

Universidade de Évora - Instituto de Investigação e Formação Avançada

Programa de Doutoramento em Bioquímica

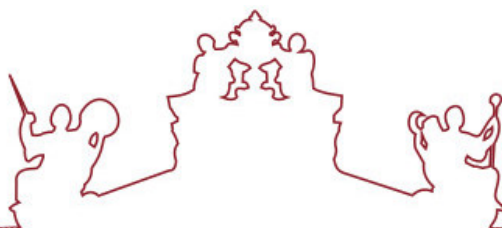
Tese de Doutoramento

**STONECOLOR: Color of commercial marbles and limestone
- causes and changes**

Luís Carlos Rosmaninho Dias

Orientador(es) | Ana Teresa Caldeira
António José Estevão Grande Candeias
José António Paulo Mirão

Évora 2020



Universidade de Évora - Instituto de Investigação e Formação Avançada

Programa de Doutoramento em Bioquímica

Tese de Doutoramento

**STONECOLOR: Color of commercial marbles and limestone
- causes and changes**

Luís Carlos Rosmaninho Dias

Orientador(es) | Ana Teresa Caldeira
António José Estevão Grande Candeias
José António Paulo Mirão

Évora 2020



A tese de doutoramento foi objeto de apreciação e discussão pública pelo seguinte júri nomeado pelo Diretor da Instituto de Investigação e Formação Avançada:

- Presidente | Filipe Themudo Barata (Universidade de Évora)
- Vogal | Maria Amélia Alves Rangel Dionísio (Universidade de Lisboa)
- Vogal | Maria Filomena Meireles Abrantes de Macedo Dinis (Universidade Nova de Lisboa)
- Vogal | Maria Clara Semedo da Silva Costa (Universidade do Algarve)
- Vogal | Luís Lopes (Universidade de Évora)
- Vogal-orientador | Ana Teresa Caldeira (Universidade de Évora)

This work was financially supported by *Fundação para a Ciência e Tecnologia* (PhD grant, SFRH/BD/111498/2015) through the *Programa Operacional do Capital Humano* (POCH) co-financed by the European Social Fund (ESF) and MEC national funds.

The projects ColourStone - Colour of commercial marbles and limestone: causes and changings (ALT20-03-0145-FEDER-000017), MEDUSA-Microorganisms Monitoring and Mitigation-Developing and Unlocking novel Sustainable Approaches (ALT20-03-0145-FEDER-000015) and INOVSTONE4.0 (POCI-01-0247-FEDER-024535) supported by the European Union through the European Regional Development Fund ALENTEJO 2020, *Fundação para a Ciência e Tecnologia* and COMPETE also funding this work.



UNIÃO EUROPEIA
Fundos Social Europeu



REPÚBLICA
PORTUGUESA

Às minhas filha e avós
To my daughters and grandparents

Acknowledgments

The execution of a PhD is not possible without the collaboration and cooperation of several people, entities and institutions. During the execution of this research I was able to count on several supports, to which I want to leave my acknowledgements.

I want to thank my supervisors Professor Doctor José Mirão, Professor Doctor Ana Teresa Caldeira and Professor Doctor António Candeias for all the scientific support, for their knowledge sharing and transmission, for the trust that they have always placed in my work, and for the fantastic people they are. I have always looked at you with great admiration and respect, which increased over the last years.

A special acknowledgement to Tânia Rosado, who has always been available to help me with whatever I need, unconditionally supporting me in even the hardest decisions. Tânia, your presence and support were fundamental, without you I have no doubt that the work would not be so “rich”! Thanks also for your companionship and moments of friendship.

A special acknowledgement also to the HERCULES Laboratory academic staff, namely Professor Doctor Cristina Dias, Professor Doctor Patrícia Moita, Professor Doctor Teresa Ferreira, Professor Doctor Jorge Teixeira, Professor Doctor Maria Rosário Martins, Professor Doctor Cristina Galacho and Professor Doctor Dora Teixeira, for all the support that was given to me when necessary, for their kindness and for always welcoming me with a smile.

I would like to thank Professor Doctor Luís Lopes, teacher at the School of Science and Technology of the University of Évora, for all his availability and scientific support, particularly in sampling campaigns.

I am grateful to the company of Ornamental Stone production and also to CEVALOR for granting the several limestone and marble lithotypes used in this PhD, which were fundamental for its execution. I also thank National Museum of Ancient Art (NMAA) and the people of the “São João da Penitência” Convent for supporting the work, namely in the execution of the Case Studies.

To the technicians of the Biotechnology Laboratory and Geosciences Laboratory of Luís António Verney College, namely D. Lena, D. Esperança and D. Sandra for all their precious help, their good spirit and for always asking me “for the girls” with great affection.

To all my colleagues and ex-colleagues of the HERCULES Laboratory for all their contribution, through knowledge transmission, constructive criticism, their availability and friendship, and for the conversations always with a good spirit. Especially to Cátia Salvador, Ricardo Vieira, Sri, Ana Coelho, Ana Manhita, Ana Margarida Cardoso, Mara Silva, Inês Cardoso, Luís Almeida, Massimo Beltrame, Carlo Bottaini, Pedro Barrulas, Milene Gil, Nuno Carriço, Lúcia Rosado, Sara Valadas, Sérgio Martins, Catarina Miguel, Sílvia Arantes, Alexandra Ferreira and Rita Vaz-Freire. A very special acknowledgement to Mafalda Costa for all her contribution, for her availability and for the shared conversations and “desk”. Your contribution was fundamental! Thank you, Mafalda for helping me in the writing phase.

To all my friends, for the friendship that has always been shown, and for knowing that even I cannot be present, you can count on me. Special thanks to the “Zés” group: Nuno Cachaço, Picasso, Coelho, André Mendes, Mosquito, Chris, Grazina, Rui Serrano and their families. Also, to the “Trupe Família”, that even physically estranged, our friendship does not fall. After this I will be more often present, I promise!

To my parents and brother for all the support shown, for the understanding and for your presence when I needed most. Despite the ups and downs, in the end the important thing is to stay together. Thank you, João for making me uncle and godfather, enriching our family with one more treasure. Thank you, mom for always being available to take care of the girls, in the tightest times.

To Catarina and my girls, probably whom I owe the most for these years. Thank you for your patience, understanding, waiting for a “better tomorrow”. These were years of great emotion, with everything that happened with Teresinha, our great warrior, we deserve only the best. I have no doubt that we will come out on top. Thank you, Catarina for all your support, patience and affection, without you it would be much more complicated! Thank you, Maria Inês and Teresinha for the fantastic moments you daily provide us, and for always having a ready smile for the parents.

To the HERCULES Laboratory, Geosciences laboratory and Biotechnology laboratory of the Chemistry Center of the University of Évora for all the support that was provided to me, essential for the execution of the work, through access to equipment, reagents and materials. I am also grateful for the support that has been provided to me in work publication and dissemination to the scientific community, which has allowed me to establish new contacts and friendships across borders. Special acknowledgement to the

Fundação para a Ciência e Tecnologia (FCT) for its financial support through the granting of a PhD scholarship.

Agradecimentos

A realização de um projeto de Doutoramento nunca é possível sem a colaboração e a cooperação de várias pessoas, entidades e instituições. Durante a execução deste projeto pude contar com vários apoios, aos quais deixo aqui o meu agradecimento.

Quero agradecer aos meus orientadores Professor Doutor José Mirão, Professora Doutora Ana Teresa Caldeira e Professor Doutor António Candeias por toda a orientação científica que me foi concedida, pela sua partilha e transmissão de conhecimento, pela confiança que sempre depositaram no meu trabalho, e também pelas fantásticas pessoas que são. Sempre olhei para vós com muita admiração e respeito, e isso só aumentou ao longo destes anos.

O meu obrigado muito especial à Tânia Rosado, que desde sempre se mostrou disponível para me ajudar no que fosse necessário, apoiando-me incondicionalmente nas decisões, mesmo nas mais difíceis. Tânia, a tua presença foi fundamental e sem ela não tenho dúvidas de que o trabalho não ficaria tão “rico”! Obrigado também pelo teu companheirismo e momentos de amizade.

Especial agradecimento vai também para o corpo docente do Laboratório HERCULES, nomeadamente à Professora Doutora Cristina Dias, Professora Doutora Dora Teixeira, Professor Doutor Jorge Teixeira, Professora Doutora Maria Rosário Martins, Professora Doutora Patrícia Moita, Professora Doutora Cristina Galacho e Professora Doutora Teresa Ferreira por todo o apoio que me foi prestado quando necessário, pela sua simpatia e por me receberem sempre com um sorriso.

Agradeço ao Professor Doutor Luís Lopes, docente da Escola de Ciência e Tecnologia da Universidade de Évora, por toda a sua disponibilidade e apoio científico, nomeadamente em campanhas de amostragem realizadas.

Agradeço à empresa de produção de Pedra Ornamental e também à CEVALOR que concederam os diversos litótipos de calcários e mármore utilizados neste projeto, e que foram fundamentais para a sua realização. Um agradecimento também ao Museu Nacional de Arte Antiga (MNAA) e às pessoas afetas ao Convento de “São João da Penitência” por apoiarem a realização do trabalho, nomeadamente na execução dos Casos de Estudo.

Às técnicas do laboratório de Biotecnologia da fase III e do laboratório de Geociências do Colégio Luís António Verney, nomeadamente a D. Lena, D. Esperança e D. Sandra,

por toda a sua ajuda preciosa, pela sua boa disposição e, por me conhecerem há já alguns anos, por me perguntarem sempre “pelas meninas” com muito carinho.

A todos os meus colegas e ex-colegas do Laboratório HERCULES por todo o seu contributo, através da transmissão de conhecimentos, críticas construtivas, pela sua disponibilidade e amizade, e pelas conversas proporcionadas sempre com boa disposição. Especialmente à Cátia Salvador, Ricardo Vieira, Sri, Ana Coelho, Ana Manhita, Ana Margarida Cardoso, Mara Silva, Inês Cardoso, Luís Almeida, Massimo Beltrame, Carlo Bottaini, Pedro Barrulas, Milene Gil, Nuno Carriço, Lúcia Rosado, Sara Valadas, Sérgio Martins, Sílvia Arantes, Alexandra Ferreira e Rita Vaz-Freire. Um agradecimento muito especial à Mafalda Costa por todo o seu contributo, pela disponibilidade sempre demonstrada e pelas conversas e “secretária” partilhadas. O teu contributo foi fundamental! Obrigado Mafalda, por me ajudares na fase da escrita.

A todos os meus amigos, pela amizade demonstrada desde sempre, e por saberem que, mesmo quando não posso estar presente, podem contar comigo. Um especial obrigado ao grupo dos “Zés”: Nuno Cachaço, Picasso, Coelho, André Mendes, Mosquito, Chris, Grazina e Rui Serrano e respetivas famílias. Também à “Trupe Família”, que mesmo afastados fisicamente, a nossa amizade não cai. Após esta fase conto estar mais vezes presente, prometo!

Aos meus pais e irmão por todo o apoio demonstrado, pela compreensão e pela vossa presença nos momentos em que mais precisei. Apesar dos altos e baixos, ao final o importante é mantermo-nos unidos. Obrigado João, por me teres tornado Tio e Padrinho, enriquecendo a nossa família com mais um tesouro. Obrigado mãe, por estares sempre disposta a cuidar das meninas, nas alturas de maior aperto.

À Catarina e às minhas meninas, provavelmente as pessoas a quem mais devo uma retribuição por estes anos. Obrigado pela compreensão, pela paciência, pela espera de um “amanhã melhor”. Foram anos de muitas emoções, com tudo o que aconteceu com a Teresinha, a nossa grande Guerreira, só merecemos o melhor. Não tenho dúvidas que sairemos por cima. Obrigado Catarina por todo o teu apoio, paciência e carinho, sem ti seria muito mais complicado! Obrigado Maria Inês e Teresinha pelos fantásticos momentos que nos proporcionam diariamente, e por estarem sempre com um sorriso pronto para os pais.

Ao Laboratório HERCULES e Laboratório de Biotecnologia do Centro de Química da Universidade de Évora por todo o apoio que me foi facultado, necessário para a execução do trabalho, através do acesso aos equipamentos, reagentes e materiais. Agradeço também

o apoio e os meios que me foram prestados na divulgação do trabalho à comunidade científica, a qual me permitiu estabelecer novos contactos e novas amizades além-fronteiras. Especial agradecimento à Fundação para a Ciência e Tecnologia (FCT) pelo suporte financeiro, através da concessão de uma Bolsa de Doutoramento.

Abstract

Historically centred in the European and Asiatic countries, the ornamental stone production is currently one of the most important sectors for the Portuguese economy. In fact, Portugal is today one of the leaders in the production of natural stone worldwide, namely in the limestone and marble exploitation. The production increment over the last several years is related with the high quality of the carbonated stones existing in the Portuguese territory together with the Portuguese experience in stone manufacture, acquired since ancient times.

In this context, colour is one of the most important visible aspects of natural stone, for the construction/restoration of new buildings and/or for Cultural Heritage preservation. Therefore, colour and discolouration of stone is currently an important research topic for the scientific community, where the association stone-colour-microorganism is still unexploited.

This PhD aimed to determine the causes that affect the colour of Portuguese marbles and limestones. Therefore, several lithotypes of natural stone with high relevance for the Portuguese natural stone industry and for Cultural Heritage assets were selected and studied. In order to characterise discolouration phenomena, the processes of natural stones' weathering were assessed, and the microbiota thriving on the stones was determined. The microorganisms' contribution for the stone discolouration phenomena was evaluated through the execution of artificial ageing assays, under controlled environment.

The results obtained allowed to identify the main chromophore components of the Portuguese carbonated stones studied. It was also finding and determined that the colour change occurred on the blue limestone is achieved through the natural weathering of pyrite, and this mechanism is accelerated when microorganisms are present. Regarding the cultural heritage assets study, it was finding that colour alterations of the stone are caused mainly by chemical and biogenic actions.

Keywords:

Ornamental stone; Limestone; Marble; Cultural Heritage; Colour; Colour change; Natural weathering; Biodeterioration; Biodeteriogenic agents; Microbial diversity; Metabolically active microorganisms.

STONECOLOR: Cor de mármore e calcários comerciais – causas e alterações**Resumo**

Tradicionalmente centrada nos países Europeus e Asiáticos, a produção de Pedra Ornamental tem-se tornado num dos mais importantes setores da economia Portuguesa. Portugal é hoje, de facto, um dos líderes ao nível mundial na produção de Pedra Natural, nomeadamente de calcários e mármore. O aumento na produção ao longo destes últimos anos está relacionada não só com a elevada qualidade das rochas carbonatadas que aqui se encontram, mas também com a experiência portuguesa no manuseamento da Pedra.

A cor, neste contexto, é um dos aspetos visíveis mais importantes na Pedra Natural, tanto na construção/restauro de novos edifícios como na preservação de Património Cultural. Deste modo, a cor e a descoloração da Pedra tem-se tornado num dos importantes tópicos de investigação para a comunidade científica, onde uma das lacunas é a falta de associação pedra-cor-microorganismo.

Com este projeto pretendeu-se contribuir para a compreensão das causas de cor em rochas carbonatadas portuguesas, como o calcário e o mármore, onde foram selecionados e estudados diversos litótipos de Pedra Natural com elevada relevância para a indústria da Pedra portuguesa e para o património cultural construído. Para caracterizar fenómenos de descoloração, foram estudados os processos de meteorização de rochas e foi determinado o estado de biocolonização do material. O contributo dos microorganismos para o fenómeno de descoloração de Pedra foi avaliado através da execução de ensaios de envelhecimento artificial, sob ambiente controlado.

Os resultados obtidos permitiram identificar os principais elementos cromóforos das rochas carbonatadas portuguesas estudadas. Foi ainda determinado que a alteração da cor no calcário azul é causada pela meteorização natural da pirite, e que este mecanismo é acelerado na presença de agentes microbianos. Relativamente ao estudo dos bens patrimoniais, foi determinado que as alterações cromáticas aqui presentes são sobretudo de origem química e biogénica.

Palavras-chave:

Pedra ornamental; Calcário; Mármore; Património Cultural; Cor; Alteração de cor; Meteorização natural; Biodeterioração; Agentes biodeteriogénicos; Diversidade microbiana; Microorganismos metabolicamente ativos.

Table of contents

Acknowledgments	vii
Agradecimentos	xi
Abstract	xv
Resumo	xvii
List of Figures	xxiii
List of Tables	xxxii
Abbreviations	xxxvii
Units	xl
Aims and Methodology	1
Chapter I. State of the Art	3
<hr/>	
1.1. Ornamental stones	5
1.1.1. Types of ornamental stone	6
1.1.2. The international production of natural building stone	7
1.1.3. Portuguese ornamental stones	9
1.1.3.1. Limestones	11
1.1.3.2. Marbles	13
1.2. Weathering and deterioration of natural stone	15
1.2.1. Deterioration induced by mechanical processes	16
1.2.2. Deterioration induced by chemical processes	20
1.2.2.1. Hydrolysis	21
1.2.2.2. Dissolution	21
1.2.2.3. Oxidation	23
1.3. Biodeterioration of stone	23
1.3.1. Organisms involved in biodeterioration of stone	25
1.3.1.1. Bacteria	25
1.3.1.2. Fungi	27
1.3.1.3. Lichens	28
1.3.2. Biodeterioration effects	29
1.3.2.1. Surface alteration	29
1.3.2.2. Chemical and mechanical alterations	29
	xix

1.4. The Colour in natural stone	31
1.4.1. The colour in carbonated natural stones	32
Chapter II. Characterisation of Portuguese carbonated stones	39
<hr/>	
2.1. Introduction	41
2.2. Material and methods	43
2.2.1. Selection of the stones	43
2.2.2. Determination of the colour parameters	44
2.2.3. Chemical and mineralogical composition	45
2.2.3.1. X-ray Fluorescence Spectrometry (XRF)	45
2.2.3.2. X-ray Diffraction (XRD)	46
2.2.3.3. Variable Pressure Scanning Electron Microscopy with Energy Dispersive Spectrometry (VP-SEM-EDS)	46
2.3. Results and discussion	47
2.3.1. Determination of the colour parameters	47
2.3.2. Chemical and mineralogical characterisation	48
Chapter III. Characterisation of the of colour alteration mechanism on the blue limestone	59
<hr/>	
3.1. Introduction	61
3.2. Materials and methods	63
3.2.1. Sampling process	63
3.2.2. Material characterisation	64
3.2.2.1. XRF	64
3.2.2.2. XRD	64
3.2.2.3. VP-SEM-EDS	64
3.2.3. Biocontamination assessment	65
3.2.3.1. Assessment of biological contamination on the building stone	65
3.2.3.2. Cell viability index	65
3.2.3.3. Isolation and characterisation of the cultivable microbial community	65
3.2.3.3.1. Characterisation of the microbial isolates	66
3.2.3.4. Characterisation of the total microbial population	68

3.3. Results and discussion	70
3.3.1. Chemical composition	70
3.3.2. Mineralogical composition and superficial texture	71
3.3.3. Biocontamination evaluation	74
Chapter IV. Evaluating the contribution of biocontamination on the blue limestone discolouration	85

4.1. Introduction	87
4.2. Materials and methods	89
4.2.1. Artificial ageing assay set-up	89
4.2.2. Macroscopic and microscopic monitoring	90
4.2.3. Colour monitoring	90
4.2.4. Assessment of the microbial population dynamics	91
4.3. Results and discussion	92
4.3.1. Determination of chromatic changes	92
4.3.2. Assessment of the microbial population	95
Chapter V. Characterisation of the colour change on carbonated stones applied in cultural heritage	105

5.1. Introduction	107
5.1.1. Limestone-built sculptures	108
5.1.2. Heritage building made of marble	109
5.2. Materials and methods	112
5.2.1. <i>In-situ</i> approach	113
5.2.2. Sampling processes	114
5.2.3. Characterisation of the material and detection of alteration products	114
5.2.4. Microbiological assessment	115
5.2.4.1. Assessment of biological contamination	115
5.2.4.2. Characterisation of the microbial population	115
5.3. Results and discussion	116
5.3.1. Case study of NMAA limestone sculptures	116
5.3.1.1. Characterisation of the material and detection of alteration products	116

5.3.1.2. Biocontamination assessment	121
5.3.2. Case study of the “São João da Penitência” Convent	128
5.3.2.1. Measurement and characterisation of the colour	130
5.3.2.2. Characterisation of the material and alteration products	130
5.3.2.3. Microbiological assessment	134
Chapter VI. Concluding remarks	143
References	149
Annexes	179
<hr/>	
Annex A. Samples obtained from the blue limestone	181
Annex B. Culture media composition	182
Annex C. Characterisation of the microbial population thriving in the samples obtained from the blue limestone	183
C.1. Microbial growth resulted from the inoculation of blue limestone samples using CDM	183
C.2. Electrophoresis of the PCR products obtained from the isolated microbial population of the blue limestone	185
C.3. HTS approach for the blue limestone samples	187
Annex D. Characterisation of the microbial population thriving in the limestone sculptures from the Portuguese NMAA	190
D.1. Microbial growth in the sculpture’s samples using CDM	190
D.2. HTS approach for the sculpture’s samples	191
Annex E. Microbial population thriving on the “São João da Penitência” Convent identified through HTS approach	195
E.1. Prokaryotic population	195
E.2. Eukaryotic population	203

List of Figures

Chapter I. State of the Art

Figure I-1. The geological rock cycle and the relationship between each type of rock	6
Figure I-2. Leading countries on the world export of natural building stones, in 2015	7
Figure I-3. Applications of stones worldwide and their proportion	8
Figure I-4. Examples of several applications of stone: Temple made of limestone and marble, Évora, Portugal (a), marble sculpture, Vatican (b), marble sarcophagus, Lisbon, Portugal (c), limestone interior flooring, Vatican (d), and marble external cladding of a Roman Catholic basilica, Lucca, Italy (e)	9
Figure I-5. Main mining sites of Portuguese ornamental stones and their geologic units	10
Figure I-6. Location of Maciço Calcário Estremenho (MCE) in the context of the Meso-Cenozoic Lusitanian Basin	11
Figure I-7. The geographical location of the Estremoz Anticline, Portugal	13
Figure I-8. Quarry located in the Estremoz Anticline	14
Figure I-9. Examples of effects promoted by historic fires in stone-built structures. Granite pillars, Brazil (a), marble columns, Greece (b), church wall constructed with argillaceous sandstone, Argentina (c)	16
Figure I-10. Effects of thermal cycling for a calcite mineral. Calcite crystal composing the marble matrix (a), contraction and expansion upon heating (b) and cooling (c)	17
Figure I-11. Examples of effects of salt deterioration in buildings made of stone. Initial flaking (left block) and sanding following the bedding plane (right block) (a), scaling (b), alveolarisation (c) and salt efflorescences (d)	19

Figure I-12. Ground moisture transported by rising capillary (a) and its practical effect in buildings (b)	20
Figure I-13. Different phase transitions of salts in building materials	20
Figure I-14. Dissolution effect in marble, built in 1832. The carved details gradually become rounded	22
Figure I-15. Environmental and substrate factors influencing the development of microbial communities in a building stone (a) and the main ways (b) in which microorganisms may affect stone	24
Figure I-16. Rosy stain on the salt damaged stone surface of a Medieval monument, Austria, promoted by halophilic bacteria and archaea	27
Figure I-17. Crustose lichens developing on calcareous stone	28
Figure I-18. Sugaring marble in the Monumental Cemetery of Bologna, Italy	30
Figure I-19. Examples of natural stone applications: the floor of the area next to Padrão dos Descobrimentos in Lisbon, Portugal (a) and interior floor of the Milano “Duomo”, Italy (b)	32
Figure I-20. Examples of the most common limestones exploited in Portugal, their macroscopic appearance and their common commercial names. Provenance from the MCE (a-i), and Algarve (j-k) regions	34
Figure I-21. Examples of the most common marbles exploited in Portugal, their macroscopic appearance and their common commercial names. Provenance from Alentejo region for all	35
Figure I-22. Examples of weathering in pieces of art made of limestone and marble. Patina formations (a, b and c) and a hardened crust formed after a past treatment (d), responsible for the detachment of a thin stone layer	37
 Chapter II. Characterisation of Portuguese carbonated stones <hr/>	
Figure II-1. Evolution of the ornamental stone’ exportation in Portugal	41

Figure II-2. Stones selected for the study. White (a), green (b) and pink (c) marbles, and red (d), yellow (e), orange (f) and blue (g) limestones	43
Figure II-3. CIE Lab 1976 colour coordinates system	45
Figure II-4. Spectral reflection profiles obtained by colourimetry technique for the white (—), green (—), pink (—), yellow (—), red (—), orange (—) and blue (—) stones	47
Figure II-5. Spectra obtained by X-ray fluorescence for the white (—) and pink (—) marbles from Estremoz and green marble (—) from Serpa	48
Figure II-6. Spectra obtained by X-ray fluorescence for the blue (—) and orange (—) limestones from MCE and for the yellow (—) and red (—) limestones from Negrais	49
Figure II-7. Significant diffractograms obtained and identification of crystalline phases on the powdered white (—) and pink (—) marbles from Estremoz and green marble (—) from Serpa. Abbreviations: m-muscovite; w-wollastonite; ch-chamosite; o-orthoclase; q-quartz; a-albite; r-rutile; c-calcite	50
Figure II-8. Significant diffractograms obtained and identification of crystalline phases on the powdered blue (—) and orange (—) limestones from MCE and yellow (—) and red (—) limestones from Negrais. Abbreviations: b-birnessite; c-calcite; p-pyrite; mrc-marcasite; q-quartz	51
Figure II-9. Microstructure, calcium distribution and point analysis obtained on the white marble from Estremoz	53
Figure II-10. Microstructure, distribution of the major elements and point/area analyses obtained on the pink marble from Estremoz (only cations were considered)	54
Figure II-11. Microstructure, distribution of the major elements and point analyses obtained on the green marble from Serpa	55
Figure II-12. Microstructure, distribution of the major elements and point analysis obtained on the yellow limestone from Negrais	56

Figure II-13. Microstructure, distribution of the major elements and point analysis on the blue limestone from MCE	57
 Chapter III. Characterisation of the of colour alteration mechanism on the blue limestone	
<hr/>	
Figure III-1. Blue limestone with blueish dark-grey and cream colour in the same outcrop	61
Figure III-2. Building blue limestone with visible alteration (a), (b)	62
Figure III-3. Sampling process of the building stone located at the floor pavements next to the Mosteiro da Batalha building (a), (b), (c) and in the waterfront of São Martinho do Porto village (d)	63
Figure III-4. Compositional spectra obtained by X-ray fluorescence for the sample of building stone, on altered (----) and non-altered (—) areas	70
Figure III-5. Micro diffractogram obtained on altered area of the building stone collected. Abbreviations: g-gypsum; c-calcite; q-quartz	71
Figure III-6. Microstructure (a), punctual analysis (b) and element mapping of calcium (c) and sulphur (d) on the altered area of the stone, performed by SEM-EDS	72
Figure III-7. Stone microstructure of non-altered (a) and altered (b) surfaces, obtained by SEM-EDS	73
Figure III-8. Determination of surface roughness parameters on non-altered (a) and altered (b) surfaces of the stone, using the 3D Roughness Reconstruction software. The mean value and standard deviation were calculated after 20 measurements	74
Figure III-9. SEM analysis on weathered sections, showing microbial contamination	75
Figure III-10. Cell viability of the microbial population present on altered areas and non-altered areas of the stone. Error bar corresponds to \pm standard deviation (n=21)	75

Figure III-11. Phylogenetic relationship between the prokaryotic isolates	81
Figure III-12. Phylogenetic relationship between the eukaryotic isolates	82
Figure III-13. Characterisation of the prokaryotic population present on limestone altered areas at (a) phylum and (b) family levels	83
Figure III-14. Characterisation of the eukaryotic population at genera level present on limestone altered areas	83
Chapter IV. Evaluating the contribution of biocontamination on the blue limestone discolouration	
<hr/>	
Figure IV-1. Scheme of the artificial ageing assays performed in lithotypes of blue limestone	90
Figure IV-2. Graphical representation of the difference in total colour (ΔE) during the artificial ageing assays for the slab without inoculation (■), slab inoculated with bacteria (■), slab inoculated with fungi (■) and slab inoculated with bacteria + fungi (■)	94
Figure IV-3. FORS spectroscopy spectra obtained for the slab stones inoculated with the mixture of bacteria + fungi, during the ageing assays. Spectra for the slab inoculated at t_{0d} (—), t_{2d} (—), t_{7d} (—), t_{15d} (—), t_{30d} (—), t_{90d} (—) and t_{180d} (—)	94
Figure IV-4. FORS spectroscopy spectra obtained for the slab without inoculation at t_{0d} (—) and t_{180d} (—)	95
Figure IV-5. Microbial proliferation on the slabs during the ageing. Slabs without inoculation (a-d) and slabs inoculated with the mixture bacteria + fungi (e-l)	99

Figure IV-6. Element mapping of calcium, sulphur, carbon, nitrogen and oxygen obtained by VP-SEM-EDS at t_{30d} on the slab containing the mixture bacteria + fungi	100
Figure IV-7. SEM micrographs on the stone slabs at t_{180d} that indicate the presence of bacteria, hyphae of filamentous fungi and spores proliferating around the calcite and gypsum crystals	100
Figure IV-8. Dynamic of the prokaryotic population inoculated on the stone slabs during the artificial ageing assays	101
Figure IV-9. Dynamic of the most representative inoculated and native prokaryotic population present on the stone slabs during the artificial ageing assay	102
Figure IV-10. Dynamic of the most representative inoculated and native eukaryotic population present on the stone slabs during the artificial ageing assays	103
 Chapter V. Characterisation of the colour change on carbonated stones applied in cultural heritage	
<hr/>	
Figure V-1. Limestone sculptures selected for the study, located at the NMAA. <i>St. John the Baptist</i> (a), <i>The Virgin and the Child</i> (b), <i>St. Paul</i> (c) and <i>Musician Angel</i> (d)	109
Figure V-2. The manueline architecture of the Convent of “São João da Penitência”	110
Figure V-3. Some of the pathologies found in the main cloister of the Convent. Dark staining on column stems (a), reddish staining with detachment of the material (b and e), and patina formations on the Tuscan pillars (c) and on the stone walls (d)	111
Figure V-4. Limestone sculptures subjected for deterioration study and details of their pathologies	112

Figure V-5. Areas selected for the methodology approach. Areas CM1 and CM2 correspond to white and yellow patinas (a, b), areas CM3 and CM4 correspond to reddish stains and fissures (c, d), areas CM5 and CM6 correspond to formation of red and dark biofilms (e, f)	113
Figure V-6. Micro-X-ray diffractograms obtained on non-altered (—) and altered (—) microsamples' surface of the <i>St. John the Baptist</i> sculpture. Abbreviations: g-gypsum; c-calcite; q-quartz	116
Figure V-7. Iron sulphide minerals' microstructure (a) and correspondent point analysis (b) on a microsample collected from the <i>St. John the Baptist</i> sculpture, obtained by VP-SEM-EDS	117
Figure V-8. Microstructure (a) and element mapping of calcium and sulphur (b) on a damaged area of the <i>St. John the Baptist</i> sculpture' surface, obtained by VP-SEM-EDS	117
Figure V-9. Micro-X-ray diffractogram on <i>Virgin and Child</i> non-altered (—) and altered (—) microsamples' surface. Abbreviations: c-calcite; s-sodalite; q-quartz; h-halite	118
Figure V-10. Microstructure (a) and element mapping of calcium, chlorine and sodium (b) on a damaged area of <i>The Virgin and the Child</i> sculpture, obtained by VP-SEM-EDS	119
Figure V-11. Micro-X-ray diffractogram performed on non-altered (—) and altered (—) microfragments' surface from the <i>St. Paul</i> sculpture. Abbreviations: g-gypsum; hy-hydrohematite; c-calcite; hm-hematite	119
Figure V-12. Microstructure (a), element mapping of calcium and iron (b) and point analysis (c, d) of iron oxides present on the microfragments' surface with reddish stains collected from the <i>Musician Angel</i> sculpture, obtained by VP-SEM-EDS	120
Figure V-13. Raman spectra of β -carotene standard (—), microfragment collected without alteration (—) and microfragment collected in the red coloured zone of the <i>Musician Angel</i> sculpture (—)	121

Figure V-13. Raman spectra of β -carotene standard (—), microfragment collected without alteration (—) and microfragment collected in the red coloured zone of the <i>Musician Angel</i> sculpture (—)	124
Figure V-14. Microstructure (a) and element mapping of calcium, carbon, oxygen, and nitrogen (b) evidencing index of biocontamination on the surface of the <i>St John the Baptist</i> sculpture, obtained by VP-SEM-EDS	122
Figure V-15. SEM micrographs on the microfragments of the <i>St. John The Baptist</i> (a), <i>The Virgin and the Child</i> (b) and <i>Musician Angel</i> (c, d) sculptures, signalling hyphae of filamentous fungi proliferating around the crystals of calcite	122
Figure V-16. Cell viability of the microbial population present in the samples collected on the sculptures' surface. Abbreviations: SJB- <i>John the Baptist</i> , SP- <i>St. Paul</i> , VC- <i>The Virgin and the Child</i> and MA- <i>Musician Angel</i> . Error bar corresponds to \pm standard deviation (n=9)	123
Figure V-17. Composition of the major prokaryotic population thriving on the limestone sculptures at genera and species levels. Abbreviations: MA – <i>Musician Angel</i> ; SP – <i>St. Paul</i> ; VC – <i>The Virgin and the Child</i> ; SJB – <i>St. John the Baptist</i>	126
Figure V-18. Aerial view of the Convent (a) and map of the main cloister with the location of the areas selected for the study (b)	128
Figure V-19. Micro-diffractograms obtained on the microfragments collected in the areas CM1 (—) and CM2 (—). Abbreviations: c – calcite; wh – whewellite; q – quartz; w – weddellite	131
Figure V-20. Surface microstructure, elemental distribution of calcium and sulphur, and point analysis of calcium sulphates, obtained by SEM-EDS on the microfragment collected in the area CM1	132
Figure V-21. Spectra obtained by X-ray fluorescence on the CM3 (—), CM4 (—) and non-altered (—) areas	133

Figure V-22. Microstructure and elemental distribution of calcium, aluminium, silicon, iron and potassium on the microfragment collected on the area CM3, obtained by SEM-EDS	133
Figure V-23. Microstructure and elemental distribution of calcium, carbon, nitrogen and oxygen, obtained by SEM-EDS for the microfragment collected on the area CM5	134
Figure V-24. Micrographs obtained on the microfragment collected on the area CM5 showing the ability of filamentous fungi to surround the calcitic matrix and penetrate the porous of the stone	135
Figure V-25. Micrographs obtained on the microfragment collected on the area CM6 showing the microscopic aspect of the biofilm (a and b), presence of microalgae (c) and some unidentified structures (d)	136
Figure V-26. Characterisation of the major eukaryotic population present on the areas of the Convent without biofilms formation, at genera level	140
Figure V-27. Characterisation of the major eukaryotic population present on the red (a) and black (b) biofilms, at genera level	141
 Annexes	
<hr/>	
Figure C-1. Electrophoresis of the PCR products performed with DNA extracted from bacteria isolates	185
Figure C-2. Electrophoresis of the PCR products performed with DNA extracted from yeast isolates	186
Figure C-3. Electrophoresis of the PCR products performed with DNA extracted from fungi isolates	186

List of Tables

Chapter I. State of the Art

Table I-1. Main physical-mechanical properties of the most common Portuguese limestones exploited at the MCE	12
---	----

Table I-2. Main physical and mechanical properties of the most common Portuguese ornamental marbles exploited at the Estremoz Anticline	15
--	----

Chapter II. Characterisation of Portuguese carbonated stones

Table II-1. Determination of the parameters $L^*a^*b^*$ for each stone, obtained through the CIEL $^*a^*b^*$ system	48
--	----

Table II-2. Determination of the peak areas (a. u.) for each element detected in the stones by X-ray fluorescence spectrometry	50
---	----

Table II-3. Minerals under crystalline form composing stones, identified by X-ray diffraction	52
--	----

Chapter III. Characterisation of the of colour alteration mechanism on the blue limestone

Table III-1. Characterisation of the bacteria isolated from the stone with chromatic alteration	76
--	----

Table III-2. Characterisation of the fungi isolated from the stone with chromatic alteration	78
---	----

Table III-3. Identification of the microorganisms isolated from the cultivable population	80
--	----

Chapter IV. Evaluating the contribution of biocontamination on the blue limestone discolouration

Table IV-1. Measurement of the colourimetric parameters and determination of the colour difference for each slab	92
---	----

Table IV-2. Microscopic monitoring of the stone slabs, through stereoscopic and scanning electron microscopy	97
---	----

Chapter V. Characterisation of the colour change on carbonated stones applied in cultural heritage

Table V-1. Characterisation of the microbial population isolated from the limestone sculptures' samples	124
Table V-2. Identification of microorganisms isolated from the limestone sculptures	125
Table V-3. Digital microscopy analyses on the selected areas, under visible and UV light	129
Table V-4. Measurement of the colourimetric parameters, using the CIELAB system	130
Table V-5. Characterisation of the isolated bacteria from the selected areas of the Convent	136
Table V-6. Characterisation of the isolated fungi from the selected areas of the Convent	138

Annexes

Table A-1. Samples of stone collected and their location	181
Table B-1. Composition of the culture media used for microbiological development	182
Table C-1. Microbial colonies growth from the inoculated samples of building stone, with and without chromatic alteration	183
Table C-2. Prokaryotic population present in the altered areas of the stone, identified through HTS approach	187
Table C-3. Eukaryotic population present in the altered areas of the stone, identified through HTS approach	

Table D-1. Cultivable microbial colonies present on the limestone sculptures	189
Table D-2. Prokaryotic population present in the <i>St. John the Baptist</i> sculpture, identified through HTS approach	190
Table D-3. Prokaryotic population present in <i>The Virgin and the Child</i> sculpture, identified through HTS approach	191
Table D-4. Prokaryotic population present in the <i>St. Paul</i> sculpture, identified through HTS approach	192
Table D-5. Prokaryotic population present in the <i>Musician Angel</i> sculpture, identified through HTS approach	192
Table E-1. Prokaryotic population present in the area CM1 of the Convent, identified through HTS approach	193
Table E-2. Prokaryotic population present in the area CM2 of the Convent, identified through HTS approach	195
Table E-3. Prokaryotic population present in the area CM3 of the Convent, identified through HTS approach	197
Table E-4. Prokaryotic population present in the area CM4 of the Convent, identified through HTS approach	197
Table E-5. Prokaryotic population present in the area CM5 of the Convent, identified through HTS approach	198
Table E-6. Prokaryotic population present in the area CM6 of the Convent, identified through HTS approach	201
Table E-7. Eukaryotic population present in the area CM1 of the Convent, identified through HTS approach	201
Table E-8. Eukaryotic population present in the area CM2 of the Convent, identified through HTS approach	203
Table E-9. Eukaryotic population present in the area CM3 of the Convent, identified through HTS approach	206
	209

Table E-10. Eukaryotic population present in the area CM4 of the Convent, identified through HTS approach	213
Table E-11. Eukaryotic population present in the area CM5 of the Convent, identified through HTS approach	216
Table E-12. Eukaryotic population present in the area CM6 of the Convent, identified through HTS approach	221

Abbreviations

ΔE	Colour difference
2D	Bi-dimensional
A	Adenine nucleotide
Al	Aluminium
Au	Gold
(aq)	Aqueous
BC	Before Christ
BSE	Backscattered electron
C	Cytosine nucleotide
C	Carbon
Ca	Calcium
Ca²⁺	Calcium (II) ion
CaCO₃	Calcite
CaC₂O₄.H₂O	Whewellite
CaC₂O₄.2H₂O	Weddellite
CaF₂	Fluorite
CaMg(CO₃)₂	Dolomite
CaSO₄.2H₂O	Gypsum
CCD	Charge Coupled Device
CDM	Culture-Dependent Methods
CIE	Commission Internationale de l'Elclairage
CIELAB	Colour space defined by the CIE
CO₂	Carbon dioxide
Cr	Chromium
CRB	Cook Rose Bengal
CVI	Cell Viability Index
DMSO	Dimethyl sulfoxide
DNA	Deoxyribonucleic acid
dNTPs	Deoxynucleotide triphosphates
EDS	Energy Dispersive Spectrometry
EN	European Normative
F	Fluorine
Fe	Iron
Fe²⁺	Iron (II) ion
Fe³⁺	Iron (III) ion
Fe₂O₃	Hematite
FeO(OH)	Hydrohematite
FeS₂	Iron sulphide
FeSO₄	Iron (II) sulphate
FORS	Fiber Optic Reflectance Spectroscopy
FWHM	Full Width at Half Maximum
(g)	Gaseous
G	Guanine nucleotide
H⁺	Hydrogen ion
H₂O	Water
H₂SO₄	Sulphuric acid
HTS	High Throughput Sequencing
IMM	Independent Market Monitoring

ITS	International Transcribed Space
K	Potassium
K₂HPO₄	Dipotassium phosphate
KAlSi₃O₈	Orthoclase
KLi₂Al(Al,Si)₃O₁₀(F,OH)₂	Lepidolite
(K,Na,Ca)(Si,Al)₄O₈	Feldspar
(l)	Liquid
Li	Litium
MCE	“Maciço Calcário Estremenho”
MEA	Malt Extract Agar
Mg	Magnesium
Mg²⁺	Magnesium (II) ion
MgCl₂	Magnesium dichloride
MgSO₄	Magnesium Sulphate
Mn	Manganese
Mn²⁺	Manganese (II) ion
Mn⁴⁺	Manganese (IV) ion
MRD	Maximum Recovery Diluent
MTT	3-(4,5-dimethylthiazol-2-yl)-2,5-diphenyltetrazolium bromide
N	Nitrogen
NA	Nutrient Agar
Na	Sodium
NaAlSi₃O₈	Albite
(Na_{0.3}Ca_{0.1}K_{0.1})(Mn⁴⁺, Mn³⁺)₂O₄·1.5H₂O	Birnessite
NaCl	Sodium chloride
NCBI	National Center for Biotechnology Information
NMAA	National Museum of Ancient Art
NO	Nitric oxide
NO₂	Nitrogen dioxide
NO_x	Nitrogen oxides
NTS	Ribosomal Non Transcribed Spacer
O	Oxygen
O₂	Oxygen
OTU	Operational Taxonomic Unit
PAR	Photosynthetically Active Radiation
PCR	Polymerase Chain Reaction
Pd	Palladium
Ra	Arithmetic average roughness
Rb	Rubidium
rDNA	Ribosomal deoxyribonucleic acid
rRNA	Ribosomal ribonucleic acid
RH	Relative Humidity
Rz	Average distance between the highest and lowest peaks
(s)	Solid
S	Sulphur
SCE	Specular Component Excluded
SDD	Silicon Drift Detector
SDS	Sodium Dodecyl Sulphate
SEM	Scanning Electron Microscopy

SEM-EDS	Scanning Electron Microscopy coupled to an Energy Dispersive Spectrometry
Si	Silicon
SiO₂	Quartz
SO₂	Sulphur dioxide
SO₄²⁻	Sulphate ion
TE	Tris-EDTA buffer
Ti	Titanium
TiO₂	Titanium oxide
UV	Ultraviolet
UV-Vis	Ultraviolet-visible
VP-SEM-EDS	Variable Pressure Scanning Electron Microscope coupled to an Energy Dispersive Spectrometry
XRD	X-ray Diffraction
XRF	X-ray Fluorescence
Zr	Zircon

Units

μA	Microampere
μg/mL	Microgram per millilitre
μL	Microlitre
μM	Micromolar
%	Percentage
°C	Celsius degree
a.u.	Arbitrary units
bp	Base pairs
cm	Centimetres
cps	Counts per second
d	Day
eV	Electron volt
g	Gram
g/L	Gram per litre
h	Hour
J	Joule
KeV	Kiloelectron volt
kg	Kilogram
kg/m³	Kilogram per cubic metre
km²	Square kilometre
kV	Kilo volt
m	Metre
M	Molar
m³	Cubic metre
mL	Millilitre
mM	Millimolar
mg/mL	Miligram per millilitre
mm	Millimetre
Mpa	Megapascal
ms	Millisecond
Mt	Milliton
nm	Nanomolar
Pa	Pascal
rpm	Rotations per minute
V	Volt
w/v	Weight per volume

Aims and methodology

Portuguese natural stone, namely limestone and marble, are currently very valuable in the national and international market. Since colour is one of the most important characteristics, it is necessary to develop new methodologies in order to keep the Portuguese natural stone at the forefront and, at the same time, to preserve and valorise the Cultural Heritage assets built of stone.

The main goals of this PhD project comprise the determination of factors that can contribute to the colour acquisition in carbonated stones, the characterisation of colour change mechanisms in stone through inorganic and/or biogenic processes, and the association of colour change with microorganisms' metabolic action.

In this way, several types of Portuguese stone were selected, according with their importance for the Portuguese economy and Cultural Heritage.

The methodology defined for this PhD intended:

- To characterise limestones and marbles, in order to determine the causes for their colour and to understand and anticipate discolouration mechanisms through multi-analytical approaches, using X-ray based methods like XRD, XRF and SEM-EDS;
- To characterise colour change mechanisms on stone using X-ray based methods;
- To identify alteration products in stones showing discolouration patterns, using X-ray based methods and Raman spectrometry;
- To assess the presence of metabolic active cells through the CVI determination (MTT cell viability);
- To characterise the biocolonisers thriving on stones with discolouration patterns, using complementary methodologies, namely culture-dependent methods and molecular approaches;
- To isolate the cultivable microbial population for further use in artificial ageing assays;
- To evaluate the microbial proliferation capacity on stone, using SEM;
- To evaluate the colour difference promoted on stone by natural weathering and biocolonisers;
- To identify the main biodeteriogenic agents involved in stone deterioration and associate these agents with colour changes on stone.

This PhD thesis is composed by six chapters; an introductory chapter, four chapters dedicated to the results and discussion, and a final chapter presenting the main conclusions obtained during this project research.

Chapter I describes the general aspects related to: a) the history of ornamental stone industry; b) the most important carbonated stones exploited in Portugal and their importance for the Portuguese economy; c) the typical mechanisms of weathering in ornamental stones; and d) the importance of colour and colour alteration for the ornamental stone industry and stone-built heritage. In Chapter II, the study of several limestones and marbles is presented with the aim to find the causes for their colour achievement using X-rays based analytical methods. Chapter III describes the colour alteration mechanism of a particular stone, which is actually one important lithotype for the Portuguese ornamental stone industry. Chapter IV is focused on the evaluation of the contribution of microbial contamination in the discolouration process of a particular stone lithotype, with the execution of ageing assays in stone slabs under controlled atmosphere. Chapter V presents two case studies in which stone is employed in artworks and monuments, and where the discolouration phenomena both by inorganic and biogenic ways were characterised. Finally, the concluding remarks and future perspectives are presented in Chapter VI, underlining the advantages of the methodologies used.

Chapter I:

State of the Art



1.1. Ornamental stones

Stone is one of the oldest and more durable building materials used by humanity since ancient times (Göbekli Tepe, 10th-8th millennium BCE), being employed to construct impressive historic structures with the purpose to last for centuries or even thousands of years (Vasconcelos and Lourenço, 2009; Schmidt, 2011; Siegesmund and Snethlage, 2011; Pereira and Marker, 2016).

Until the 20th century, the availability of stone resources determined the appearance of entire cities. Without the transportation facilities that we have nowadays, nearby sources provided the stones to build important structures like castles, churches, and other buildings. Stones were transported over long distances only for exceptional cases (Siegesmund and Snethlage, 2011).

The EN 12670 document (Natural Stone - Terminology, 2001) defined that natural building stones are natural resource rocks with a wide range of applications in the international market, such as construction, reconstruction and restoration of monuments and buildings. Properties like porosity, water absorption, flexural and compressive strength, and colour are the main characteristics of natural building stones (Siegesmund and Snethlage, 2011; Contrafatto and Cosenza, 2014; Kuprina et al., 2014), and these materials can be used for (Amaral et al., 2015) load bearing and floors (e.g. cladding panels) or for decorative purposes (e.g. sculptures).

The exploitation of ornamental stone is done according with its purposes. Generally, the highest demands are required to produce decorative objects, where is expected a great homogeneity of stone' characteristics, and as a result a very high price can be reached. On the other hand, gravestone sector generally requires a regular structural formation and petrography of the rock (Mosch, 2009). Over time, the methods of exploitation of natural stones have significantly changed. The quarrying techniques have been developed substantially during the industrialisation process, and nowadays drilling and cutting equipment is used in quarries on a daily basis. Thus, today it is possible to exploit very large blocks and further reduce the block size close to the quarry.

Nevertheless, these materials can be differentiated into hard and soft rocks. Generally, soft rocks like sandstones or limestones are materials where mechanical processing is relatively easy, while hard rocks like granite or basalt are more difficult to process.

1.1.1. Types of ornamental stone

Ornamental stones can be differentiated by their genesis conditions. Therefore, three main types of ornamental stone can be distinguished (Amaral et al., 2015) namely igneous, sedimentary and metamorphic. These three types of rock compose the geological rock cycle (Schon, 2015) which are interconnected (Fig. I-1).

The igneous or magmatic rocks (granites for example) are formed in the mantle or at/near the surface, resulting from the cooling and solidification of magma deep in the earth's crust. This type of rocks can be subdivided into plutonic (intrusive) and volcanic (extrusive) and are characterised by their texture, mineralogy and chemical composition (Bell and Pankhurst, 1979; Gill, 2010; Marks et al., 2011). On the other hand, sedimentary rocks are originated from weathering and erosion of original rocks. After transport the new sedimentary rocks are originated through the deposition of small particle or by precipitation of dissolved compounds from water through chemical and biological processes (Siegesmund and Sneathlage, 2011; Schon, 2015). Finally, metamorphic rocks result from previously existing rocks (igneous, sedimentary or even metamorphic) that are subjected to high pressure and/or temperature that occur usually deep within the Earth (Bucher and Grapes, 2011). Metamorphism involves a change in the texture, mineralogy or chemical composition of the rock, that is caused by physical or/and chemical processes (Bucher and Grapes, 2011; Schon, 2015).

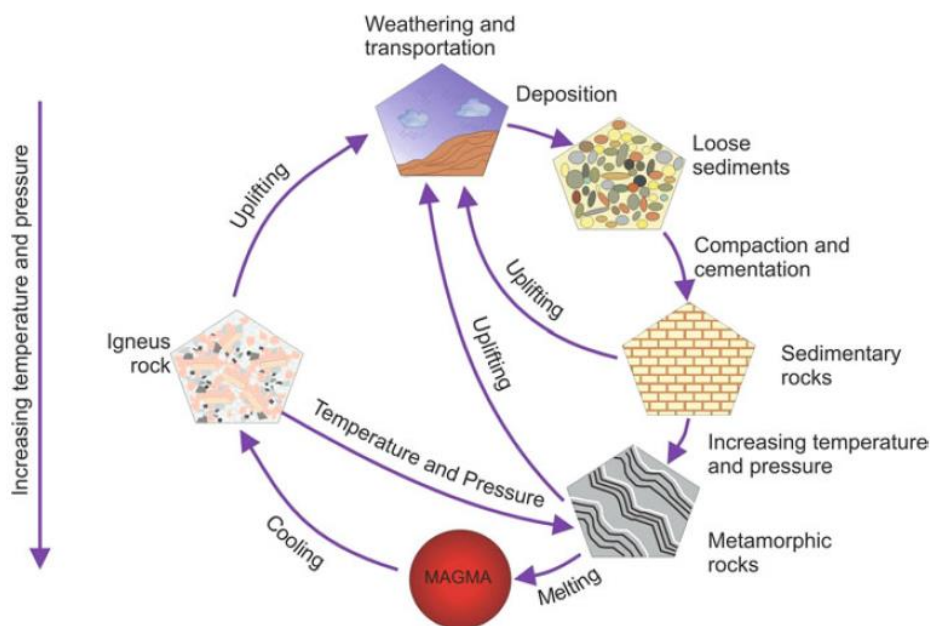


Figure I-1. The geological rock cycle and the relationship between each type of rock (Siegesmund and Sneathlage, 2011).

1.1.2. The international production of natural building stone

The building stone industry is part of an important sector of the natural resource exploitation in several countries. The worldwide main exporters of natural stone are located in the Asian and European continents (Rana et al., 2016). About 92% of the natural stone world export is provided by 10 countries, which five are European (Fig. I-2).

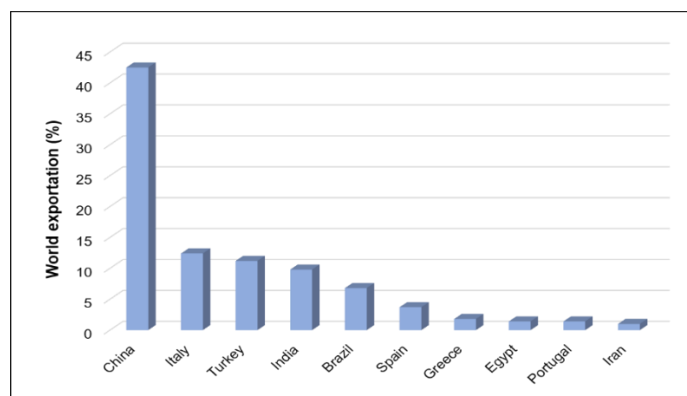


Figure I-2. Leading countries on the world export of natural stones, in 2015. Source: Global Trade Atlas, processing by IMM.

The main exporting countries of stone are able to sell more than 1 Mt/year of material in the international market. On the other hand, the list of importing countries is led by Germany, Italy, China and Spain (Rana et al., 2016). The process of globalisation enabled the availability of thousands of different kinds of natural building stone in the market (Duggal, 1998; Howe, 2001), and these numbers are still rising.

The major European stone producers have direct connection with the Mediterranean Sea and have a long tradition in the use of this building material. 90% of the ornamental stone production in Europe is supported by southern European countries, including Portugal (Lo Vetro and Martini, 2016). Their regional geology and long tradition in the field of natural stone manufacture place these countries in a privileged position. Currently, Portugal is able to sell more than 2,5Mt/year of ornamental stone, which about 1Mt is marble and limestone. However, in the last several years the European contribution for the worldwide natural building stone production has declined. This is mainly related with the enhancement of the stone processing capacities of countries like China, India, Brazil or South Korea, which are also characterised by distinctly lower labour costs (Terezopoulos, 2004; Zhou et al., 2015).

Over the last decades, the construction industry has started to replace some of these natural resources by other materials like concrete, steel, brick, glass or artificial stone. However, the natural building stone materials remain very popular all over the world. This is mostly due to their harmonious appearance, their variability of applications in the architecture (Fig. I-3) and their prestigious character, which is evident in many public buildings and sculptures (Fig. I-4). Even in modern architecture where other materials are dominant, it is the natural stones that will characterise the most emblematic and impressive buildings.

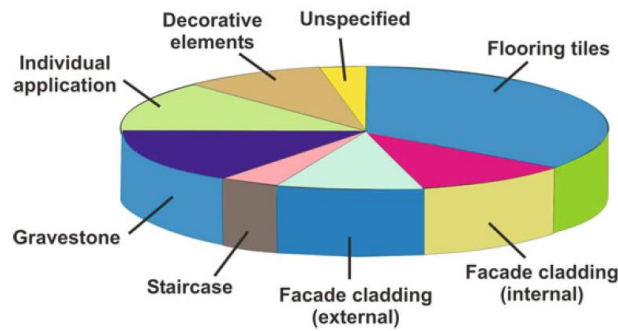


Figure I-3. Applications of stones worldwide and their proportion (Siegesmund and Snethlage, 2011).

Regarding the several lithotypes existing, the calcareous stones are the most widely used, while other types such as siliceous stones exhibit less impact in the worldwide stone industry (Amaral et al., 2015; Careddu et al., 2018).

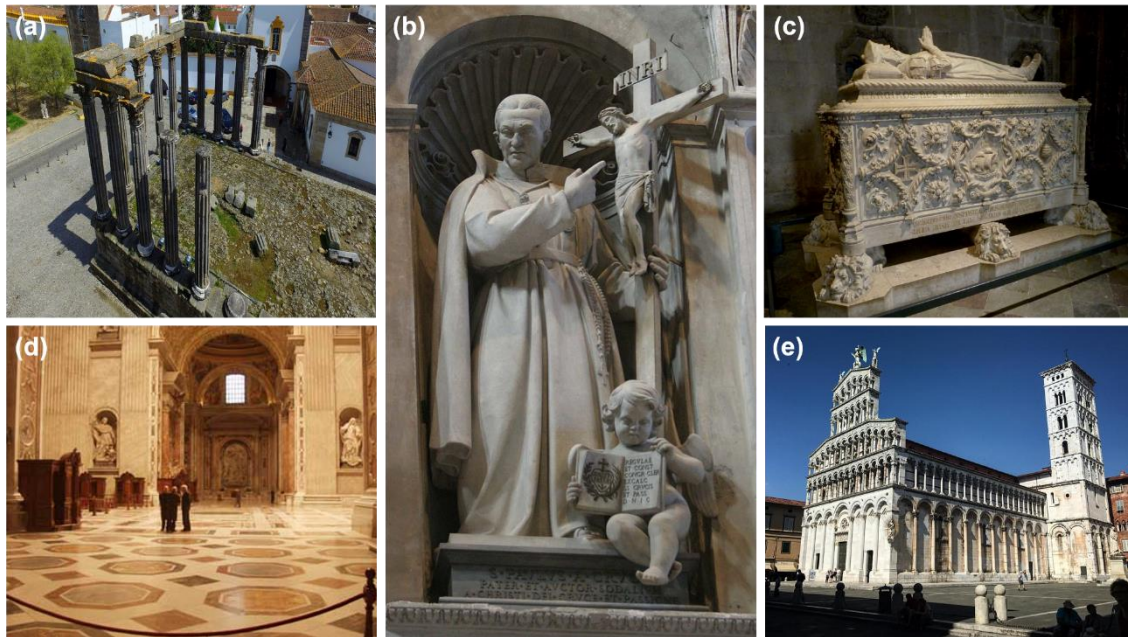


Figure I-4. Examples of several applications of stone: Temple made of limestone and marble, Évora, Portugal (a), marble sculpture, Vatican (b), marble sarcophagus, Lisbon, Portugal (c), limestone interior flooring, Vatican (d), and marble external cladding of a Roman Catholic basilica, Lucca, Italy (e).

1.1.3. Portuguese ornamental stones

Besides its relatively small territory, Portugal has a great geological diversity (Fig. I-5). It is characterised by the presence of igneous, metamorphic and sedimentary rocks from the Neoproterozoic to the Cenozoic (Carvalho et al., 2012a). This diversity makes the country a notable place that offers a wide variety of geological resources, especially natural stone (Carvalho et al., 2012a; Barros et al., 2014; Emídio et al., 2014; Sousa, 2014; Silva and Leal, 2015).

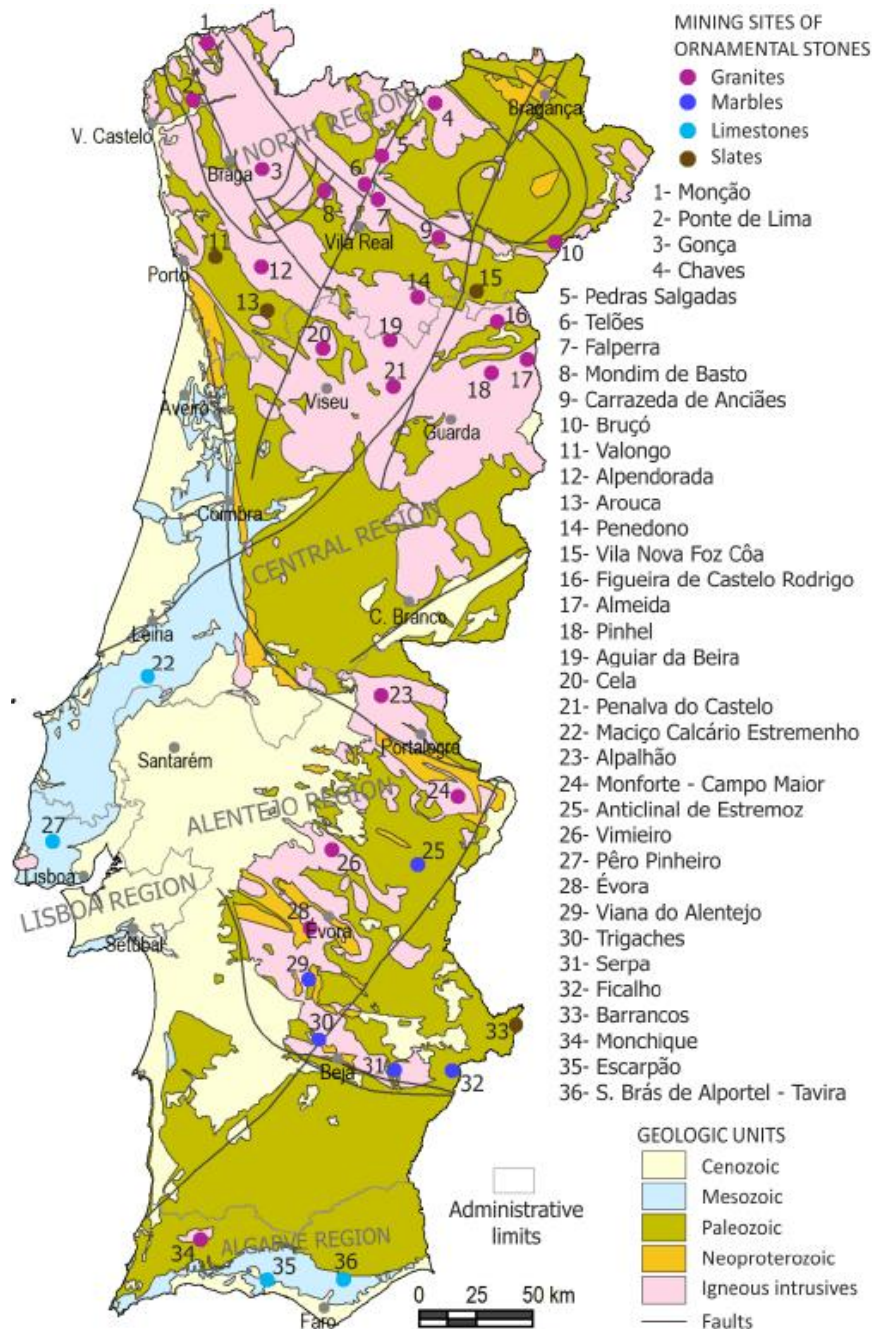


Figure I-5. Main mining sites of Portuguese ornamental stones and their geologic units (Carvalho et al., 2012a).

The continuous use of stone over the centuries allowed the acquisition of knowledge and experience that places Portugal within the main worldwide providers of stone-made work (Leite and da Silva, 2013; Lopes, 2016), including both contemporaneous architectonic productions and the manufacture and restoration of emblematic monuments. Recently, Lopes (2016) described some examples which demonstrate that Portuguese companies working with Portuguese stones are leaving footprints in monuments and buildings of worldwide reference, namely in Europe and Northern America.

1.1.3.1. Limestones

In Portugal, limestones usually occur in coastal areas, namely in the Algarve and Lusitanian basins. The latter is where the main mining site for ornamental limestones is located (Carvalho and Lisboa, 2018) – the Estremenho Limestone Massif (“Maciço Calcário Estremenho” or MCE in Portuguese). This geomorphologic unit fits in the context of the Meso-Cenozoic Lusitanian Basin (Fig. I-6) and possesses a well-known lithostratigraphy that is composed by carbonated rocks tectonically upraised, dated to the Jurassic (Mesozoic) (Azerêdo, 2007; Carvalho et al., 2012b; Amaral et al., 2015).

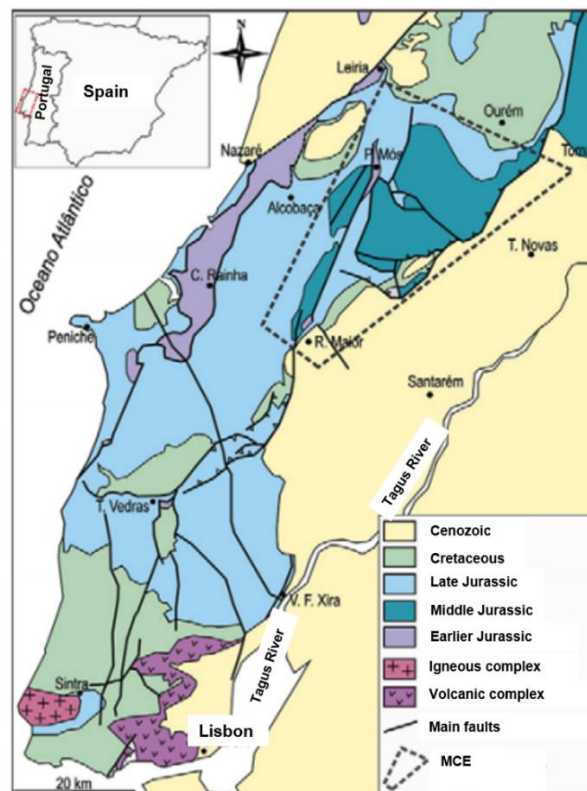


Figure I-6. Location of the Maciço Calcário Estremenho (MCE) in the context of the Meso-Cenozoic Lusitanian Basin (adapted from Carvalho et al., 2012b).

In this region, exploitation is carried out by several dozen quarries where limestones from two main lithostratigraphic units are exploited, the Moleanos and Pé da Pedreira Members, dated from the Middle Jurassic age. Nevertheless, limestones from other lithostratigraphic units, such as the Codaçal Member, and the Serra d’Aire and Montejunto Formations, are also exploited (Carvalho et al., 2012a; Carvalho et al., 2012b; Carvalho and Lisboa, 2018). In this region, the limestones’ exploitation had increased exponentially in the last decades of the last century, so its demand is relatively recent.

However, nowadays these stones are one of the most requested stones in Portugal, mainly by the Chinese market. The stratigraphic orientation and the simple geological structure make the exploitation of these materials very favourable.

Most of limestones from the MCE are characterised by the presence of grains cemented by small amounts of translucent calcite, forming fine to coarse-grained calciclastic sparitic rocks (grainstones and rudstones). Its grains are composed of carbonate particles (intraclasts, oolites or oncolites) and skeletal fossil fragments of marine organisms. In the market, these materials are recognized by their high quality, conferred by their physical and mechanical properties (table I-1). Sintra, Pêro Pinheiro and Negrais are places where Cretaceous limestones are also extensively exploited for ornamental purposes, which the most traditional are Lioz, Amarelo Negrais, Encarnado Negrais, Encarnadão de Lameiras and Abancado (Carvalho et al., 2003).

Table I-1. Main physical-mechanical properties of the most common Portuguese limestones exploited at the MCE (Carvalho et al., 2012a).

Feature	Variation range
Compressive strength [MPa]	44 – 246
Flexural strength under concentrated load [MPa]	4.4 – 23.4
Apparent density [kg/m ³]	2190 – 2710
Open porosity [%]	0.1 – 16.5
Water absorption at atmospheric pressure [%]	0.1 – 8.9
Linear thermal expansion coefficient [$\times 10^{-6}/^{\circ}\text{C}$]	2.7 – 5.1
Rupture energy [J]	2 – 5
Abrasion resistance [mm]	17.5 – 28.0

The exploitation of limestones in the Algarve region (Carvalho et al., 2012a) is done near the villages of Escarpão (Albufeira), Mesquita (S. Brás de Alportel) and Santo Estêvão (Tavira). The mining site of Escarpão is very strict and exploits a blueish grey limestone from the Late Jurassic that is used mainly for aggregates. Here, if some strata exhibit fewer fractures, the stone can be also mined for ornamental purposes. Around ten large exploitation centres are situated in the regions of Mesquita and Santo Estêvão, but

currently their activity is very limited. In these places, the variety of limestone exploited is known as Brecha Algarvia (Carvalho et al., 2013a), also dated from the Later Jurassic. Brecha Algarvia is a bioclastic and partially bio-edified limestone, and their breccia appearance is given by the presence of coarse elements and variations of greyish and reddish colourations (Carvalho et al., 2012a; Carvalho et al., 2013a).

1.1.3.2. Marbles

The major source of Portuguese marble is the famous geological structure known as Estremoz Anticline. The Estremoz Anticline, located in the Alentejo region within the Ossa-Morena Zone (Fig. I-7), is the main production centre of this material, displaying outcrop marbles with ornamental quality for over 27 km² (Lopes, 2003; Brilha et al., 2005; da Fonseca et al., 2013; Lopes and Martins, 2014; Menningen et al., 2018). An anticline is characterised by the tectonic deformation of initially horizontal strata, forming an arch-like shaped fold structure with the oldest rocks at its core. Along with MCE, the Estremoz Anticline shares the leading position in the production of ornamental stones in Portugal (Carvalho et al., 2003; da Fonseca et al., 2013; Carvalho and Lisboa, 2018).



Figure I-7. The geographical location of the Estremoz Anticline, Portugal.

The exploitation of marble here located is done since around 370 BC (Martins and Lopes, 2011; da Fonseca et al., 2013), and it is known that in the Roman Period the mined material had already been used for structural and decorative purposes. A great number of mining sites in the area provide phenomenal geological windows (Fig. I-8) that in some places can reach about 150 m in depth (Brilha et al., 2005; Carvalho et al., 2012a).

Because of this historical and geological relevance, they are considered part of the Portuguese geological heritage (Brilha et al., 2005; Carvalho et al., 2012a).

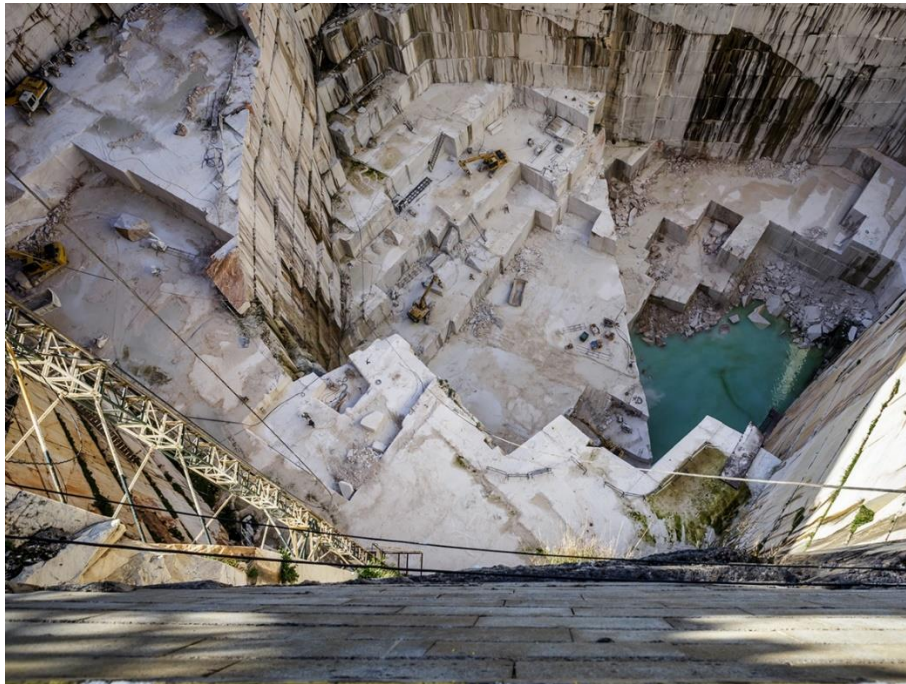


Figure I-8. Quarry located in the Estremoz Anticline. ©Nelson Cristo

Despite the effects of the different Variscan Orogeny deformation phases (Lopes, 2003; Carvalho et al., 2008) that strongly affect its exploitability, the importance of the production centre of the Estremoz Anticline is revealed by the existence of about 150 quarries (Carvalho et al., 2012a). These quarries are distributed in 5 regions: Borba, Estremoz, Lagoa, Pardais, and Vigária. Lagoa, Pardais, and Vigária are in the municipality of Vila Viçosa.

These marbles are characterised by fine to medium-grained texture and exhibit excellent mechanical and physical properties (Table I-2) and also unique aesthetic features. They exhibit a wide range of colours, from white to cream, pink, grey or black (Moura, 2007). The most valuable are the pure white and the pinkish varieties, whose large volumes can be exploited, thus placing Portugal at the forefront of the world marble production.

Other regions such as Trigaches, Viana do Alentejo, Vila Verde de Ficalho and Serpa have small mining sites, where the potential of marble production is smaller when compared with those situated in the Estremoz Anticline. This is due to the higher degree of fracturation of the marble in these places (Carvalho et al., 2012a). The marble from

Viana do Alentejo present a medium to coarse-grained texture and it is characterised by its green colour with typical dark green to brownish stripes. The marble from Trigaches present a very coarse-grained texture and have a grey colouration. Regardless of their importance, some of these mining sites are already out of service.

Table I-2. Main physical and mechanical properties of the most common Portuguese ornamental marbles exploited at the Estremoz Anticline (Carvalho et al., 2012a).

Feature	Variation range
Compressive strength [MPa]	52 – 141
Flexural strength under concentrated load [MPa]	4.9 – 19.3
Apparent density [kg/m ³]	2710 – 2790
Open porosity [%]	0.2 – 0.5
Water absorption at atmospheric pressure [%]	0.0 – 0.2
Linear thermal expansion coefficient [$\times 10^{-6}/^{\circ}\text{C}$]	4.1 – 14.0
Rupture energy [J]	5 – 11
Abrasion resistance [mm]	15.5 – 26.5

1.2. Weathering and deterioration of natural stone

Despite being considered one of the most resistant materials used in construction, stone, like any other building material, is also susceptible to deterioration processes (Franzoni et al., 2013; Sassoni and Franzoni, 2014; Rodrigues, 2015). There are several types of deterioration that can affect building stone, either mechanical, chemical or biochemical. In monuments and buildings, these processes are initiated and handled through the interaction between stone and exogenic factors like environmental conditions, pollution or organisms' proliferation (Fitzner, 2004; Cutler and Viles, 2010; Graue et al., 2013; Sassoni and Franzoni, 2014; Siedel and Siegmund, 2014; Rodrigues, 2015).

1.2.1. Deterioration induced by mechanical processes

In general, the mechanical damage in stone is the result of a strength that is above its mechanical resistance. Defective soil settlement, poor design of the buildings or catastrophic events are considered the main factors responsible for the strongest damages observed in buildings (Parisi and Augenti, 2013; Ozguven and Ozcelik, 2014; Saloustros et al., 2015). Other factors like growth of vegetation may result in the breaking of stone masonry, frequently seen in archaeological sites.

Stone is not a good thermal conductor, which makes fire also a factor capable of inducing stress on it. In this case, the surface of the stone will expand causing a literal shattering, phenomenon also known as conchoidal fracture (Fig. I-9). The heat may also result in a change of the mineralogical composition that will increase the susceptibility of the material to deterioration (Dionísio et al., 2009; McCabe et al., 2010; Mendes et al., 2012; Ozguven and Ozcelik, 2013; Kompaníková et al., 2014; Ozguven and Ozcelik, 2014; Martinho et al., 2017; Martinho and Dionísio, 2018).



Figure I-9. Examples of effects promoted by historic fires in stone-built structures. Granite pillars, Brazil (a), marble columns, Greece (b), church wall constructed with argillaceous sandstone, Argentina (c) (Siegesmund and Snethlage, 2011).

Despite this, fire can also be used to finish stone, a process known as “flame-finish” that became popular in the 70’s because of its rustic appearance. This process may induce the formation of considerable fissures in the stone, increasing its capacity to absorb moisture (Grissom et al., 2000).

Vibrations can also induce mechanical stress in the stone that may be caused by traffic (e.g. airplanes and trains), machinery work, etc. These vibrations will induce alternating tensile and compressive forces in the building structures, and the effects will be higher for already cracked stones. Generally, vibration does not cause damage directly but certainly may increase the overall deterioration rate.

Other factors must be considered for mechanical damage in stone, such as:

a) **thermal cycling** (Yavuz et al., 2010; Smith et al., 2011; Shushakova et al., 2013; Andriani and Germinario, 2014; Ghobadi and Babazadeh, 2015), an abrupt modification of the stones' temperature may result in its volume expansion/contraction when the temperature increases/decreases. This effect occurs commonly in calcite, dolomite, quartz, albite, gypsum, micas and clays, for example. Even without a wide variation in temperature, the repeated cycle of heating and cooling will eventually lead the deterioration of the stone over time. Regarding the common minerals that may compose stones, calcite is the only mineral that expands in one direction and contracts in the other (Winkler, 1994). Thus, limestones and marbles are the most susceptible to thermal cycling (Fig. I-10). This factor can lead to “sugaring”, a granular decohesion of the matrix, or to “bowing”, a deformation of stone slabs that is being studied more intensely due to the increasing use of stone for cladding (Siegesmund et al., 2008a; Siegesmund et al., 2008b; Menningen et al., 2018). Additionally, it is known that the presence of moisture enhances the deterioration effects caused by thermal cycling (Koch and Siegesmund, 2004);

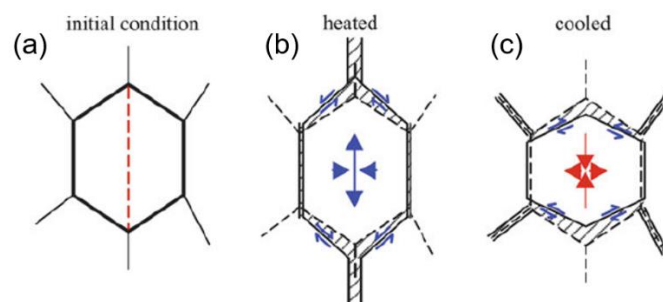


Figure I-10. Effects of thermal cycling for a calcite mineral. Calcite crystal composing the marble matrix (a), contraction and expansion upon heating (b) and cooling (c) (adapted from Siegesmund et al., 2004).

b) **Hygric and hydric swelling** (Espinosa-Marzal et al., 2011; Berthonneau et al., 2012; Charola and Wendler, 2015; Berthonneau et al., 2016), a change in the air relative

humidity, that affects more extensively the stones containing clays in its composition like sandstones and limestones, since their structure makes them particularly susceptible to retain moisture and to expand-contract processes. This phenomenon induces characteristic decay patterns like delamination parallel to the bedding layer and spalling (Rodríguez-Navarro et al., 1997; Sebastián et al., 2008). Different clay minerals have distinct capacities to adsorb water, and in some cases the crystalline swelling phenomenon can double its volume (Siegesmund and Snethlage, 2011). For the materials without clays or phyllosilicates in their composition, the hygric expansion results from the disjoining pressure. Nevertheless, it seems that thermal cycling can induce much stronger swelling than changes in relative humidity (Siegesmund and Snethlage, 2011);

c) **Crystal phase development** (Gentilini et al., 2012; Vásquez et al., 2013; Serafeimidis and Anagnostou, 2014; Benavente et al., 2015), a formation and confined growth of new phases within empty spaces of building stones, that generates a pressure called “crystallisation pressure”. This could be considered the major mechanical damage mechanism in stones, having been first documented more than a century ago. Tensile stress within the solid matrix of the stone may be induced if these pressures are achieved in the pores of the stone and exceed the stone’s strength. Typical examples of this type of damage are the crystallisation of ice which may result from freeze-thaw cycles (Ruedrich et al., 2011; Freire-Lista et al., 2015; Martins et al., 2015) or the crystallisation of salts like sodium chloride (Desarnaud et al., 2016), calcium sulphates (Marszalek, 2016), etc.

For many authors, the action of salts is considered the major threat that can cause deterioration of stone (Doehne, 2002; Rothert et al., 2007; Doehne and Price, 2010; Kramar et al., 2011; Ghobadi and Babazadeh, 2015), which can be reflected under deterioration patterns (Fig. I-11) like delamination, blistering, disintegration, scaling, alveolarisation and efflorescences. The alteration patterns will depend on the type of material and the conditions of the salt crystallisation, such as the amount of available water.

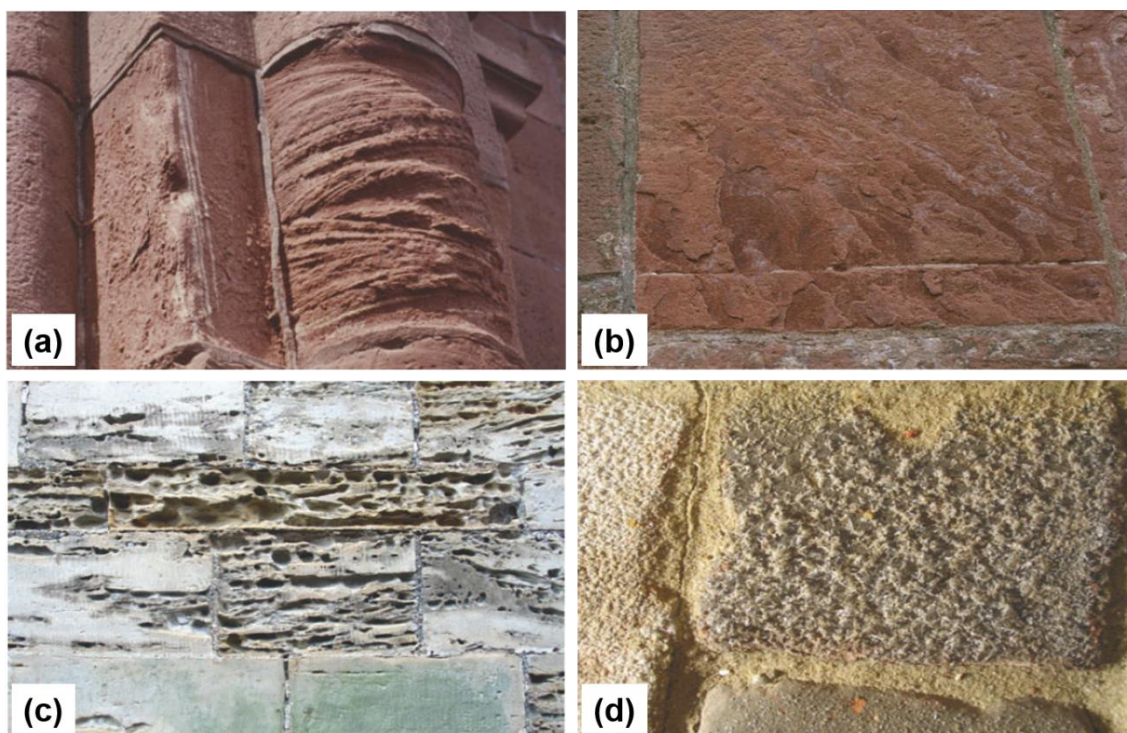


Figure I-11. Examples of effects of salt deterioration in buildings made of stone. Initial flaking (left block) and sanding following the bedding plane (right block) (a), scaling (b), alveolarisation (c) and salt efflorescence (d) (adapted from Siegesmund and Snethlage, 2011).

The most important sources of salt enrichment in building materials are the deposition of salts from the atmosphere, namely sulphates and nitrates, anthropogenic air pollutants, sea spray from the marine environment, ground moisture and the use of alkaline materials (e.g. Portland cement, cleaning products or consolidation materials) (Vignati et al., 2010; Kloppmann et al., 2011; D'Agostino, 2013; Li et al., 2014). Sea salt particles, for some authors are considered the major cause of decay of monuments located in coastal sites (Zezza et al. 1995). This source can contribute with several ions, such as sodium, potassium, magnesium, chloride, calcium, and sulphate, where sodium and chloride are the major components, composing around 90 % of the sea salt spray (Kolev et al., 2013). On the other hand, ground moisture can contribute with potassium, sodium, magnesium, chloride, calcium, bicarbonate, sulphate and nitrate. When saturated groundwater is in hydraulic contact with stone, these ions are transported into the structure through capillary rise (Hall and Hoff, 2007; Karagiannis et al., 2016). After the water's evaporation, efflorescence or subflorescence can be formed on the surface of the stone (Fig I-12) or within the pores of the stone, respectively.

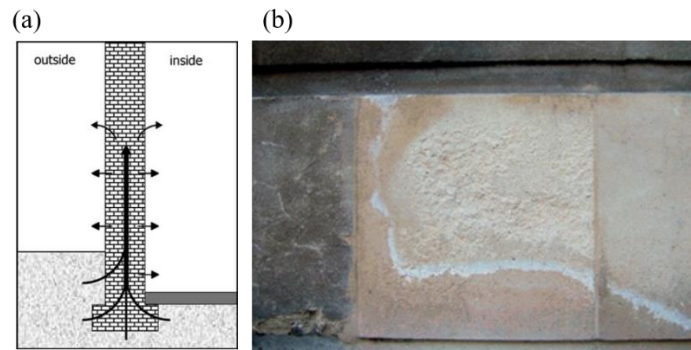


Figure I-12. Ground moisture transported by rising capillarity (a) and its practical effect in buildings (b) (adapted from Siegesmund and Sneathlaga, 2011).

A wide number of salts can be formed in building stone, according to three different phase transitions (Fig I-13). These phase transitions are interconnected and are mostly dependent of their solubility in water, the porosity of the material, the relative humidity and temperature.

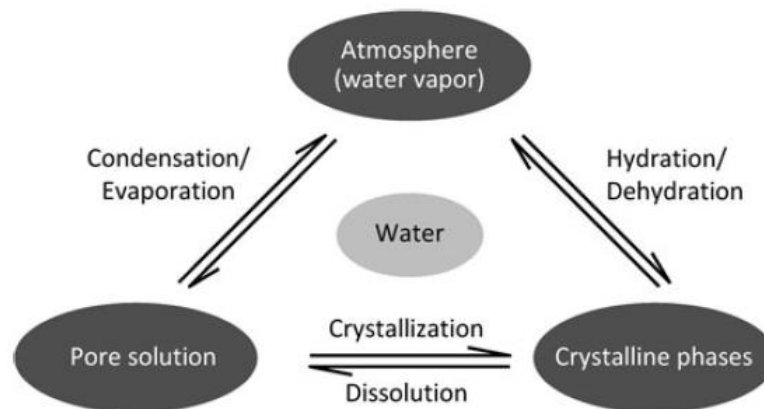


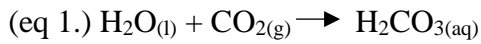
Figure I-13. Different phase transitions of salts in building materials (adapted from Steiger, 2005).

In nature, the processes described above do not act alone, and the pathologies observed in a damaged stone are most probably a result of their interaction, which can occur simultaneously or sequentially.

1.2.2. Deterioration induced by chemical processes

Since many minerals present in building stones are thermodynamically unstable under the earth's atmosphere (White and Buss, 2014; Earle, 2015), they may be subjected to chemical deterioration. The characteristics of the changes are highly conditioned by the

mineral and the environmental conditions. Generally, chemical weathering is greatest in warm and wet climates, and less significant in cold and dry climates. The most important components that contribute to chemical weathering are water (from the atmosphere or ground-water), oxygen and carbon dioxide (Earle, 2015). When combined with water, carbon dioxide produces weak carbonic acid (eq. 1) which after dissociation forms hydrogen and carbonate ions (eq. 2):

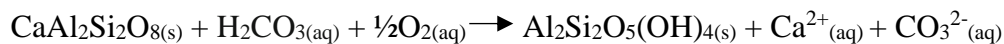


which is fundamental for the most chemical weathering processes.

1.2.2.1. Hydrolysis

The hydrolysis process in stone occur when the minerals, especially silicate minerals (Earle, 2015), react with weakly acidic waters changing its chemical composition. Most natural waters at the surface are slightly acidic due to the carbon dioxide from the air or ground water, originating carbonic acid (Millero, 2009; Sánchez-España et al., 2014).

As an example, the hydrolysis reaction of calcium plagioclase, a common feldspar found in igneous rock, contacting acidic waters will originate kaolinite, dissolved calcium and carbonate ions, according with the following reaction:

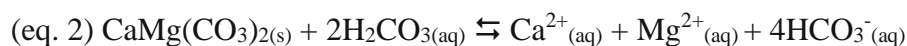
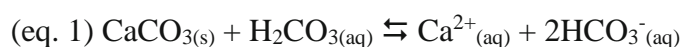


where similar reactions could also be applied for sodium or potassium feldspars.

Another examples of hydrolysis of silicate minerals is the transformation of pyroxene to clay minerals like chlorite or smectite, and conversion of olivine to the clay mineral serpentine.

1.2.2.2. Dissolution

Generally, the dissolution of the minerals composing building stones is related with the CO₂ amount and atmosphere pollutants. One of the most relevant reactions that lead stone deterioration is the dissolution of carbonate minerals, namely calcite (eq. 1) and dolomite (eq. 2), associated with acid water:



where irreversible damages can be induced in the stones, mainly for those with calcite and dolomite as the major minerals (Fig. I-14).

It is known that rainwater is the main source of liquid water in building stones (Rosso et al., 2016). Here, damages caused by dissolution may promote the appearance of distinct patterns that follow the exposure to direct rainfall, its flow and surface runoff (Vazquez et al., 2016). Although most of the minerals that compose rocks present a very low solubility in water, the exposure and infiltration of water over centuries are sufficiently long to impute significant damages in historic buildings.



Figure I-14. Dissolution effect in marble, built in 1832. The carved details gradually become rounded (adapted from Abulude et al., 2018).

Since the presence of H_2CO_3 enhances the solubility of carbonate materials, natural dissolution of carbonate materials occurs, known as karst effect (Cardell-Fernández et al., 2002). However, “acid deposition” either by acid precipitation or dry deposition of particulates and gaseous pollutants like SO_2 , NO , and NO_2 , is the major source of H_2CO_3 in building materials, which increases significantly the natural rates of mineral dissolution. In the recent years, it is known that the pH of rainwater is continuous decreasing, at least in North America, Europe and Asia (Yanxia and Qing, 2009; Gaddamwar, 2011; Sudalma et al., 2015, Earle, 2015), where pH values can reach 4. In acidic fogs even lower pH values can be registered, around 2 (Siegesmund and Sneathlge, 2011).

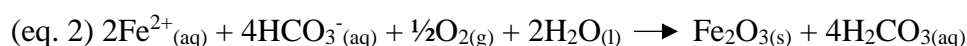
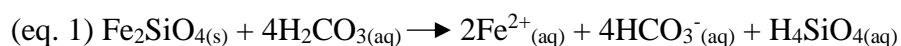
After dissolution reactions, the major compounds that may be formed in carbonated stones like limestone and marble are calcium sulphate in the form of gypsum ($\text{CaSO}_4 \cdot 2\text{H}_2\text{O}$), and calcium oxalate patinas (Charola et al., 2007; Corvo et al., 2010), like whewellite ($\text{CaC}_2\text{O}_4 \cdot \text{H}_2\text{O}$) and weddellite ($\text{CaC}_2\text{O}_4 \cdot 2\text{H}_2\text{O}$). The genesis of these compounds may induce the formation of white or black crusts. The black colouration in

gypsum crusts is related with the embedding of pollutant particles that can be originated from several different sources (Schiavon, 1991; Mérillou et al., 2010; Sánchez et al., 2011).

1.2.2.3. Oxidation

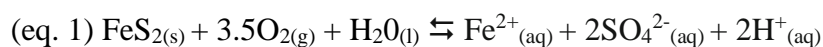
The phenomenon of oxidation in stone occurs commonly in those minerals containing iron (II), such as clays, sulphides and carbonates (Nordstrom, 2011). Since these minerals contact the Earth's surface, they can react with oxygen in air, and consequently rusts. These reactions begin (Grafe et al., 2000) with the electrons transfer from iron (reducing agent) to oxygen (oxidising agent). With higher incidence in humid to semi humid climates, these reactions may be followed by hydration of the compounds released, making them more susceptible to physical weathering.

As an example of mineral oxidation, olivine (Fe_2SiO_4) is converted into hematite (Fe_2O_3) due to the oxidation of the iron (eq. 2) after its dissolution (eq. 1), where silicic acid is released (Earle, 2015):



where the same mechanism can be applied to almost any other ferromagnesian silicate (e.g. biotite, pyroxene, amphibole).

Another example is the oxidation of the iron in iron sulphides. Here the mineral (e.g. pyrite) may react with water and oxygen to form sulphuric acid (eq. 1) and then sulphates compounds will be formed. If salts are present in these mechanisms, the iron tends to rust more quickly, as a result of electrochemical reactions.



Some authors refer that the stability of the iron minerals as well as the minerals containing iron have a significant importance for the colour of the stone (Winkler, 1997), since the colour of iron oxides may range from yellow to brown hues.

1.3. Biodeterioration of stone

Hueck (1965) defined biodeterioration as “any undesirable change in the properties of a material caused by the vital activities of organisms”. Microorganisms are capable of growing all over the world. Despite being a poor nutrient material, stone provides

sufficient conditions for microbiota development (Fig. I-15a). Here, the microorganisms can be considered epilithic if they develop on the stone surface, or endolithic if they develop within the stone (McNamara et al., 2006; Cutler and Viles, 2010). Microorganisms may play a considerable role in the formation of rocks process, namely in the precipitation of carbonate sediments in seawater through CO₂ uptake by bacteria and algae, for example. However, they also play a major role in the deterioration of rocks, a process called biodeterioration (Fig. I-15b). Some authors even consider that the weathering of stone in the presence of living organisms is some ten thousand times faster than without the biogenic agents' presence (Gu et al., 2011; Siegesmund and Snelthage, 2011; Gaylarde et al., 2012).

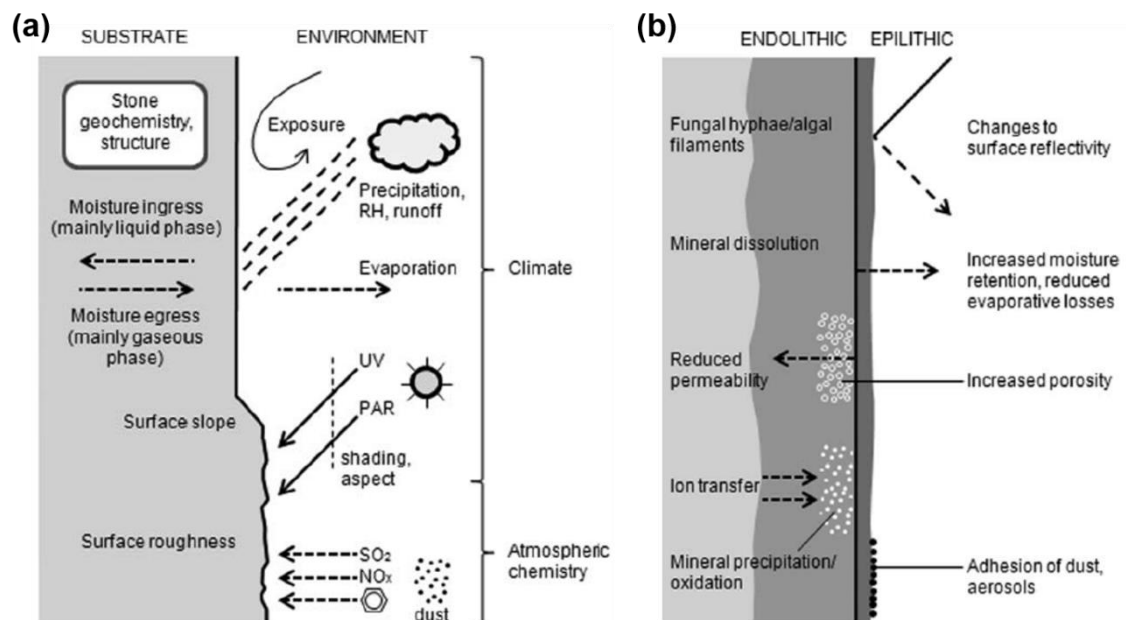


Figure I-15. Environmental and substrate factors influencing the development of microbial communities in a building stone (a) and the main ways (b) in which microorganisms may affect stone (adapted from Cutler and Viles, 2010).

Guillite (1995) defined bioreceptivity as “the ability of a material to be colonised by living organisms”. Considering that the most important factor for colonisation is the availability of water, porous stones that can retain high amounts of water have an higher bioreceptivity. It is known that bacteria communities generally need higher amounts of water than fungi, since fungi communities tolerate periods of complete dryness in a dormant state (Liu et al., 2006; Feofilova et al., 2012; Sterflinger et al., 2012). However,

bacteria tolerate salty environments on and inside the stone (Rivadeneira et al., 2004; Jafari et al., 2012).

As shown in figure I-16a, stones are good substrates for the interaction among several types of microorganisms, demonstrated by the complex composition of communities found in highly altered surfaces. This susceptibility, also known as bioreceptivity, will increase according to the physical and chemical properties of the stone, like water availability and circulation, surface roughness and mineralogical composition (Miller et al., 2009; Jim and Chen, 2011; Miller et al., 2012; Vázquez-Nion et al., 2018).

1.3.1. Organisms involved in biodeterioration of stone

1.3.1.1. Bacteria

Bacteria are mostly single-cell organisms and, although they cannot be seen by the naked eye, they are capable of contributing to visible deterioration phenomena, such as sanding, etching and discolouration of stone (Warscheid and Braams, 2000; Scheerer et al., 2009). Different types of bacteria can intervene in the mechanisms of biodeterioration, such as chemoheterotrophic, chemolithotrophic, phototrophic, micro-algae, halophilic and archaea (Tomaselli et al., 2000; de Felice et al., 2010; Dakal and Cameotra, 2012; Kusumi et al., 2013; Li et al., 2016; Mihajlovski et al., 2017).

Chemoheterotrophic bacteria need organic carbon to develop. In stone, organic carbon may be provided by airborne organic contamination, animal stools, dripping water, and organic compounds present in the original substrate or by metabolites of autotrophic bacteria. As their action produces organic pigments and organic acids, they are considered as important deteriogenic agents in the chromatic alteration and biogenic corrosion of stone (Banciu, 2013; Piñar et al., 2014a). On the other hand, the growth of chemolithotrophic bacteria is not dependent on the presence of organic carbon sources. These microorganisms are capable of developing through the oxidation of minerals containing sulphur, iron, ammonia or manganese present in the stones' composition. Usually, the iron and manganese oxidation by bacteria result in the formation of a blackish stain that may cover the stone surface. In the ammonia oxidation, both nitrite and nitrate ions are released, which can lead the formation of nitrous and nitric acids promoting a further corrosion of the stone through dissolution. The same mechanism takes place with the sulphur oxidation, whose action will lead the formation of sulphuric and sulphurous

acids (Siegesmund and Snethlage, 2011; Hedrich and Johnson, 2013; Pokorna and Zabranska, 2015).

If enough light and water are available in a stone, phototrophic bacteria can develop on it, since they are able to grow through sunlight absorption, using the well-known process called photosynthesis, where CO₂ is also needed. Some strains need sulphur to develop in addition to sunlight, water, and CO₂, performing an “anoxic” photosynthesis, since they do not produce oxygen. The most common groups of phototrophic bacteria are algae and cyanobacteria (formerly known as blue-green algae), since they are capable of colonising stone in all climate regions of the earth (Crispim and Gaylarde, 2004; Hallmann et al., 2013; Keshari and Adhikary, 2013; Gaylarde et al., 2017). Despite the fact algae are primarily aquatic organisms, they have managed to well adapt to terrestrial conditions, and nowadays are considered to be cosmopolitan organisms as they colonise all types of environments. Some authors stated their capacities to tolerate temperature changes in the range from 0 to 85°C (Vojtková, 2017). Chlorophyll production by algae and cyanobacteria will induce the formation of green layers on the stones’ surface, but these organisms may also produce other compounds for photoprotection like carotenoids and scytonemin pigments. The production of these compounds may induce orange or brown colouration on the stone (Aires-Barros et al., 2001; Domonkos et al., 2013; Leverenz et al., 2015; Toth et al., 2015; Zavrel et al., 2015; Kirilovsky and Kerfeld, 2016). It has been also established that algae and cyanobacteria produce organic acids that disturb the building substrate and thus enable the development of other microorganisms responsible for biodegradation like bacteria and fungi (Vojtková, 2017). Cyanobacteria and algae are characterised by the high resistance to UV-radiation and desiccation, and on stone often develop in close association with lichens (Siegesmund and Snethlage, 2011; Honegger et al., 2013; Rikkinen, 2013). In addition, algae may also precipitate in the formation of a crust as they produce the so-called extracellular polymer substances, which have been identified on the surfaces of a range of urban structures (El-Sheekh et al., 2012).

Halophilic and archaea bacteria are characterised by their tolerance to very high temperature values and extreme salt stress levels. The salt crusts, as well as salt efflorescence, provide a proper environment for halophilic and halotolerant bacteria and archaea development. Their action may induce the formation of pink or purple pigments (Banciu, 2013; Ettenauer et al., 2014; Piñar et al., 2014b; Zanardini et al., 2016), leading to typical pinkish stain (Rosado et al., 2014a) on stone surfaces (Fig. I-16). *Halobacillus*,

Bacteroidetes, *Rubrobacter* and *Salinisphaera* are common moderately halophilic bacteria, while *Halococcus* and *Halobacterium* are the most important genera of archaea.



Figure I-16. Rosy stain on the salt damaged stone surface of a Medieval monument, Austria, promoted by halophilic bacteria and archaea (Siegesmund and Snethlage, 2011).

1.3.1.2. Fungi

Fungi are multicellular organisms, capable of forming hyphae (cell filaments) on and in stones. The development of these filaments enables fungi to spread over the stones' surface and penetrate its pores. Fungi have high erosive effect in stone since they are capable of penetrate stone over 1 cm in depth. For this reason, for many authors fungi are considered the most important endoliths in building stone (Scheerer et al., 2009; Gaylarde et al., 2012; Hallmann et al., 2014; Municchia et al., 2014; Salvadori and Municchia, 2016; Gleason et al., 2017). Additionally, more than 60 species have been identified and reported in building stone substrates around the world, including limestone and marble (Cutler and Viles, 2010; Cutler et al., 2013; Onofri et al., 2014; Gutarowska et al., 2015).

On stone, hyphomycetes strains (*Cladosporium*, *Alternaria*, *Epicoccum*, *Phoma* and *Aureobasidium*) are dominant in moderate or humid climates (Isola et al., 2013; Sterflinger and Piñar, 2013; Gehlot and Singh, 2018) which have the capacity to form mycelia in the porous space. In semi-arid and arid environments, the fungal communities are mainly composed by the so-called black yeasts (*Sarcinomyces*, *Hortaea*, *Trimmatostroma*, *Exophiala*, *Coniosporium*, *Knufia* and *Capnobotryella*) which commonly develop in association with lichens (Marvasi et al., 2012; Sterflinger and Piñar, 2013; Martino, 2016; Gehlot and Singh, 2018). Fungi as well as green algae communities have been associated with biofouling and bioweathering, but also with

patination, dark staining and black crusts, promoting discolouration of stone surfaces (Cutler and Viles, 2010; Schiavon et al., 2013; Sazanova et al., 2014; Karaca et al., 2015; Ortega-Morales et al., 2016; Gadd, 2017; Kirtzel et al., 2017). Moreover, biopitting – a deterioration phenomenon promoted by both chemical and mechanical ways – can be caused by fungi communities. The pits diameter and depth can achieve up to 2 cm, predominantly in calcareous stone like marble and limestone (Sterflinger and Piñar, 2013; Mohammadi and Maghbol-Balasjin, 2014; Martino, 2016).

The fungi communities develop thick walls, making them particularly resistant against heat (up to 80°C) and mechanical or chemical attacks such as biocides and other antimicrobial treatments (Silva, 2017).

1.3.1.3. Lichens

Lichen is an organism that is formed from the symbiosis of algae and cyanobacteria living among filaments of several fungi species. This synergism enables the lichen to live in a nutrient-poor environment and in stone surfaces inserted in arid habitats. Several kinds of lichens can be formed on rocks and stone, but crustose lichens are the most predominant ones (Fig. I-17). Moreover, these organisms are considered the most common colonisers of calcareous stone all over the world (Gaylarde and Gaylarde, 2005, de la Rosa et al., 2013; de la Rosa et al., 2014; Salvadori and Municchia, 2016; Sohrabi et al., 2017), and are especially dangerous for the integrity of stone since they develop a structure called thallus that penetrates inside the cracks and fissures. The lichens growth may create a pattern of pitting (de la Rosa et al., 2012), and the surface covering may also create a landscape effect coloured with several shades.



Figure I-17. Crustose lichens developing on calcareous stone.

1.3.2. Biodeterioration effects

1.3.2.1. Surface alteration

All the organisms mentioned before produce a wide variety of organic pigments that may have different biochemical functions. However, these pigments can induce changes on the surface of the stone, like colour alteration through the formation of biopatinas. Siegesmund and Snethlage (2011) described some examples:

a) Chlorophyll, released by cyanobacteria and algae, appears in different shades of green, and nearly black when the microbial layers become dry and cells are in a dormant state;

b) Carotenoids, released to support the photosynthesis process or as a UV-radiation absorber, are produced by photosynthetic organisms and may display a wide variety of colourations such as brown, red, orange, yellow and purple;

c) Melanin, released for protection against UV-radiation, desiccation or radioactivity, is produced by many fungi strains, particularly by black fungi, and may be coloured of dark brown and black.

Some of the organic pigments are excreted by the metabolically active organisms, while others are only released after cell death. It is known that organic pigments incorporated in calcareous rocks like limestone and marble, originate a biogenic stain (Saiz-Jimenez et al., 2012, Martin-Sanchez et al., 2013) that can remain visible for many decades.

Biofilm formation may induce changes in the stones' surface appearance. Biofilms are defined to be a layer of microorganisms whose thickness can range from several microns up to 5 mm or more. The formation of biofilms will favour the retention of dirt particles, pollen, dust and fly ash, which will feed the communities and further increase the biofilm development. This retention may result in an increasingly dirty appearance with the inherent aesthetical alteration (Cutler and Viles, 2010; McCabe et al., 2015).

1.3.2.2. Chemical and mechanical alterations

As mentioned above, microorganisms thriving on stone materials can penetrate them over several millimetres or even centimetres in depth. This capacity may influence considerably the chemical and physical properties of the stone and accelerates the deterioration process. It is known that lichens release organic acids or complexing agents capable of leaching out Na, Mg, Ca, K, Fe and other elements of the matrix of the stone.

However, some authors defend that intact lichen crusts might protect the stone from weathering agents like wind, rain, and sunlight, and their elimination will turn the surface of the stone rougher and therefore more susceptible to weathering (Warscheid and Braams, 2000; Llop et al., 2013; Pinna, 2014).

Among the most important damage effects on stones caused by lichens and fungi is the micropitting – a formation of shallow cavities on the stone. This phenomenon is a consequence of a chemical dissolution achieved through the liberation of oxalic acid by these microorganisms, which further reacts with the calcareous stone and originate calcium oxalate crystals (Monte, 2003). Thus, crusts of calcium oxalates may have biogenic origin, and predominantly occur on the calcareous stone, namely limestone and marble (Rosado et al., 2013a; Gadd et al., 2014; Sturm et al., 2015; Unkovic et al., 2017).

Due to their metabolic activity, fungi, cyanobacteria and heterotrophic bacteria produce several organic acids (oxalic, gluconic, succinic, malic, fumaric, acetic and citric). The production of these acids is significantly influenced by the available nutrients and minor elements such as Fe, Mg or Mn (Siegesmund and Snethlage, 2011). Therefore, an increment of environmental pollution will increase acid production and thus enhance stone decay through the dissolution of carbonates and other minerals. According to their composition, the acid attack may result in several damages for the stone, namely sugaring of marble (Fig. I-18) or sanding of limestone and sandstone.



Figure I-18. Sugaring marble in the Monumental Cemetery of Bologna, Italy (adapted from Sassoni and Franzoni, 2014b).

On the other hand, chemolithotrophic bacteria produce inorganic acids like nitric, nitrous, sulphuric and sulphurous, through the oxidation of ammonium or reduced sulphur compounds (Gottschalk, 2012), which are considerably high corrosive for several materials, including natural stones. The metabolic activity of bacteria and fungi thriving in the stone porous will result in an increase of the concentration of CO₂ (Uroz et al., 2009) which, in the presence of water, carbonic acid might be formed. Even being considered a weak acid, the carbonic acid can contribute for the dissolution of calcite in limestone, marble and other stones.

Nevertheless, there are some bacteria that has the ability to precipitate calcium carbonate in the form of calcite, a process called biomineralisation, which commonly occur in building stone. Moreover, some studies have emerged in order to improve the durability of stone through biomineralisation (Dhami et al., 2013; Andrei et al., 2017; Li et al., 2018a).

In summary, deterioration and biodeterioration is the result of several interacting factors that cannot be clearly distinguished, from physical and chemical weathering, which both are part of stone decay. Therefore, weathering processes must always be regarded as a result of combined elements acting together.

1.4. The colour in natural stone

Used since ancient times for architectural purposes, stone has generally been chosen considering aesthetic aspects such as colour and its symbolism (Jones, 1999). Nowadays, colour of building stones is still one of the most important characteristics that define their aesthetic characteristics (Fig. I-19), and one of the main macroscopic characteristics that leads to their appreciation and application as a building material. In conjunction with the mechanical properties of the stone, colour is considered very important for its marketability, since it is based on its appearance (Selonen et al., 2000; Benavente et al., 2002).



Figure I-19. Examples of natural stone applications: the floor of the area next to “Padrão dos Descobrimentos” in Lisbon, Portugal (a) and interior floor of the Milano “Duomo”, Italy (b) (adapted from Amaral et al., 2015).

Small variations in the stone and colour are tolerated, but uniformity in the production-scale is highly required. According to Selonen et al. (2000), ornamental stones can be classified as one-coloured or multicoloured. The colour of one-coloured stones is homogeneous along the entire exploitation site, but flaws can appear in the form of inclusions, clusters or stripes of minerals. On the other hand, the multicoloured stones have higher variations, which is often the case for gneisses or gneissose granites. Generally, strong and unusual colours seem to be desirable in the global building stone market, but national preferences also exist, often related with the culture and the religion of a particular country.

1.4.1. The colour in carbonated natural stones

Carbonated rocks, like marble and limestone, are essentially composed by calcite, which is one of the most abundant minerals in the surface of the Earth. In the pure state, the mineral is colourless or white, but owing to the presence of several impurities can be of almost any colour, such as red, yellow, blue, green, pink, lavender, brown or black ^[1, 2]. Considering this, the colour of these carbonated rocks may be achieved by the modification of the colour of calcite minerals, or by incorporation of outlandish minerals in the rock.

¹ www.geology.com, accessed at March 2019;

² www.mindat.org, accessed at March 2019;

Previously, it has been demonstrated that the colouration of common colourless minerals can be achieved or changed through the incorporation of impurities, such as transition metals with the 3d orbitals partially occupied (Nassau, 2001; Cairncross and McCarthy, 2007). For calcite, it was found that several colourations as green, blue, purple, brown or pink can be originated through the incorporation of small amounts of iron, cobalt, manganese, nickel, copper or zinc. Additionally, like fluorite (CaF_2), it was demonstrated that radiation can influence the colour of calcite, giving it tones of amber, light orange or even blue (Gaft et al., 2008; Kalita and Wary, 2014). This phenomenon can be achieved through luminescence, which is the return of an excited electron into the fundamental state, releasing energy in the form of a photon. The excitation state can be reached by gamma, UV or X-ray radiation, or by the presence of trace elements (Laanait et al., 2015; Costagliola et al., 2017; Kabacińska et al., 2017; Kabacińska et al., 2019).

Despite this, carbonate rocks may have multiple minerals in their composition, that can interfere in the colouration of the rock. Some of them are considered evident, such as chlorites in marbles that can induce a strong green colouration. Iron oxides also seem to play an important role in the colouration of some carbonated rocks, due to their chromophore capacity (Gil et al., 2007; Yuanfeng et al., 2012; Grossi et al. 2015). The redox conditions occurring during the rocks' formation will interfere with the chemical speciation of iron, which may originate distinct colours (Calogero et al., 2000). Clay minerals, phyllosilicates or organic matter may also confer colour, although some difficulty in their identification. For these cases, the colour of the stones may range from dark/black (rocks highly rich in organic matter) to amber.

The colour of the most common limestones exploited in Portugal ranges from white-cream in the MCE, to vivid yellowish or reddish colours at the Pêro Pinheiro region, and also reddish and greyish colours at the Algarve region (Fig. I-20).

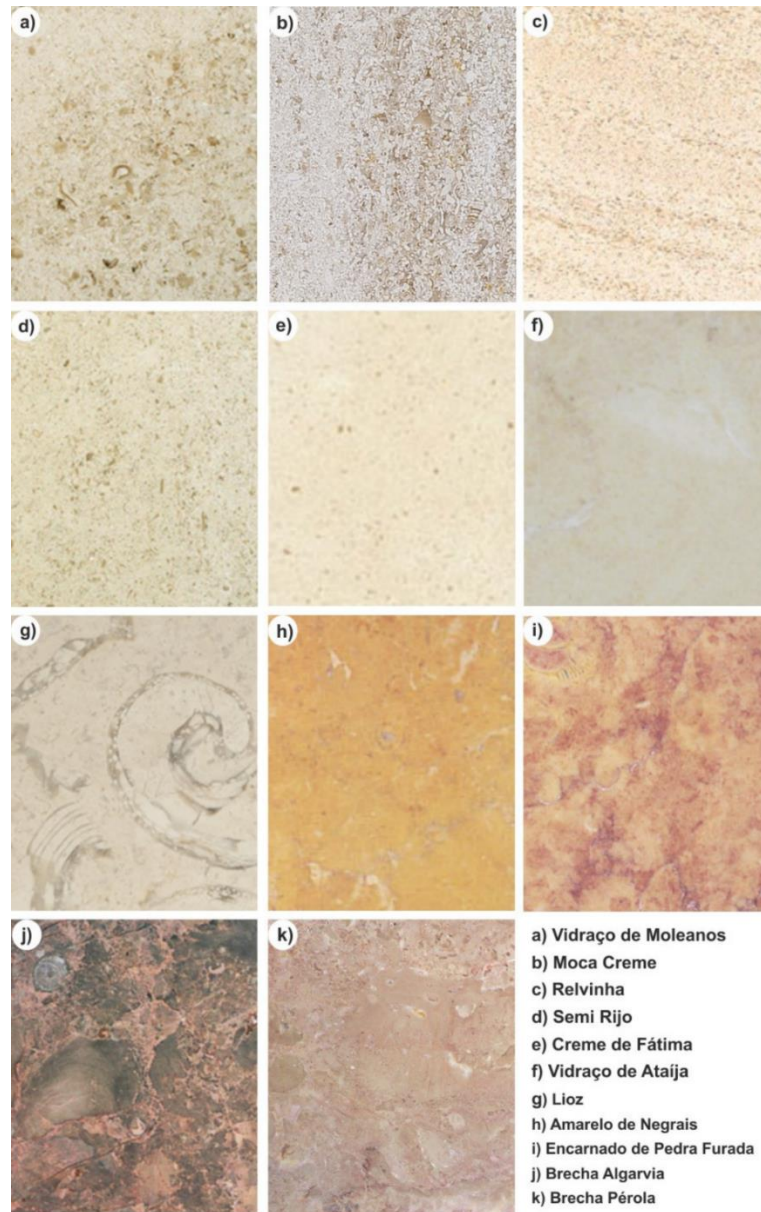


Figure I-20. Examples of the most common limestones exploited in Portugal, their macroscopic appearance and their common commercial names. Provenance from the MCE (a-i), and Algarve (j-k) regions (Carvalho et al., 2012a).

Regarding the colouration of the Portuguese marbles, they present a wide range that goes from white to dark grey (Moura, 2007). However, the most common varieties (Fig. I-21) are the white and light cream with more or less abundance of greyish to reddish stripes, while the most valuables are the pure white and the pinkish varieties. The commercial names may differ for the same lithotype, according to the quarry owner.

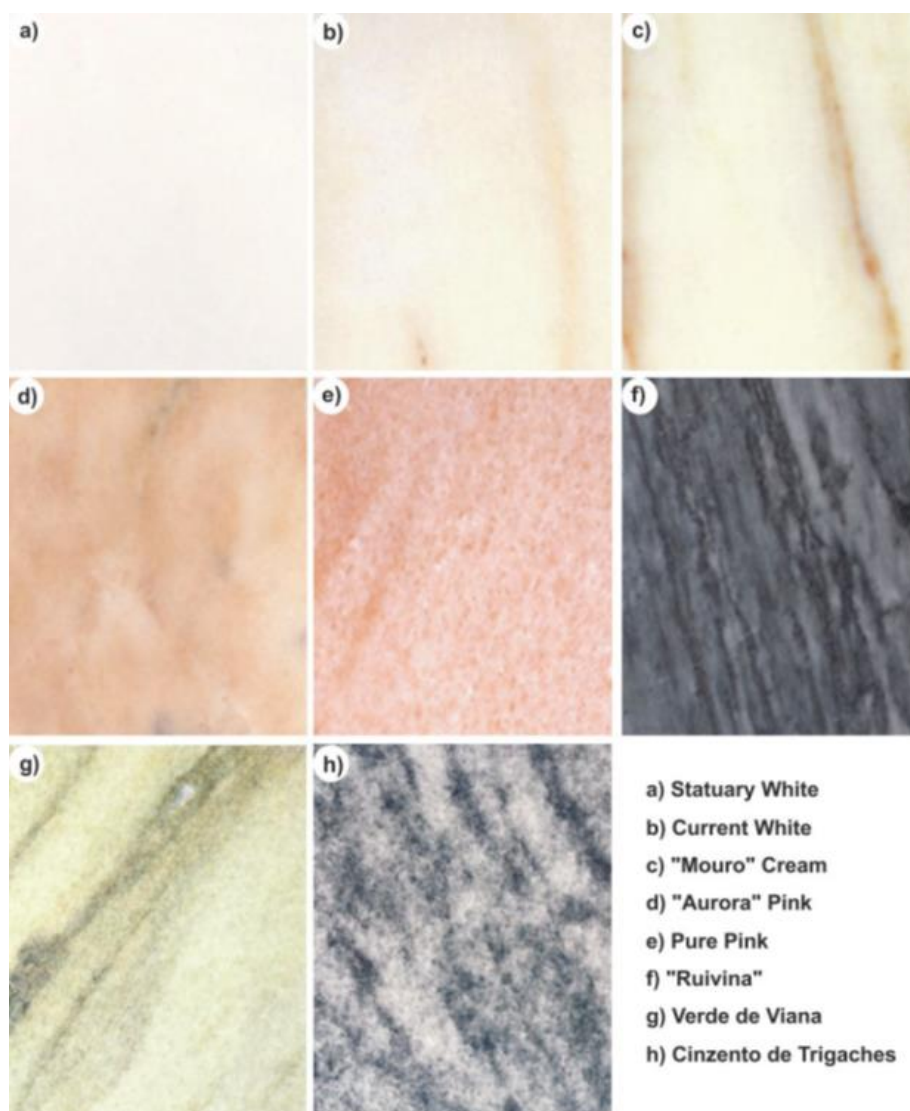


Figure I-21. Examples of the most common marbles exploited in Portugal, their macroscopic appearance and their common commercial names. Provenance from Alentejo region for all (Carvalho et al., 2012a).

Colour change is considered one of the major problems facing the conservation of natural stone, with significant impact in their economic value, as well as in the cultural heritage context. Discolouration processes are responsible for the appearance of unaesthetic patterns that affect negatively the appreciation of the architectonic object or the artwork. As mentioned above, the original colour may be changed by either inorganic or organic pathways, which in most of the cases operate together.

The inorganic weathering processes of rocks are well-known. Besides this, in the framework of ornamental stones where the aesthetic details are essential, factors like human activity (Viles, 2002; McAllister, 2016; Fatorić and Seekamp, 2017) and the

commercial finishing of the surface (Grissom et al., 2000; Urosevic et al., 2013) may originate discolouration patterns that are unpredictable.

Nevertheless, chromatic changes can be related with the geochemical/mineralogical features of the stone. For example, reddish or yellowish appearance in carbonates after their dissolution can be originated by the presence of a great amount of iron or mineral inclusions in the rock (Valls del Barrio et al., 2002). Another example is the weathering of clay-limestones that may induce accumulation of clay minerals in the surface - which will give a different colour to the stone. Also, sulphides are known to corrode stone with time and can cause discolouration (Selonen et al., 2000). Probably the most common discolouration process is the weathering of stone in buildings and monuments that results in the formation of a thin patina (Fig. I-22) which gives a different colour to the stone. U.V. radiation is also known to be capable of induce colour alteration on stones through luminescence phenomena. Unfortunately, some of the conservation and restoration works (Fig. I-23), e.g. consolidants incorrectly applied, also result in a colour alteration for some stones (Grossi et al., 2007; Pouli et al., 2012; Grossi and Benavente, 2016).

Furthermore, as previously mentioned in the biodeterioration section, the colonisation of external surfaces of the buildings and monuments can induce, apart from the mechanical damages, an aesthetically unacceptable appearance with a staining conferred by biogenic pigments (Rosado et al., 2014a; Mihajlovski et al., 2015; Morillas et al., 2015). In the last years, the biodeterioration of stone monuments has been an important topic of research (St.Clair et al., 2004; Rosado et al., 2016; Salvadori and Municchia, 2016; Pinheiro et al., 2019), although systematic studies that can associate stone-microorganism-colour are still missing. The main reason for that is the extreme difficulty in the microorganism's identification in non-controlled environments. Even so, the biotechnological investigation community has been developing new approaches and methodologies that allow the microorganisms' identification (Schuster et al., 2007) successfully applied in biodeterioration studies (Tan et al., 2015; Aguilar et al., 2016; Dias et al., 2018; Gallego et al., 2019).



Figure I-22. Examples of weathering in pieces of art made of limestone and marble. Patina formations (a, b and c) and a hardened crust formed after a past treatment (d), responsible for the detachment of a thin stone layer (adapted from Rodrigues, 2006).

The colour and discolouration of natural stones for construction purposes is a very critical and important topic of study since these phenomena can lead to very costly conservation works in monuments, and high costs for building stone companies in the new buildings' construction. It is important that our country continues to invest in new technologies, in order to maintain itself in the forefront of the building stone industry. The perspective of this PhD research project has been the development of strategies for the determination of the colour origin in carbonated ornamental stones. This was done in limestone and marbles, to therefore understand their chromatic alteration processes, with particularly attention on the microbial contribution. Several Portuguese limestones and marbles were selected and studied according with their importance for built-heritage and for the new buildings' industry. Additionally, some heritage artworks and heritage building made of stone were selected as case studies under the framework of this PhD, representing different scenarios and conditions.

Chapter II:

Characterisation of Portuguese carbonated stones



Publications and dissemination:

- Papers:
 - **L. Dias**, F. Sitzia, C. Lisci, L. Lopes and J. Mirão, “Microscopia e Microanálise no estudo de Pedras Ornamentais carbonatadas”, *Boletim de Minas – DGEG-Direção-Geral de Energia e Geologia* (paper submitted).
- Communications in Conferences:
 - L. Lopes, J. Mirão and **L. Dias**, “Limestone and marbles from Portugal: Colors, textures and patterns”. I Workshop on Heritage Stones, Salamanca, Spain, October 2-4, 2018;
 - J. Mirão, **L. Dias**, I. Cardoso, P. Barrulas, P. Moita and A. Candeias, “Geochemistry and mineralogy to industry: from stone degradation to BIM”, GlobalStone 2018, Ilheus (Bahia), April 26-29, 2018;
 - **L. Dias**, T. Rosado, P. Barrulas, L. Lopes, A. Manhita, C. Dias, J. Mirão, A. Candeias, A. T. Caldeira, “Alteração cromática de calcários ornamentais”. Jornadas do Departamento de Química da Universidade de Évora, Portugal, April 10, 2018;
 - **L. Dias**, T. Rosado, P. Barrulas, A. Manhita, L. Lopes, J. Mirão, A. T. Caldeira, A. Candeias, “Limestone chromatic changes – a case study”. Natural Stone for Cultural Heritage, Prague, Czech Republic, September 19-22, 2017;
 - J. Mirão, **L. Dias**, I. Cardoso, P. Barrulas, A. T. Caldeira, P. Moita, C. Dias, L. Lopes and A. Candeias, “Stone chemical and mineralogical research in Hercules Laboratory, Portugal”. IVth International Stone Congress 2017, Izmir, Turkey, March 20-25, 2017;
 - **L. Dias**, P. Barrulas, L. Lopes, P. Moita, A. T. Caldeira, J. Mirão, “X-ray based analytical methods and the color of marbles and limestones used in architecture”, SCIX2016 – The Great Scientific Exchange, Minneapolis, Minnesota, USA, September 18-23, 2016.

2.1. Introduction

As previously mentioned, Portugal has a great geological diversity in its territory and has a strong ornamental stone industry throughout all its history. Over the last centuries, the Portuguese stone has been used for several purposes such as public monuments, small works of art or in private houses. Some authors report that nowadays Portuguese stone is applied in hundreds of thousands of buildings (Lopes and Martins, 2014). The high-quality Portuguese carbonated stones are characterised by the high proportion of calcite (CaCO_3). These materials have been exploited since ancient times (Maciel and Coutinho, 1990; Martins and Lopes, 2011; da Fonseca et al., 2013), placing the country in the forefront of natural stone production, as marble, limestone and granite. Therefore, Portugal is one of the leaders in the production of ornamental stone (Carvalho et al., 2000; Carvalho et al., 2013b), offering a wide variety of natural stone.

Since the ornamental stone industry is an important sector for the Portuguese economy (Fig. II-1), having reached over than 400M€ in 2019^[3], Portugal must continue to support technological development and offer new services/specifications, as after-sales services and material certification. Creation and implementation of manuals for the application of Portuguese carbonated stones is encouraged, to a greater valorisation of the Portuguese ornamental stone.

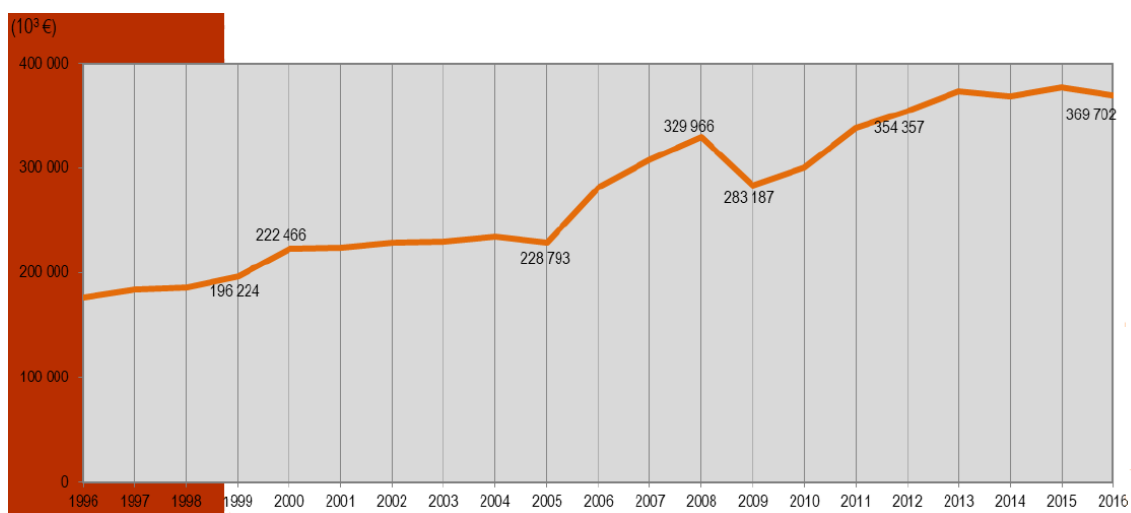


Figure II-1. Evolution of the ornamental stone exportation in Portugal (DGEG, 2017). Values for marble and limestone reach to about 250M€.

³ <https://www.assimagra.pt/>, accessed at December 2019;

Colour is one of the main visible characteristics that lead to the appreciation of stone and its use as building material. Since the stone discolouration has become a critical issue with strong influence in its commercial value, the colour and discolouration of carbonated stones is one of the major challenges for the ornamental stone scientific community. Therefore, it is essential to understand how the colouration of each of these materials is achieved.

This chapter aims to characterise Portuguese marbles and limestones based on their colour and their importance for the Portuguese market and cultural heritage, using X-ray based analytical methods. Therefore, it is expected that this work might be a contribution to determine the mineralogical and geochemical factors that can impute colouration in stone, and somehow, anticipate possible mechanisms of colour alteration.

2.2. Material and Methods

2.2.1. Selection of the stones

Several limestones and marbles were selected considering their economic importance for the actual Portuguese market and for cultural heritage assets. The stones collected were cut to obtain several slabs of each lithotype. White, green and pink marbles, and red, yellow, orange and blue limestones were selected (Fig. II-2).

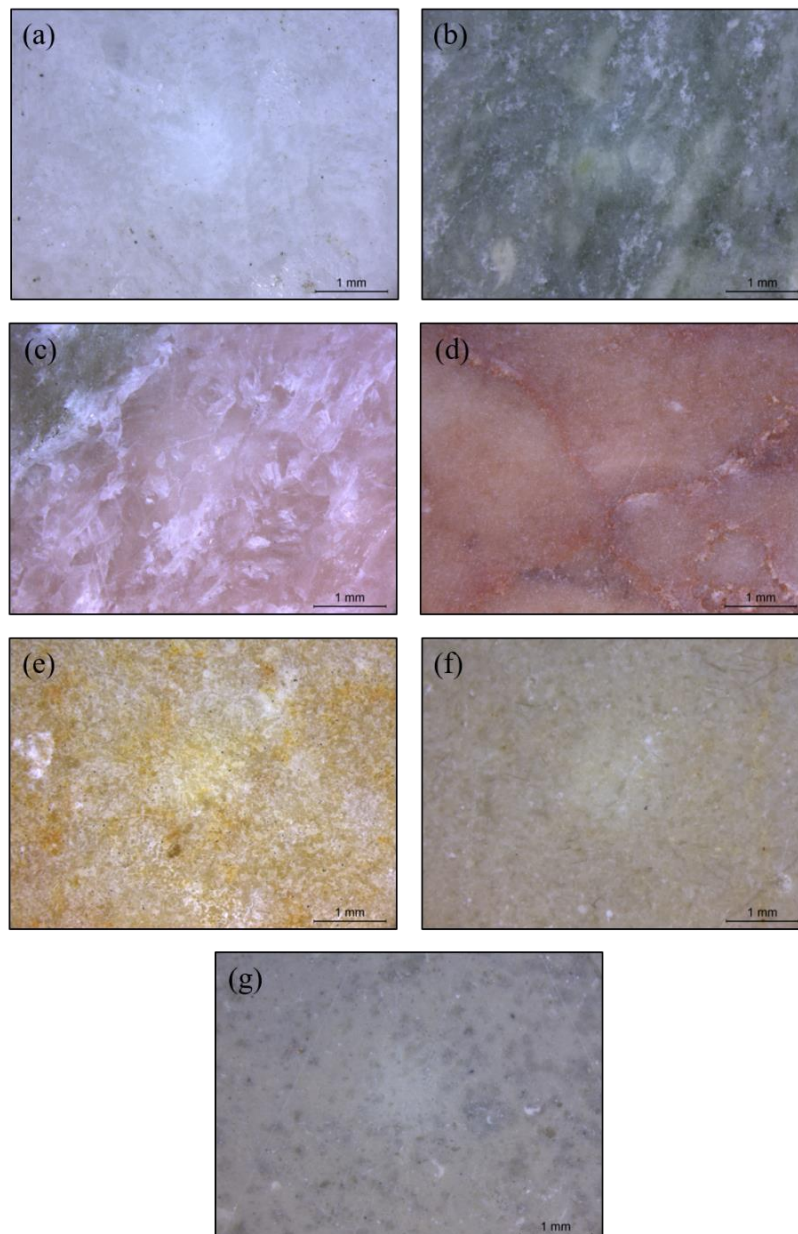


Figure II-2. Stones selected for the study. White (a), green (b) and pink (c) marbles, and red (d), yellow (e), orange (f) and blue (g) limestones.

The white and pink marbles (Fig. II-2a and II-2c), varieties of a Heritage Stone Global Resource “Estremoz Marbles” (Lopes, 2020), are exploited in the Estremoz Anticline where, as previously mentioned, are located the largest Portuguese marble exploitations. These lithotypes are very popular natural stones with a fine grain. They were used to construct important buildings in the past, and currently, are mainly used for contemporary architecture projects, for interior design as staircases, floorings and façades, decorative objects and home decorations. The green marble (Fig. II-2b) has been exploited in southern Portugal, Serpa. Features a medium to thin grain, with several accessory greenish minerals and calcitic whitish patches. This marble has been commonly used for extensive interior flooring and wall cladding.

The red and yellow limestones (Fig. II-2d and II-2e), varieties of “Lioz” a Heritage Stone Global Resource (Lopes, 2020), are exploited in the region of Pêro Pinheiro - Negrais, north of Lisbon. These two limestones are characterised by having some white fossils and patches in their composition, which currently are mainly used for internal and external claddings and pavements. On the other hand, the orange and the blue limestones (Fig. II-2f and II-2g) are extracted in the MCE, where the largest Portuguese limestone exploitations are located. The blue limestone has a thin grain, a compact appearance, and it presents lighter and darker areas and dark blue spots. The orange limestone has a thin grain, compact appearance and it presents lighter and darker areas, dark red spots, as well as some occasional well defined dark brownish veins. Currently, these very popular limestones are mainly used for masonry, façades and interior and exterior flooring. In addition, due to their hardness, these stones have a considerable reputation and international demand.

The stones were characterised by determining their colourimetric parameters, and their chemical and mineralogical composition using X-ray based methods.

2.2.2. Determination of the colour parameters

The colour characterisation was carried out through the determination of the colourimetric parameters of the CIE L^*a^*b (CIELAB) space. This method was defined in 1976 as an international standard for colour measurement by the *Commission Internationale d'Eclairage* (CIE), and determines saturation, hue and lightness (Beck et al., 2016). According to this system, the colour of an object is determined by the three coordinates L^* , a^* and b^* located in the colour space (Fig. II-3). The coordinate L^*

corresponds to grades of lightness from 0 (black) to 100 (white). The coordinate a^* is based on the green (negative values)/red (positive values) axis, and the coordinate b^* refers to the blue (negative values)/yellow (positive values) axis. The data were collected on the surface of several slabs of each stone with a portable DataColor CheckPlusII spectrophotometer (Lawrenceville, NJ) equipped with an integrating sphere. The experimental conditions included diffuse illumination 8° (in agreement with CIE publication No15.2.Colorimetry), SCE, Standard Illuminant/Observe D65/ 10° and a measurement area of 5mm. The results are the mean value of nine measurements for each stone lithotype.

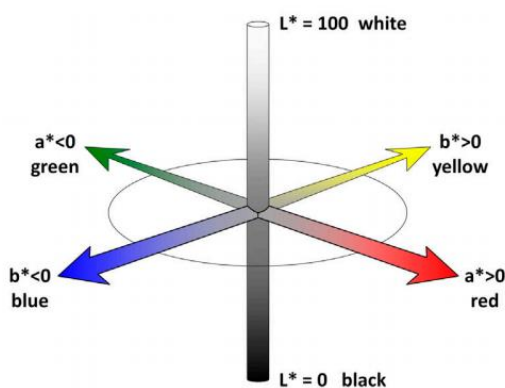


Figure II-3. CIE Lab 1976 colour coordinates system (adapted from Beck et al., 2016).

2.2.3. Chemical and mineralogical composition

2.2.3.1. X-ray Fluorescence Spectrometry (XRF)

The XRF spectrometry allows to detect the major elements and some trace elements. The measurements were done with a handheld Bruker Tracer III/IV-SD operated with an XFlash[®] Silicon Drift Detector (SDD) with 145eV of resolution. The X-ray generator was operated at 40 kV and 30 μ A current under low vacuum conditions, with an acquisition time of 120 s. The data were processed using the software ARTAX 7.4.0. The peak areas were calculated after data normalisation with the $RhK\alpha$.

The analyses were performed on stone without any previous preparation. The data presented are the mean value of nine spectra acquired for each lithotype.

2.2.3.2. X-ray Diffraction (XRD)

The mineralogical composition of the stones was characterised through X-ray diffraction with a commercial Bruker D8 Discover diffractometer with CuK α radiation tube operating at 40 kV and 40 mA. The XRD patterns were measured between 3° to 75° 2 θ , using a step size and recording time per step of 0,05° and 1s, respectively. The crystalline phases were identified with the PDF-ICDD Powder Diffraction Database (International Centre for Diffraction Data), using the Bruker EVA software (version 3.0).

The XRD experiments were carried out on powdered samples.

2.2.3.3. Variable Pressure Scanning Electron Microscopy with Energy Dispersive Spectrometry (VP-SEM-EDS)

The SEM-EDS analysis was performed with a scanning electron microscope HITACHI S3700N coupled to a microanalysis system QUANTAX EDS equipped with a BRUKER XFlash[®] Silicon Drift Energy Dispersive Detector, with 129 eV spectral resolution at the FWHM/Mn K α . The EDS data was processed using standardless tools in the software Esprit1.9. The BSE detector was used to detect slight changes in the chemical composition of the material surfaces. When the surface was chemically heterogeneous, elemental compositional maps were acquired and punctual analyses were obtained. The microscope was operated with a 20 kV accelerating voltage and 40 Pa chamber atmosphere.

The stones were analysed without any previous preparation.

2.3. Results and discussion

Several marble and limestone with different colourations were characterised using X-ray based methods and colourimetry, in order to discriminate their composition and colour, representing a starting point for the main aim of this thesis, the comprehension of colour alteration.

2.3.1. Determination of the colour parameters

In order to measure the colour of the stones, colourimetry technique was performed. The spectral reflection curves, which graphs the reflectance of the stone as a function of wavelengths, were obtained (Fig. II-4) and the parameters of the CIEL*a*b* system were determined (Table II-1). These data allowed to get the chrominance for the different stones, and show the heterogeneity existing among them.

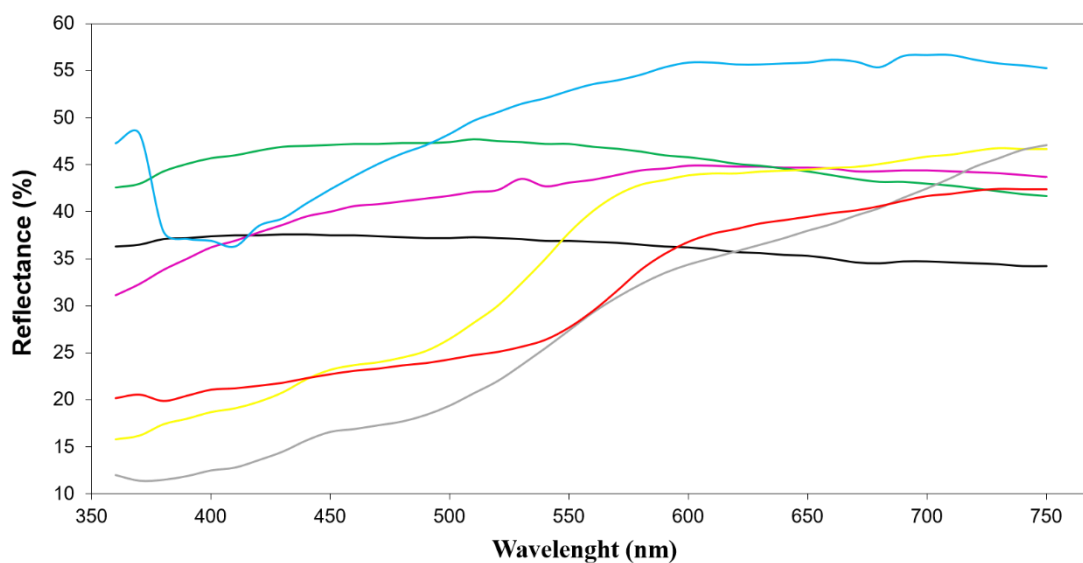


Figure II-4. Spectral reflection profiles obtained by colourimetry technique for the white (—), green (—), pink (—), yellow (—), red (—), orange (—) and blue (—) stones.

This colourimetric characterisation is very useful, namely for the determination of changes in the spectral reflection profile in the future and, consequently, variation in the chrominance, using a non-invasive approach (Grossi et al., 2007).

Table II-1. Determination of the parameters $L^*a^*b^*$ for each stone, obtained through the CIEL^{*} a^*b^* system. The mean value and standard deviation were calculated after 9 measurements.

Stone	L^*	a^*	b^*
White marble	67.12 ± 3.39	-0.81 ± 0.09	-1.22 ± 0.32
Green marble	62.72 ± 2.34	-2.6 ± 0.18	1.97 ± 0.97
Pink marble	68.83 ± 0.97	2.26 ± 0.23	6.05 ± 1.01
Red limestone	59.58 ± 0.95	15.29 ± 1.78	16.97 ± 1.81
Yellow limestone	67.05 ± 0.37	6.19 ± 0.24	20.86 ± 0.57
Orange limestone	56.62 ± 6.04	8.17 ± 0.53	20.95 ± 0.56
Blue limestone	53.45 ± 1.19	0.05 ± 0.14	4.87 ± 0.24

2.3.2. Chemical and mineralogical characterisation

In order to determine the major and some trace elements that can intervene in the stones' colouration, X-ray fluorescence spectrometry was performed. The spectra obtained for the different stones are shown in the figures II-5 and II-6, which allowed to calculate the peak areas for each chemical element identified (Table II-2).

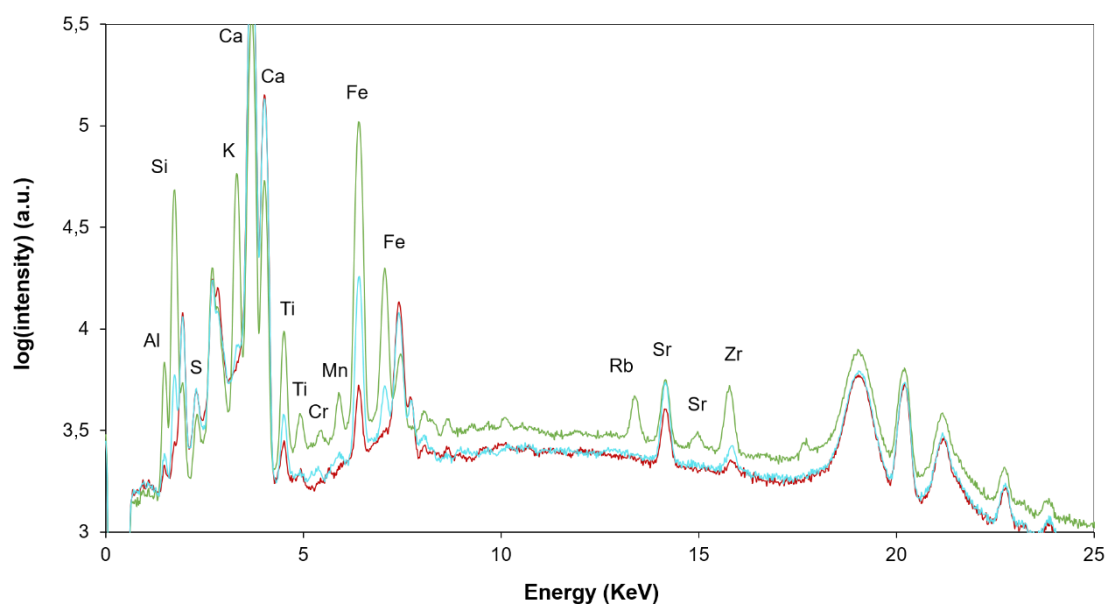


Figure II-5. Spectra obtained by X-ray fluorescence for the white (—) and pink (—) marbles from Estremoz and green marble (—) from Serpa.

As expected, the white marble was the material that presented the purest calcium carbonate, since shows less elemental enrichment. On the other hand, the stones that presented the richest and wider diversity in their elemental composition were the green marble and blue limestone. In these stones, in addition to the major elements, it was possible to determine the presence of some trace elements like rubidium and zirconium.

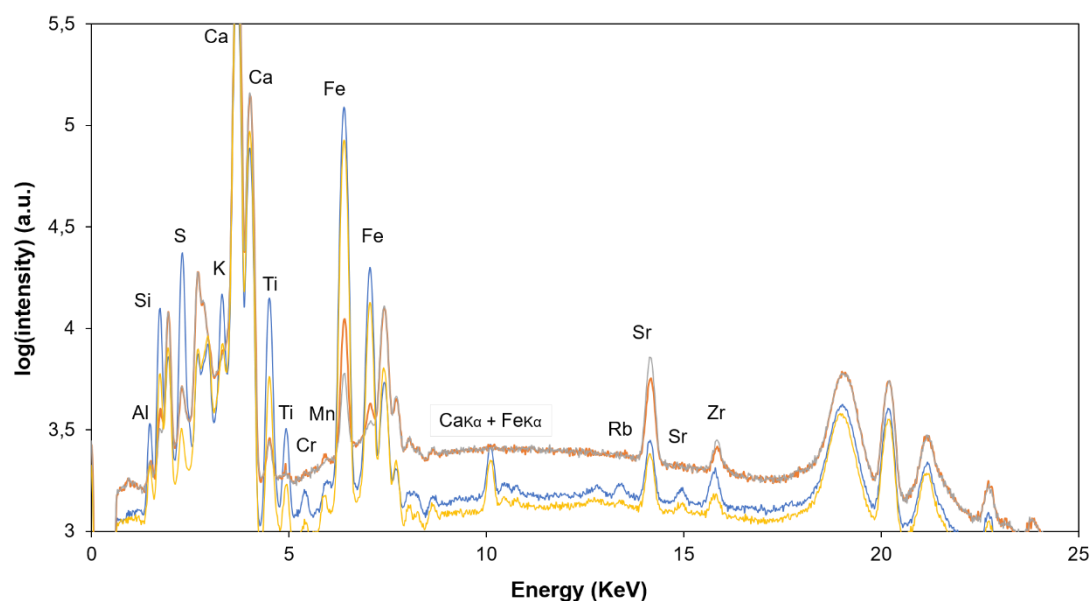


Figure II-6. Spectra obtained by X-ray fluorescence for the blue (—) and orange (—) limestones from MCE and for the yellow (—) and red (—) limestones from Negrais.

In addition to calcium, some stones like the pink, green, orange and blue stones exhibit enrichment in aluminium, silicon, potassium and iron. This data may suggest that these stones have outlandish minerals – possibly micas or clays – incorporating the calcite during the formation processes of the rocks. Complementarily, the blue limestone revealed high amounts of sulphur and iron which prompted further investigation within this PhD. The red and yellow stones did not exhibit potassium and have a small quantity of major elements like aluminium, silicon, manganese and titanium, which can suggest that these stones exhibit less incorporation of outlandish minerals in the rocks. Special attention must be given to the presence of manganese in the pink and blue stones, since there are minerals that contain small quantities of ions like Mn^{2+} and Mn^{4+} that can be coloured (Cairncross and McCarthy, 2015) to pink or to black, respectively.

Table II-2. Determination of the peak areas (a. u.) for each element detected in the stones by X-ray fluorescence spectrometry. The values were calculated after 9 spectra acquisitions.

Stone	Al	Si	S	K	Ca	Ti	Mn	Fe	Cu	Zn	Cr	Rb	Sr	Zr
White marble	4	11	0	0	11204	13	0	43	7	2	1	0	36	4
Green marble	43	398	7	525	3485	79	20	1193	9	6	6	30	49	41
Pink marble	7	42	13	36	10471	25	6	212	14	0	3	0	58	8
Yellow limestone	4	21	10	0	10787	13	2	119	10	2	1	0	65	6
Red limestone	5	16	13	0	10957	11	1	48	10	3	1	0	91	7
Orange limestone	24	141	288	167	7924	211	7	2183	6	4	6	10	34	12
Blue limestone	12	71	9	80	11214	90	8	1713	9	4	1	0	32	7

In order to identify the minerals composing the carbonated stones under crystalline form, XRD was performed (Fig. II-7 and II-8). The results were analysed and compared with the data obtained previously, from XRF spectrometry.

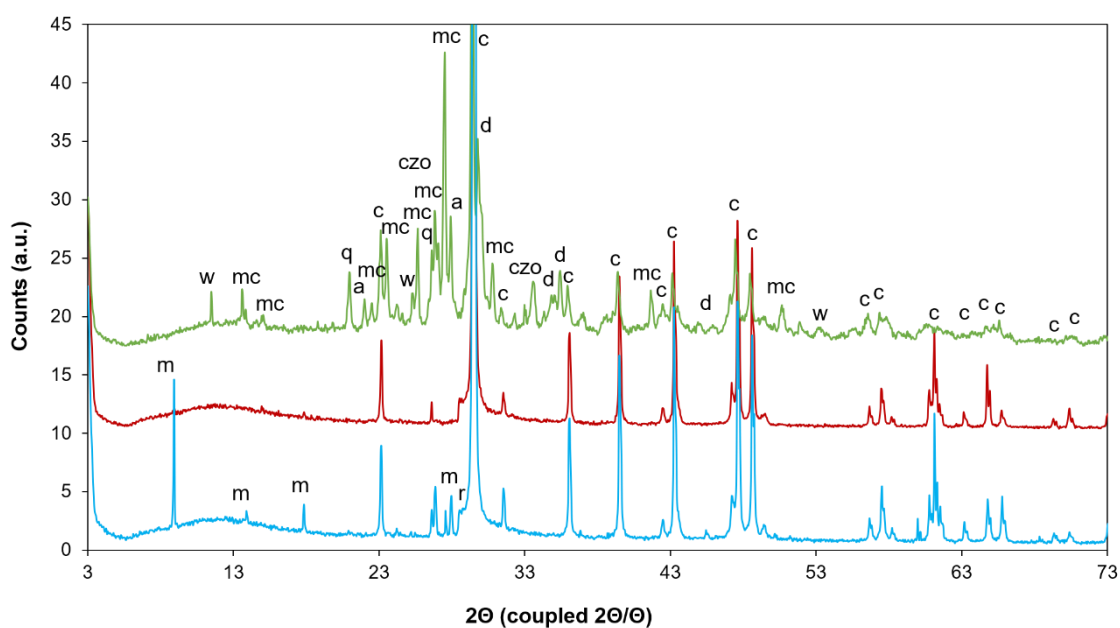


Figure II-7. Significant diffractograms obtained and identification of crystalline phases on the powdered white (—) and pink (—) marbles from Estremoz and green marble (—) from Serpa. Abbreviations: m-muscovite; w-wollastonite; mc-microcline; q-quartz; a-albite; r-rutile; c-calcite; czo-clinozoisite; d-diopside.

The diffractograms of the powdered carbonated stones showed that all stones are essentially calcitic - since no dolomite was identified - and all of them exhibit some quartz (SiO_2) in its composition. Additionally, it was possible to identify some minerals incorporating the calcite, such as:

- muscovite ($\text{KAl}_2(\text{AlSi}_3\text{O}_{10})(\text{F},\text{OH})_2$) and rutile (TiO_2) in the pink marble;
- microcline (KAlSi_3O_8), diopside ($\text{CaMgSi}_2\text{O}_6$), albite ($\text{NaAlSi}_3\text{O}_8$) and clinozoisite ($\text{Ca}_2\text{Al}_3(\text{SiO}_4)_3(\text{OH})$) in the green marble;
- birnessite ($\text{Na}_{0.3}\text{Ca}_{0.1}\text{K}_{0.1}(\text{Mn}^{4+},\text{Mn}^{3+})_2\text{O}_4 \cdot 1.5\text{H}_2\text{O}$), pyrite (FeS_2) and marcasite (FeS_2) in the blue limestone;
- birnessite in the orange limestone.

Table II-3 summarises the minerals identified for each stone.

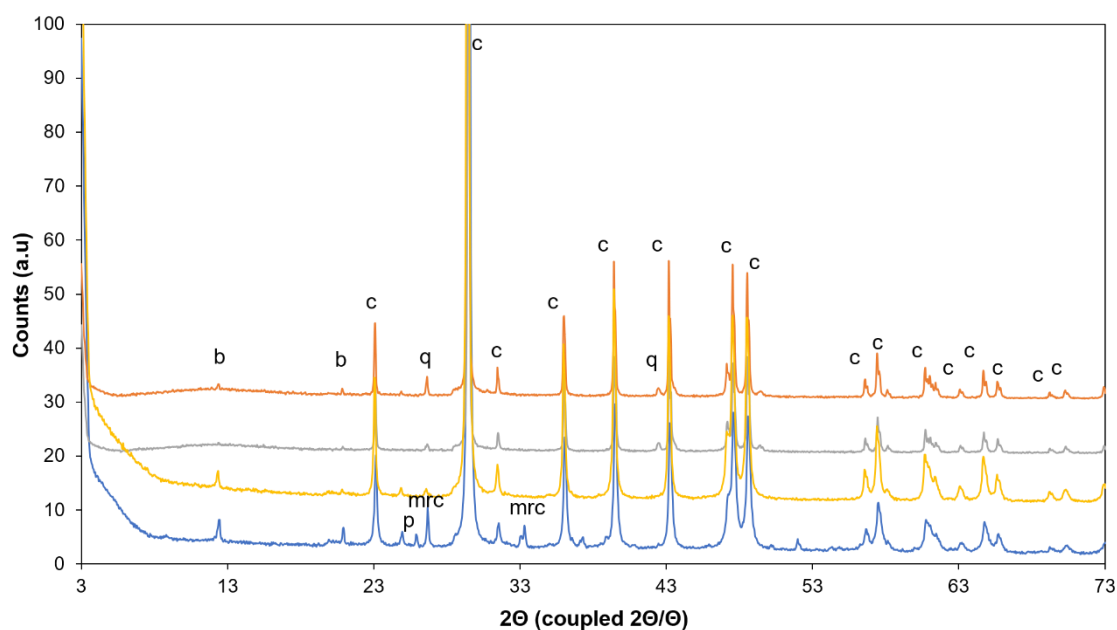


Figure II-8. Significant diffractograms obtained and identification of crystalline phases on the powdered blue (—) and orange (—) limestones from MCE and yellow (—) and red (—) limestones from Negrais. Abbreviations: b-birnessite; c-calcite; p-pyrite; mrc-marcasite; q-quartz.

The presence of muscovite, a hydrated potassium aluminum silicate that belongs to the micas' group, in the pink marble is compatible with the X-ray spectrum obtained for this stone that shows the presence of Al, Si and K.

Regarding the green marble, the identification of microcline and albite is also compatible with the data obtained from the XRF analysis, since these minerals belong to the feldspars' family. In addition to wollastonite and diopside, the clinozoisite, a mineral belonging to the epidote minerals' family was also identified in this stone. The identification of pyrite and marcasite in the blue limestone is compatible with the high

amounts of sulphur and iron observed by XRF. The presence of the element manganese could in part be associated with the presence of birnessite in the stones.

Table II-3. Minerals under crystalline form composing stones, identified by X-ray diffraction.

Stone	Minerals I.D.
Estremoz white marble	Calcite, quartz
Estremoz pink marble	Calcite, quartz, muscovite, rutile
Serpa green marble	Calcite, quartz, microcline, diopside, albite, wollastonite, clinozoisite
Negraiz yellow limestone	Calcite, quartz, birnessite
Negraiz red limestone	Calcite, quartz
MCE orange limestone	Calcite, quartz, birnessite
MCE blue limestone	Calcite, quartz, pyrite, marcasite, birnessite

Besides XRD and XRF analyses, VP-SEM-EDS was also performed, since it allows to obtain information about the morphology, microstructure and it is a complementary tool for the determination of the chemical composition. It was possible to observe the higher porosity degree of the limestones in comparison with marbles. On the other hand, 2D elemental mapping and point analyses allowed to determine how the major elements detected by the X-ray fluorescence spectrometry are distributed.

On the white marble, it was possible to detect calcium carbonate (Fig. II-9) and few silicon oxides, while on the pink marble were identified some iron oxides, phyllosilicates, calcium titanium silicates (Fig. II-10) as well as calcium phosphates, zirconium silicates and silicon oxides.

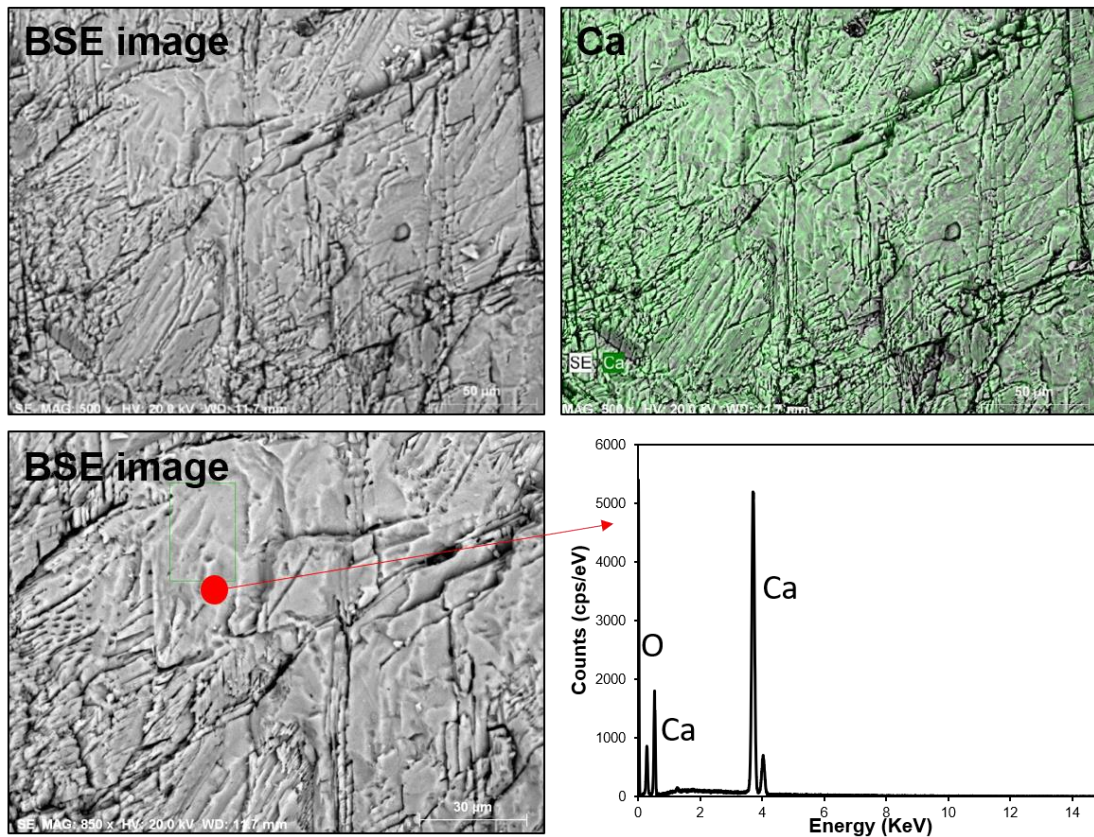


Figure II-9. Microstructure, calcium distribution and point analysis obtained on the white marble from Estremoz.

The pinkish colouration of this marble can be achieved by the incorporation of iron in the calcite or by the presence of iron oxides spread along the calcitic matrix (Fig. II-10). The presence of phyllosilicates like calcium titanium silicates (maybe sphena) in this pink marble can also be associated to the greenish vein's, a visible characteristic of this stone (Fig. II-2c), since these minerals may exhibit a green colouration (Mazdab et al., 2007; Ospitali et al., 2008; Randive et al., 2015).

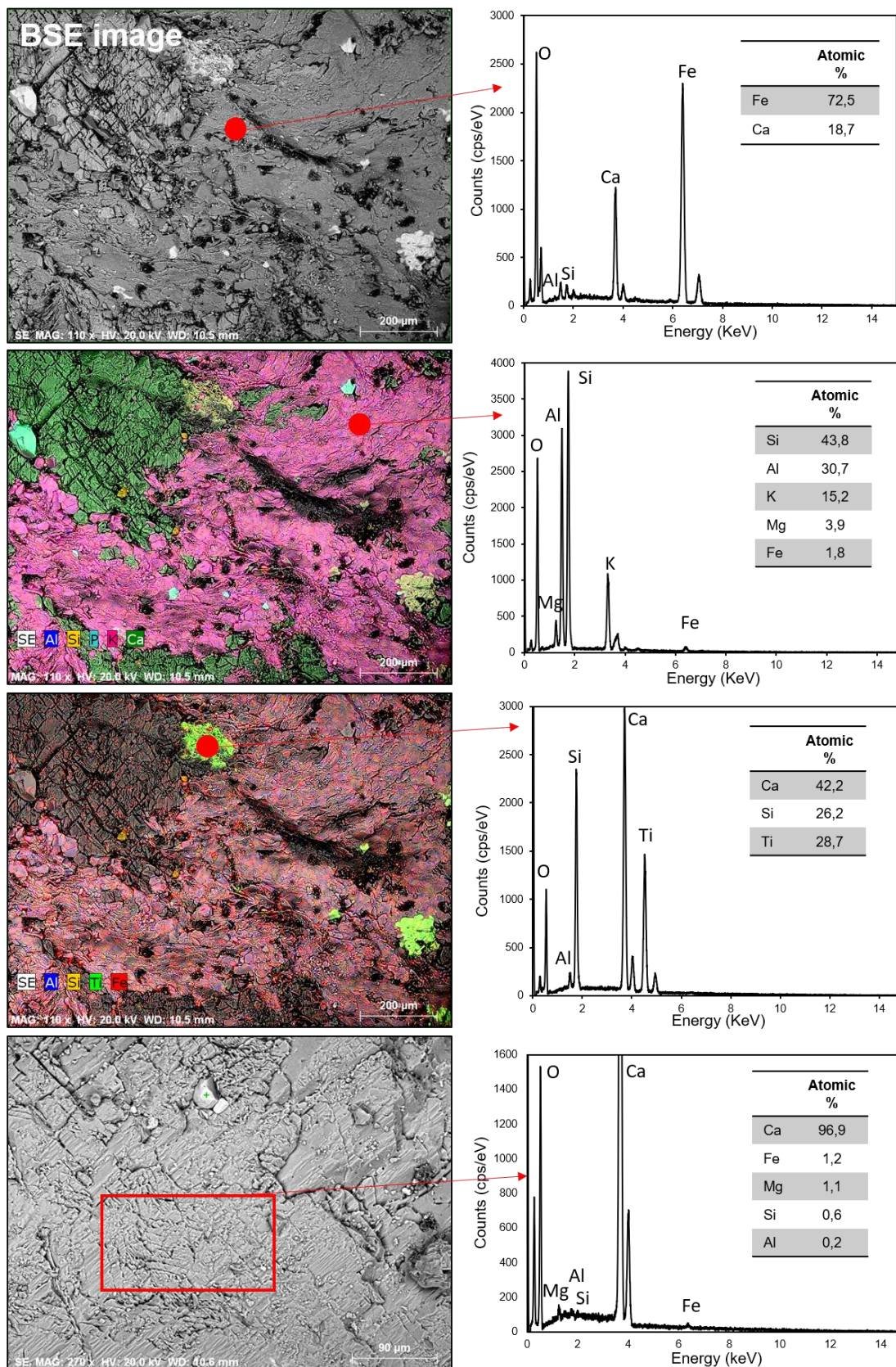


Figure II-10. Microstructure, distribution of the major elements and point/area analyses obtained on the pink marble from Estremoz (only cations was considered).

The green marble displays large areas containing what seems to be potassium feldspars. Complementing with the XRD results these areas may be associated with the microcline mineral. In this stone, it was also identified alkaline feldspars and possible epidote (Fig. II-11), silicon oxides, calcium phosphates, zirconium silicates, iron oxides and iron sulphides. Clinozoisite, a mineral of epidote group, is greenish which may contribute for the achievement of the greenish colour of this marble.

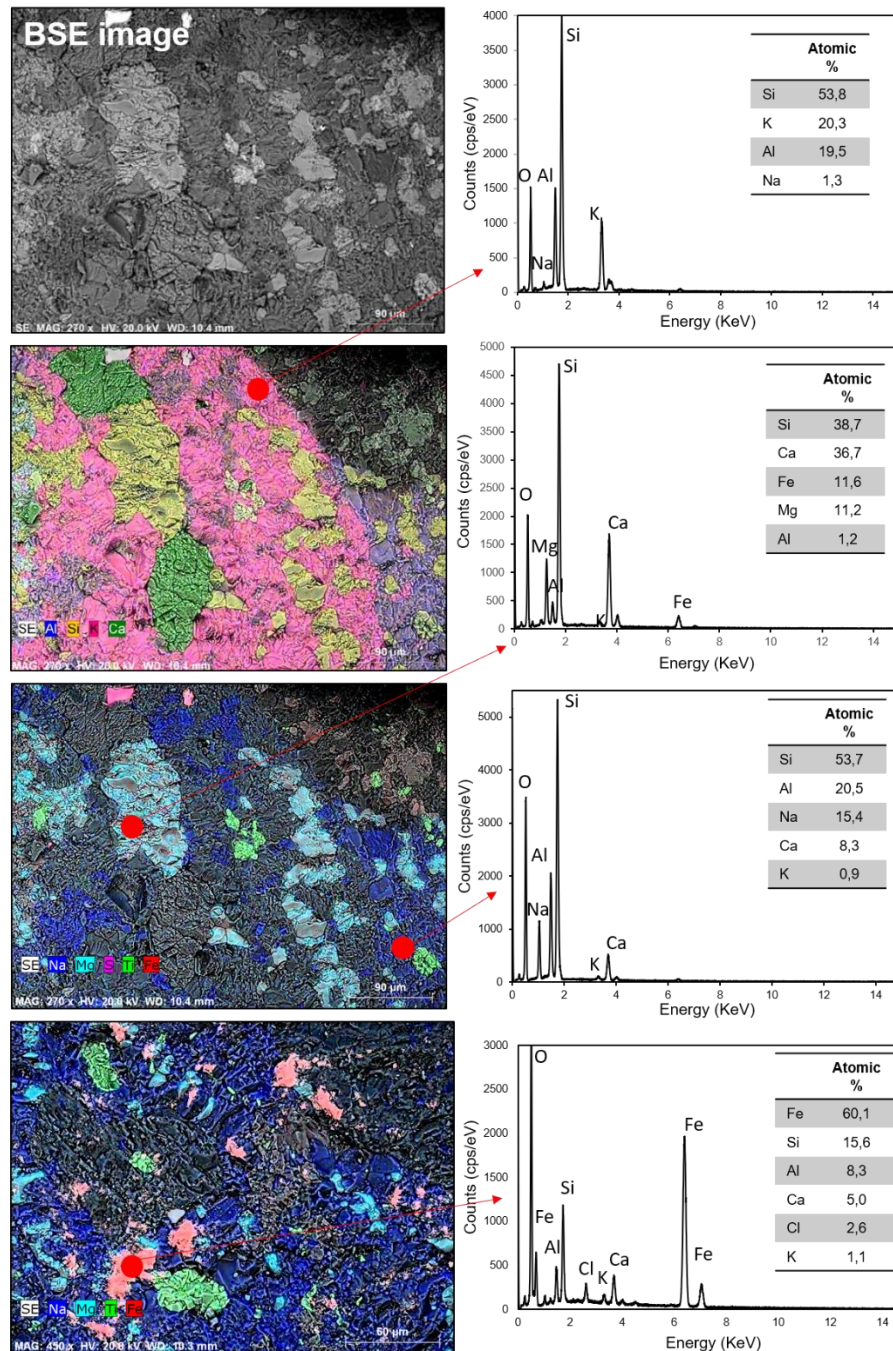


Figure II-11. Microstructure, distribution of the major elements and point analyses obtained on the green marble from Serpa.

The data obtained on the yellow (Fig. II-12), red and orange stones revealed the presence of calcium carbonates, silicon oxides, iron oxides and few clays. Iron oxides may have different colours ^[4] such as yellow, red, brown or orange, and their incorporation in the rocks can contribute actively for the colouration of these stones.

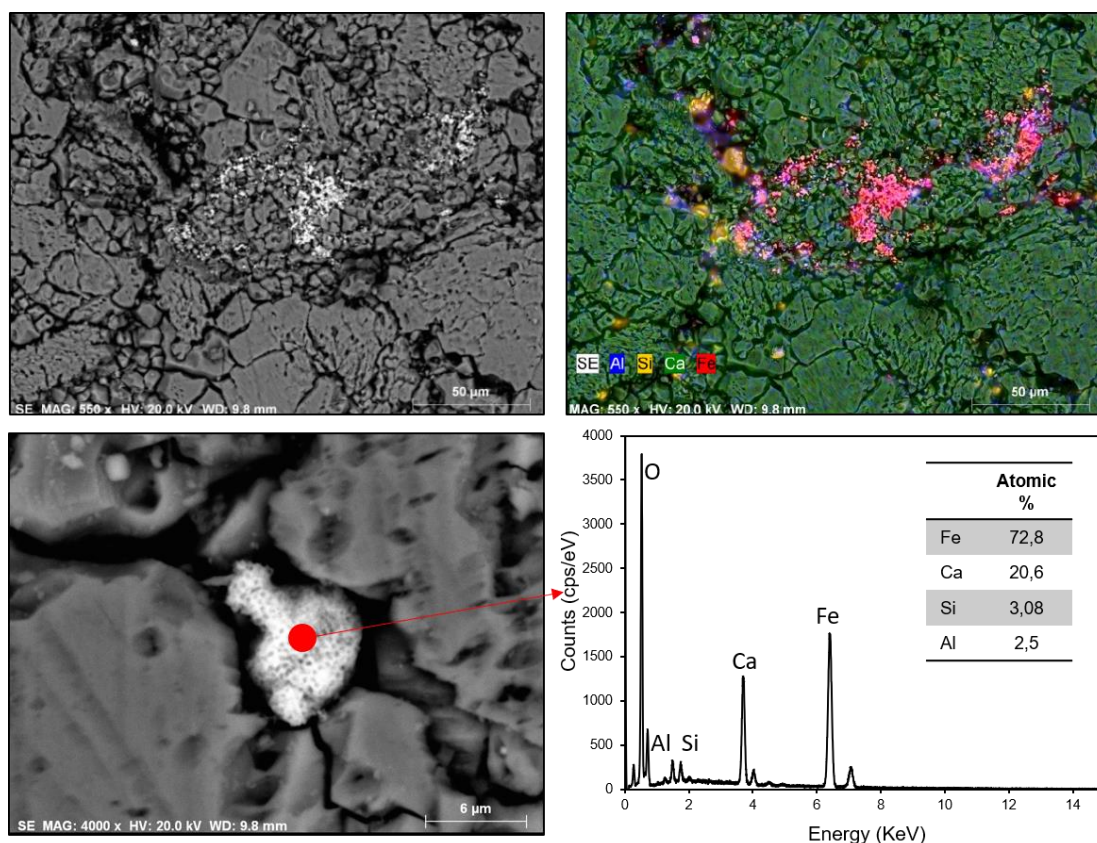


Figure II-12. Microstructure, distribution of the major elements and point analysis obtained on the yellow limestone from Negrais.

The EDS analysis of the blue limestone revealed the presence of some silicon oxides, and a great amount of iron sulphides (Fig. II-13), corroborating the XRF and XRD data. In part, the blue colour of this limestone can be achieved by the charge transfer of Fe^{2+} to Fe^{3+} , since the colour of Fe^{2+} is green and Fe^{3+} is yellow. It is also known that this limestone has a great amount of organic matter content, that probably contributes for the blueish colour of these stones.

⁴ www.webmineral.com, accessed at February 2019;

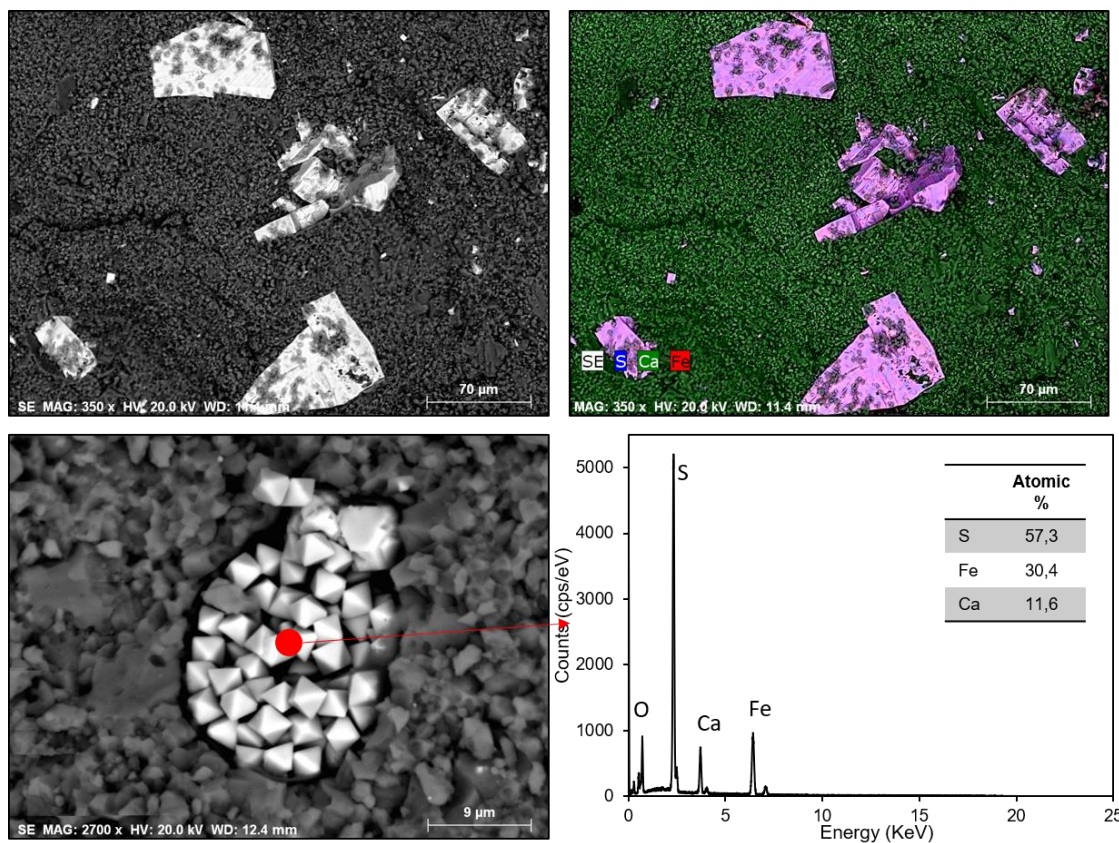


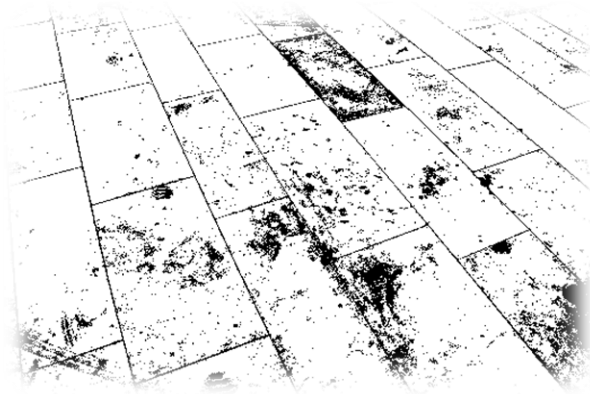
Figure II-13. Microstructure, distribution of the major elements and point analysis on the blue limestone from MCE.

The X-ray based methods used in this study, namely XRF, XRD and SEM-EDS, showed to be an effective and useful approach to do a preliminary screening for limestones and marbles characterisation. The study contributes to better knowledge about the composition of Portuguese ornamental stones, namely limestones and marbles typically used in historic heritage and new buildings. Therefore, with this knowledge in mind, the implementation of methodologies for stone application (e.g. surface finishing, avoid particular places to do the installation, etc.) is encouraged, in order to predict and prevent changes in their phase composition and consequently, its colour alteration. This information could be available to the companies through independent laboratories.

Currently, the blue limestone is vastly produced and used for both national and international applications. For this PhD, the blue limestone lithotype was selected in order to characterise its discolouration mechanism and study the influence of the microbial communities in this process.

Chapter III:

Characterisation of the colour alteration mechanism on the blue limestone



Publications and dissemination:

- Papers:
 - **L. Dias**, T. Rosado, A. Coelho, P. Barrulas, L. Lopes, P. Moita, A. Candeias, J. Mirão, A. T. Caldeira (2018). “Natural limestone discolouration triggered by microbial activity – a contribution”. *AIMS Microbiology* **4**(4): 594-607. DOI: 10.3934/microbiol.2018.4.594.

- Communications in Conferences:
 - **L. Dias**, T. Rosado, A. Coelho, L. Lopes, J. Mirão, A. T. Caldeira, A. Candeias, “Limestone chromatic changes: a microbial-mediated inorganic process”. TECHNART2017 – Non-destructive and microanalytical techniques in art and cultural heritage, Bilbao, Spain, May 2-6, 2017;
 - **L. Dias**, T. Rosado, P. Barrulas, L. Lopes, J. Mirão, A. T. Caldeira, A. Candeias, “Degradação de pedra ornamental: Alteração de cor em calcário aplicado”, XII Congresso Ibérico de Arqueometria, Burgos, Spain, October 25-28, 2017 (Winner of the Best Panel Presentation Award).

This Chapter was written based on an article published with scientific peer review entitled “Limestone chromatic changes triggered by microbial activity” (Dias et al., 2018).

3.1. Introduction

After the characterisation of some important Portuguese carbonated stones, a lithotype of building stone – the blue limestone – was selected in order to characterise its mechanism of colour alteration by spontaneous weathering. This stone is exploited in one of the most important regions for the Portuguese ornamental stone industry, the MCE, and have different geological ages. Currently, this product is widely used as building stone in major contemporaneous architecture projects, which its marketability and exportation levels have increased over the last years. Companies selling this lithotype have been losing millions in the replacement in the of the altered stone, especially in the stone that was exported. It has also been relevant in the past, in important monuments, and it is utmost importance to understand its deterioration mechanism. Its name came from the blueish dark-grey colour, apparently due to the charge transfer of Fe^{2+} to Fe^{3+} and the presence of organic matter. This ornamental stone coexists sometimes with a cream limestone, that may appear in the same outcrop (Fig. III-1).



Figure III-1. Blue limestone with blueish dark-grey and cream colour in the same outcrop. ©Luís Lopes

Besides its economic and cultural importance, it is known that this limestone is susceptible to weathering processes that are still unknown, inducing its colour alteration and causing aesthetic patterns that are unacceptable (Fig. III-2). The alteration has been reported in both indoor and outdoor environment, causing costly repairs to the companies.



Figure III-2. Building blue limestone with visible alteration (a), (b). ©Luís Lopes

Despite the inorganic processes that intervene in the rocks' weathering are generally well-known, it is necessary to study the colonisation effects of building surfaces by microorganisms that can cause discolouration. Moreover, the inorganic weathering can create the conditions to the biological colonisation that will increase the alterations rate, therefore the reinforcing mechanisms of inorganic-biological alteration must be stressed.

This chapter intends to describe the inorganic processes of the natural weathering of the stone and, furthermore, perform the assessment of the biocolonisation of the material in previously applied stone with visible discolouration. The multi-analytical approach used allowed to describe the colour alteration mechanism of the stone, as well as to characterise the prokaryotic and eukaryotic population colonising this stone, which somehow might be related with its discolouration.

3.2. Materials and methods

3.2.1. Sampling process

Sampling was performed in building stone showing chromatic alterations. Two different sites containing applications of this lithotype were selected, which one is the area that surrounds the Mosteiro da Batalha building ($39^{\circ} 32' 54''$ N $8^{\circ} 58' 48''$ O) (Fig. III-3 a, b) and the other is the waterfront of São Martinho do Porto village ($39^{\circ} 30' 47''$ N $9^{\circ} 8' 8''$ O) (Fig. III-3 d). In both cases, the blue limestone was applied in the floor pavement. Generally, the sampling regions have a warm and temperate climate, as the yearly average temperature is 15.7°C and the yearly average rainfall is 710 mm.



Figure III-3. Sampling process of the building stone located at the floor pavements next to the Mosteiro da Batalha building (a), (b), (c) and in the waterfront of São Martinho do Porto village (d). ©Luís Lopes

The stone applied in both places shows the pathology previously discriminated (Fig. III-2), where samples were collected using an electric core drill (annex A). Due to the rock heterogeneity and in order to avoid an excessive number of variables, sampling was performed in close altered and non-altered sections (table A-1), ensuring the representativeness.

Microfragments were also collected for biocontamination assessment in altered and non-altered sections. The collection of these microfragments was done under semi-aseptic conditions with sterile scalpels and microtubes. The microfragments were mechanically shaken with a Maximum Recovery Diluent (MRD) during 24 h, at 150 rpm, to promote the cell disaggregation from the stone.

3.2.2. Material characterisation

3.2.2.1. XRF

To determine the chemical composition, X-ray fluorescence spectrometry analyses were performed with a handled Bruker Tracer III-SD, using the same equipment and methodology described in the section 2.2.3.1. of the Chapter II. The analyses were performed directly on the collected samples.

3.2.2.2. XRD

To obtain the mineralogical composition, μ -XRD was performed with a Bruker D8 Discover diffractometer equipped with a Goebel mirror and a linear detector Bruker Lynxeye. Diffraction were performed with a $\text{CuK}\alpha$ radiation tube operating at 40 kV and 40 mA. The XRD patterns were measured between 3° to 75° 2θ , using a step size and recording time per step of $0,05^\circ$ and 1s, respectively. A laser-video sample alignment system and a motorised XYZ stage were used. The crystalline phases were identified with the PDF-ICDD Powder Diffraction Database (International Centre for Diffraction Data), using the Bruker EVA software (version 3.0).

The XRD experiments were carried out in the exposed surface of the stone, using a 1-millimetre X-ray collimator. The data were taken from sections with and without alteration patterns.

3.2.2.3. VP-SEM-EDS

The SEM-EDS analyses were performed with a HITACHI S3700N interfaced with a QUANTAX EDS microanalysis system, using the same features and methodology described in the section 2.2.3.3. of the Chapter II. Additionally, the surface roughness parameters were determined through a Phenom ProX Desktop SEM equipped with the 3D Roughness Reconstruction software.

3.2.3. Biocontamination assessment

3.2.3.1. Assessment of biological contamination on the building stone

The stone microfragments collected were coated with a gold/palladium layer in an SCD030 Balzers Union sputter-coater, and the surface of the stone was carefully examined in the SEM HITACHI S3700N, using an accelerating voltage of 10 keV in secondary electrons mode, to assess the microbial communities' presence.

3.2.3.2. Cell viability index

The cell viability index (CVI) of the biocontaminants present in the stone was assessed by the 3-(4,5-dimethylthiazol-2-yl)-2,5-diphenyltetrazolium bromide (MTT) assay, according to the method previously described by Mosmann (Mosmann, 1983) and adapted for cultural heritage materials (Rosado et al., 2013b).

90 μ L of each extracted suspension from stone with and without chromatic alteration were incubated with 300 μ L of MTT stock solution (0.5 mg/mL) for 4 h, at 37°C in the dark. After this, 350 μ L of DMSO/ethanol (1:1) were added to promote the dissolution of the formazan crystals formed. The final suspension was centrifuged at 10.000 rpm for 15 min and the absorbance of the supernatant was determined by spectrophotometry at 570 nm.

Each assay was performed in triplicate.

3.2.3.3. Isolation and characterisation of the cultivable microbial community

Each extracted solution was inoculated in different media (see the composition in Annex B), specific for each type of microorganism: NA (Nutrient Agar) for bacteria growth, MEA (Malt Extract Agar) and CRB (Cook Rose Bengal) for filamentous fungi. The cultures were incubated at 30°C during 24-48h and at 28°C during 4-5 days for the development of bacteria and fungi, respectively. After this period, the plates stayed in incubation at the same temperature to detect slow microbial development. The distinct single colonies obtained were sub-cultured onto Petri dish and maintained at 4°C until processing.

3.2.3.3.1. Characterisation of the microbial isolates

The distinct single colonies were characterised based on their macroscopic and microscopic features like texture, colour, hyphae morphology and, where applicable, their reproductive structures. The fungal isolates were stained with methylene blue and observed with a lens objective 50x, using an optical microscope Motic BA410E and digitally recorded by a MoticomPro 282B camera. On the other hand, the bacterial isolates were stained with Gram reagent and observed in the optical microscope with a lens objective 100x.

Molecular characterisation of the isolates was performed by sequencing 16S rDNA or ITS region for bacterial or fungi isolates respectively. The samples' preparation was performed as follows.

The genomic DNA of the prokaryotic population was extracted using a methodology adapted from the method described by Rinta-Kanto et al. (Rinta-Kanto et al., 2005). The cells were collected onto filters and suspended in 100 μ L of 1X TE lysis buffer solution and 15 μ L of lysozyme (2 mg/mL) were added and vortexed. The samples were thereafter incubated in a bath at 37°C for 20 min to promote the cells' disruption. After that, 15 μ L of α -chymotrypsin (4 mg/mL) in 10% SDS were added to the samples that therefore were incubated at 50°C during 30 min. After this period, 100 μ L of phenol/chloroform/isoamyl alcohol (25:24:1) were added and gently shaken for a few seconds. The aqueous phase was transferred to new tubes, and 200 μ L of 100% ethanol + 30 μ L of 3M sodium acetate were added. The DNA precipitated overnight at -20°C. The preparations were centrifuged at 11900 g for 25 min. The supernatant was discarded, and the DNA pellets were left at air-dry, and therefore resuspended in 1X TE buffer, pH=8. The DNA samples were stored at -20°C until further utilisation.

The genomic DNA of the eukaryotic population was extracted according with the method described by Sambrook et al. (Sambrook et al., 1989) and by Pitcher et al. (Pitcher et al., 1989). After the fungal isolates' incubation, the colonies were macerated and transferred to microtubes containing 300 μ L of microspheres. 700 μ L of lysis buffer were added and the microtubes were vortexed for 30 s and placed in the ice for 30 s (3X). The microtubes were then incubated for 1h at 65°C. After this period, the microtubes' content was centrifuged at 13500 rpm for 10 min at 4°C. Its supernatant was recovered to new microtubes and 700 μ L RNase (100 μ g/mL) were added and incubated at 37°C for 1 h. After this period, 600 μ L chloroform/isoamyl alcohol (24:1) were added, mixed by

inversion, and centrifuged at 10000 rpm for 10 min. The supernatant was recovered for new microtubes, which 50 μL of sodium acetate and 1250 μL of 100% ethanol were added. The microtubes were centrifuged at 13000 rpm for 15 min and the supernatant was discarded. The sediment was washed with 1 mL of 70% ethanol (2X) and the mixture was centrifuged at 10000 rpm for 10 min and the supernatant was therefore discarded. The microtubes were left at 37°C to promote dryness, and thereafter the extracted DNA was resuspended with 100 μL of TE buffer and kept at 4°C until processing.

The genomic DNA extracted from prokaryotic and eukaryotic population was quantified by UV-Vis spectrophotometry, using a microplate reader Thermo Scientific MULTISKAN GO μDrop , with a quantification software coupled (SkanTY RE MultiScan 3.2.). This photometric method is based on the equation of Lambert-Beer, $A = c \times l \times \epsilon$, where the molar absorptivity constant (ϵ) of the DNA is 0,020 ($\mu\text{g}/\text{mL}$) cm^{-1} and the optical depth is 0,051 cm.

The amplification of the DNA was done by polymerase chain reaction using the specific primers. For bacteria, 16S rDNA was amplified using the forward primer 5'-CCAGCA GCC GCG GTA ATA CG-3', corresponding to nucleotides 518 to 537 of the *E. coli* 16S rRNA gene (Rahmani et al., 2006), and the reverse primer 785R with the sequence 5'-CTA CCA GGG TAT CTA ATC C (Amann et al., 1995). For eukaryotic, the region containing partial portions of the small subunit (18S), both internal transcribed spacers (ITS) and the 5.8S of the rDNA repeat unit was amplified using the oligonucleotides primers ITS1 (5'-TCCGTAGGTGAACCTGCGG-3') and ITS4 (5'-TCCTCCGCTTATTGATATGC-3') (Anderson and Cairney, 2004).

The reactional mixture was composing by: 17.6 μL of sample; 2.5 μL of H_2O RNase free; 2.5 μL of reaction buffer (10X) + MgCl_2 (25mM); 2.5 μL of dNTPs (2mM); 0.1 μL of Primer reverse (1 μM); 0.1 μL of Primer forward (1 μM); 0.2 μL of Taq DNA polymerase. The reactional mixtures were inserted in a thermal cycler MJ Mini Bio-Rad, and PCR reactions were carried out with initial denaturing at 95°C for 5 min, followed by 40 cycles at 94°C for 60 s, 50°C for 60 s, and 72°C for 2 min, finishing with 1 cycle of 6 min extension at 72°C for the bacteria population. For fungi, PCR reactions were carried out with initial denaturing at 95°C for 3 min followed by 36 cycles at 94°C for 50 s, 56°C for 50 s, and 72°C for 60 s, finishing with 1 cycle of 10 min extension at 72°C. PCR products were analysed through agarose gel (1%) electrophoresis. The electrophoresis was performed at 100 V and the gel was revealed in the UV transilluminator Bio Rad Gel DocTM XR⁺. NZYDNA Ladder VII was used as molecular weight marker.

The nucleotides' sequences were aligned with those retrieved from the GenBank (NCBI) databases for the homology analysis using the BLASTN 2.8.0 program. The sequence alignment was performed using the BioEdit 7.0.5.3 program against the nearest neighbours. A neighbour-joining tree of the aligned sequences was constructed using the software MEGA V.7 (Tamura et al., 2011).

3.2.3.4. Characterisation of the total microbial population

The metagenomic DNA was extracted from the stone using QIAmp DNA Stool Mini Kit (Qiagen, Limburg, Netherlands), with slight modifications of the manufacturer's instructions.

The bacterial and fungal communities were characterised by Illumina Sequencing for the 16S rRNA V3-V4 region and Internal Transcribed Spacer 2, respectively.

The DNA was amplified for the hypervariable regions with specific primers and further reamplified in a limited-cycle PCR reaction to add sequencing adaptor and dual indexes. First, PCR reactions were performed for each sample using 2X KAPA HiFi HotStart Ready Mix. In a total volume of 25 μ L, 12.5 ng of template DNA and 0.2 μ M of each PCR primer.

For bacteria the following primers were used: forward primer Bakt_341F 5'-CCTACGGGNGGCWGCAG-3' and reverse primer Bakt_805R 5'-GACTACHVGGGTATCTAATCC-3' (Herlemann et al., 2011; Klindworth et al., 2013). For fungi, a pool of forward primers was used: ITS3NGS1_F 5'-CATCGATGAAGAACGCAG-3', ITS3NGS2_F 5'-CAACGATGAAGAACGCAG-3', ITS3NGS3_F 5'-CACCGATGAAGAACGCAG-3', ITS3NGS4_F 5'-CATCGATGAAGAACGTAG-3', ITS3NGS5_F 5'-CATCGATGAAGAACGTGG-3', and ITS3NGS10_F 5'-CATCGATGAAGAACGCTG-3' with the reverse primer ITS3NGS001_R 5'-TCCTSCGCTTATTGATATGC-3' (Tedersoo et al., 2014).

The PCR conditions involved 3 min of denaturation at 95°C, followed by 25 cycles of 98°C for 20 s, 55°C for 30 s and 72°C for 30 s and a final extension at 72°C for 5 min. Negative controls were included for all amplification reactions. Electrophoresis of the PCR products was undertaken in a 1% (w/v) agarose gel and the ~490 bp V3-V4 and ~390 bp ITS2 amplified fragments were purified using AMPure XP beads (Agencourt, Beckman Coulter, USA) according to manufacturer instructions. Second PCR reactions added indexes and sequencing adaptors to both ends of the amplified target region by the

use of 2X KAPA HotStart Ready Mix, 5 μ L of each index (i7 and i5) (Nextera XT Index Kit, Illumina, San Diego, CA) and 5 μ L of the first PCR product in a total volume of 50 μ L. The PCR conditions involved a 3 min denaturation at 95°C, followed by 8 cycles of 95°C for 30 s, 55°C for 30 s and 72°C for 30s and a final extension at 72°C for 5 min. Electrophoresis of the PCR products was undertaken in a 1% (w/v) agarose gel and the amplified fragments were purified using AMPure XP beads (Agencourt, Beckman Coulter, USA) according to the manufacturer instructions.

The amplicons were quantified by fluorimetry with PicoGreen dsDNA quantification kit (Invitrogen, Life Technologies, Carlsbad, California, USA), pooled at equimolar concentrations and paired-end sequenced with the V3 chemistry in the MiSeq® according to manufacturer instructions (Illumina, San Diego, CA, USA) at GenoInseq (Cantanhede, Portugal). They were multiplexed automatically by the Miseq® sequencer using the CASAVA package (Illumina, San Diego, CA, USA) and quality-filtered with PRINSEQ software (Schmieder and Edwards, 2011) using the following parameters: 1) bases with average quality lower than Q25 in a window of 5 bases were trimmed, and 2) reads with less than 220 bases were discarded for V3-V4 samples and less than 100 bases for ITS2 samples.

The forward and reverse reads were then merged by overlapping paired-end reads using the AdapterRemoval v2.1.5 (Schubert et al., 2016) software with default parameters.

The QIIME package v1.8.0 (Caporaso et al., 2010) was used for Operational Taxonomic Units (OTU) generation, taxonomic identification and sample diversity and richness indexes calculation.

Sample IDs were assigned to the merged reads and converted to FASTA format (split_libraries_fastq.py, QIIME). Chimeric merged reads were detected and removed using UCHIME (Edgar et al., 2011) against the Greengenes v13.8 database (DeSantis et al., 2006) for V3-V4 samples and UNITE/QIIME ITS v12.11 database (Abarenkov et al., 2010) for ITS2 samples (script identify_chimeric_seqs.py, QIIME).

OTUs were selected at 97% similarity threshold using the open reference strategy. First, merged reads were pre-filtered by removing sequences with a similarity lower than 60% against Greengenes v13.8 database for V3-V4 samples and UNITE/QIIME ITS v12.11 database for ITS2 samples. The remaining merged reads were then clustered at 97% similarity against the same databases listed above. Merged reads that did not cluster in the previous step were again clustered into OTU at 97% similarity. OTUs with less

than two reads were removed from the OTU table. A representative sequence of each OTU was then selected for taxonomy assignment (pick_rep_set.py, assign_taxonomy.py; QIIME).

3.3. Results and discussion

In order to investigate the mechanism of colour alteration of the blue limestone and the relation between the biocolonisation state and weathering, a multidisciplinary approach was accomplished. This problem strongly affects the aspect and integrity of the stone, leading to costly conservation work, which answers are needed. Thus, complementary analytical methodologies contributed with relevant information to understand the process of the colour alteration and the association between inorganic alteration and biological colonisation of the stone surface.

3.3.1. Chemical composition

The samples were firstly analysed by handheld X-Ray fluorescence, on stone with chromatic alteration and non-altered sections. The elements as Ca, Si, Al, K, Sr, Fe and Mn seem to be present in similar quantities for the areas with and without chromatic alteration. Nevertheless, in the spectrum obtained on the chromatic altered area stands out a clear enrichment in sulphur (Fig. III-4).

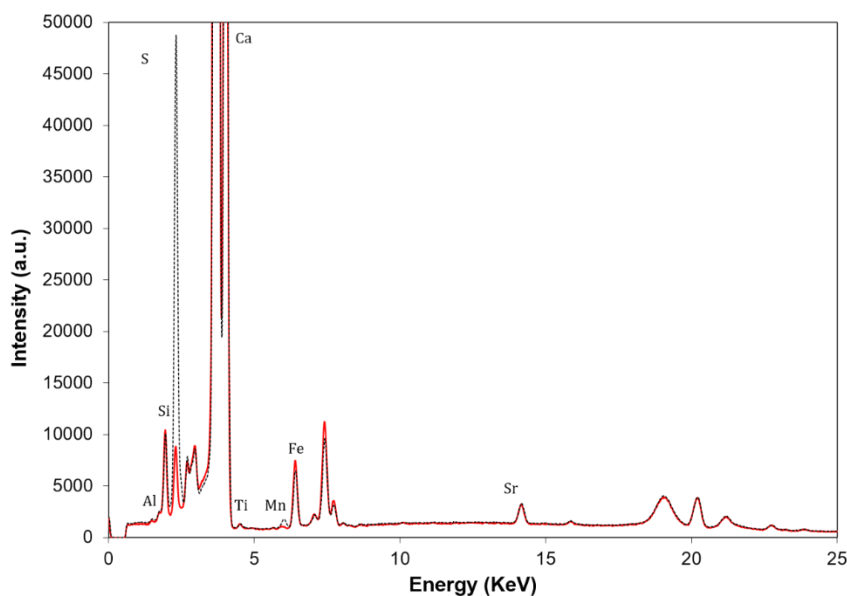


Figure III-4. Compositional spectra obtained by X-ray fluorescence for the sample of building stone, on altered (----) and non-altered (—) areas.

3.3.2. Mineralogical composition and superficial texture

According to the section 2.3.2. of the previous chapter, the mineralogical study of the blue limestone without any alteration pattern revealed the presence of calcite, quartz, pyrite, marcasite and birnessite in its composition. The microdiffraction (Fig. III-5) performed on altered areas of the stone surface revealed an enrichment in gypsum ($\text{CaSO}_4 \cdot 2\text{H}_2\text{O}$).

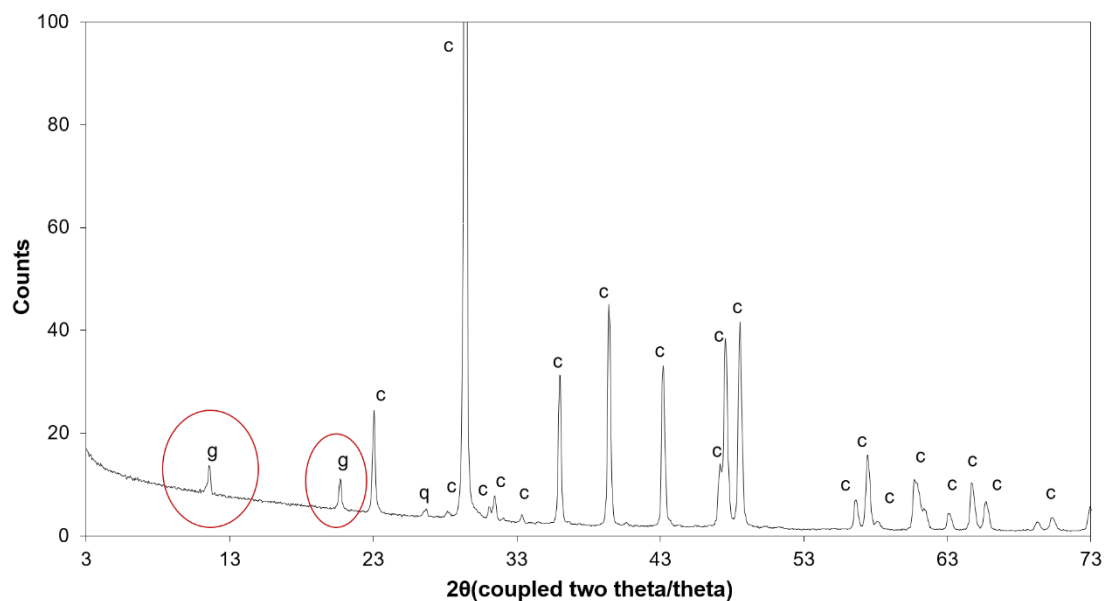


Figure III-5. Micro diffractogram obtained on altered area of the building stone collected. Abbreviations: g-gypsum; c-calcite; q-quartz.

The determination of gypsum on altered surface areas was corroborated with SEM-EDS, with the coexistence of calcium and sulphur in the same regions, as demonstrated in the bi-dimensional elemental mapping and punctual analysis performed (Fig. III-6). The results are compatible with the data obtained through X-ray fluorescence, where altered sections show a large content in sulphur.

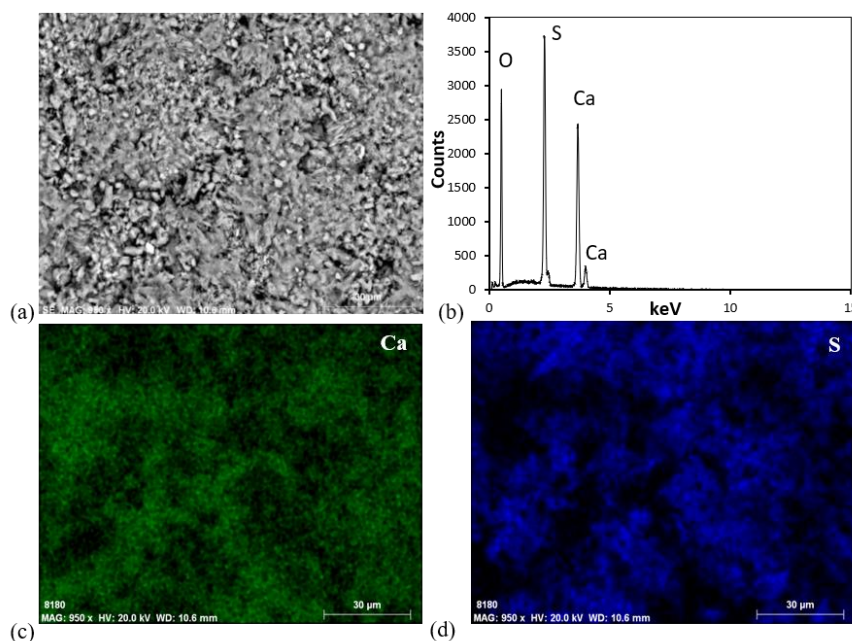
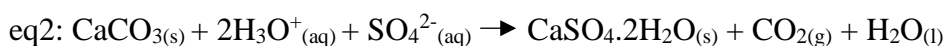
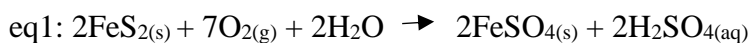


Figure III-6. Microstructure (a), punctual analysis (b) and element mapping of calcium (c) and sulphur (d) on the altered area of the stone, performed by SEM-EDS.

The formation of calcium sulphates can be resulted by the weathering of iron sulphide minerals (Ritsema and Groenenberg, 1993; Móricz, et al., 2012), found in this stone in a large amount, according with the section 2.3.2. of the chapter II. Based on the geochemical and mineralogical data of many previous studies, the chemical oxidation mechanism of FeS_2 has been proposed (Chen et al., 2014). Thus, when exposed to water and oxygen, FeS_2 can react to form sulphuric acid, H_2SO_4 (eq1), and calcium sulphates may be formed after the reaction of sulphuric acid with available carbonates of the stone (Móricz, et al., 2012; Chen et al., 2014), according to the reaction present in eq2. This reaction (eq1) implies the sulphur oxidation and loss of sulphur atoms in the iron sulphide structure.



Additionally, SEM analyses allowed to observe differences in the surfaces' microstructure, where the stone surface with chromatic alterations seems less compact (Fig. III-7), which can be attributed to the loss of the polishing effect, probably caused by the carbonates' dissolution.

The roughness parameters were measured in the SEM Phenom, using the 3D Roughness Reconstruction software. The software provides the measurement of two roughness parameters, Ra and Rh. While Ra smooths all measurements into one average, Rz averages only the greatest deviations. The higher values of Ra and Rh (Fig. III-8) obtained for the altered surfaces are indicative of a greater roughness when compared with non-altered surfaces.

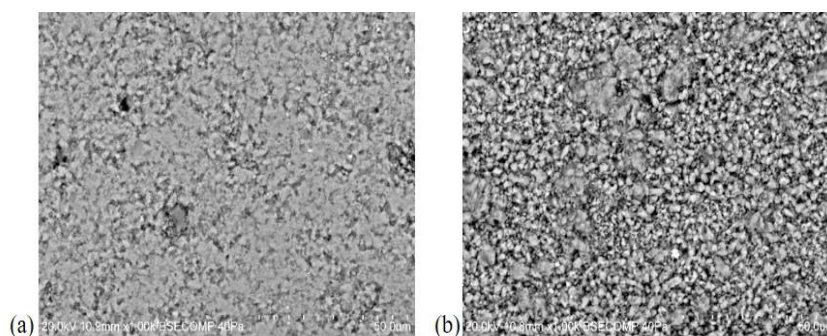


Figure III-7. Stone microstructure of non-altered (a) and altered (b) surfaces, obtained by SEM-EDS.

As suggested above, the oxidation of the iron sulphides originates an acidic solution that will induce the dissolution of the stone, creating micro-cavities in the stone surface, and consequently a change in its roughness. This may create favourable conditions to microbial proliferation on the surface of the stone (Muynck et al., 2011; Miller et al., 2012; Korkanç and Savran, 2015), since the biocolonisers' capacity of penetration and anchoring increases.

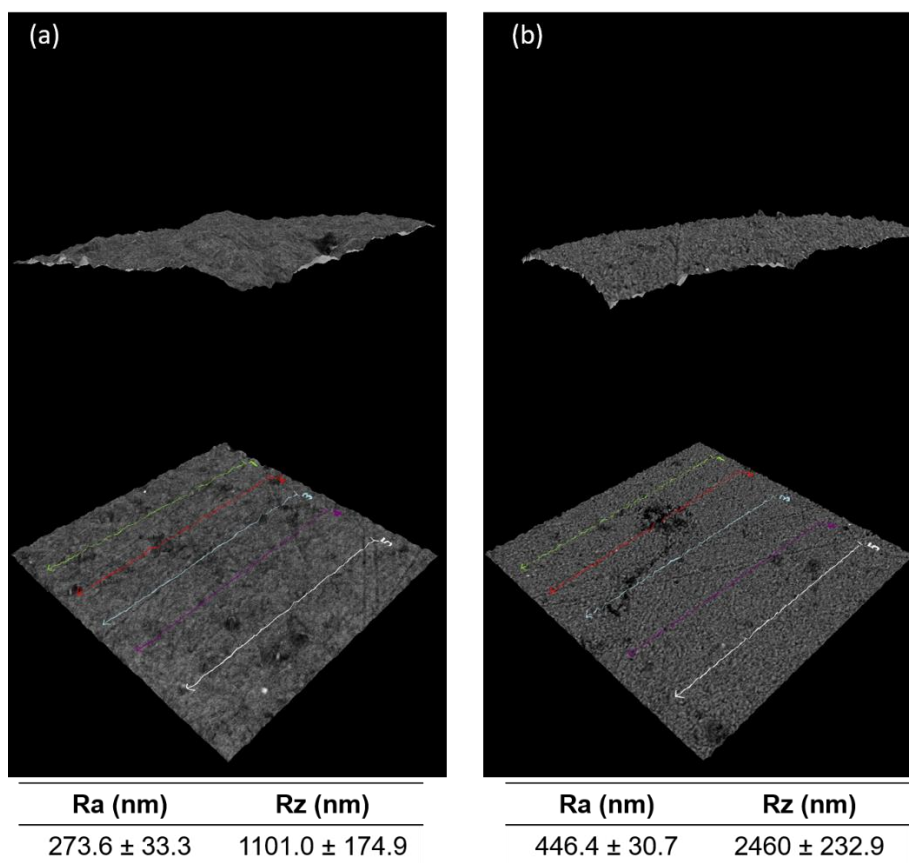


Figure III-8. Determination of surface roughness parameters on non-altered (a) and altered (b) surfaces of the stone, using the 3D Roughness Reconstruction software. The mean value and standard deviation were calculated after 20 measurements.

3.3.3. Biocontamination evaluation

The SEM using the secondary electrons mode allowed a further insight into the presence of microbial communities thriving on the stones with chromatic alteration and their capacity to proliferate within the stone surface (Fig. III-9). The micrographs obtained show the presence of filamentous fungi and spores on these surfaces. Using this technique, no biocolonisation was observed on non-altered surfaces.

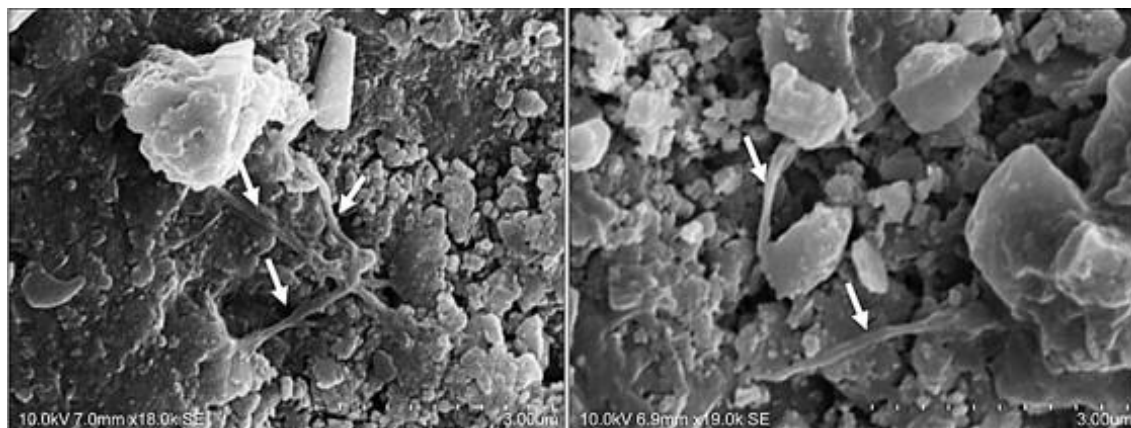


Figure III-9. SEM analysis on weathered sections, showing microbial contamination.

Regarding the cell viability index (CVI), performed in seven different altered and non-altered areas, the methodology adopted showed that the samples collected on chromatic altered areas seem to indicate higher levels, when compared with the non-altered areas (Fig. III-10), whose high CVI degree potentiates metabolic activity. This method was previously optimised to cultural heritage biodeterioration studies and demonstrates to be simple, fast, and very sensitive (Rosado et al., 2013b), giving an overview about the presence of biocolonisers and a preliminary screening of their metabolic activity.

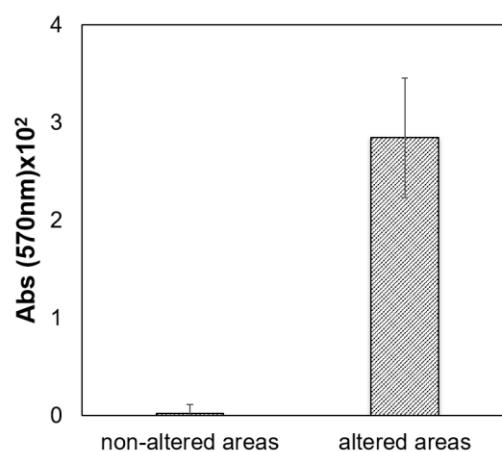



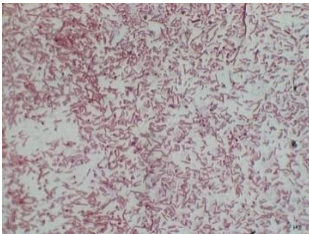

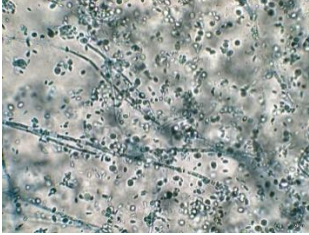

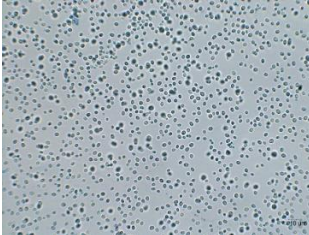

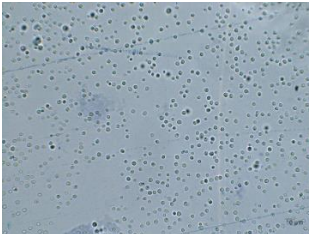
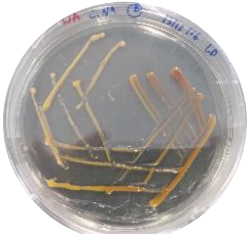
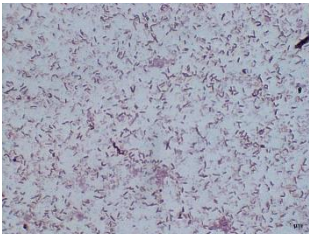
Figure III-10. Cell viability of the microbial population present on altered areas and non-altered areas of the stone. Error bar corresponds to \pm standard deviation (n=21).


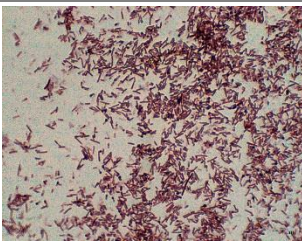

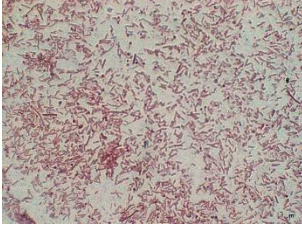

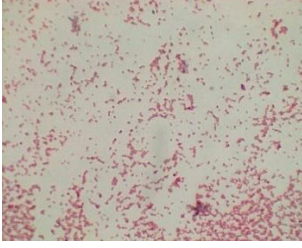

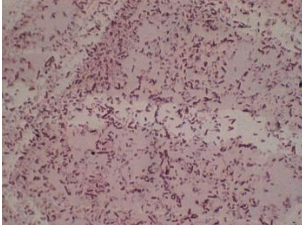

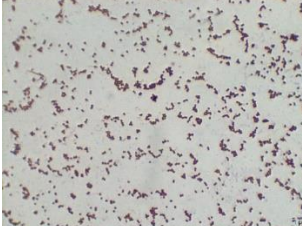
Some of the conventional methods traditionally used to characterise microbial population were performed in this study. The culture-dependent methods revealed that the samples from the altered areas of the stone had predominantly a higher and wider microbial growth when compared with the non-altered areas (Annex C.1). The samples

presenting the higher and wider microbial growth were C1, C2 and C3. On the other hand, the samples C4 and C5 had a moderate microbial development, while the sample C6 had not any microbial development using the NA, MEA and CRB culture media.

The cultivable population was characterised based on their macroscopic and microscopic features. Ten single-colonies of bacteria (Table III-1) and eight single-colonies of fungi (Table III-2) were obtained.

Table III-1. Characterisation of the bacteria isolated from the stone with chromatic alteration.


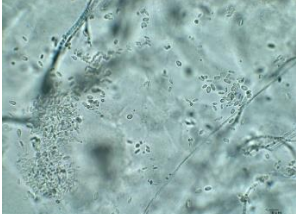



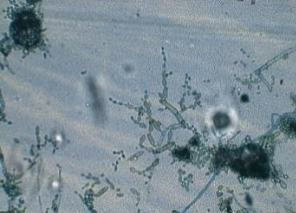

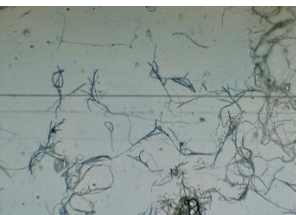

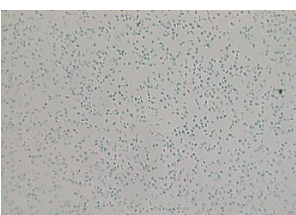




Code	Macroscopic features	Microscopic features	
C1P_A			Bacilli (Gram+)
C1A_A			Cyanobacteria 1
C1A_B			Cocos (Gram+)
C1NA_A			Cocos (Gram+)
C1NA_B			Bacilli (Gram+)


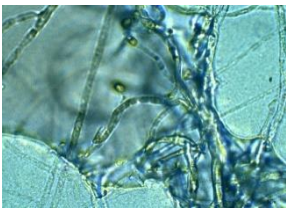
Code	Macroscopic features	Microscopic features	
C3P_A			Bacilli (Gram+)
C3A_b1			Bacilli (Gram+)
C3A_b2			Cocos (Gram-)
C3A_b3			Bacilli (Gram-)
C4A_b1			Cocos (Gram+)

For the bacterial isolates, it was possible to distinguish them according to their morphology: cocos or bacilli.

On the other hand, the cultivable fungi population is composed by several strains of yeast and filamentous fungi.

Table III-2. Characterisation of the fungi isolated from the stone with chromatic alteration.

Code	Macroscopic features	Microscopic features	
C1A_a'			Sterile mycelium
C1A_b			Sterile mycelium
C1A_c			<i>Cladosporium</i> sp.
C1A_d			Sterile mycelium
C2A_a			Yeast
C3_B			Sterile mycelium
C3_D			<i>Cladosporium</i> sp.

Code	Macroscopic features	Microscopic features	
C5A_A			Sterile mycelium

Based on macroscopic and microscopic characteristics, it was possible to discriminate one yeast and two microorganisms from the genus *Cladosporium* in the fungi isolates. For the other isolates it was not possible to identify their reproductive structures, being denominated by sterile mycelium, the vegetative part of any fungus.

Besides this, the isolates were identified by 16S, 18S and ITS sequencing. The DNA extracted was amplified (Annex C.2) through Polymerase Chain Reaction (PCR) with the specific primers previously described.

According with the best matches of the database used, the cultivable bacteria population (Table III-3) is essentially composed of bacteria belonging to the families Bacillaceae and Micrococcaceae. It is composed of four different microorganisms from the genus *Bacillus*, which two of them have high similarities with the species of *Solibacillus silvestris* and other has high similarity with the species *Bacillus cereus*. Moreover, it is composed of species of the genera *Exiguobacterium*, *Arthrobacter*, *Micrococcus*, and microorganisms with high similarity with the species *Kocuria rosea* and *Microbacterium murale*.

Table III-3. Identification of the microorganisms isolated from the cultivable population.

Code	Closest related type strain on basis of 16S and 18S rRNA gene and ITS	Similarity	Accession Numbers (NCBI)	Family	Class	Phylum
C1P_A	<i>Bacillus cereus</i>	96%	EF195169	Bacillaceae	Bacilli	Firmicutes
C1A_A	<i>Exiguobacterium</i> sp.	95.1%	X86064	Bacillaceae	Bacilli	Firmicutes
C1A_B	<i>Kocuria rosea</i>	94.3%	DQ060382	Micrococcaceae	Actinobacteria	Actinobacteria
C1NA_A	<i>Micrococcus</i> sp.	97%	JN181252	Micrococcaceae	Actinobacteria	Actinobacteria
C1NA_B	<i>Microbacterium murale</i>	93.9%	KR476461	Microbacteriaceae	Actinobacteria	Actinobacteria
C3P_A	<i>Solibacillus silvestris</i>	93.8%	EU249562	Bacillaceae	Bacilli	Firmicutes
C3A_b1	<i>Solibacillus silvestris</i>	93.6%	AJ006086	Bacillaceae	Bacilli	Firmicutes
C3A_b2	<i>Arthrobacter</i> sp.	95.1%	AJ785761	Micrococcaceae	Actinobacteria	Actinobacteria
C3A_b3	<i>Bacillus</i> sp.	95.2%	KP728948	Bacillaceae	Bacilli	Firmicutes
C4A_b1	<i>Exiguobacterium</i> sp.	96%	JX945789	Bacillaceae	Bacilli	Firmicutes
C2A_a	<i>Rhodotorula mucilaginosa</i>	99%	MG020687.1	Sporidiobolaceae	Pucciniomycetes	Basidiomycota
C1A_a'	<i>Phoma</i> sp.	99%	MH029124.1	Didymellaceae	Dothideomycetes	Ascomycota
C1A_b	<i>Phoma herbarum</i>	99%	LC085217.1	Didymellaceae	Dothideomycetes	Ascomycota
C1A_c	<i>Cladosporium ramotenellum</i>	99%	MG548565.1	Davidiellaceae	Dothideomycetes	Ascomycota
C1A_d	<i>Phoma herbarum</i>	98%	MH858359.1	Didymellaceae	Dothideomycetes	Ascomycota
C3_B	<i>Phoma</i> sp.	96%	KF411578.1	Didymellaceae	Dothideomycetes	Ascomycota
C3_D	<i>Cladosporium</i> sp.	100%	MG975642.1	Davidiellaceae	Dothideomycetes	Ascomycota
C5A_A	<i>Schizophyllum commune</i>	98%	MF280930.1	Schizophyllaceae	Agaricomycetes	Basidiomycota

The figure III-11 shows the phylogenetic tree constructed for the isolated bacteria and reveal two main clusters. One cluster with six microorganisms from the phylum Firmicutes (*Bacillus* sp, two *Solibacillus silvestris*, *Bacillus cereus*, and two

Exiguobacterium sp.), and the other cluster is formed with Actinobacteria (*Microbacterium murale*, *Kocuria rosea*, *Micrococcus* sp. and *Arthrobacter* sp.).

Previous studies showed that some of these microorganisms have already been found in limestone-built heritage showing signs of deterioration, such as *Solibacillus silvestris* (Skipper et al., 2016), *Bacillus cereus* (Sasso et al., 2013; Skipper et al., 2016) and other microorganisms belonging to the genera *Bacillus* (Banciu et al., 2013; Sasso et al., 2013; Skipper et al., 2016; Andrei et al., 2017), *Exiguobacterium* (Sasso et al., 2013; Andrei et al., 2017), *Arthrobacter* (Jroundi et al., 2010; Banciu et al., 2013; Sasso et al., 2013; Andrei et al., 2017) and *Kocuria* (Jroundi et al., 2010; Banciu et al., 2013). Besides this, some authors suggested the capability of some of these microorganisms to induce extracellular precipitation of calcium carbonates in decayed limestones (Oriol et al., 1993; Castanier et al., 2000).

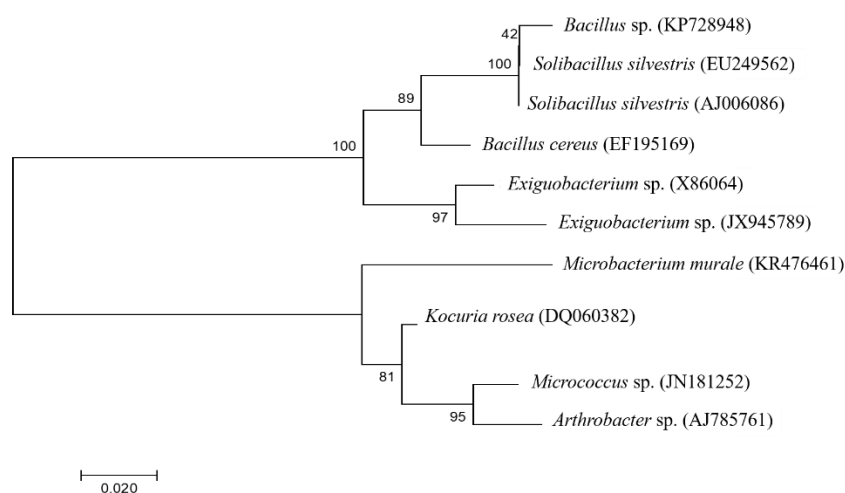


Figure III-11. Phylogenetic relationship between the prokaryotic isolates.

The fungi population isolated (Table III-3) belongs mainly to the class Dothideomycetes, and it is composed of different species of the genera *Phoma* and *Cladosporium*. The presence of a species with high similarity with *Schizophyllum commune* complete the composition of the isolated fungi population.

Figure III-12 shows the phylogenetic tree for the eukaryotic isolates. The two major clusters are composed of four isolated sequences belonging to the genus *Phoma*, and two isolated sequences that belong to the genus *Cladosporium*.

Some microorganisms of the genus *Cladosporium* has been associated with stone weathering, causing deterioration patterns as discolouration (Grbic and Vukojevic, 2009;

Hallmann et al., 2011) and is considered one of the most abundant genera found on calcareous stone of historic monuments (Miller et al., 2008). *Schizophyllum commune* not only has been related to the biodeterioration of stone but, moreover, has also been used as a model organism to study the role of filamentous basidiomycete fungi in black slate' bioweathering (Kirtzel et al., 2017).

Regarding the yeast population, a microorganism with high similarity with *Rhodotorula mucilaginosa* was isolated. This species has also been found previously on historic buildings and related to its biodeterioration (Páramo-Aguilera et al., 2012).

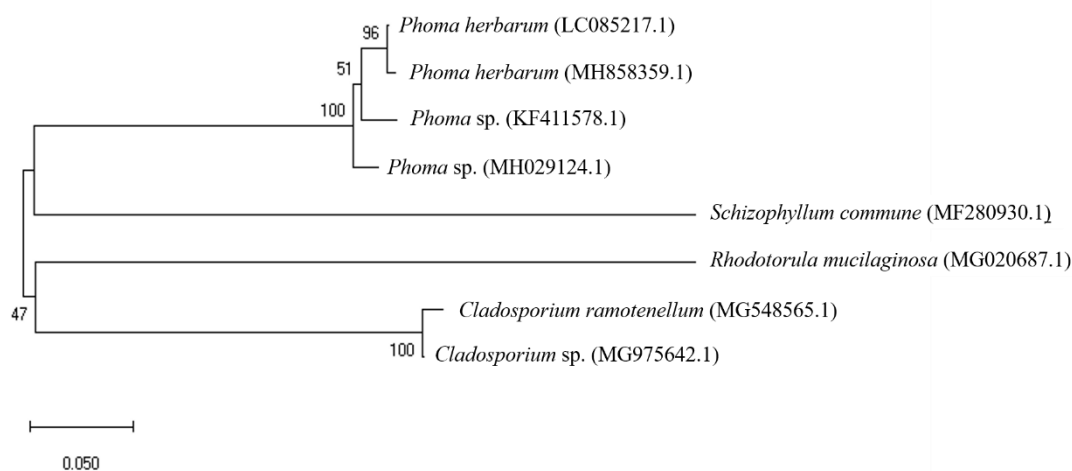


Figure III-12. Phylogenetic relationship between the eukaryotic isolates.

Most of the isolates obtained in this work have been related with stone weathering, in both ornamental stone and historic monuments made of stone. The isolated strains are deposited in the microbial collection of the Unity of Biodegradation and Biotechnology from the HERCULES Laboratory – Évora University, opening the possibility to its further use to assess their effects on colonisation of stones.

It is thought that only less than 1% of the estimated microbial diversity are cultivable (Dupont et al., 2014). Thus, high-throughput sequencing (HTS) approaches allowed to characterise in detail the total microbial community present on the limestone altered areas, for both prokaryotic and eukaryotic population (Annex C.3).

For the prokaryotic population the dominant phyla (Fig. III-13a) were Actinobacteria (87.2%) and Proteobacteria (7.1%), while the prevalent families (Fig. III-13b) were Geodermatophilaceae (36.8%), Micrococcaceae (19.4%) and Nocardioidaceae (10.9%). The most abundant genus is *Modestobacter* (25.3%), previously related with degradation

in cultural heritage made of limestone (Urzi et al., 2001). Other less representative genera were also identified, like *Geodermatophilus*, *Agrococcus*, *Arthrobacter* and *Deinococcus*.

For eukaryotic population, the predominant genera identified were *Coniosporium* and *Cladosporium* (Fig. III-14). As referred above, species of *Cladosporium* has been related with stone weathering, but *Coniosporium* species may also have an important role (De Leo et al., 1999). This approach confirmed also the presence of microorganisms belonging to the genera *Cladosporium* and *Phoma*, previously isolated.

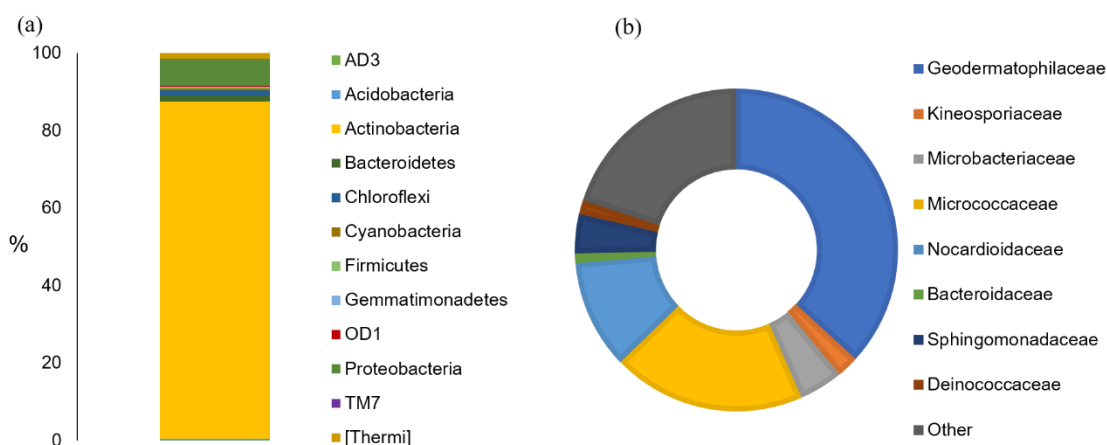


Figure III-13. Characterisation of the prokaryotic population present on limestone altered areas at (a) phylum and (b) family levels.

These results seem to indicate that the main biocolonisers of this limestone are bacterial communities, in particular Actinobacteria have the most important role in the colonisation of this material.

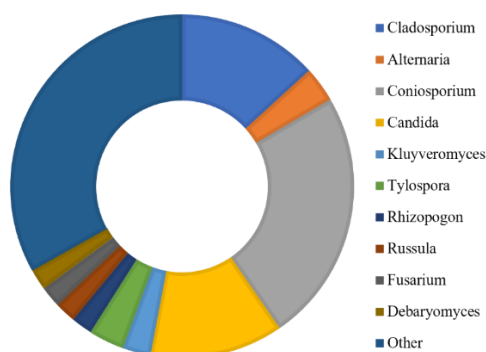


Figure III-14. Characterisation of the eukaryotic population at genera level present on limestone altered areas.

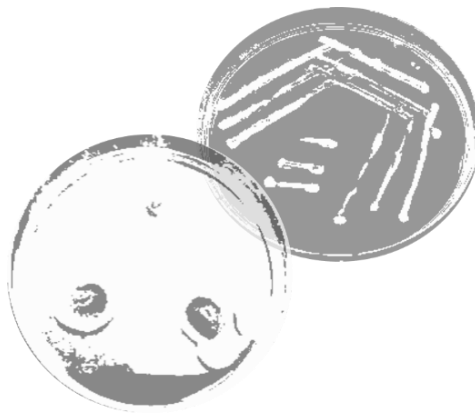
Both conventional and HTS approaches encompassed and give useful information about the presence of biocontamination, allowing the characterisation of the microbial diversity. In this work, important and detailed description about the communities able to develop on the blue limestone was provided, and the possibility to use the isolated microorganisms for simulation assays.

The results point out that these changes in the stone mineralogy through natural weathering may provide favourable conditions to microbial proliferation on the damaged surfaces, due to the increment of the surface roughness and further enhancement of the microorganisms' capacity to penetrate and anchor within the damaged surface. Therefore, the inorganic initial surface alteration promotes the biocolonisation that will increase the degradation rate, creating a cause-effect cycle.

This study constitutes an important contribution to understand the mechanism of colour alteration occurred on the blue limestone, and the results point out the possible influence of the communities in the natural degradation process (Fig. III-10) of the stones.

Chapter IV:

Evaluating the contribution of biocontamination on the blue limestone discolouration



Publications and dissemination:

- Papers:
 - **L. Dias**, T. Rosado, A. Candeias, J. Mirão, A. T. Caldeira. “Linking ornamental stone discolouration to its biocolonisation state”. *Building and Environment* (paper submitted).

- Communications in Conferences:
 - **L. Dias**, T. Rosado, A. Candeias, J. Mirão and A. T. Caldeira. “Colour change in carbonated stones enhanced by microbial activity”. Encontro Ciência 2019, Lisbon, Portugal. July 8-10, 2019.

4.1. Introduction

The conservation of natural stone applied in historic monuments or new buildings remains a challenge for the conservators-restorers. Although stone being a piece of cultural symbolism for many societies, the efforts of the scientific community have not been completely successful, in order to understand the complex issues of its deterioration. As previously mentioned, one of the most important characteristic and visible aspect that affects the features of natural stone is the colour, since discolouration creates unacceptable aesthetic patterns, and consequently a negative impact on their appreciation and economic value. There are too many factors that may induce weathering and subsequent discolouration of natural stone, and for many authors the main important ones are its composition, atmospheric conditions and biodeteriogenic agents (Polo et al., 2010; Orihuela et al., 2014).

In this context, one of the main gaps of the scientific community is the lack of association stone-microorganisms-colour because, for many decades, chemical and physical deterioration with non-biogenic origin were believed to be the main causes of stone deterioration (Villa et al., 2016). Most of stone buildings and monuments are exposed to outdoor environment and, consequently, are subjected to biological colonisation through endolithic, chasmolithic and epilithic ways. The mineralogical composition, porosity and surface roughness are properties that define the susceptibility of the stone substrata to biological colonisation, through the settlement, anchorage and development of the biocolonisers (Tiano, 2002; Miller et al., 2009; Jim and Chen, 2011; Gómez-Cornelio, 2012; Miller et al., 2012; Vázquez-Nion et al., 2018). Nutritional characteristics and stone surface finishing can influence the spatial and temporal development of the colonisers able to grow on it (Tiano, 2002). Moreover, some stone lithotypes are more susceptible to colonisation, that is commonly the case for limestone, since its degree of porosity is higher when compared with other stones (Cuzman et al., 2011; Miller et al., 2012; Pranjic et al., 2015).

One typical and important case of natural discolouration occurs on the blue limestone. The weathering of this stone results in the formation of calcium sulphates on the stone surface and, as it was previously suggested in the Chapter III, this alteration can promote biocolonisation which will increase the deterioration rate, creating a cause-effect cycle. In this way, there is a possibility that the alteration of the surface roughness may potentiate the microorganisms' ability to anchor and penetrate within the damaged

surface of the stone. This relationship needs to be fully investigated, and therefore demonstrate how the microbial proliferation influence the colour change rate on the blue limestone.

With this need in mind, this work aims to determine how the biocolonisers contributes for the discolouration process occurred on the blue limestone. For this purpose, accelerated artificial ageing was performed under controlled environmental parameters, using slabs of blue limestone. The stone slabs were inoculated with microorganisms previously isolated from blue limestone showing colour alteration patterns, collected in a real context, according with the previous Chapter. The colour and the microbial proliferation were evaluated and determined for 180 days.

4.2. Materials and methods

In order to investigate the effect of microbial agents in the natural discolouration process of the blue limestone, accelerated ageing assays were performed for 180 days, using stone slabs. A polished surface was used to mimic a finished stone and the stone slabs were placed in a water-contact condition, thus providing the conditions described in the section 3.3.2. of the Chapter III in order to induce its natural weathering. The communities' dynamic was studied for the inoculated and native communities of the stone. The microorganisms used for the inoculation of the slabs were those obtained from the blue limestone showing colour alteration patterns, previously described in the table III-3 of the previous Chapter.

4.2.1. Artificial ageing assay set-up

To inoculate the stone slabs, six isolated bacteria and five isolated fungi with high genetic similarity with *Arthrobacter* sp., *Bacillus* sp., *Exiguobacterium* sp., *Kocuria rosea*, *Microbacterium murale*, *Solibacillus silvestris*, *Phoma* sp, *Phoma herbarum*, *Cladosporium ramotenellum*, *Cladosporium* sp. and *Schizophyllum commune* were selected.

Fresh cultures of the bacteria and fungi isolates were inoculated in NA and MEA (Annex B), and incubated at 30°C and 28°C, during 2 and 7 days, respectively. After this, three different mixtures of microbial population were prepared, using sterile saline solution (NaCl 0.9%). One mixture is composed of six bacterial microorganisms (denominated mix of bacteria), another of five fungi microorganisms (denominated mix of fungi) and the last one is composed of the both previous mixtures (denominated mix of bacteria + fungi).

The blue limestone was collected in a quarry located in the MCE and carried to the laboratory in sterile bags, where were placed at 4°C until processing. Slabs were prepared (1,5 x 1,5 x 1,5 cm) in semi-aseptic conditions and inoculated with 1 mL of the different mixtures (mix of bacteria, mix of fungi, mix of bacteria + fungi) and incubated at 28°C and 30°C for 180 days. One slab was left without inoculation in order to study the native population of the stone. To maintain a high relative humidity, 1 mL of sterile water was periodically added (every 15 days) on the slabs. The assays were performed in triplicate.

The stone slabs were monitored under aseptic conditions at 0, 2, 7, 14, 30, 90 and 180 days after the inoculation, in order to determine the colourimetric alterations and to evaluate the dynamics of the microbial population (Fig. IV-1).

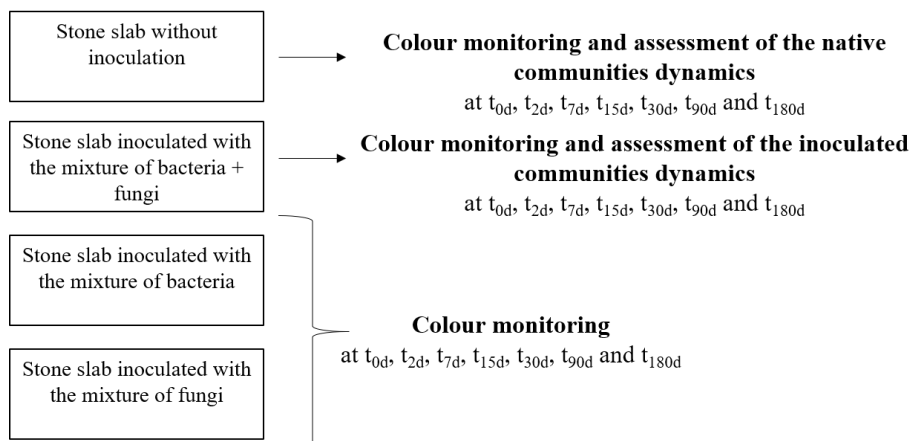


Figure IV-1. Scheme of the artificial ageing assays performed in lithotypes of blue limestone.

4.2.2. Macroscopic and microscopic monitoring

The macroscopic appearance of the stone slabs during the assay was recorded using a camera Nikon D3100.

At microscopic level, the slabs were observed using the stereoscopic microscope LEICA M205C, equipped with a digital camera Leica DFC295 (Leica Microsystems, Wetzlar, Germany), and a SEM coupled to an EDS spectrometer in order to get the particular details of each slab, using the same conditions described in the section 2.2.3.3. of the Chapter II.

After the 180 days, the stone slabs were coated with an Au/Pd target during 60 s and carefully examined by SEM at high vacuum mode, using 10 kV accelerating voltage to assess the microbial proliferation with higher resolution.

4.2.3. Colour monitoring

The colour of the stones' surface was monitored using the colourimetric parameters of the CIELAB space, previously described in the section 2.2.2. of the Chapter II, and also through Fiber Optic Reflectance Spectroscopy (FORS).

Using the CIELAB space, as previously mentioned, the L^* value refers to the luminosity variable, while a^* and b^* are the chromaticity coordinates. According to Mokrzycki and Tatol (2011), the colour difference (ΔE) can be obtained with the

following equation:

$$\Delta E = ((\Delta L)^2 + (\Delta a)^2 + (\Delta b)^2)^{1/2}$$

Where $\Delta L = L^*_{\text{txdays}} - L^*_{\text{t0days}}$; $\Delta a = a^*_{\text{txdays}} - a^*_{\text{t0days}}$; $\Delta b = b^*_{\text{txdays}} - b^*_{\text{t0days}}$.

The measurement of the colourimetric parameters was performed in aseptic conditions. Five distinct points of each stone slab were studied, with three measurements per point. The results are an average of these measurements.

The FORS spectroscopy analyses were performed using a portable spectrophotometer ASEQ LR1-T v.2, in the range of 300-1000 nm, with a spectral resolution of 1 nm, a time exposure of 100-200 ms, 5 scans during 5 s. The spectra were acquired using the software ASEQ CheckTR. Each slab was analysed in five distinct points, with three measurements per point.

4.2.4. Assessment of the microbial population dynamics

The study of the microbial population dynamic was performed by high-throughput sequencing (HTS), using the methodology previously described in the section 3.2.3.4. of the Chapter III.

4.3. Results and discussion

The action of biocolonisers on the blue limestone was investigated through artificial ageing tests, where the chromatic parameters and the proliferation capacity of the microbial community were evaluated, and its dynamics were characterised.

The colour was determined by spectroscopy techniques, and the dynamic of the microbial population during the ageing period was monitored through microscopic and HTS approaches. The complementary data contributed with relevant information to associate the effect induced by the microbial proliferation on the natural discolouration of this lithotype.

4.3.1. Determination of chromatic changes

To determine with accuracy the effects on its original colouration, the limestone slabs were analysed by non-invasive micro-analytical techniques.

The parameters $L^*a^*b^*$ were determined during the artificial ageing assays. The measurement of the colour difference (ΔE) was performed using the formula described in the section 4.2.3. and the results obtained are shown in the table IV-1.

Table IV-1. Measurement of the colourimetric parameters and determination of the colour difference for each slab.

Slab stone	Colourimetric parameters			ΔE	
	L^*	a^*	b^*		
t_{0d}	C	54.36 ± 1.29	0.76 ± 0.24	5.19 ± 0.87	0
	B	53.75 ± 2.20	0.75 ± 0.21	4.85 ± 0.93	0
	F	55.74 ± 2.84	0.67 ± 0.23	4.98 ± 0.69	0
	B+F	54.16 ± 0.95	0.67 ± 0.18	4.88 ± 0.64	0
t_{2d}	C	56.87 ± 1.86	0.67 ± 0.16	5.03 ± 0.68	2.52
	B	50.49 ± 2.83	0.82 ± 0.27	4.65 ± 0.96	3.27
	F	51.74 ± 3.06	0.69 ± 0.23	4.67 ± 0.75	4.03
	B+F	48.86 ± 3.13	0.95 ± 0.29	5.18 ± 1.05	5.33
t_{7d}	C	56.12 ± 1.34	0.72 ± 0.20	5.11 ± 0.75	1.76
	B	50.92 ± 2.40	0.84 ± 0.27	4.57 ± 0.94	2.85
	F	51.40 ± 2.82	0.66 ± 0.24	4.44 ± 0.88	4.42
	B+F	48.96 ± 1.16	0.91 ± 0.22	5.06 ± 0.72	5.21
t_{15d}	C	51.50 ± 1.95	0.93 ± 0.24	5.10 ± 1.01	2.17
	B	52.74 ± 2.62	0.86 ± 0.25	4.60 ± 0.92	1.42
	F	53.47 ± 3.43	0.75 ± 0.21	4.54 ± 0.82	2.43

Slab stone	Colourimetric parameters			ΔE	
	L*	a*	b*		
B+F	51.05 ± 0.95	0.96 ± 0.12	5.07 ± 0.52	5.22	
t _{30d}	C	55.37 ± 3.52	0.86 ± 0.27	5.07 ± 0.95	1.02
	B	54.99 ± 3.30	0.86 ± 0.21	4.73 ± 0.86	1.79
	F	53.92 ± 2.96	0.78 ± 0.24	4.32 ± 0.87	2.04
	B+F	51.53 ± 1.29	1.06 ± 0.26	5.04 ± 0.77	2.67
t _{90d}	C	53.01 ± 4.17	0.98 ± 0.28	4.54 ± 0.79	1.51
	B	52.20 ± 2.73	1.07 ± 0.25	5.07 ± 0.77	1.94
	F	54.74 ± 2.87	0.77 ± 0.27	3.95 ± 0.96	1.71
	B+F	52.23 ± 1.58	1.03 ± 0.18	4.78 ± 0.57	1.98
t _{180d}	C	54.13 ± 3.15	0.46 ± 0.22	3.54 ± 0.65	1.65
	B	52.79 ± 6.07	0.51 ± 0.30	3.65 ± 0.77	1.97
	F	53.15 ± 4.55	0.49 ± 0.19	3.33 ± 0.63	3.9
	B+F	48.36 ± 1.16	0.71 ± 0.16	4.04 ± 0.49	5.87

C – slab without inoculation; B – slab inoculated with bacteria; F – slab inoculated with fungi; B+F – slab inoculated with bacteria + fungi.

The results showed that the slabs inoculated with microorganisms exhibited always a higher ΔE , when compared with the slabs without inoculation (Fig. IV-2). Moreover, the slabs that presented the higher ΔE were those inoculated with a microbial population composed of the mixture of bacteria + fungi. On the other hand, the inoculated slabs that presented the lower ΔE values were those containing the mixture composed only of bacteria. After the 180 days, the ΔE was 1.64 for the slabs without inoculation, 1.97 for the slabs inoculated with bacteria, 3.90 for the slabs inoculated with fungi and 5.87 for the slabs inoculated with the mixture of bacteria + fungi.

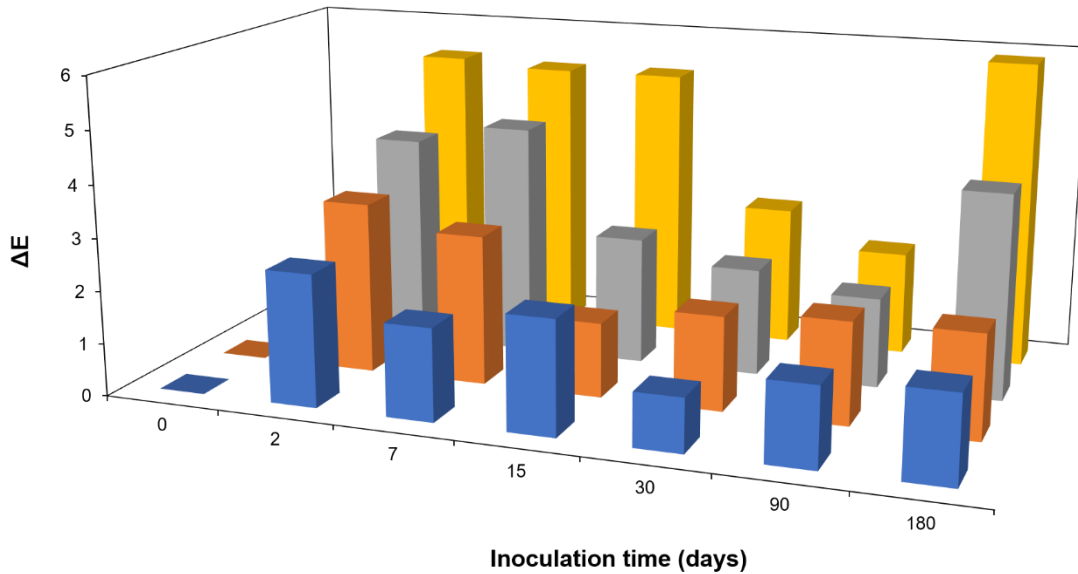


Figure IV-2. Graphical representation of the difference in total colour (ΔE) during the artificial ageing assays for the slab without inoculation (■), slab inoculated with bacteria (■), slab inoculated with fungi (■) and slab inoculated with bacteria + fungi (■).

Complementarily, FORS spectroscopy was performed on the stone slabs presenting the higher discolouration – the stone inoculated with the mixture of bacteria + fungi (Fig. IV-3). The results obtained showed a gradual change in the spectra along the ageing period, namely a vertical shift in the reflectance spectrum. The maximum shift is achieved for the spectrum obtained at the end of the artificial ageing, 180 days after the inoculation. Previous studies associated vertical shift of an reflectance spectrum with discolouration effects due to roughness modification of the substratum (Simonot and Elias, 2002).

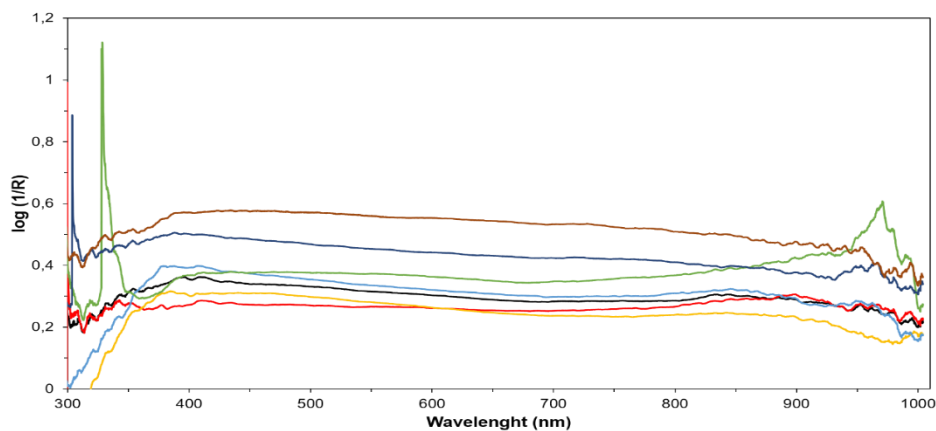


Figure IV-3. FORS spectroscopy spectra obtained for the slab stones inoculated with the mixture of bacteria + fungi, during the ageing assays. Spectra for the slab inoculated at t_{0d} (—), t_{2d} (—), t_{7d} (—), t_{15d} (—), t_{30d} (—), t_{90d} (—) and t_{180d} (—).

To validate these results, spectra at t_{0d} and t_{180d} were obtained from the slabs without any inoculation (Fig. IV-4), and the data collected revealed only slight differences between the two spectra since they nearly overlap. Therefore, the data obtained suggest that biocolonisation of this stone can increment the change of the stone surface.

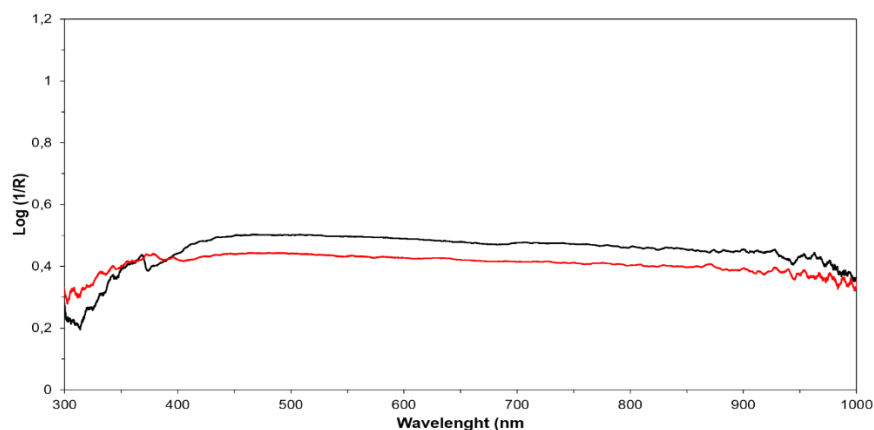


Figure IV-4. FORS spectroscopy spectra obtained for the slab without inoculation at t_{0d} (—) and t_{180d} (—).

The FORS spectroscopy results combined with colourimetry data suggest that biocolonisation of this limestone may have an effective contribution in its discolouration, since higher surface discolouration occurs when inoculated colonisers are present. This effect was more evident in the slabs that were inoculated with the microbial population composed of bacteria + fungi.

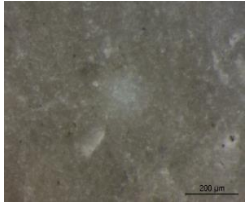
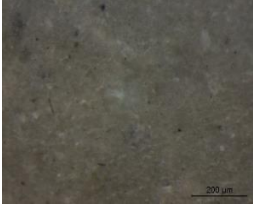

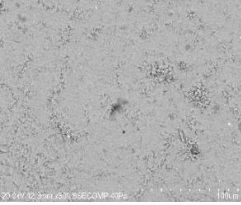
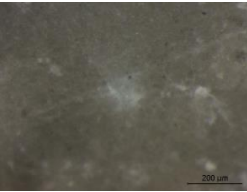
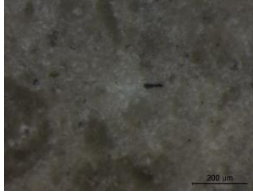
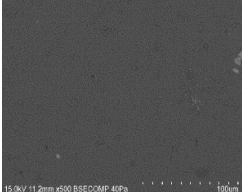
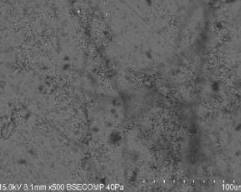
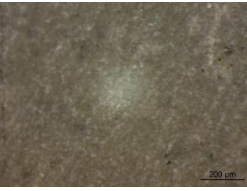
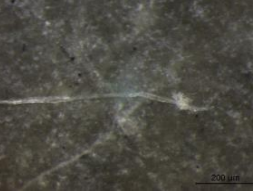

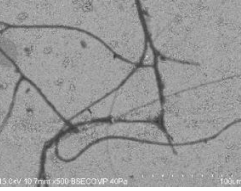


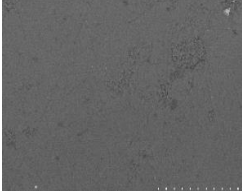
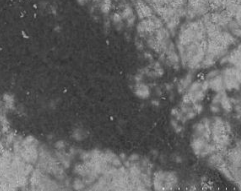
4.3.2. Assessment of the microbial population

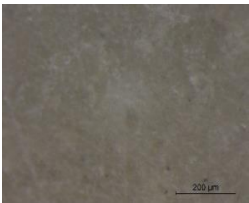
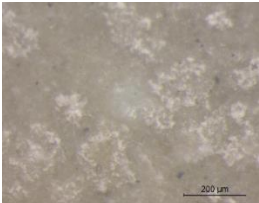
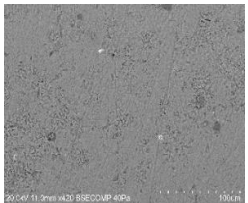
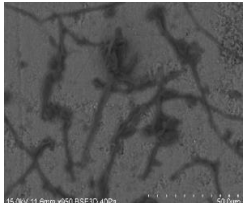
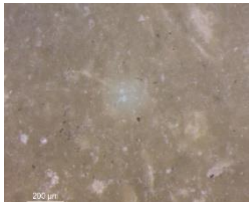
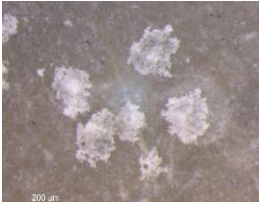
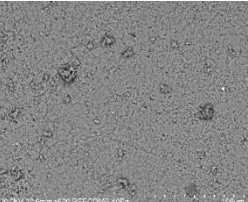
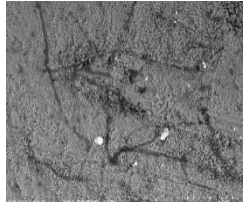
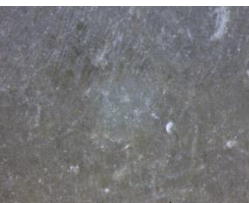
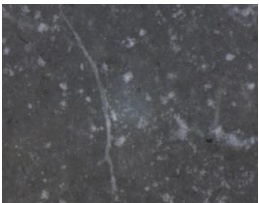
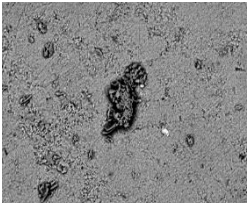
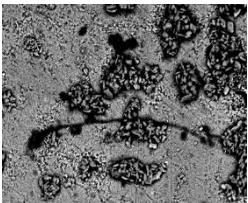
The microscopic features and the proliferation capacity of the microbial communities in this material were assessed (Table IV-2). Progressive formation of gypsum crystals on the surface of the stone slabs was observed, as well as the continuous ability of biological communities to develop on the substratum during the period of the ageing assays, without any addition of nutrients. Also noteworthy is the slight discolouration detected on the stone slabs by stereoscopic microscopy after the 15th day of inoculation, corroborating the colourimetric and FORS data.

The micrographs obtained by SEM revealed that this limestone seems to have a high susceptibility to biocolonisation, since that progressive development of microbial communities was observed throughout the artificial ageing (Fig. IV-5). After 30 days of inoculation, it was possible to observe already a considerable index of microbial agents'

proliferation, as well as formation of calcium sulphates resulted from the natural weathering of this stone.

Table IV-2. Microscopic monitoring of the stone slabs, through stereoscopic and scanning electron microscopy.

Inoculation time (days)	Stereoscopic microscope		SEM	
	No inoculation	B + F*	No inoculation	B + F*
0				
2				
7				
15				

Inoculation time (days)	Stereoscopic microscope		SEM	
	No inoculation	B + F*	No inoculation	B + F*
30				
90				
180				

*B+F – stone slab inoculated with the mixture bacteria + fungi.

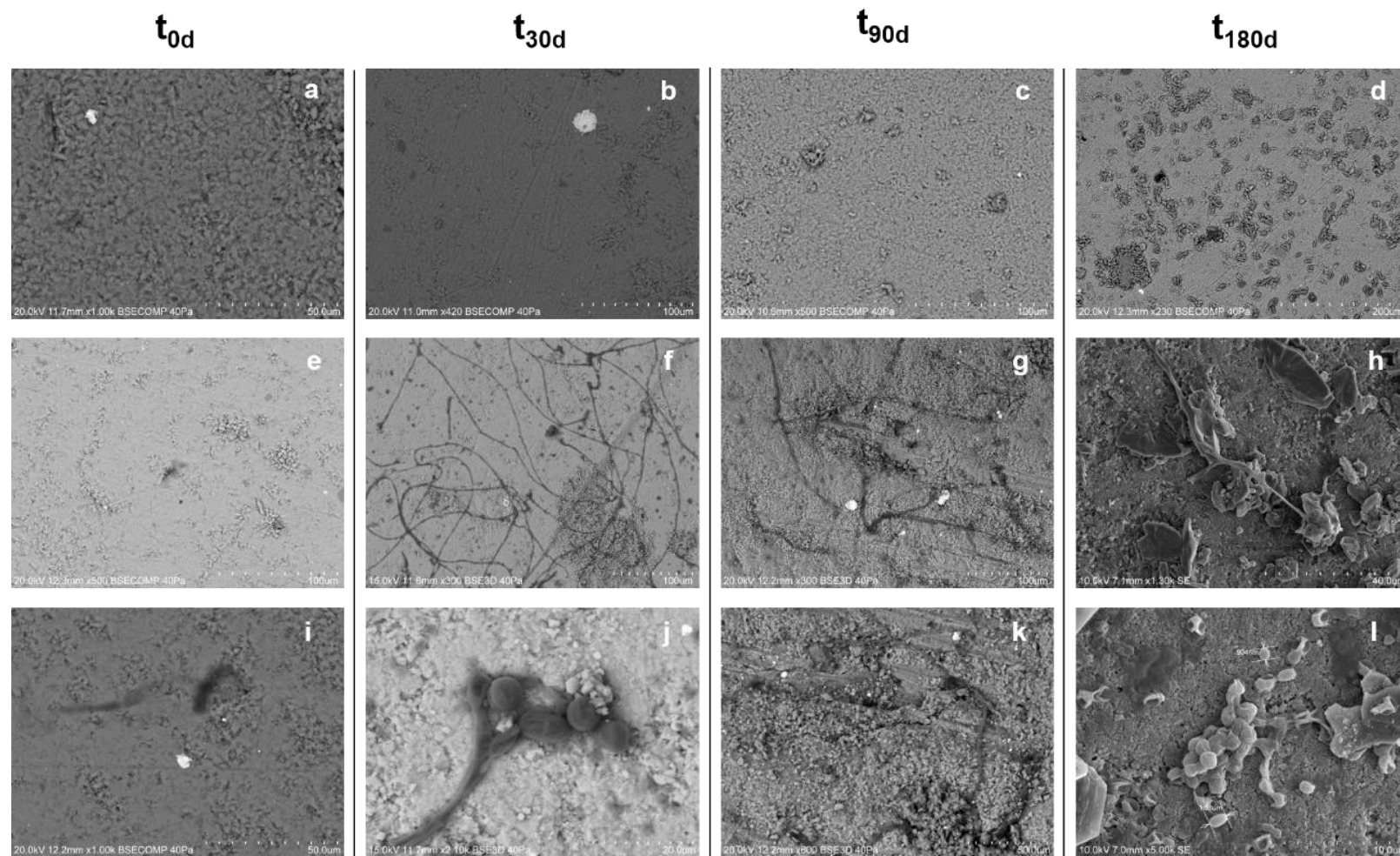


Figure IV-5. Microbial proliferation on the slabs during the ageing. Slabs without inoculation (a-d) and slabs inoculated with the mixture bacteria + fungi (e-l).

Using the EDS detector, it was possible to determine the presence of elements like carbon, nitrogen and oxygen, which are indicators of the presence of organic material, while sulphur and calcium reveals the formation of calcium sulphates (Fig. IV-6).

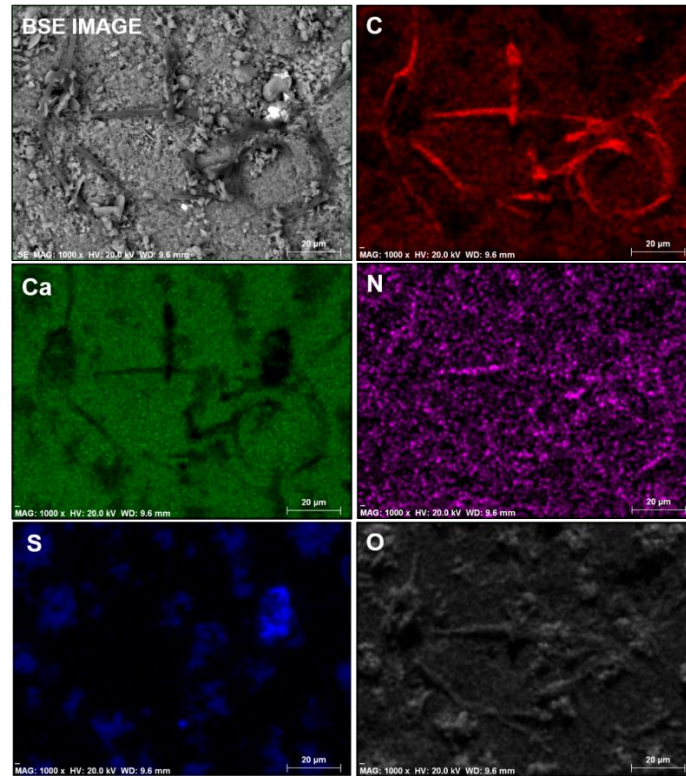


Figure IV-6. Element mapping of calcium, sulphur, carbon, nitrogen and oxygen obtained by VP-SEM-EDS at t_{30d} on the slab containing the mixture bacteria + fungi.

The micrographs acquired after the 180 days of inoculation revealed that the microbial population was composed mainly by filamentous fungi, spores and bacteria that were proliferating around the calcite and gypsum crystals (Fig. IV-7).

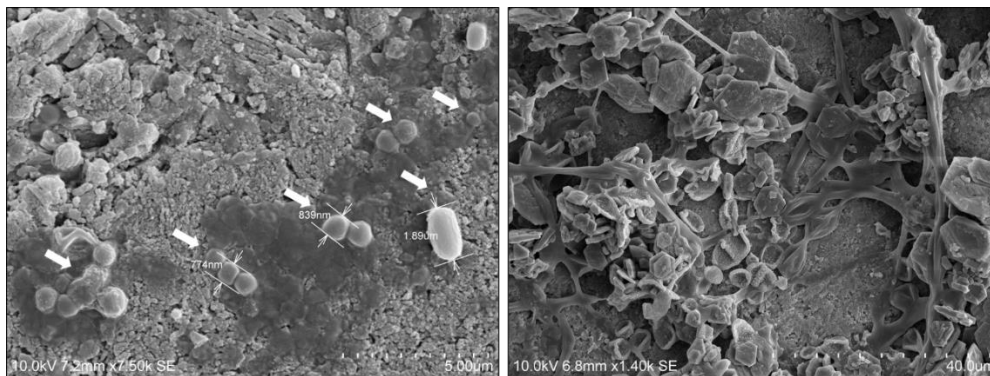


Figure IV-7. SEM micrographs on the stone slabs at t_{180d} that indicate the presence of bacteria, hyphae of filamentous fungi and spores proliferating around the calcite and gypsum crystals.

The microbial population developed and its evolution during the assay were characterised through HTS using the Illumina[®] MiSeq platform. The stone slabs were inoculated with 3 different microbial mixtures, as described above in the section 4.2. The presence of native population on the stone and their evolution were also assessed.

Regarding the inoculated bacteria (Fig. IV-8), after 15 days of inoculation the dominant genus was *Solibacillus* (3.4%), followed by the genera *Arthrobacter* (2.2%), *Microbacterium* (0.9 %) *Exiguobacterium* (0.9%), *Bacillus* (0.6%) and *Kocuria* (0.2%). After the 180 days of inoculation, microorganisms belonging to the genus *Arthrobacter* are the dominant (7.2%), followed by the genera *Bacillus* (2.6%), *Exiguobacterium* (1.8%), *Microbacterium* (1.4%) and *Kocuria* (0.7%). Microorganisms belonging to the genus *Solibacillus* were not identified at t_{90d} and t_{180d} . The results pointed out that the microorganisms belonging to the genus *Arthrobacter* revealed the ability to develop on this substratum, even when they are competing with microorganisms of other genera, since their relative percentage raised along the 180 days of the artificial ageing assays.

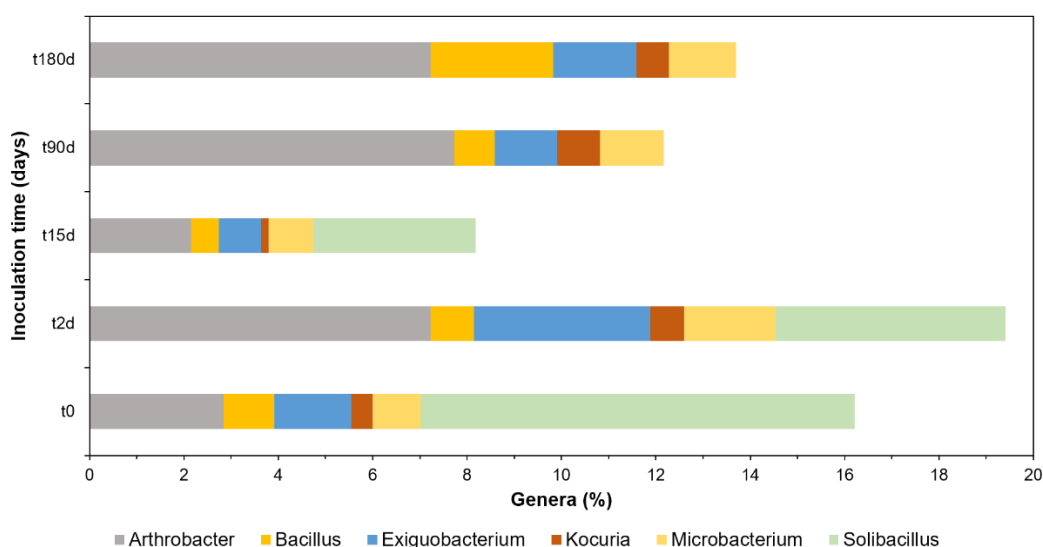


Figure IV-8. Dynamic of the prokaryotic population inoculated on the stone slabs during the artificial ageing assays.

Considering the total communities (namely inoculated and native population), the most representative prokaryotic population (Fig. IV-9) at the beginning of the inoculation is composed of microorganisms belonging to the genus *Microbispora* (17.3 %). The proliferation of these microorganisms remained stable along the time, as well as the microorganisms belonging to the genera *Enterobacter* and *Exiguobacterium*. The

microorganisms of the genus *Solibacillus* had a slight decrease over time, while the microorganisms of the genera *Zhihengliuella* and *Arthrobacter* had a slight increase. At t_{2d} , the genus *Pseudomonas* turned up into the dominant genus until the end of the artificial ageing, composing 38.9 % of the prokaryotic population. The genus *Lactococcus* was part of the dominant genera until the 15 days of the inoculation. After the 180 days of inoculation, the prokaryotic population was mostly composed of microorganisms of the genus *Pseudomonas* (38.9%), followed by the genera *Zhihengliuella* (11.6%), *Microbispora* (9.5%), *Arthrobacter* (7.2%), *Enterobacter* (2.9%), *Exiguobacterium* (2.4%) and *Solibacillus* (1.6%). Previous studies indicate that microorganisms belonging to the genera *Microbispora*, *Enterobacter*, *Exiguobacterium* and *Solibacillus* have been found on ornamental stone and on historical limestone buildings in biodeterioration context (Piñar et al., 2010; Ettenauer et al., 2011; Niyomyong et al., 2012), while *Pseudomonas* were previously described as carbonatogenic microorganisms using ornamental stone as substratum (Piñar et al., 2010).

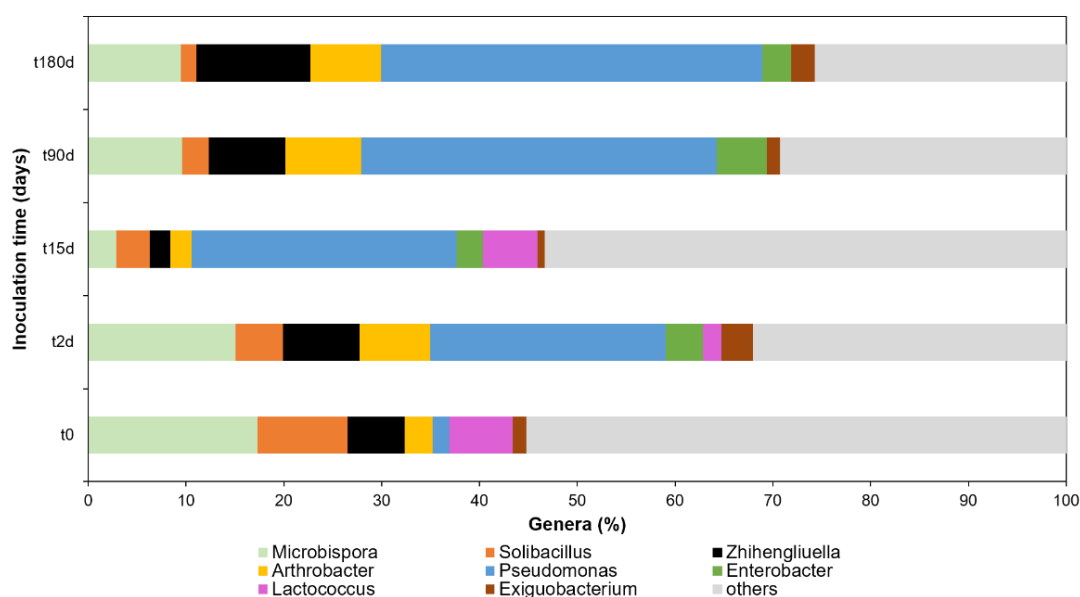


Figure IV-9. Dynamic of the most representative inoculated and native prokaryotic population present on the stone slabs during the artificial ageing assay.

Regarding the eukaryotic population (Fig. IV-10), at the beginning of the ageing assays the major microorganisms identified belong to the genera *Mycosphaerella* (38.3%), *Didymella* (33.9%) and *Fusarium* (6.5%). After 7 days of the inoculation, the microorganisms belonging to the genus *Fusarium* revealed a pronounced development

on the stone slabs, being the major genus identified in this period (24.7%), followed by the genera *Hannaella* (17.5%), *Devriesia* (9.3%), *Dirina* (4.7%), *Chaetomium* (3.1%) and *Penicillium* (3%). After 30 days of the inoculation, the major fungi population was equally composed of microorganisms belonging to the genera *Penicillium* (19.4%), *Fusarium* (18.5%), *Chaetomium* (18.2%) and *Hannaella* (17.4%). At the end of the ageing assays, the fungi population was mainly composed of *Didymella* (41.4%), *Fusarium* (34.8%) and *Mycosphaerella* (12%).

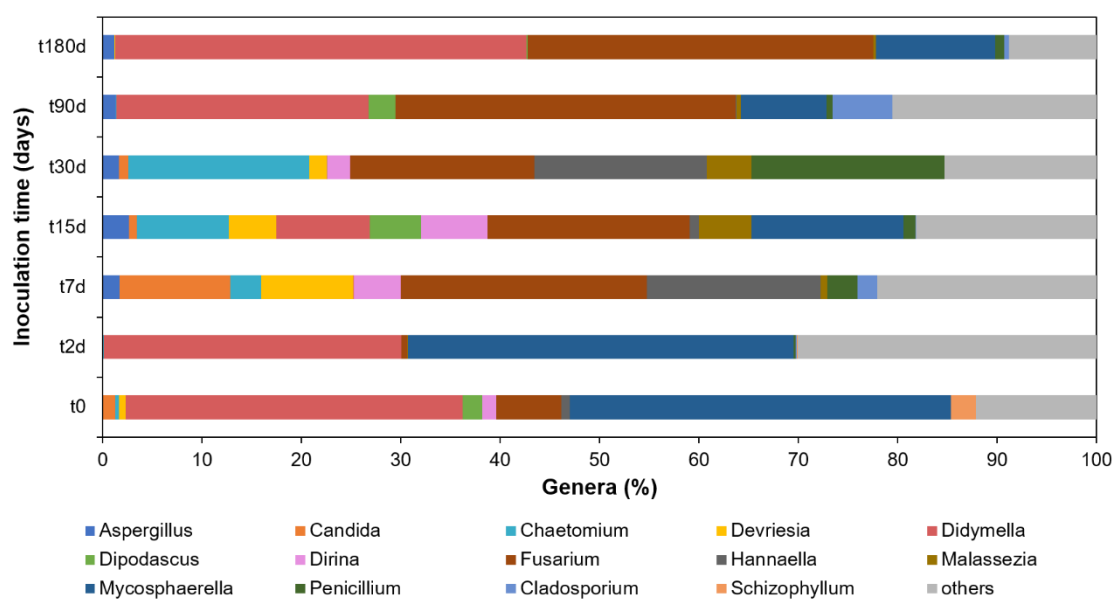


Figure IV-10. Dynamic of the most representative inoculated and native eukaryotic population present on the stone slabs during the artificial ageing assays.

Some of these microorganisms have already been associated or isolated from stone materials. For example, microorganisms of the genera *Fusarium* and *Penicillium* have the ability to form biofilms “in vitro” on limestone, sandstone and granite materials (de la Torre et al., 1993), and have also been related with biofilms’ formation on surfaces of historic buildings made of limestone (Mitchell and Gu, 2000; Rosa-García et al., 2011; Gómez-Cornelio et al., 2012), or even on concrete (Gu et al., 1988). Additionally, microorganisms of the genera *Hannaella* and *Chaetomium* has recently been reported to be a part of a patina formed on a weathered limestone (Li et al., 2018b), and microorganisms of the genera *Chaetomium* and *Dirina* were suggested to play an important role in the transformation of limestone minerals through their weathering (Burford et al., 2003; Llop et al., 2013; Seaward, 2014; Cañaveras et al., 2015).

The inoculated fungi population had an insignificant evolution when compared with the native fungi population, which can be another indicator that bacteria may play the major role in the biodeterioration of this stone.

The execution of this methodology seems to be useful for the evaluation of the contribution of biogenic colonisation on the natural weathering of this important ornamental stone lithotype. The data obtained instrumentally revealed that the rates of the discolouration increased for the stone slabs inoculated with microorganisms, when compared with stone slabs without inoculation. This rate increment was particularly higher when the biocolonisers were composed of both fungi and bacteria population. Additionally, it was possible to evaluate the great capacity of microbial growth on this material, since that microbial development increased period after period (Fig. IV-6). As described in the previous Chapter, this is much probably related with the increase of the surface roughness of the stone and further microorganisms' capacity to anchor and penetrate within it.

On the other hand, it was possible to evaluate the dynamics of the microbial population that colonise this material during the artificial ageing assays, using HTS, a faster, reliable and precise technology. Thus, it was possible to identify the microorganisms that may play the major role in the biodeterioration of this lithotype. The most predominant microorganisms at the end of the artificial ageing belong to the genera *Pseudomonas*, *Zhihengliuella*, *Microbispora*, *Arthrobacter*, *Enterobacter*, *Exiguobacterium* and *Solibacillus* for the bacterial population, and *Didymella*, *Fusarium* and *Mycosphaerella* for the fungi population.

Chapter V:

Characterisation of the colour change
on carbonated stones applied in
cultural heritage



Publications:

- Papers:
 - **L. Dias**, T. Rosado, A. Candeias, J. Mirão, A. T. Caldeira (2019). A change in composition, a change in colour: The case of limestone sculptures from the Portuguese National Museum of Ancient Art, *Journal of Cultural Heritage*. DOI: 10.1016/j.culher.2019.07.025;
 - T. Rosado, **L. Dias**, M. Lança, C. Nogueira, R. Santos, M.R. Martins, A. Candeias, J. Mirão and A.T. Caldeira (2019). “Assessment of microbiota present on outdoor stone materials using high throughput sequencing approaches”, *MicrobiologyOpen* (under revision).

- Communications in Conferences:
 - **L. Dias**, T. Rosado, A. Candeias, J. Mirão, A. T. Caldeira, “A closer look into limestone sculptures’ degradation from the Portuguese National Museum of Ancient Art”. I Workshop on Heritage Stones, Salamanca, Spain, 2-4 October 2018;
 - T. Rosado, **L. Dias**, A. Candeias, J. Mirão, A.T. Caldeira, “Biocolonisation of Cultural Heritage stone materials”. Web of Knowledge, Évora, Portugal, 17-19 May 2018;
 - **L. Dias**, C. Salvador, A. Candeias, J. Mirão, A. T. Caldeira, “Characterization and biodegradation evaluation in a limestone sculpture”, SPB2016-XIX National Congress of Biochemistry, Guimarães, Portugal, 8-10 December 2016.

Part of this Chapter was written based on an article published with scientific peer review entitled “A change in composition, a change in colour: The case of limestone sculptures from the Portuguese National Museum of Ancient Art” (Dias et al., 2019).

5.1. Introduction

An important part of our cultural heritage assets is made of stone, since has always been a prime material of choice due to its beauty and properties (Eyssautier-Chuine et al., 2015). Specifically, colour is a key-factor in selecting a particular stone. Like any other material, stone is subjected to deterioration mechanisms, that can be caused by external (temperature, humidity, air pollution, biogenic agents, etc) or internal (e.g. composition, bioreceptivity) factors (El-Gohary, 2007; Polo et al., 2010). It is known that the main harmful deterioration agents which commonly may affect carbonated stones are water, soluble salts and biodeteriogenic agents, that can induce physical and chemical deterioration (Pires et al., 2010; Polo et al., 2010).

As previously mentioned in the Chapter I, water can disaggregate stone through the phenomenon of hygric and hydric swelling. Water may hydrate or hydrolyse minerals and can also transport compounds able to oxidise/reduce elements of minerals. Additionally, water may introduce soluble minerals in solution like hydrous and anhydrous forms of chlorides, carbonates, and sulphates of Ca, Na and Mg which, after precipitation, have a strong effect in limestone deterioration (Pires et al., 2010).

Moreover, many biodeteriogens, organisms that are involved in deterioration processes like bacteria, fungi, algae, and lichens can be found in stone (Polo et al., 2010; Abdelhafez et al., 2012; Dakal and Cameotra, 2012). Usually, the composition of the microbial populations present on a stone is very complex, which is the result from a successive colonisation of different communities over several years (Abdelhafez et al., 2012). In this case, the mechanical damage is mainly caused by the penetration of fungal structures into the stone and by the tallus expansion /contraction under environmental conditions' changes such as humidity. Furthermore, as mentioned in the Chapter I, chemical dissolution can occur through the reaction between the carbonates and the acids secreted by the biodeteriogenic agents (Charola et al., 2007; Corvo et al., 2010; Doehne and Price, 2010). Biodeteriogenic agents can also induce staining on stone, which is dependent of the compounds produced by the biodeteriogens (Polo et al., 2010). Carotenoids, which are mainly produced by filamentous fungi and yeasts, as well as by

some species of bacteria, algae and lichens (Rosado et al., 2014a) impart yellow to red hues to the stones.

To predict or prevent the loss of our common heritage, it is necessary to be able to characterise the different lithotypes existing, describe its deterioration model and measure its extent. Only after, it is possible to comprehend the behaviour of a stone placed in a particular environment (Doehne and Price, 2010). There is an emergent need to preserve our cultural heritage, thus it is necessary to give the right indications to create the best opportunities for the conservator-restorers to do their work in the appropriate way.

In this chapter, two types of calcareous stone applied in historic artworks and monuments – limestone and marble – were selected as case studies. These materials show diverse types of pathologies and are placed under different environment conditions. This work aims to characterise the stones and alteration products formed, and their main microbial colonisers, in order to determine the causes for the deterioration of these historical and cultural heritage assets.

5.1.1. Limestone-built sculptures

Considered one of the major challenges for conservator-restorers, the deterioration of artworks may result in the decay of its matrix and, consequently, the loss of carved details and original intention of the sculptor (El-Gohary, 2007). It is known that the storage/exposure of our heritage to indoor environments does not mean that the artworks are protected against harmful levels of deterioration agents (Corvo et al., 2010).

Four sculptures (Fig. V-1) from the Portuguese National Museum of Ancient Art (NMAA, Lisbon) (38° 42' 16.654'' N 9° 9' 42.527'' O) with aesthetic and structural damages were selected for this study, in order to characterise their chromatic alterations and some material loss. The sculptures *St. John the Baptist*, *St. Paul* and *The Virgin and the Child* are attributed to the sculptor João de Ruão and are dated to the 16th century. The other sculpture, *Musician Angel*, was created in the Workshop of the Portal of the Monastery of Batalha directed by Master Huguet and is dated to the 15th century. The sculptures have been maintained under indoor environment conditions but in different rooms (both with windows occasionally opened) and exhibit different types of pathologies.



Figure V-1. Limestone sculptures selected for the study, located at the NMAA. *St. John the Baptist* (a), *The Virgin and the Child* (b), *St. Paul* (c) and *Musician Angel* (d).

5.1.2. Heritage building made of marble

Estremoz (Portugal) has been since antiquity one of the most exploited sources of marble in the Mediterranean. As mentioned before in the Chapter I, the Estremoz Anticline is the main centre of Portuguese marble exploitation and one of the most important at worldwide. In the Middle Ages, marbles from Estremoz were used for the construction of castles, palaces and other buildings (Lopes and Martins, 2012). Since the 15th century, these marbles became used both nationally and internationally, having been exported to other continents by Portuguese explorers. After this period, these marbles began to be searched for ornamental purposes and are currently present in several national and international monuments (Lopes and Martins, 2012).

One of the national building made of marble from Estremoz, the Convent of “São João da Penitência” (38° 50’ 44’’ N 7° 35’ 30’’ O) (Fig. V-2), was selected in order to understand the deterioration processes that are affecting the features of the stone, namely its colour and strength. This Convent, situated in Estremoz, in the eastern side of the main square of the village (Rossio Marquês de Pombal), was founded in 1501-02 by the King

Manuel I. Here, climate is wet and temperate, and the yearly average temperature and average rainfall are 15.6°C and 699 mm, respectively.



Figure V-2. The manueline architecture of the Convent of “São João da Penitência” ^[5].

The Convent was instituted in 1519, being the only Monastery of the Knights of Rhodes in Portugal and subsequently was incorporated into the Order of Malta. The church is contemporary of 16th century structural design, boasting of Manueline architecture. The area was enlarged in the 17th century with a second archway, supported by Tuscan pillars. Each wing has ten arches, subdivided into four twin arches and two simple ones (Crespo, 1949; Mandeiros, 2001).

The main cloister, made of marble, has been subjected to deterioration, leading to appearance of unacceptable aesthetic patterns, namely staining and loss of cohesion (Fig. V-3).

⁵ www.cm-estremoz.pt, accessed at February 2019;



Figure V-3. Some of the pathologies found in the main cloister of the Convent. Dark staining on column stems (a), reddish staining with detachment of the material (b and e), and patina formations on the Tuscan pillars (c) and on the stone walls (d).

This study intends to characterise the stone, to detect the alteration products and assess the microbial colonisers, in order to determine the causes of the colour alteration and the loss of the cohesion in specific areas of the Convent.

5.2. Materials and methods

The sculptures show two different types of pathologies, which are affecting their original colour and integrity (Fig. V-4). The *St. John the Baptist* and *The Virgin and the Child* sculptures show white stains for almost the entire surface, while the *St. Paul* and *Musician Angel* sculptures show red stains and loss of material. On average, the yearly temperature and relative humidity values of the floor where the sculptures are placed range between 18.5-23.5 °C and 40-65 %, respectively.



Figure V-4. Limestone sculptures subjected for deterioration study and details of their pathologies.

On the other hand, the Convent of “São João da Penitência” has the main cloister made of marble. In the cloister, six areas were signalised by having a colour alteration on the stone surface, namely areas with white and yellow patinas, red stains and fissures, and areas with reddish and blackish biofilms (Fig. V-5). These areas were chosen for being representative of the diverse pathologies that are affecting the marble of this building. A non-altered surface of the stone was selected in order to use it as a control specimen.



Figure V-5. Areas selected for the methodology approach. Areas CM1 and CM2 correspond to white and yellow patinas (a, b), areas CM3 and CM4 correspond to reddish stains and fissures (c, d), areas CM5 and CM6 correspond to formation of red and dark biofilms (e, f).

To study the marble from the Convent, an *in-situ* approach was initially performed using the methodologies following described.

5.2.1. *In-situ* approach

Optical images were recorded using a digital microscope (Dinolite, 430 nm, Anmo Electronics Corporation) with a magnification between 45x-75x in the reflected visible and UV light.

Colour measurement was performed using the same methodology described in the section 2.2.2. of the Chapter II, through the CIELAB chromatic space. The colour of each

area was measured on three different points. The data reported represent the mean value of these measurements.

Elemental composition study was done *in-situ*, through X-ray fluorescence spectrometry analyses using a portable Bruker Tracer III-SD adopting the same methodology described in the section 2.2.3.1. of the Chapter II. In this study, no vacuum was applied.

5.2.2. Sampling processes

The sampling processes for the sculptures and building were done under strict conservation requirements, in order to minimise the structural and aesthetic impact on the artworks, stone pillars and walls. This was closely monitored by the curators and conservator-restorers.

The microfragments' collection was done under semi-aseptic conditions using sterile scalpels, swabs, and microtubes. The samples collected for biocontamination assessment were placed in a suspension of transport MRD medium solution and conserved at 4°C until processing.

5.2.3. Characterisation of the material and detection of alteration products

The mineralogical composition was characterised by X-ray microdiffraction using the methodology previously described in the section 3.2.2.2. of the Chapter III. The data were acquired on altered and non-altered areas, without any previous sample preparation.

The elemental composition was determined through Variable Pressure Scanning Electron Microscopy with Energy Dispersive Spectrometry coupled (VP-SEM-EDS), with the features described previously in the section 2.2.3.3. of the Chapter II. The microfragments were analysed without any previous preparation.

The microfragments were also analysed by Raman Spectroscopy, using a HORIBA Xplora Raman microscope, with a CCD (Charge Coupled Device) detector to assess the presence of metabolic activity indicators. A laser with a wavelength of 638 nm and a filter of 10% was applied. Raman spectra were calibrated using the 520.5 cm⁻¹ band of a silicon wafer and were obtained by accumulating 10 acquisitions of 30 s, with a spectral resolution of 5 cm⁻¹. The spectra deconvolution was performed using LabSpec and the identification was made using the *software* Spectral IDTM 13. No sample preparation was required.

5.2.4. Microbiological assessment

5.2.4.1. Assessment of biological contamination

The CVI for each sculpture was assessed as described previously in the section 3.2.3.2. of the Chapter III. The method was performed in three different areas of each sculpture, and each assay was performed in triplicate.

Stone microfragments from both limestone sculptures and marble building were coated with Au/Pd target during 60 s and observed in the Scanning Electron Microscope at high vacuum mode, using 10kV accelerating voltage to assess the microbial communities' presence.

5.2.4.2. Characterisation of the microbial population

Samples collected for biological assays were mechanically stirred during 24 h. After this period, 100 µL of each sample were inoculated in different culture media, using the methodology described in the section 3.2.3.3. of the Chapter III. The distinct single colonies obtained were sub-cultured onto Petri dish and maintained on slants at 4°C until the DNA extraction.

The genomic DNA of the isolates obtained was extracted and amplified using the methodology described in the section 3.2.3.3.1. of the Chapter III. The amplification of the DNA was done using the specific primers 518F/785R and ITS1/ITS4. The PCR products obtained from the microbial isolates were purified and sequenced. The nucleotides sequences were aligned with those retrieved from the GenBank (NCBI) databases for the homology analysis using the BLASTN 2.8.0 program. For the building marble, the isolated population were not characterised by molecular approach.

HTS approach was performed using the methodology described in the section 3.2.3.4. of the Chapter III, where it was possible to determine the microbial population present on the sampled areas.

5.3. Results and discussion

Limestone and marble have been some of the most appreciated materials since antiquity for construction and decorative purposes. In this study, Portuguese limestones and marble vastly used nationally and internationally were studied through the application of a multidisciplinary approach. Complementary analytical methodologies for the materials characterisation and detection of alteration products combined with the biocolonisation assessment, contributed with relevant information to comprehend the association between the chemical and mineralogical alteration and the biological colonisation of these historical and cultural heritage assets.

5.3.1. Case study of NMAA limestone sculptures

5.3.1.1. Characterisation of the material and detection of alteration products

Regarding the *St. John the Baptist* sculpture, the stone used to produce this sculpture is characterised by the association of blue with cream colour, particularly visible in the head section (Fig. V-4). In addition of calcite, the non-altered areas revealed the presence of quartz (SiO_2) and large amounts of iron sulphide minerals (Fe_2S) in the stone matrix (Fig. V-6 and V-7). These results, and according with the lithological features of the stone, might indicate that this sculpture was produced with the blue limestone lithotype from the MCE, previously characterised in the Chapter II.

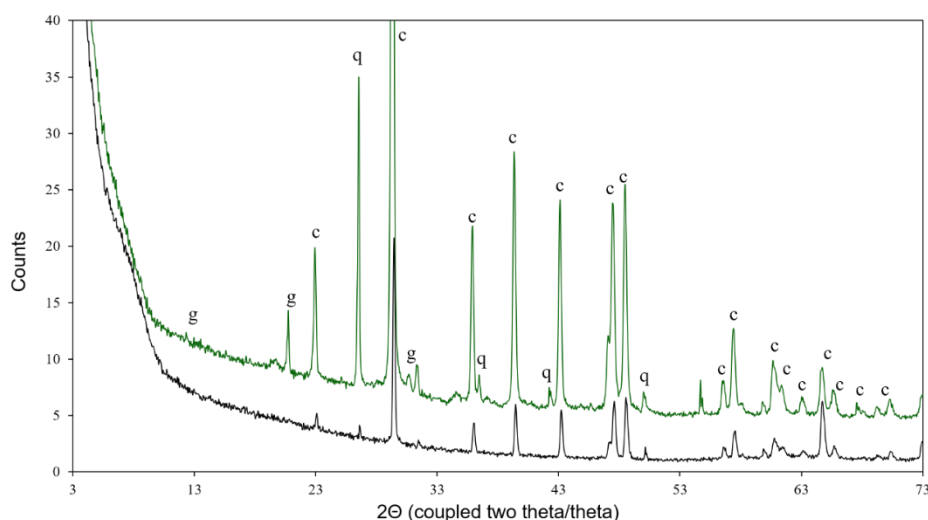


Figure V-6. Micro-X-ray diffractograms obtained on non-altered (—) and altered (---) microsamples' surface of the *St. John the Baptist* sculpture. Abbreviations: g-gypsum; c-calcite; q-quartz.

On the altered surfaces showing white stains, the formation of calcium sulphates was identified (Fig. V-6). As mentioned before in the Chapter III, the crystallisation of calcium sulphates is probably related with the natural weathering processes occurred in the iron sulphide minerals (Ritsema and Groenenberg, 1993; Móricz et al., 2012) that are present in the stone.

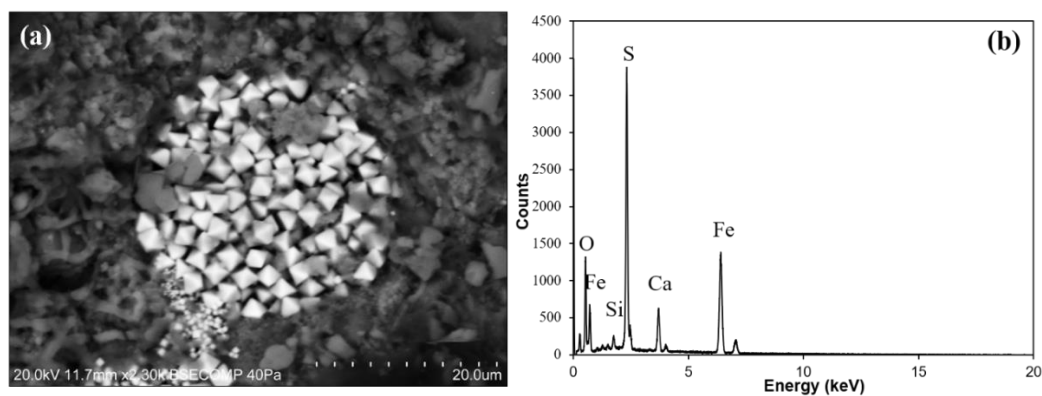


Figure V-7. Iron sulphide minerals' microstructure (a) and correspondent point analysis (b) on a microsample collected from the *St. John the Baptist* sculpture, obtained by VP-SEM-EDS.

In previous studies, some authors highlighted the preponderance of salt crystallisation role in the deterioration of this type of materials (Rothert et al., 2007; Marzal and Scherer, 2008; Doehne and Price, 2010; Kramar et al., 2011; Ghobadi and Babazadeh, 2015). Therefore, this phenomenon might be related with the calcite micro-cracking observed in this sculpture (Fig. V-8).

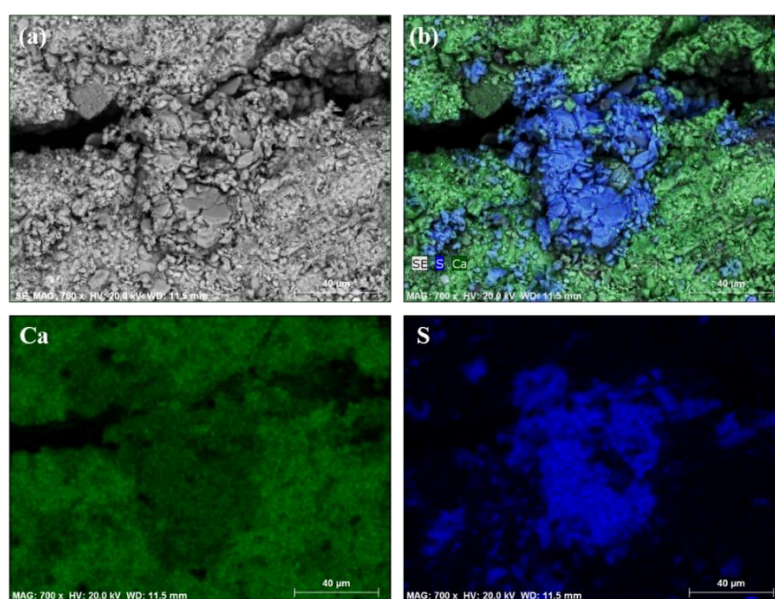


Figure V-8. Microstructure (a) and element mapping of calcium and sulphur (b) on a damaged area of the *St. John the Baptist* sculpture' surface, obtained by VP-SEM-EDS.

Formation of gypsum crystals, although in smaller amounts, was also observed on *The Virgin and the Child* sculpture. Furthermore, halite crystals were identified (Fig. V-9) which may also contribute for the deterioration of the calcite matrix (Fig. V-10). In this sculpture, no sulphide minerals were found in the stone. Thus, the formation of these efflorescence can be originated through the interaction of the material with the environment that surrounds the sculpture, given particular consideration to the pollutant SO₂ (Saiz-Jimenez, 2004; Corvo et al., 2010) and sea spray (Slamova et al., 2012). As previously mentioned, the museum is situated in Lisbon, a city with intense traffic and close to the Atlantic Ocean, which may affect the indoor environment. In fact, some authors state that the outdoor/indoor air exchange, caused by open windows and doors, and museum ventilation systems, is the main contributing factor to indoor air pollution (Krupinska et al., 2013). Additionally, pollutants can also be transferred into museums by tourists or museum personnel (Krupinska et al., 2013).

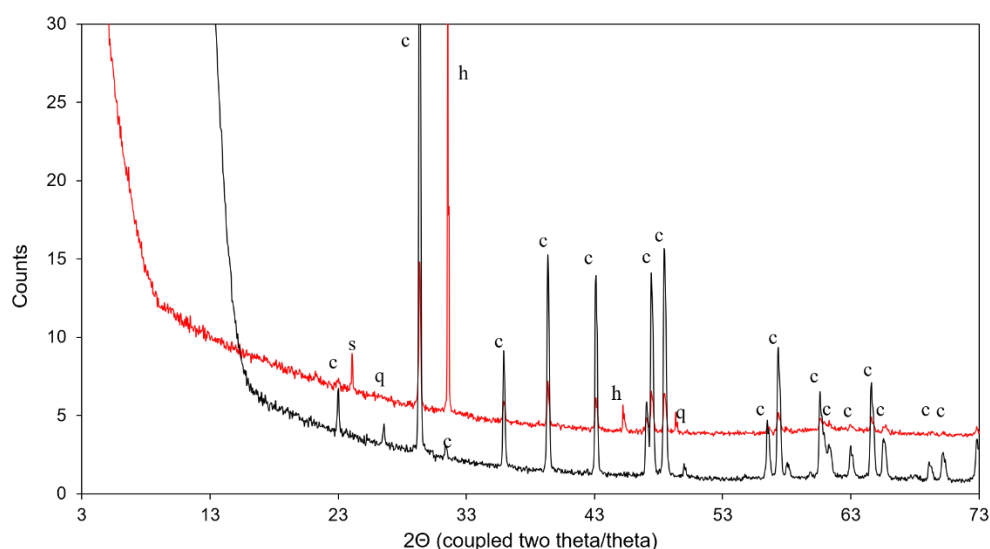


Figure V-9. Micro-X-ray diffractogram on *Virgin and Child* non-altered (—) and altered (—) microsamples' surface. Abbreviations: c-calcite; s-sodalite; q-quartz; h-halite.

It is known that the crystallisation of soluble salts, like gypsum and halite, can induce mechanical stress in the stone pores, causing irreversible damages for the material (Gázquez et al., 2015). In fact, the crystallisation pressure created by salts, for many authors, is considered one of the most severe threats to our common cultural heritage (Espinosa-Marzal and Scherer, 2010; Flatt et al., 2014; Gázquez et al., 2015; Desarnaud et al., 2016).

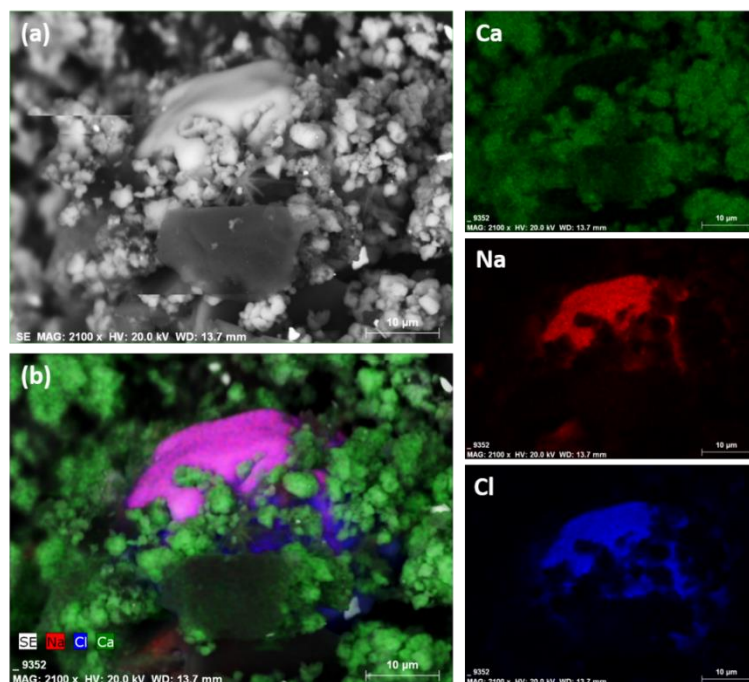


Figure V-10. Microstructure (a) and element mapping of calcium, chlorine and sodium (b) on a damaged area of *The Virgin and the Child* sculpture, obtained by VP-SEM-EDS.

As previously mentioned, the *St. Paul* and *Musician Angel* sculptures exhibit red stains and occasional loss of material. The elemental and mineralogical study performed on the stained areas of the *St Paul* sculpture revealed high concentration of iron oxides (Fig. V-11 and V-12), namely hematite (Fe_2O_3) and hydrohematite ($\text{FeO}(\text{OH})$).

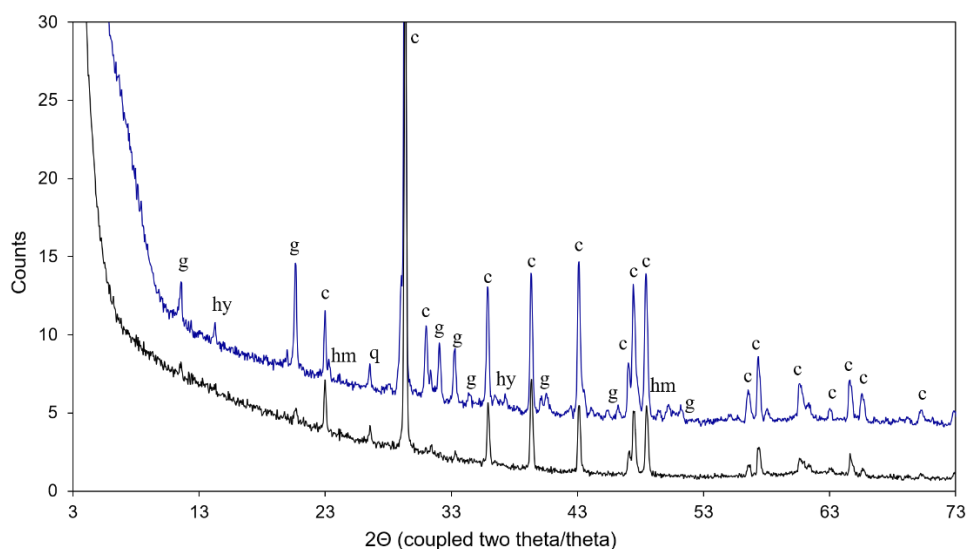


Figure V-11. Micro-X-ray diffractogram performed on non-altered (—) and altered (---) microfragments' surface from the *St. Paul* sculpture. Abbreviations: g-gypsum; hy-hydrohematite; c-calcite; hm-hematite.

According to previous studies, the incorporation of these minerals as a secondary alteration product can stain the rock a red hue (Matero and Tagle, 1995; Weiss et al., 2005; Bams and Dewaele, 2007; Thompson, 2012; Spile et al., 2016). For this case, biocontamination may have played an essential role (Mamet et al., 1997; Bose et al., 2014), as some bacteria may catalyse the oxidation of Fe^{2+} to Fe^{3+} , leading to precipitation and deposition of Fe^{3+} (Hedrich et al., 2011). Low quantities of iron oxides were also found in non-altered areas and identified using SEM-EDS, suggesting they are present in the stone matrix. Their absence in the X-ray diffractograms can be explained by their low crystallinity or by the use of copper radiation, causing an increased background, and limiting the identification of these minerals when present in small amounts (Mos et al., 2018).

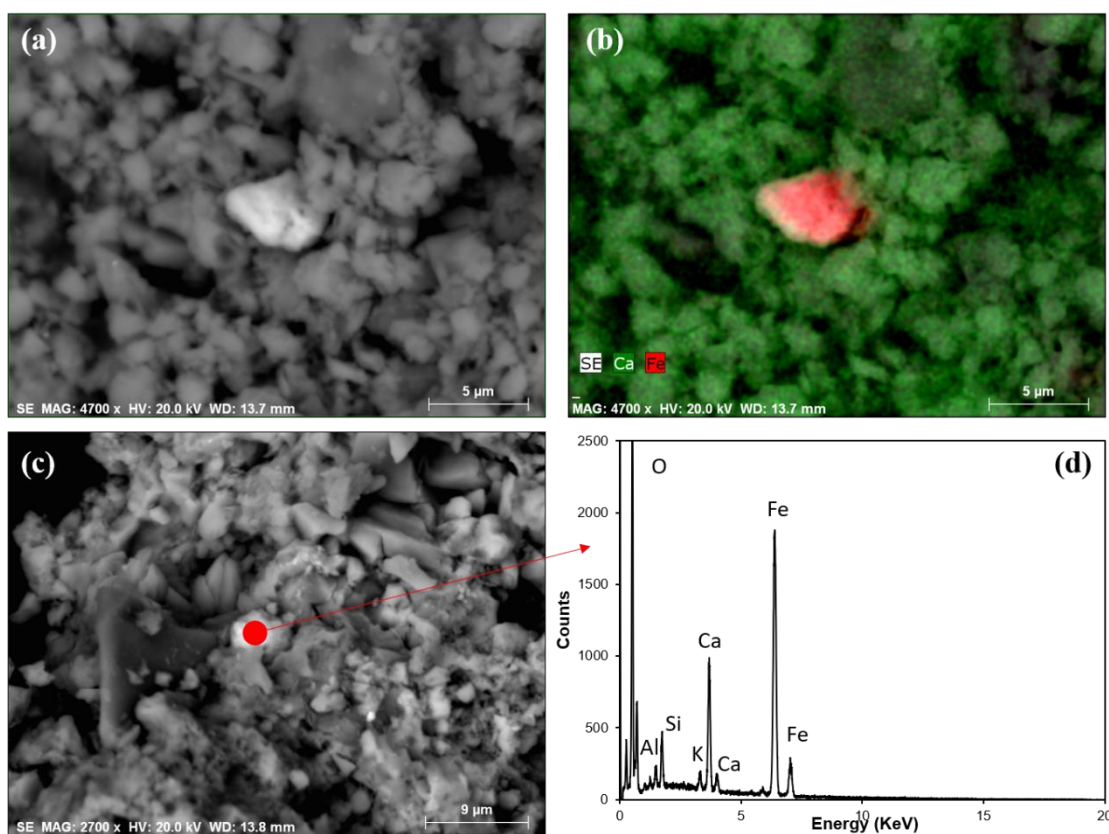


Figure V-12. Microstructure (a), element mapping of calcium and iron (b) and point analysis (c, d) of iron oxides present on the microfragments' surface with reddish stains collected from the *Musician Angel* sculpture, obtained by VP-SEM-EDS.

Raman spectroscopy analyses allowed to detect carotenoids on the *Musician Angel* sculpture (Fig. V-13), a pigmented compound that can be produced by the metabolic activity of some microorganisms (Rosado et al., 2014a; Nupur et al., 2016) and may

display yellow to red hues (Rosado et al., 2014a). Besides it can be an indicative sign of biocontamination, the presence of these compounds in the sculpture surface probably contribute to the reddish stains observed on the *Musician Angel* sculpture.

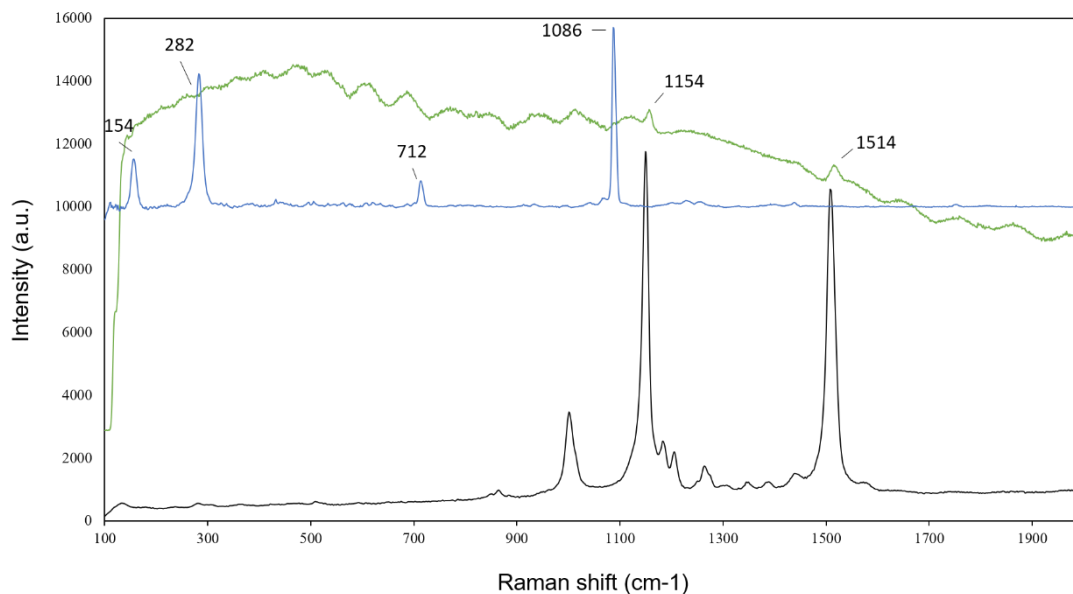


Figure V-13. Raman spectra of β -carotene standard (—), microfragment collected without alteration (—) and microfragment collected in the red coloured zone of the *Musician Angel* sculpture (—). The bands at 154, 282, 712 and 1086 can be attributed to calcite (Edwards et al., 2000), while β -carotene can be identified based on bands at 1154 and 1514 (Rosado et al., 2014a).

5.3.1.2. Biocontamination assessment

VP-SEM-EDS analysis allowed a further insight into the presence of microbial communities thriving on these sculptures and their capacity to proliferate within the stone surface (Fig. V-14). The detection of elements like carbon, oxygen, and nitrogen by EDS are indicators of the presence of organic/biological material.

Complementarily, SEM micrographs showed the presence of microbial agents like filamentous fungi on the surface of the sculptures (Fig. V-15), with a higher incidence in the *Musician Angel* sculpture. Furthermore, it was possible to observe the proliferation of these structures around the crystals of calcite.

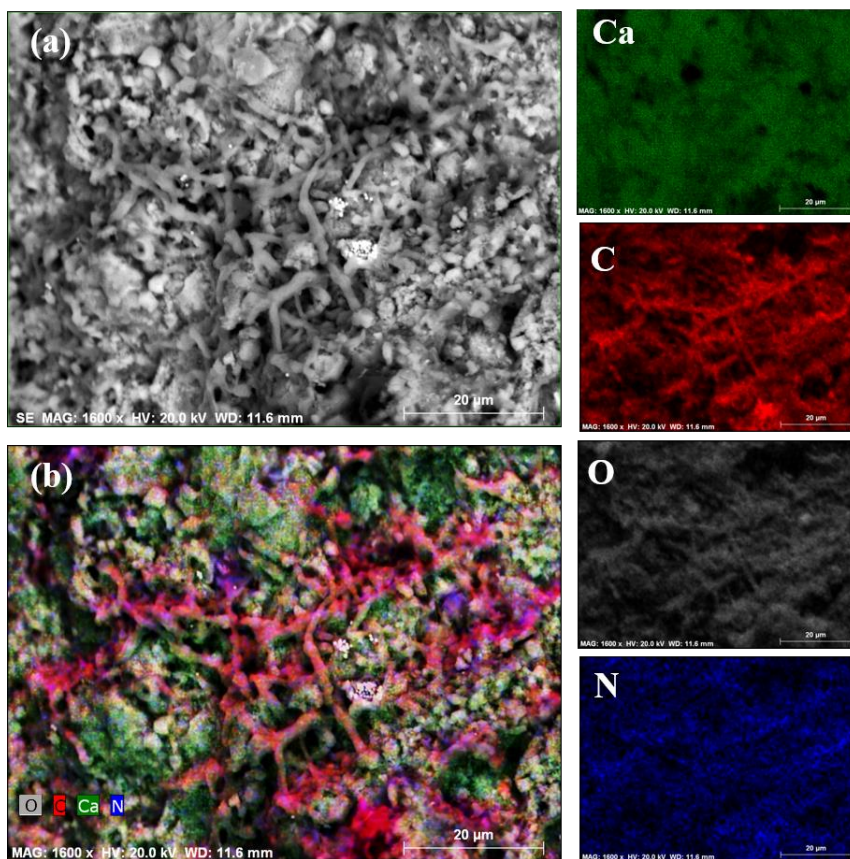


Figure V-14. Microstructure (a) and element mapping of calcium, carbon, oxygen, and nitrogen (b) evidencing index of biocontamination on the surface of the *St John the Baptist* sculpture, obtained by VP-SEM-EDS.

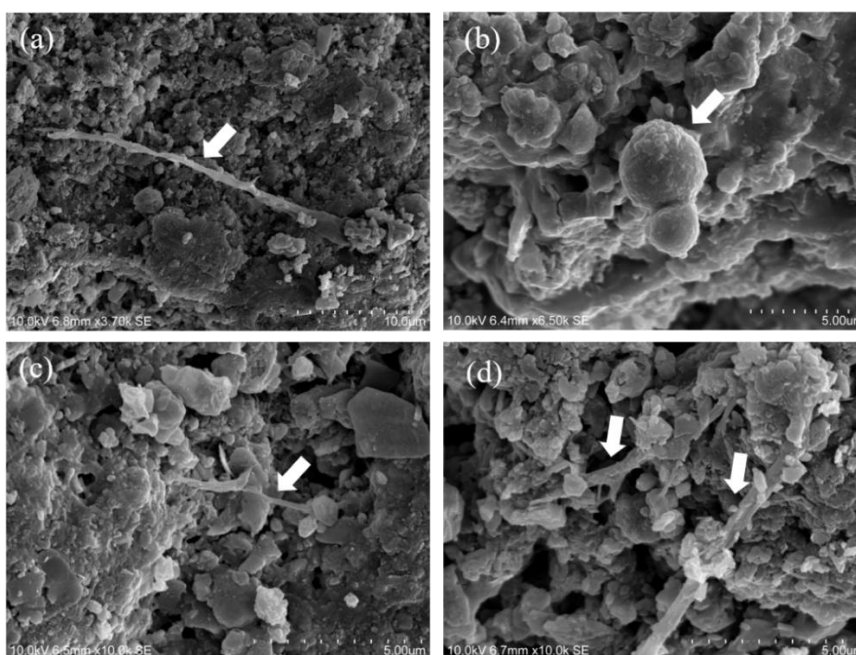


Figure V-15. SEM micrographs on the microfragments of the *St. John The Baptist* (a), *The Virgin and the Child* (b) and *Musician Angel* (c, d) sculptures, signalling hyphae of filamentous fungi proliferating around the crystals of calcite.

Regarding the cell viability index, the method used shows that the *Musician Angel* sculpture presents higher CVI levels when compared with the other sculptures (Fig. V-16). This higher CVI degree indicates a greater potential for metabolic activity of the microbial agents for the *Musician Angel* sculpture.

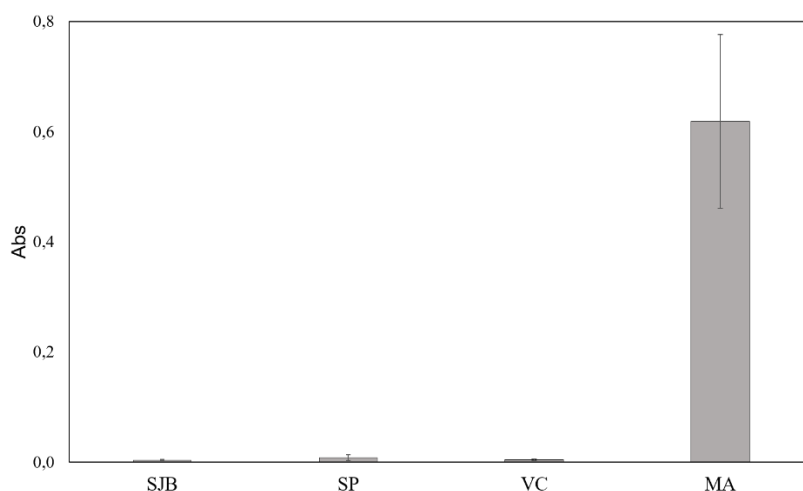
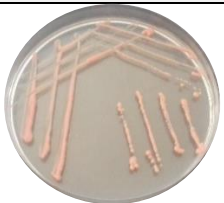



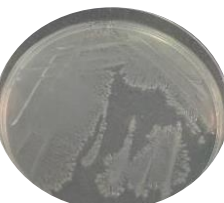
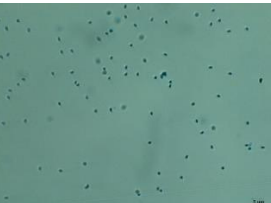

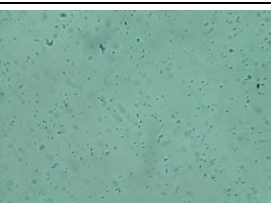





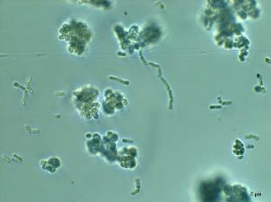


Figure V-16. Cell viability of the microbial population present in the samples collected on the sculptures' surface. Abbreviations: SJB-*John the Baptist*, SP-*St. Paul*, VC-*The Virgin and the Child* and MA-*Musician Angel*. Error bar corresponds to \pm standard deviation (n=9).

CDM allowed the characterisation of cultivable isolated population, which it was proven to be mainly composed of prokaryotic microorganisms (Annex D.1). The samples that had the higher microbial development belong to the *Musician Angel* sculpture, thus corroborating the results described above (Fig. V-15 and V-16).

The cultivable population was further characterised based on their macroscopic and microscopic features. Two single-colonies were obtained for the *St. John the Baptist* sculpture, one single-colony for the *St. Paul* sculpture, three single-colonies for the *The Virgin and the Child* sculpture and one single-colony for the *Musician Angel* sculpture (Table V-1).

Table V-1. Characterisation of the microbial population isolated from the limestone sculptures' samples.

Sculpture	Macroscopic features	Microscopic features	
<i>St. John the Baptist</i>			Coccus
			<i>Penicillium</i> sp.
<i>St. Paul</i>			Bacilli
<i>Virgin and the Child</i>			Coccus
			Coccus
			Bacilli
<i>Musician Angel</i>			Black yeast

Some of the isolated population was sequenced. The DNA extracted was amplified by PCR and the PCR products were purified, quantified and sequenced. According to the best matches of the database used, was possible to identify microorganisms with high similarities with *Staphylococcus aureus*, *Pseudomonas stutzeri*, *Bacillus licheniformis* and *Aureobasidium* sp. (Table V-2). Previous studies referred that, in moderate or humid climates, some hyphomycetes strains (*Alternaria*, *Cladosporium*, *Epicocum*, *Aureobasidium* and *Phoma*) usually form mycelia in the porous space of stones (Sterflinger and Piñar, 2013; Martino, 2016), which consequentially will induce damages in the stone matrix. In addition, some authors emphasised the *Pseudomonas stutzeri* ability to reduce nitrates present in altered stone surfaces (Palla and Barresi, 2017), and related *Staphylococcus aureus* and *Bacillus* to limestone deterioration (Ekarim, 2017).

Table V-2. Identification of microorganisms isolated from the limestone sculptures.

Sculpture	Closest related type strain on basis of 16 S and 18S rRNA gene	Similarity	Accession number (NCBI)	Familiy	Class	Phylum
MA	<i>Aureobasidium</i> sp.	100%	KX611011.1	Dothioraceae	Dothideomycetes	Ascomycota
VC	<i>Pseudomonas stutzeri</i>	100%	KY770794.1	Pseudomonadaceae	Gammaproteobacteria	Proteobacteria
SP	<i>Bacillus licheniformis</i>	99%	JN998742.1	Bacillaceae	Bacilli	Firmicutes
SJB	<i>Staphylococcus aureus</i>	100%	GQ214333.1	Staphylococcaceae	Bacilli	Firmicutes

MA – *Musician Angel*; VC – *The Virgin and the Child*; SP – *St. Paul*; SJB – *St. John the Baptist*.

Considering that the main colonisers of the sculptures are majorly prokaryotic, HTS was performed allowing the detailed characterisation of the prokaryotic population thriving on the sculptures' surface (Annex D.2). The results obtained demonstrate that the prokaryotic population thriving on the *St. John the Baptist*, *The Virgin and the Child* and *St. Paul* sculptures (Fig. V-17) is predominantly composed of *Lactococcus* sp. (around 80%) and *Lactococcus raffinolactis* (around 8.5%). For the *Musician Angel* sculpture, the main prokaryotic population is composed of *Lactococcus* sp. (55.9%), *Bacillus aryabhatai* (20.2%) and *Lactococcus raffinolactis* (5.9%). 272 different species were identified on the *Musician Angel* sculpture, 232 on the *St. John the Baptist* sculpture, 212

on the *St. Paul* sculpture while 176 different species were identified on *The Virgin and the Child* sculpture. All the prokaryotic population identified on the sculptures belongs to the Bacilli class, except those that belong to the genus *Pseudomonas*. Particularly, microorganisms of Bacilli class have been identified on many limestone historical buildings with signs of deterioration (Sasso et al., 2013; Banciu, 2013; Skipper et al., 2016). Besides their abundance on stone-built heritage located outdoor, the microorganisms of the Bacilli class have been also found on indoor stone-built artworks (Pangallo et al., 2009) where more extensive studies are missing.

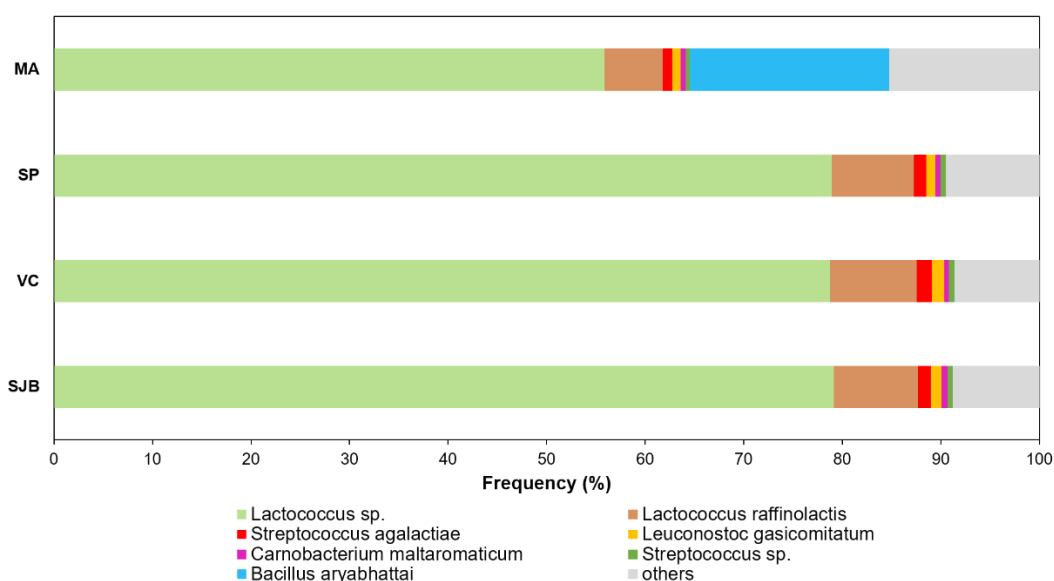


Figure V-17. Composition of the major prokaryotic population thriving on the limestone sculptures at genera and species levels. Abbreviations: MA – *Musician Angel*; SP – *St. Paul*; VC – *The Virgin and the Child*; SJB – *St. John the Baptist*.

The similarities in the prokaryotic population colonising the *St. John the Baptist*, *The Virgin and the Child* and *St. Paul* sculptures is understandable given that these sculptures are kept in the same room, and therefore are subjected to the same micro-environment conditions. The fact that the *Musician Angel* sculpture, which is displayed in a different room inside the museum, revealed a wider variety of prokaryotic population further validates this hypothesis.

The HTS results corroborate the determination of the CVI levels, since the *St. John the Baptist*, *The Virgin and the Child* and *St. Paul* sculptures showed similar levels of CVI, unlike the *Musician Angel* sculpture. The higher CVI level of this sculpture and its

wider microbial population variety can possibly be related with the different display location of the sculpture in the museum.

The multi-analytical approach encompasses and give useful information about the composition of the material, detection of alteration products and the presence of microorganisms. The data obtained provided an important and detailed description of the communities able to develop in these materials, in an indoor environment. The results revealed that the aesthetical and structural damages in these sculptures might be related with the formation of efflorescence and iron oxides concentration, as well as with the microbial proliferation. These factors are making a practical contribution for the colour alteration and the detachment of the material.

5.3.2. Case study of the “São João da Penitência” Convent

For this study, marble exploited in the Estremoz anticline, one of the most appreciated marbles worldwide, was selected to investigate the factors that are leading its deterioration. The marble is applied in the “São João da Penitência” Convent, situated in the main square of the Estremoz village. According with the pathologies found in the main cloister, three broad categories form the research work – patina formation, staining and biofilm formation. The areas CM1 and CM2 show formation of patinas on the surface of the stone, the areas CM3 and CM4 exhibit signs of staining, and the areas CM5 and CM6 show biofilms formation. These areas are distributed along the main cloister (Fig. V-18).

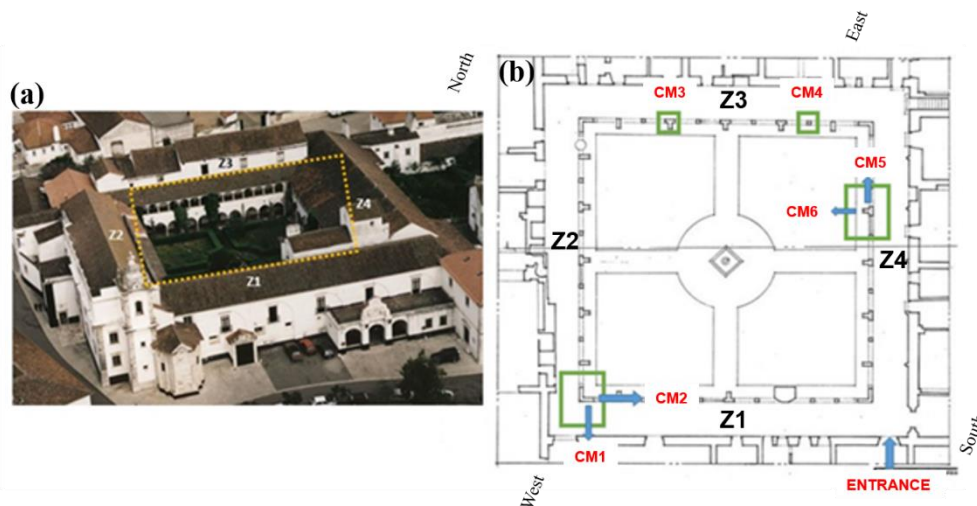






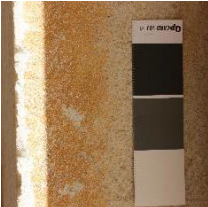

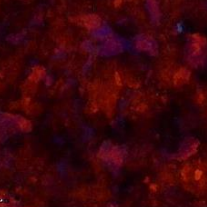

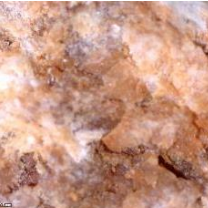









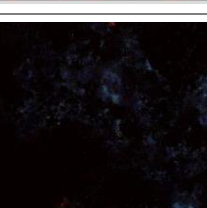


Figure V-18. Aerial view of the Convent (a) and map of the main cloister with the location of the areas selected for the study (b). green squares represent the sampling areas.

The pathologies present in the selected areas were observed in detail. Some areas exhibited fluorescence emission under the UV light, with higher intensity for the areas CM5 and CM6 (Table V-3), which is an indicative of organic material presence on the surface of the stones.

Table V-3. Digital microscopy analyses on the selected areas, under visible and UV light.

Area I.D.	Area detail	Digital Microscope 430 nm	
		Vis	UV
Non-altered			
CM1			
CM2			
CM3			
CM4			
CM5			
CM6			

5.3.2.1. Measurement and characterisation of the colour

Using the CIELAB system, the colourimetric parameters were measured and the ΔE was determined using a non-altered stone surface as reference (Table V-4). It is possible to state that colour of the damaged areas is seriously compromised, since the ΔE values are very high. The areas that exhibit the highest differences in colour are CM5 and CM6, corresponding to the areas that have biofilms formation on the stone surface.

Table V-4. Measurement of the colourimetric parameters, using the CIELAB system.

Area I.D.	L*	a*	b*	ΔE
Non-altered	72.74 \pm 4.64	0.6 \pm 1.34	5.33 \pm 3.01	-
CM1	91.52 \pm 2.41	1.84 \pm 0.58	6.40 \pm 2.04	18.85
CM2	66.98 \pm 3.95	8.69 \pm 3.53	25.00 \pm 6.03	22.02
CM3	41.58 \pm 8.57	10.94 \pm 1.16	17.21 \pm 2.69	34.31
CM4	63.82 \pm 5.49	8.77 \pm 1.73	16.50 \pm 2.13	16.46
CM5	36.05 \pm 4.33	13.46 \pm 3.02	15.55 \pm 2.21	40.19
CM6	27.64 \pm 1.68	1.82 \pm 0.51	4.25 \pm 1.34	45.12

5.3.2.2. Characterisation of the material and alteration products

Frequently, degradation of carbonated stones occurs in the presence of dust deposited on the rough stone surfaces. The deposits not only change the visual appearance of the stone but also increase the water retention, thus increasing the degradation processes. In the microfragments collected in the areas presenting patina formation (CM1 and CM2), calcium oxalates weddellite ($\text{CaC}_2\text{O}_4 \cdot 2\text{H}_2\text{O}$) and whewellite ($\text{CaC}_2\text{O}_4 \cdot \text{H}_2\text{O}$) were detected (Fig. V-19).

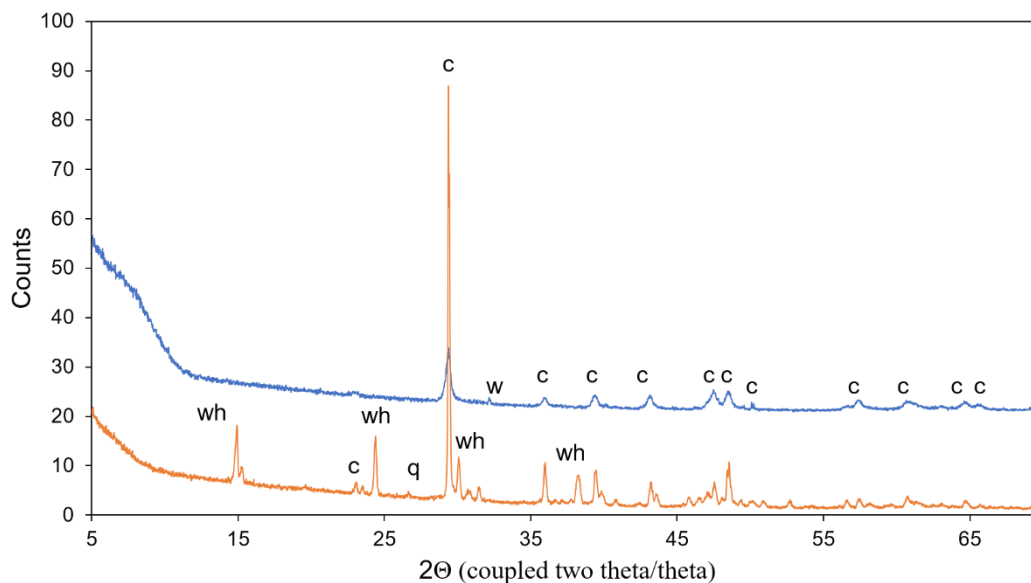


Figure V-19. Micro-diffractograms obtained on the microfragments collected in the areas CM1 (—) and CM2 (—). Abbreviations: c – calcite; wh – whewellite; q – quartz; w – weddellite.

As previously mentioned in Chapter I, these compounds may result from the calcium dissolution, a common occurrence in the carbonated stones like limestone and marble (Charola et al., 2007; Corvo et al., 2010). Calcium oxalates formation can be originated from biological or chemical pathways. Despite some authors consider that these compounds can derive from past conservation treatments (Rampazzi, et al., 2004), these compounds have been used as strong indicator of the presence of microorganisms, since oxalic acid is a common metabolite resulted from microbial activity on stone (McNamara and Mitchell, 2005; Burford et al., 2006; Corvo et al., 2010; Frank-Kamemetskaya et al., 2012). Additionally, some sulphates were identified on these areas as calcium sulphates (Fig. V-20), which can suggest that atmospheric SO₂ also may play an important contribution (Siegesmund and Snelthage, 2011) for the degradation of this stone.

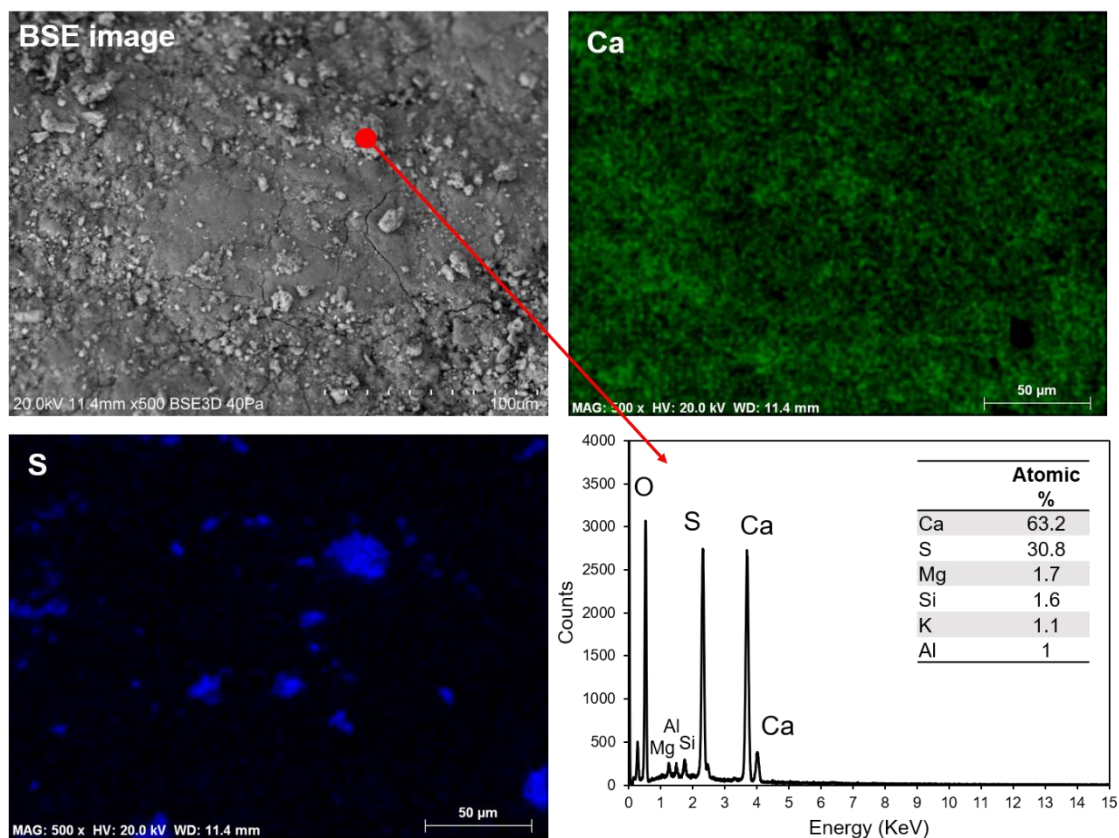


Figure V-20. Surface microstructure, elemental distribution of calcium and sulphur, and point analysis of calcium sulphates, obtained by SEM-EDS on the microfragment collected in the area CM1.

The areas CM3 and CM4 show reddish stains. Besides the proximity of both areas, the staining seems to be achieved by two different ways. The stain observed in the area CM3 is characterised as a red spot on a porous area, while the stain observed in the area CM4 is characterised by the accumulation of red pigmentation in stone fissures (Fig. V-5).

The data obtained reveal that the area CM3 has a larger enrichment in iron when compared with non-altered areas (Fig. V-21), which can indicate that this element is present as an impurity in the calcite, since the ion Fe^{3+} can replace Ca^{2+} or, more typically, enter directly in the CaCO_3 matrix (Polikreti and Maniatis 2004).

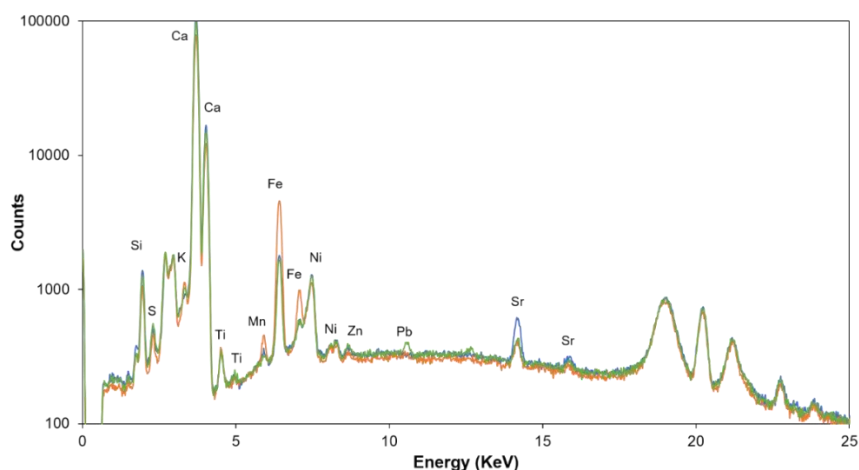


Figure V-21. Spectra obtained by X-ray fluorescence on the CM3 (—), CM4 (—) and non-altered (—) areas.

Additionally, elemental mappings obtained for both areas showed the coexistence of iron, aluminium, silicon and potassium in the same particles (Fig. V-22) which is compatible with the presence of “Terra Rossa”. This is a relatively common material formed in calcareous stone, predominantly in areas with a Mediterranean climate (Foster et al., 2004; Haldar and Tisljar, 2014).

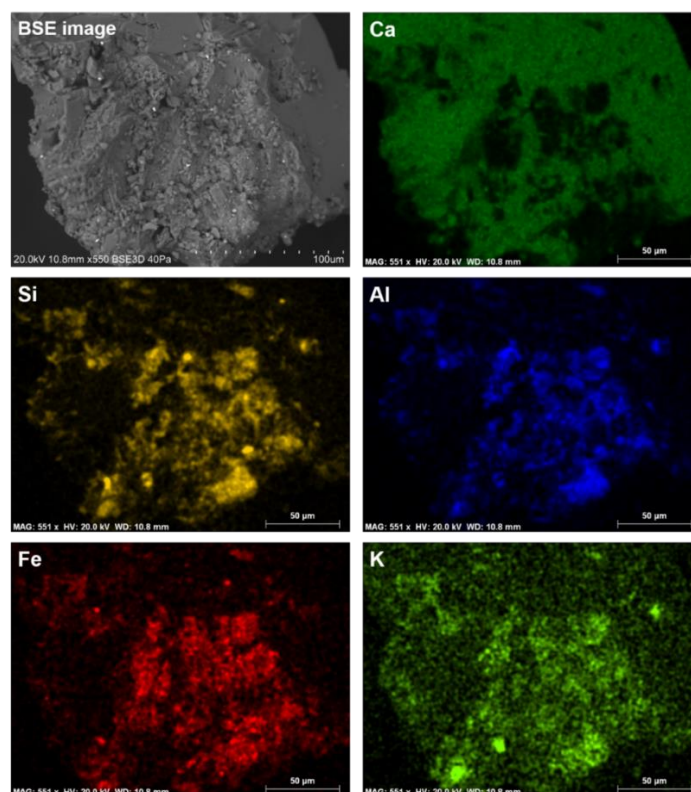


Figure V-22. Microstructure and elemental distribution of calcium, aluminium, silicon, iron and potassium on the microfragment collected on the area CM3, obtained by SEM-EDS

“Terra Rossa” is a formation owing to chemical degradation of limestone which typically cover calcareous bedrock stones such as crystalline limestone or marble, or deposits of unconsolidated calcareous with terrestrial or marine origin (Foster et al., 2004; Vingiani et al., 2018). It marks the transition of brown earth to red laterite soil and is a reddish clay residue resulting from the dissolution of the carbonated stones (Olson et al., 1980). It can form a discontinuous layer which varies between a few centimetres to a few meters (Durn, 2003; Vingiani et al., 2018).

5.3.2.3. Microbiological assessment

The areas CM5 and CM6 show red and black biofilms formation, respectively. These biofilms here formed cover all the surface of the stone. Therefore, the microbial communities thriving on it were assessed. It was possible to detect the coexistence of C, N and O in the same regions (Fig. V-23) which is an indicative of the presence of organic/biologic material over the calcium carbonate matrix.

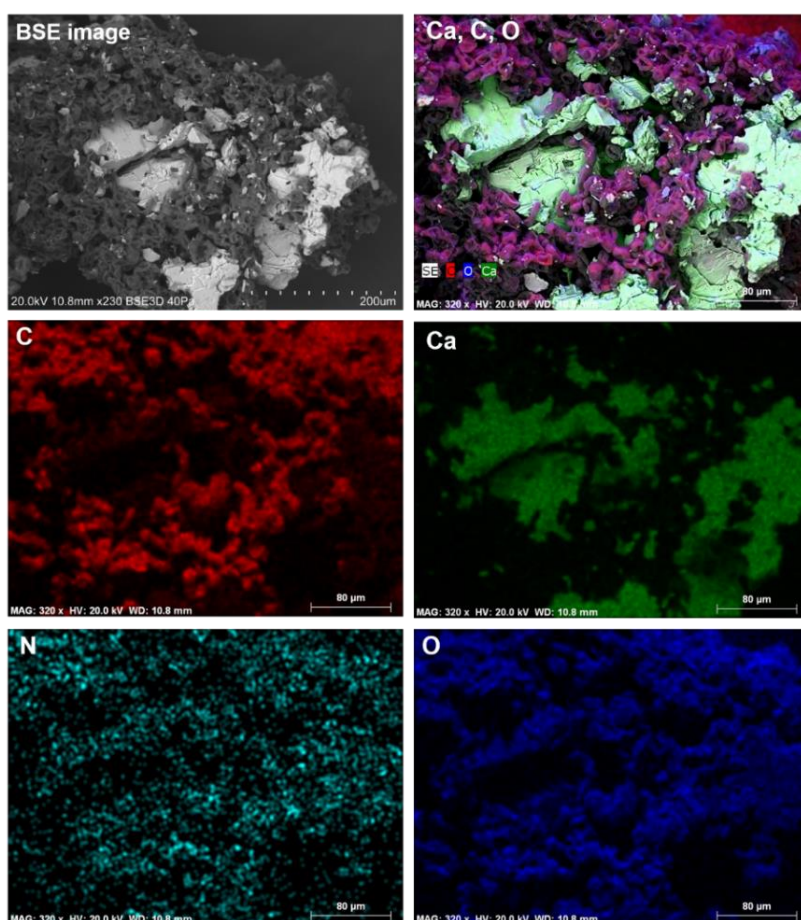


Figure V-23. Microstructure and elemental distribution of calcium, carbon, nitrogen and oxygen, obtained by SEM-EDS for the microfragment collected on the area CM5.

SEM micrographs allowed to determine how the biofilms have been developing and their impact on the surface of the stone. On the area CM5 (red biofilm) it was possible to observe the ability of filamentous fungi to surround and penetrate the porous of the stone (Fig. V-24). It was observed above the deleterious effects of the development of these organisms on this area (Fig. V-3b), where a relatively large piece of stone was completely detached from the rest of the structure.

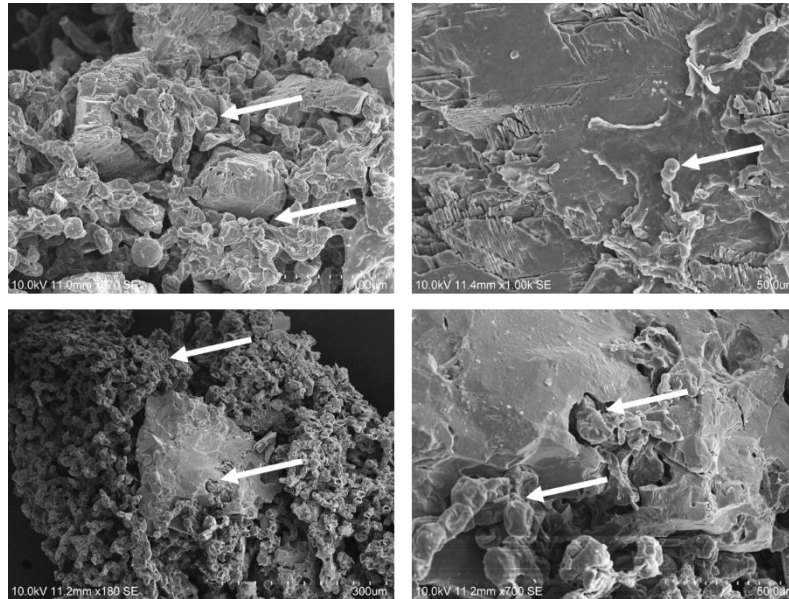


Figure V-24. Micrographs obtained on the microfragment collected on the area CM5 showing the ability of filamentous fungi to surround the calcitic matrix and penetrate the porous of the stone.

On the other hand, the area CM6 (black biofilm) revealed the presence of diatoms, microalgae and filamentous fungi (Fig. V-25), which suggest a wider diversity of the microbial community here thriving, when compared with the area CM5.

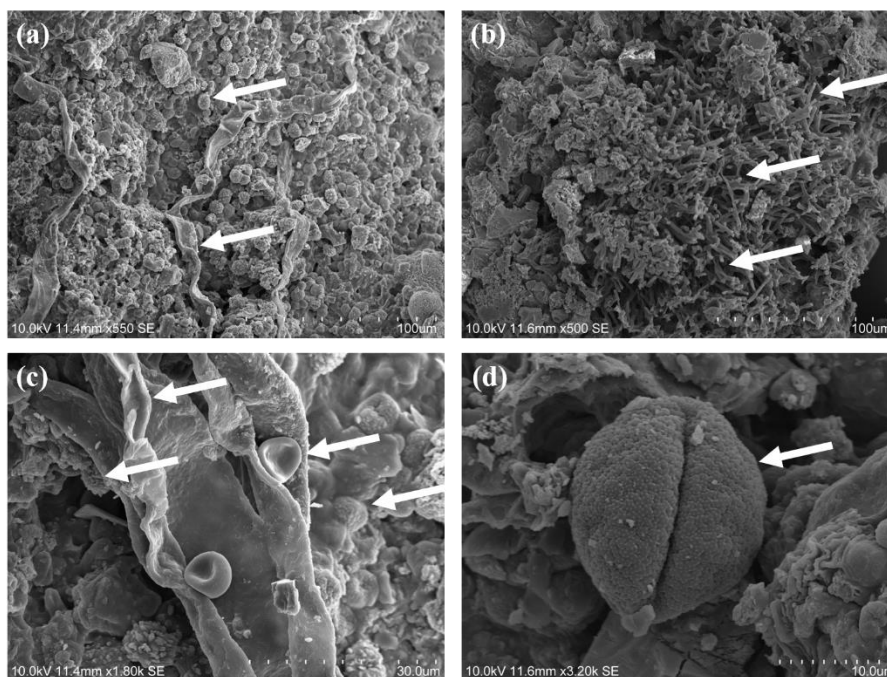
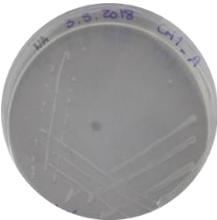
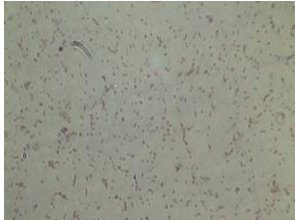
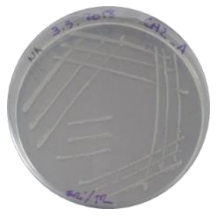
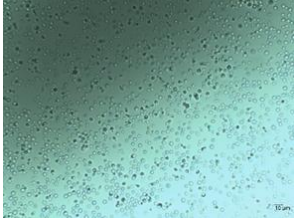
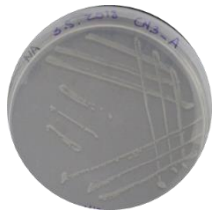
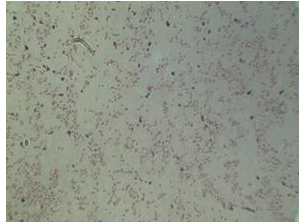

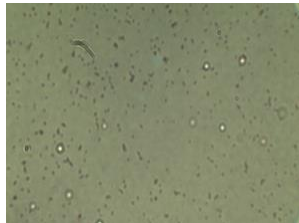

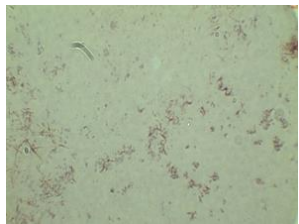
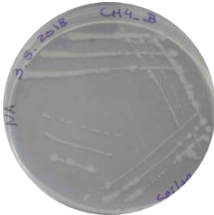
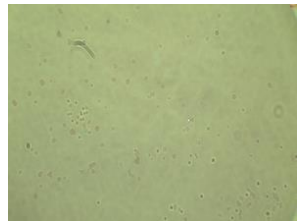

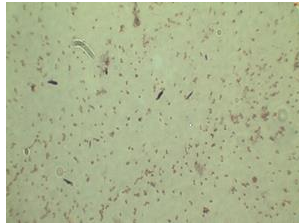

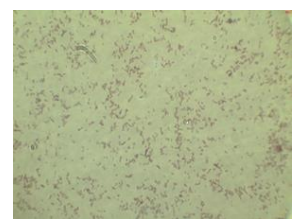


Figure V-25. Micrographs obtained on the microfragment collected on the area CM6 showing the microscopic aspect of the biofilm (a and b), presence of microalgae (c) and some unidentified structures (d).

For a more accurate characterisation of the population that is colonising the Convent, both culture-dependent methods and HTS approach were performed. The cultivable bacteria population is predominantly composed of microorganisms with the morphology *Bacillus* and *Coccus* (Table V-5).

Table V-5. Characterisation of the isolated bacteria from the selected areas of the Convent.

Code	Macroscopic features	Microscopic features
CM1_A		 <i>Coccus</i> (Gram +)
CM2_A		 <i>Bacillus</i> sp. (Gram +)


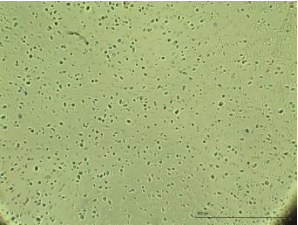

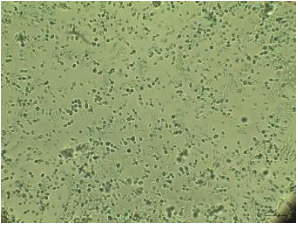

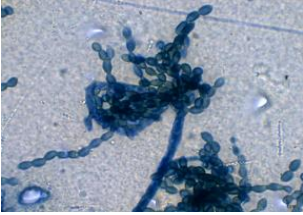
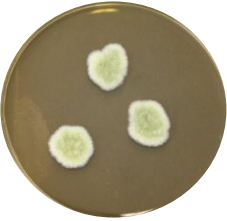
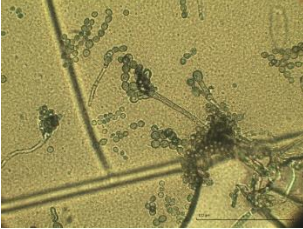

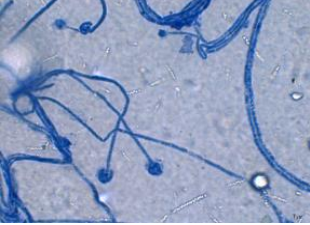
CM3_A			<i>Bacillus</i> sp. (Gram -)
CM3_B			Coccus (Gram +)
CM4_A			<i>Bacillus</i> sp. (Gram -)
CM4_B			Coccus (Gram +)
CM5_A			Coccus (Gram -)
CM6_A			Coccus (Gram +)


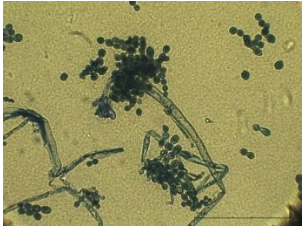


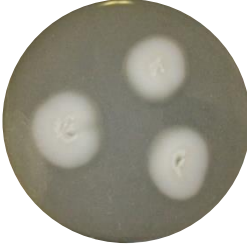
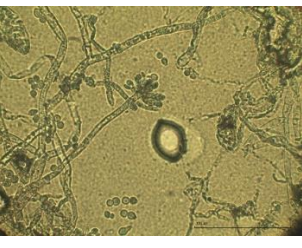
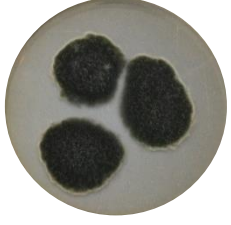
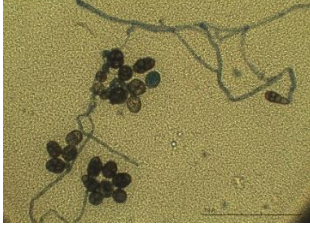
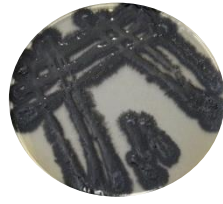

HTS approach allowed to complement the characterisation of the prokaryotic population (Annex E.1), which show that the population thriving in the stone of the Convent is mainly composed of microorganisms belonging to the phyla Proteobacteria, Actinobacteria and Cyanobacteria, while the most representative genera are *Pseudomonas*, *Rubrobacter*, *Geodermatophilus*, *Erwinia* and *Anabaena*. Previously, has

been reported that microorganisms belonging to the genera *Rubrobacter* and *Geodermatophilus* were already isolated from deteriorated stone monuments (Urzi et al., 2001; Laiz et al., 2009; Li et al., 2016).

On the other hand, the cultivable fungi population is composed of black yeasts and microorganisms belonging to the genera *Rhodotorula*, *Aspergillus*, *Mucor*, *Penicillium*, *Alternaria*, *Cladosporium* (Table V-6).

Table V-6. Characterisation of the isolated fungi from the selected areas of the Convent.

Code	Macroscopic features	Microscopic features	
CM1_1			Yeast
CM3_1			<i>Rhodotorula</i> sp.
CM3_2			<i>Cladosporium</i> sp.
CM3_3			<i>Aspergillus</i> sp.
CM3_4			<i>Mucor</i> sp.

CM4_3			<i>Aspergillus</i> sp.
CM4_5			<i>Aspergillus</i> sp.
CM4_6			Mycelium
CM5_5			<i>Alternaria</i> sp.
CM6_1			Black Yeast

Complemented by HTS approach (Annex E.2), the fungi population that are colonising the areas without formation of visible fungal biofilms is mainly composed of microorganisms that belong to the phyla Ascomycota and Basidiomycota, while the most representative genera are *Cladosporium*, *Alternaria*, *Stagonosporopsis*, *Mycosphaerella*, *Stemphylium*, *Aureobasidium* and *Vishniacozyma* (Fig. V-26).

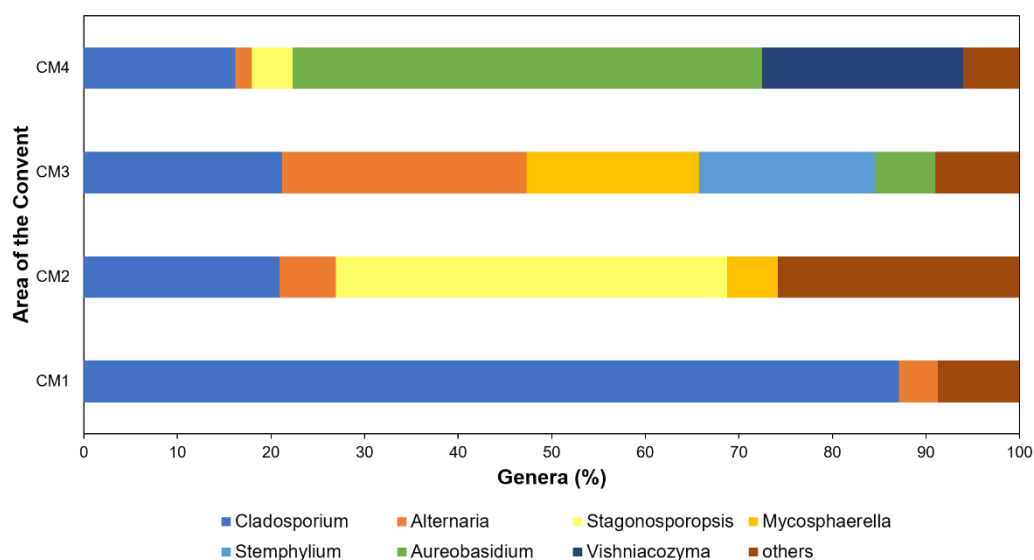


Figure V-26. Characterisation of the major eukaryotic population present on the areas of the Convent without visible fungal biofilms formation, at genera level.

As mentioned before, fungi have the ability to excrete acids like oxalic, glyoxylic, citric, acetic, formic or fumaric which can react with the carbonates. The most commonly fungi found in cultural heritage materials are *Penicillium* sp. and *Cladosporium* sp. both responsible for soiling (Sterflinger, 2010). Additionally, Grote in 1986 has suggested that microorganisms of the genera *Alternaria*, *Cladosporium*, *Fusarium* and *Penicillium* have the ability to oxidise iron and manganese on stone (Sterflinger, 2000). Regarding the areas CM1 and CM2, calcium oxalates presence is a strong indicator of microbial activity on the stone of this Convent, namely through the proliferation of microbiota like bacteria, fungi, algae and lichens (Rosado et al., 2013a; Gadd et al., 2014; Sturm et al., 2015; Unkovic et al., 2017). As mentioned before, the oxalic acid excreted reacts with calcareous stone (Monte, 2003) which consequently can form a thin membrane of calcium oxalate (patina).

The predominant population identified on the area CM5 (red coloured biofilm) belong to the phyla Ascomycota (76.48%) and Basidiomycota (7.56%), while the most

representative genera on this area are *Sordaria*, *Cladosporium*, *Aureobasidium*, *Guehomyces*, *Mycosphaerella* and *Vishniacozyma* (Fig. V-27a). For the area CM6 (black coloured biofilm) the predominant fungi population belong to the phyla Ascomycota (78.51%) and Basidiomycota (3.62%), while the most representative genera are *Cladosporium*, *Thelebolus*, *Aureobasidium*, *Alternaria*, *Vishniacozyma*, *Neodevriesia* and *Gibberella* (Fig. V-27b).

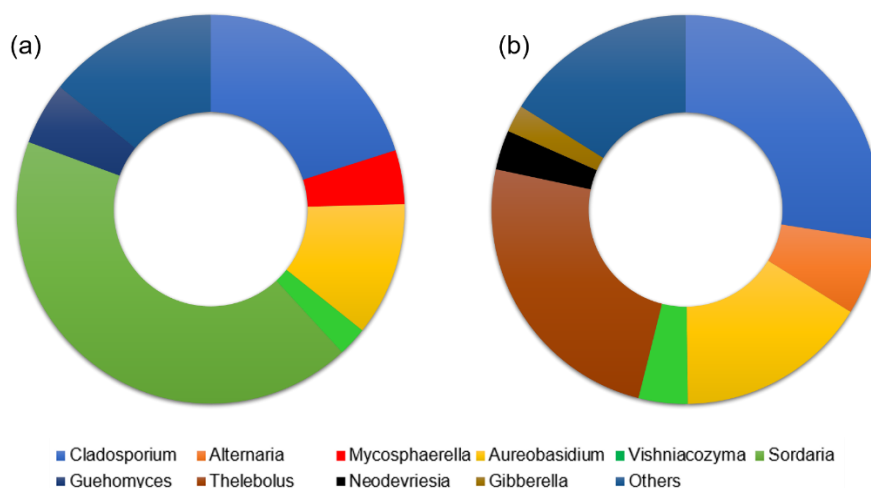


Figure V-27. Characterisation of the major eukaryotic population present on the red (a) and black (b) biofilms, at genera level.

The red colouration of the biofilm formed on the area CM5 is achieved due to the proliferation of microorganisms or/and excreted metabolites. These may include the microorganisms belonging to the genera *Sordaria*, since some phenotypes exhibit ascospores with a red colour (Lichtenstein, 2017), also *Cladosporium* since some colonies exhibit a vivid red pigmentation due to the excretion of large quantities of a perylenequinone metabolite (Robeson and Jalal, 1992), *Aureobasidium* since colonies belonging to this genus can have a red colour (Wickerham, 1975) or *Rubrobacter* since that has already been correlated with red pigmentation on stone (Rosado et al., 2019).

On the other hand, strains belonging to the genera *Cladosporium*, *Aureobasidium* and *Alternaria* are also known to form black coloured biofilms (Zammit et al., 2009; Heinrichs et al., 2013). Specifically, the species *Aureobasidium pollulans*, identified on this area, is one of the so-called black yeast (Gao et al., 2013; Kemler et al., 2017), a group strongly associated to biofouling and bioweathering (Cutler and Viles, 2010). Thus, the results obtained suggest that microorganisms of the genera *Aureobasidium*, *Cladosporium* and *Alternaria* can be the main responsible for the biofilm colouration.

In this study, *in-situ* approach using non-invasive and non-destructive techniques, as well as analyses of microfragments were carried out to evaluate the deterioration of the marble applied in the Convent “São João da Penitência”. The detection and characterisation of its alteration products and the biocolonisers thriving on it were performed. The three different pathologies detected on the stone – patina formation, staining and biofilm formation – were correlated with geochemical or/and biogenic origin.

Chapter VI:

Concluding remarks



Currently, colour and discolouration of ornamental stones is an extremely important issue that needs to be fully understood. The companies that exploit and sell ornamental stones have been losing millions in the stone replacement in new buildings. The prediction and prevention of colour alteration processes on stone remains a task for the scientific community, while the preservation and safeguard of heritage artworks and buildings made of stone represent a challenge for the conservator-restorers.

This research contributed for the characterisation of Portuguese carbonated stones based on their colour, in order to predict and prevent further alterations. It also allowed to describe the colour change mechanisms of some of the most important Portuguese ornamental stones, and of stones applied in heritage artworks and building. On the other hand, the study revealed the microbial population thriving on these stones.

The results highlighted the effect of the microbial agents' action in the deterioration processes of stone, that contribute for the stone discolouration and accelerate the deterioration rate. The methodology used in this project proved to be very effective in the characterisation of colour alteration mechanisms in stone and can be adapted to other stone lithotypes and other artworks for diagnostic and rehabilitation. In this way, it will be possible to contribute to maintain the Portuguese stone in the international market forefront and for the cultural heritage safeguard.

The strategies outlined under the framework of this research has proven that:

- The application of X-ray based methods is useful in stone characterisation and in finding the causes of its colour, using simple sample preparation methods or even without sample processing;
- X-ray based methods and Raman spectroscopy are useful in the characterisation of alteration products resulted from the stone discolouration;
- The application of MTT assays allowed to determine the cell viability index of these materials, giving an overview about the presence of biocontamination and its relationship with altered areas of the stone;
- The combined application of CDM and HTS approaches is useful for microbiota identification on stone substrata to further may relate it with bioweathering;
- The natural weathering and consequent discolouration of the blue limestone, one of the more important ornamental stone for the Portuguese industry, is due to FeS_2 oxidation whose is present in relatively high amounts. This weathering increases the surface roughness of the stone;

- Areas of the blue limestone showing colour alteration patterns are related with high levels of biocolonisation;
- The roughness increment of the stone surface caused by its weathering, possibly contributes to an increasing capacity of microorganisms to anchor the substrata;
- The main colonisers of the blue limestone lithotype are bacteria;
- CDM allowed the obtention of high microbial cells' concentration from stone with alteration patterns, for further use in artificial ageing assays;
- The discolouration rate of the blue limestone was proven to be higher when both bacteria and fungi are present;
- SEM allowed to monitor the microbial development on stone and its interaction with the material, during the artificial ageing assays;
- The HTS approach allowed to determine the microbiota dynamics during the artificial ageing performed on the blue limestone lithotype. After 180 days the prokaryotic population was mostly composed of microorganisms of the genera *Pseudomonas* (38.9%), *Zhihengliuella* (11.6%), *Microbispora* (9.5%), *Arthrobacter* (7.2%), *Enterobacter* (2.9%), *Exiguobacterium* (2.4%) and *Solibacillus* (1.6%), and the eukaryotic population was mostly composed of microorganisms of the genera *Didymella* (41.4%), *Fusarium* (34.8%) and *Mycosphaerella* (12%);
- The methodology adopted allowed to characterise the colour alteration mechanisms and the microbial population thriving on cultural heritage artworks and building made of stone, kept under indoor or outdoor environments;
- The discolouration patterns observed on the limestone sculptures can be mostly attributed to the stone-environment interaction. The four sculptures studied are colonised mainly by prokaryotic population, whose microbial diversity was wider for the *Musician Angel* sculpture, where carotenoids were also detected.
- The historic marble building shows colour alteration patterns that are mainly attributed to calcium oxalates formation (resulted from biogenic action), iron concentration in stone, and biofilms formation;
- The biofilms formed in this marble are predominantly composed by eukaryotic colonisers. The presence of the microorganisms of the genera *Sordaria*, *Aureobasidium* and/or *Rubrobacter* can induce red-coloured biofilms formation, while the blackish-coloured biofilm can be achieved by the presence of microorganisms of the genera *Cladosporium*, *Aureobasidium* and *Alternaria*.

In the near future, discolouration mechanisms of other stone lithotypes must be investigated, in order to make Portuguese stone a more valuable finish and building material. This knowledge will be very useful for the ornamental stone industry, as well as for the preservation of cultural heritage artworks and buildings. Creation of databases containing these data for each type of Portuguese stone would be interesting.

Regarding the blue limestone weathering, a solution should be found that would allow isolate the pyrite crystals to may prevent its oxidation. Several coating solutions have been tested for applied stone coating and this would be an interesting way forward with the application of, for example, phosphate/silicate solutions or nanopowders to microencapsulate the pyrite present in the stone. Alternatively, a full pyrite oxidation may be attempted prior to the application of stone, using oxidizing solutions.

Cultural heritage artworks maintained under indoor environments are also a concern. The air quality and thermo-hygric conditions should be monitored to assess air composition and detect pollutant levels that surround the artworks, in order to improve better conditions for their preservation. Since the alterations are mostly irreversible, the conservator-restorers must act as soon as possible. It is also important to study the biodiversity present in a museum environment, since these places receive thousands of visitors every year.

Biological contamination on stone under indoor or outdoor environments should be regularly monitored, as the environmental conditions can differ, and the presence of inactive microorganisms represents a potential risk. Furthermore, mitigation strategies should be applied in these materials. There are new natural biocides emerging in the market, which makes their development and application an interesting alternative to the conventional products usually applied.

References



- Abarenkov K, Henrik Nilsson R, Larsson K et al. (2010). The UNITE database for molecular identification of fungi – recent updates and future perspectives. *New Phytologist* **186** (2): 281–285. DOI: 10.1111/j.1469-8137.2009.03160.x;
- Abdelhafez AAM, El-Wekeel FM, Ramadan EM and Abed-Allah AA (2012). Microbial deterioration of archaeological marble: Identification and treatment. *Annals of Agricultural Science* **57** (2): 137-144. DOI: 10.1016/j.aosas.2012.08.007;
- Abulude FO, Ogunmola DN, Alabi MM and Abdulrasheed Y (2018). Atmospheric deposition: Effects on sculptures. *Chemistry International* **4** (2): 136-145. ISSN: 2410-9649;
- Aguilar M, Richardson E, Tan B, Walker G, Dunfield PF, Bass D, Nesbo C, Foght J and Dacks JB (2016). *The Journal of Eukaryotic Microbiology* **63** (6): 732-743. DOI: 10.1111/jeu.12320;
- Aires-Barros L, Basto MJ, Dionísio A and Charola AE (2001). Orange coloured surface deposits on stones from the Monastery of Batalha (Portugal) and from Nearby Historic Quarries: Characteristics and Origins. *Restoration of Buildings and Monuments* **7**(5): 491-506. DOI: 10.1515/rbm-2001-5594;
- Amann RI, Ludwig W and Schleifer KH (1995). Phylogenetic identification and in situ detection of individual microbial cells without cultivation. *Microbiological Reviews* **59** (1): 143-169;
- Amaral PM, Fernandes JC, Pires V and Rosa LG (2015). Ornamental Stones. *in* Materials for construction and Civil Engineering, eds. M. C. Gonçalves and F. Margarido. Springer International Publishing, Switzerland. pp: 397-445. DOI: 10.1007/978-3-319-08236-3_9;
- Anderson IC and Cairney JWG (2004). Diversity and ecology of soil fungal communities: increased understanding through the application of molecular techniques. *Environmental Microbiology* **6** (8): 769-779. DOI: 10.1111/j.1462-2920.2004.00675.x;
- Andrei AS, Păușan MR, Tămaș T, Har N, Barbu-Tudoran L, Leopold N and Banciu HL (2017). Diversity and Biomineralization Potential of the Epilithic Bacterial Communities Inhabiting the Oldest Public Stone Monument of Cluj-Napoca (Transylvania, Romania). *Frontiers in Microbiology* **8**: 372. DOI: 10.3389/fmicb.2017.00372;
- Andriani GF and Germinario L (2014). Thermal decay of carbonate dimension stones: fabric, physical and mechanical changes. *Environmental Earth Sciences* **72** (7): 2523-2539. DOI: 10.1007/s12665-014-3160-6;
- Azerêdo AC (2007). Formalização da litostratigrafia do Jurássico Inferior e Médio do Maciço Calcário Estremenho (Bacia Lusitânica), *Comunicações Geológicas* **94**: 29-51;
- Bams V and Dewaele S (2007). Staining of white marble. *Materials Characterization* **58** (11): 1052-1062. DOI: 10.1016/j.matchar.2007.05.004;
- Banciu HL (2013). Diversity of endolithic prokaryotes living in stone monuments – mini-review. *Studia Ubb Biologia*, LVIII, **1**: 99-109;

Barros RS, Oliveira DV, Varum H, Alves CAS and Camões A (2014). Experimental characterization of physical and mechanical properties of schist from Portugal. *Construction and Building Materials* **50**: 617-630. DOI: 10.1016/j.conbuildmat.2013.10.008;

Beck K, Janvier-Badosa S, Brunetaud X, Torok A and Al-Mukhtar M (2016). Non-destructive diagnosis by colorimetry of building stone subjected to high temperatures. *European Journal of Environmental and Civil Engineering* **20**: 643-655. DOI: 10.1080/19648189.2015.1035804;

Bell KG and Pankhurst RJ (1979). The interpretation of igneous rocks, *Springer/Chapman & Hall*, U.K. ISBN-10: 041253410X;

Benavente D, Martínez-Verdú F, Bernabeu A, Viqueira V, Fort R, García del Cura MA, Illueca C and Ordóñez S (2002). Influence of surface roughness on color changes in building stones. *Color research and application* **28** (5): 343-351. DOI: 10.1002/col.10178;

Benavente D, Brimblecombe P and Grossi CM (2015). Thermodynamic calculations for the salt crystallisation damage in porous built heritage using PHREEQC. *Environmental Earth Sciences* **74** (3): 2297-2313. DOI: 10.1007/s12665-015-4221-1;

Benedetti D, Bontempi E, Pedrazzani R, Zacco A and Depero LE (2007). Transformation in calcium carbonate stones: some examples. *Phase Transitions* **81** (2-3): 155-178. DOI: 10.1080/01411590701514342;

Berthonneau J, Grauby O, Bromblet P, Vallet JM, Dessandier D and Baronnet A. Role of swelling clay minerals in the spalling decay mechanism of the “Pierre Du Midi” limestone (South-east of France). 12th International Congress on the Determination and Conservation of Stone, Columbia University, New York, USA, 2012;

Berthonneau J, Bromblet P, Cherblanc F, Ferrage E, Vallet JM and Grauby O (2016). The spalling decay of building bioclastic limestones of Provence (South East of France): From clay minerals swelling to hydric dilation. *Journal of Cultural Heritage* **17**: 53-60. DOI: 10.1016/j.culher.2015.05.004;

Bose A, Gardel E, Vidoudez C, Parra E and Girguis P (2014). Electron uptake by iron-oxidizing phototrophic bacteria. *Nature Communications* **5**: 3391. DOI: 10.1038/ncomms4391;

Brilha J Andrade C, Azerêdo A, Barriga FJAS, Cachão M, Couto H, Cunha PP, Crispim JA, Dantas P, Duarte LV, Freitas MC, Granja HM, Henriques MH, Henriques P, Lopes L, Madeira J, Matos JMX, Noronha F, Pais J, Piçarra J, Ramalho MM, Relvas JMRS, Ribeiro A, Santos A, Santos VF and Terrinha P (2005). Definition of the Portuguese frameworks with international relevance as an input for the European geological heritage characterisation, *International Union of Geological Sciences* **28** (3): 177-186;

Burford EP, Kierans M and Gadd GM (2003). Geomycology: fungi in mineral substrata. *Mycologist* **17** (3): 98-107. DOI: 10.1017/S0269915X03003112;

- Burford EP, Hillier S and Gadd GM (2006). Biomineralization of fungal hyphae with calcite (CaCO₃) and calcium oxalate mono- and dihydrate in carboniferous limestone microcosms. *Geomicrobiology Journal* **23** (8): 599-611. DOI: 10.1080/01490450600964375;
- Bucher K and Grapes R (2011). Petrogenesis of Metamorphic Rocks. Springer-Verlag Berlin Heidelberg, Germany. ISBN: 978-3-540-74168-8;
- Cairncross B and McCarthy T (2015). Understanding minerals & crystals. Struik Nature, Cape Town, South Africa. ISBN: 978-1431700844;
- Calogero S, Bertelle M, Antonelli F and Lazzarini L, (2000). A Mössbauer study of some coloured marbles (cipollino mandolato, rosso antico and fior di pesco): implications on the nature of their colour. *Journal of Cultural Heritage*, **1**: 429–444. DOI: 10.1016/S1296-2074(00)01098-0;
- Cañaveras JC, Fernandez-Cortes A, Elez J, Cuezva S, Jurado V, Miller AZ, Rogerio-Candellera MA, Benavente D, Hernandez-Marine M, Saiz-Jimenez C and Sanchez-Moral S (2015). The deterioration of Circular Mausoleum, Roman Necropolis of Carmona, Spain. *Science of The Total Environment* **518-519**: 65-77. DOI: 10.1016/j.scitotenv.2015.02.095;
- Caporaso J G, Kuczynski J et al. (2010). QIIME allows analysis of high-throughput community sequencing data. *Nature Methods* **7** (5): 335-336. DOI: 10.1038/nmeth.f.303;
- Cardell-Fernández C, Vleugels G, Torfs K and Van Grieken R (2002). The processes dominating Ca dissolution of limestone when exposed to ambient atmospheric conditions as determined by comparing dissolution models. *Environmental Geology* **43**: 160-171. DOI: 10.1007/s00254-002-0640-x;
- Careddu N, Dino GA, Danielsen SW and Prikryl R (2018). Raw materials associated with extractive industry: An overview. *Resources Policy* **59**: 1-6. DOI: 10.1016/j.resourpol.2018.09.014;
- Carvalho J, Manuppella G and Moura AC (2000). Calcários ornamentais Portugueses. *Boletim das Minas* **37**: 223-232;
- Carvalho JMF, Manuppella G and Moura AC (2003). Portuguese ornamental limestones, International Symposium on Industrial Minerals and Building Stones, Istanbul, September 15-18;
- Carvalho JMF, Henriques P, Falé P and Luís G (2008). Decision criteria for the exploration of ornamental-stone deposits: Application of the marbles of the Portuguese Estremoz Anticline, *International Journal of Rock Mechanics & Mining Sciences* **45**: 1306-1319. DOI: 10.1016/j.ijrmms.2008.01.005.
- Carvalho JMF, Carvalho C, Lisboa JV, Moura AC and Leite MM. (2012a). Portuguese ornamental stones. In: Global Stone Congress 2012, Borba, Portugal, 16-20;
- Carvalho JMF, Lisboa JV, Prazeres CM and Sardinha RJ (2012b). Rochas ornamentais do Maciço Calcário Estremenho: Breve caracterização dos recursos, dos centros de produção e delimitação preliminar de áreas potenciais, *Boletim de Minas* **47** (1): 5-26;

Carvalho JMF, Lisboa JV, Moura AC, Carvalho C, Sousa LM and Leite MM (2013a). Evaluation of the portuguese ornamental stone resources, *Key Engineering Materials* **548**: 3-9. DOI: 10.4028/www.scientific.net/KEM.548.3;

Carvalho JMF, Carvalho CI, Lisboa JV, Moura AC, and Leite MM (2013b). Portuguese ornamental stones. *Geonovas* **26**: 15-22;

Carvalho JMF and Lisboa JV (2018). Ornamental stone potential areas for land use planning: a case study in a limestone massif from Portugal. *Environmental Earth Sciences* **77**: 206. DOI: 10.1007/s12665-018-7382-x;

Castanier S, Le Metayer-Levrel G, Oriol G, Loubiere JF and Perthuisot JP (2000). Bacterial carbonatogenesis and applications to preservation and restoration of historic property. In: Ciferri O, Tiano P, Mastromei G (eds) *Of Microbes and Art: The role of microbial communities in the degradation and protection of cultural heritage*. Plenum, New York, pp 201–216. DOI: 10.1007/978-1-4615-4239-1_14;

Charola AE, Puhlinger J and Steiger M (2007). Gypsum: a review of its role in the deterioration of building materials. *Environmental Geology* **52** (2): 339-352. DOI: 10.1007/s00254-006-0566-9;

Charola AE and Wendler E (2015). An Overview of the Water-Porous Building Materials Interactions. *Restoration of Buildings and Monuments* **21** (2-3): 55-65. DOI: 10.1515/rbm-2015-2006;

Chen Y, Li J, Chen L, Hua Z, Huang L, Liu J, Xu B, Liao B and Shu W (2014). Biogeochemical processes governing natural pyrite oxidation and release of acid metalliferous drainage. *Environmental Science & Technology* **48** (10): 5537-5545. DOI: 10.1021/es500154z;

Contrafatto L and Cosenza R (2014). Behaviour of post-installed adhesive anchors in natural stone. *Construction and Building Materials* **68**: 355-369. DOI: 10.1016/j.conbuildmat.2014.05.099;

Corvo F, Reyes J, Valdes C, Villaseñor F, Cuesta O, Aguilar D and Quintana P (2010). Influence of air pollution and humidity on limestone materials degradation in historical buildings located in cities under tropical coastal climates. *Water Air Soil Pollution* **205** (1): 359-375. DOI: 10.1007/s11270-009-0081-1;

Costaglia A, Vandenborre J, Blain G, Baty V, Haddad F and Fattahi M (2017). Radiolytic dissolution of calcite under gamma and helium ion irradiation. *The Journal of Physical Chemistry* **121** (44): 24548-24556. DOI: 10.1021/acs.jpcc.7b07299;

Crespo M (1949). Estremoz e o seu termo “regional”. Edição Fac-Similada, Estremoz, Portugal;

Crispim CA and Gaylarde CC (2004). Cyanobacteria and biodeterioration of cultural heritage: a review. *Microbial Ecology* **49**: 1-9. DOI: 1007/s0024800310525;

Cutler N and Viles H (2010). Eukaryotic microorganisms and stone biodeterioration. *Geomicrobiology Journal* **27** (6-7): 630-646. DOI: 10.1080/01490451003702933;

- Cutler NA, Oliver AE, Viles HA, Ahmad S and Whiteley AS (2013). The characterisation of eukaryotic microbial communities on sandstone buildings in Belfast, UK, using TRFLP and 454 pyrosequencing. *International Biodeterioration & Biodegradation* **82**: 124-133. DOI: 10.1016/j.ibiod.2013.03.010;
- Cuzman OA, Tiano P, Ventura S and Frediani P (2011). Biodiversity on Stone Artifacts, The Importance of Biological Interactions in the Study of Biodiversity, Dr. Jordi Lopez-Pujol (Ed.), InTech. ISBN: 978-953-307-751-2;
- D'Agostino D (2013). Moisture dynamics in an historical masonry structure: The Cathedral of Lecce (South Italy). *Building and Environment* **63**: 122-133. DOI: 10.1016/j.buildenv.2013.02.008;
- Dakal TC and Cameotra SS (2012). Microbially induced deterioration of architectural heritages: routes and mechanisms involved. *Environmental Sciences Europe* **24**: 36-48. DOI: 10.1016/j.aos.2012.08.007;
- De Leo F, Urzi C and de Hoog GS (1999). Two *Coniosporium* species from rock surfaces. *Studies in Mycology* **43**: 70-79;
- DeSantis TZ, Hugenholtz P, Larsen N, Rojas M, Brodie EL, Keller K, Huber T, Dalevi D, Hu P and Andersen GL (2006). Greengenes, a Chimera-Checked 16S rRNA Gene Database and Workbench Compatible with ARB. *Applied and Environmental Microbiology* **72** (7): 5069–5072. DOI: 10.1128/AEM.03006-05;
- Desarnaud J, Bonn D and Shahidzadeh N (2016). The Pressure induced by salt crystallization in confinement. *Nature Scientific Reports* **6**: 30856. DOI: 10.1038/srep30856;
- DGEG. (2017) Informação Estatística da Indústria Extrativa. Direção Geral de Energia e Geologia. (<http://www.dgeg.pt/>). Accessed at February 2019;
- Dhami NK, Reddy MS and Mukherjee A (2013). Biomineralization of calcium carbonates and their engineered applications: a review. *Frontiers in Microbiology* **4**: article 314. DOI: 10.3389/fmicb.2013.00314;
- Dias L, Rosado T, Coelho A, Barrulas P, Lopes L, Moita P, Candeias A Mirão J and Caldeira AT (2018). Natural limestone discolouration triggered by microbial activity—a contribution. *AIMS Microbiology* **4** (4): 594-607. DOI: 10.3934/microbiol.2018.4.594;
- Dias L, Rosado T, Candeias A, Mirão J and Caldeira AT (2019). A change in composition, a change in colour: The case of limestone sculptures from the Portuguese National Museum of Ancient Art. *Journal of Cultural Heritage*, article in press. DOI: 10.1016/j.culher.2019.07.025;
- Dionísio A, Braga MAS and Waerenborgh JC (2009). Clay minerals and iron oxides-oxyhydroxides as fingerprints of firing effects in a limestone monument. *Applied Clay Science* **42** (3-4): 629-638. DOI: 10.1016/j.clay.2008.05.003;
- Doehne E (2002). Salt weathering: a selective review. Geological Society, London, *Special Publications* **205**: 51-64. DOI: 10.1144/GSL.SP.2002.205.01.05;

Doehne E and Price CA (2010). *Stone Conservation: An overview of current research*. Second edition, Getty Publications, California, USA. ISBN: 978-1-60606-046-9;

Domonkos I, Kis M, Gombos Z and Ughy B (2013). Carotenoids, versatile components of oxygenic photosynthesis. *Progress in Lipid Research* **52** (4): 539-561. DOI: 10.1016/j.plipres.2013.07.001;

Duggal SK (1998) – *Building Materials*. First edition. Taylor & Francis, New York, USA. ISBN: 90-5410-764-2;

Dupont S, Carre-Mlouka A, Domart-Coulon I, Vacelet J and Bourguet-Kondracki M (2014). Exploring cultivable *Bacteria* from the prokaryotic community associated with the carnivorous sponge *Asbestopluma hypogea*. *FEMS Microbiology Ecology* **88** (1): 160-174;

Durn G (2003). Terra Rossa in the Mediterranean region: Parent materials, composition and origin. *Geologia Croatica* **56** (1): 83-100;

Earle S (2015). *Physical Geology*. BCcampus Open Ed. ISBN: 978-1-989623-70-1;

Edgar RC, Haas BJ, Clemente JC, Quince C and Knight R (2011). UCHIME improves sensitivity and speed of chimera detection. *Bioinformatics* **27** (16): 2194–2200. DOI: 10.1093/bioinformatics/btr381;

Edwards HGM, Newton EM and Russ J (2000). Raman spectroscopic analysis of pigments and substrata in prehistoric rock art. *Journal of Molecular Structure* **550-551**: 245-256. DOI: 10.1016/S0022-2860(00)00389-6;

Ekarim E (2017). Microbial deterioration of limestone of Sultan Hassan mosque, Cairo-Egypt and suggested treatment. *International Journal of ChemTech Research* **10** (5): 535-552. ISSN: 0974-4290;

El-Gohary M (2007). Degradation of limestone buildings in Jordan: Working effects and conservation problems “A critical study according to international codes of practice”. *Adumatu* **16**: 7-24. ISSN: 1319-8947;

El-Sheekh MM, Khairy HM and El-Shenody R (2012). Algal production of extra and intra-cellular polysaccharides as an adaptive response to the toxin crude extract of *Microcystis aeruginosa*. *Iranian Journal of Environmental Health Science & Engineering* **9**:10;

Emídio F, de Brito J, Gaspar PL and Silva A (2014). Application of the factor method to the estimation of the service life of natural stone cladding. *Construction and Building Materials* **66**: 484-493. DOI: 10.1016/j.conbuildmat.2014.05.073;

Espinosa-Marzal R and Scherer G (2010). Advances in understanding damage by salt crystallization. *Accounts of Chemical Research* **43** (6): 897-905. DOI: 10.1021/ar9002224;

Espinosa-Marzal RM, Hamilton A, McNall M, Whitaker K and Scherer GW (2011). The chemomechanics of crystallization during rewetting of limestone impregnated with sodium sulfate. *Journal of Materials Research* **26** (12): 1472-1481;

- Ettenauer J, Piñar G, Sterflinger K, Gonzalez-Munõz MT, Jroundi F (2011). Molecular monitoring of the microbial dynamics occurring on historical buildings during and after the *in situ* application of different bio-consolidation treatments. *Science of The Total Environment* **409** (24): 5337-5352. DOI 10.1016/j.scitotenv.2011.08.063;
- Ettenauer JD, Jurado V, Piñar G, Miller AZ, Santner M, Saiz-Jimenez C and Sterflinger K (2014). Halophilic Microorganisms Are Responsible for the Rosy Discolouration of Saline Environments in Three Historical Buildings with Mural Paintings. *Plos One* **9** (8): e103844. DOI: 10.1371/journal.pone.0103844;
- Eyssautier-Chuine S, Vaillant-Gaveau N, Gommeaux M, Thomachot-Schneider C, Pleck J and Fronteau G (2015). Efficacy of different chemical mixtures against green algal growth on limestone: A case study with *Chlorella vulgaris*. *International Biodeterioration & Biodegradation* **103**: 59-68. DOI: 10.1016/j.ibiod.2015.02.021;
- Fatorić S and Seekamp E (2017). Are cultural heritage and resources threatened by climate change? A systematic literature review. *Climatic Change* **142** (1-2): 227-254. DOI: 10.1007/s10584-017-1929-9;
- de Felice B, Pasquale V, Tancredi N, Schierillo S and Guida M (2010). Genetic fingerprint of microorganisms associated with the deterioration of an historical tuff monument in Italy. *Journal of Genetics* **89** (2): 253-257. DOI: 10.1007/s12041-010-0035-9;
- Feofilova EP, Ivashechkin AA, Alekhin AI and Sergeeva YE (2012). Fungal spores: Dormancy, germination, chemical composition, and role in biotechnology (review). *Applied Biochemistry and Microbiology* **48** (1): 1-11. DOI: 10.1134/S0003683812010048;
- Fitzner B (2004). Documentation and evaluation of stone damage on monuments. Proceedings of the 10th International Congress on Deterioration and Conservation of Stone, Stockholm, Sweden. ISBN: 978-916-311-458-8;
- Flatt R, Caruso F, Sanchez A and Scherer G (2014). Chemomechanics of salt damage in stone. *Nature Communications* **5**: 4823. DOI: 10.1038/ncomms5823;
- Foster J, Chittleborough DJ and Barovich K. Genesis of a Terra Rossa soil over marble and the influence of a neighbouring texture contrast soil at Delamere, South Australia. Supersoil2004: 3rd Australian New Zealand Soils Conference, University of Sidney, Australia, 5-9 December, 2004;
- da Fonseca BS, Galhano C and Vilão A (2013). Utilization of Estremoz marbles sawing sludge in ceramic industry – Preliminary Approach. *Civil and Environmental Research* **3** (9): 68-74. ISSN: 2224-5790;
- Frank-Kamemetskaya O, Rusakov A, Barinova E, Zelenskaya M and Vlasov D (2012). The formation of oxalate patina on the surface of carbonate rocks under the influence of microorganisms. In: Broekmans M (eds) Proceedings of the 10th International Congress for Applied Mineralogy (ICAM). Springer, Berlin, Heidelberg. DOI: 10.1007/978-3-642-27682-8_27;

Franzoni E, Sassoni E, Scherer GW and Naidu S (2013). Artificial weathering of stone by heating. *Journal of Cultural Heritage* **14** (3): 85-93. DOI: 10.1016/j.culher.2012.11.026;

Freire-Lista DM, Fort R and Varas-Muriel MJ (2015). Freeze–thaw fracturing in building granites. *Cold Regions Science and Technology* **113**: 40-51. DOI: 10.1016/j.coldregions.2015.01.008;

Gadd GM, Bahri-Esfahani J, Li Q, Rhee YJ, Wei Z, Fomina M and Liang X (2014). Oxalate production by fungi: significance in geomycology, biodeterioration and bioremediation. *Fungal Biology Reviews* **28** (2-3): 36-55. DOI: 10.1016/j.fbr.2014.05.001;

Gadd GM (2017). Fungi, Rocks, and Minerals. *Elements* **13** (3): 171-176. DOI: 10.2113/gselements.13.3.171;

Gaddamwar AG (2011). Analytical study of rain water for the determination of polluted or unpolluted zone. *International Journal of Environmental Sciences* **1** (6): 1317-1322. ISSN: 0976-4402;

Gaft M, Nagli L, Panczer G, Waychunas G and Porat N (2008) – The nature of unusual luminescence in natural calcite CaCO₃. *American Mineralogist* **93** (1): 158-167. DOI: 10.2138/am.2008.2576;

Gallego S, Devers-Lamrani M, Rousidou K, Karpouzas DG and Martin-Laurent F (2019). Assessment of the effects of oxamyl on the bacterial community of an agricultural soil exhibiting enhanced biodegradation. *Science of The Total Environment* **651** Part I: 1189-1198. DOI: 10.1016/j.scitotenv.2018.09.255;

Gao M, Su R, Wang K, Li X and Lu W (2013). Natural antifouling compounds produced by a novel fungus *Aureobasidium pullulans* HN isolated from marine biofilm. *Marine Pollution Bulletin* **77** (1-2): 172-176. DOI: 10.1016/j.marpolbul.2013.10.008;

Gaylarde CC and Gaylarde PM (2005). A comparative study of the major microbial biomass of biofilms on exteriors of buildings in Europe and Latin America. *International Biodeterioration & Biodegradation* **55** (2): 131-139. DOI: 10.1016/j.ibiod.2004.10.001;

Gaylarde CC, Gaylarde PM and Neilan BA (2012). Endolithic Phototrophs in Built and Natural Stone. *Current Microbiology* **65** (2): 183-188. DOI: 10.1007/s00284-012-0123-6;

Gaylarde C, Baptista-Neto JA, Ogawa A, Kowalski M, Celikkol-Aydin S and Beech I (2017). Epilithic and endolithic microorganisms and deterioration on stone church facades subject to urban pollution in a sub-tropical climate. *The Journal of Bioadhesion and Biofilm Research* **33** (2): 113-127. DOI: 10.1080/08927014.2016.1269893;

Gázquez F, Rull F, Medina J, Sanz-Arranz A and Sanz C (2015). Linking groundwater pollution to the decay of 15th-century sculptures in Burgos Cathedral (northern Spain). *Environmental Science and Pollution Research* **22** (20): 15677-15689. DOI: 10.1007/s11356-015-4754-6;

Gehlot P and Singh J (2018). Fungi and their Role in Sustainable Development: Current Perspectives. *Springer Singapore*, first edition. DOI: 10.1007/978-981-13-0393-7;

Gentilini C, Franzoni E, Bandini S and Nobile L (2012). Effect of salt crystallisation on the shear behaviour of masonry walls: An experimental study. *Construction and Building Materials* **37**: 181-189. DOI: 10.1016/j.conbuildmat.2012.07.086;

Ghobadi MH and Babazadeh R (2015). Experimental Studies on the Effects of Cyclic Freezing–Thawing, Salt Crystallization, and Thermal Shock on the Physical and Mechanical Characteristics of Selected Sandstones. *Rock Mechanics and Rock Engineering* **48** (3): 1001-1016. DOI: 10.1007/s00603-014-0609-6;

Gil M, Carvalho ML, Seruya A, Candeias AE, Mirão J and Queralt I (2007) – Yellow and red ochre pigments from southern Portugal: Elemental composition and characterization by WDXRF and XRD. *Nuclear Instruments and Methods in Physics Research A* **580**: 728–731. DOI: 10.1016/j.nima.2007.05.131;

Gill R (2010). Igneous rocks and processes – A practical guide. First edition, John Wiley & Sons, UK. ISBN: 978-1-4443-3065-6;

Gleason FH, Gadd GM, Pitt JI and Larkum AWD (2017). The roles of endolithic fungi in bioerosion and disease in marine ecosystems. I. General concepts. *Mycology* **8** (3): 205-215. DOI: 10.1080/21501203.2017.1352049;

Gómez-Cornelio S, Mendonza-Veja J, Gaylarde CC, Reyes-Estebanez M, Morón-Ríos A, Rosa-García SC and Ortega-Morales BO (2012). Succession of fungi colonizing porous and compact limestone exposed to subtropical environments. *Fungal Biology* **116** (10): 1064-1072. DOI: 10.1016/j.funbio.2012.07.010;

Gottschalk G (2012). Bacterial metabolism. *Springer Science & Business Media*. ISBN: 978-146-840-465-4;

Grafen H, Horn E, Schlecker H and Schindler H (2000). Corrosion. Ullmann's Encyclopedia of Industrial Chemistry. Wiley-VCH, Germany. DOI: 10.1002/14356007.b01_08;

Graue B, Siegesmund S, Oyhantcabal P, Naumann R, Licha T and Simon K (2013). The effect of air pollution on stone decay: the decay of the Drachenfels trachyte in industrial, urban, and rural environments—a case study of the Cologne, Altenberg and Xanten cathedrals. *Environmental Earth Sciences* **69** (4): 1095-1124. DOI: 10.1007/s12665-012-2161-6;

Grbic MVL and Vukojevic JB (2009). Role of fungi in biodeterioration process of stone in historic buildings. *Matica Srpska Proceedings for Natural Sciences* **116**: 245-251. DOI:10.2298/ZMSPN0916245L;

Grissom CA, Charola AE and Wachowiak MJ (2000). Measuring surface roughness on stone: Back to basics, *Studies in Conservation* **45** (2): 73-84. DOI: 10.1179/sic.2000.45.2.73;

Grossi CM and Benavente D (2016). Colour changes by laser irradiation of reddish building limestones. *Applied Surface Science* **384**: 525-529. DOI: 10.1016/j.apsusc.2016.05.031;

Grossi D, Del Lama EA, Garcia-Talegon J, Iñigo AC and Vicente-Tavera (2015). Evaluation of colorimetric changes in the Itaquera granite of the Ramos de Azevedo monument, São Paulo, Brazil. *International Journal of Conservation Science* **6**(3): 313-322. ISSN: 2067-533X;

Grossi CM, Brimblecombe P, Esbert RM and Alonso FJ (2007). Color changes in architectural limestones from pollution and cleaning. *Color Research and Application* **32**: 320–331. DOI: 10.1002/col.20322;

Gu JD, Ford TE, Berke NS and Mitchell R (1988). Biodeterioration of concrete by the fungus *Fusarium*. *International Biodeterioration & Biodegradation* **41** (2): 101-109. DOI: 10.1016/S0964-8305(98)00034-1;

Gu JD, Ford TE, Mitchel R (2011). Microbial degradation of materials: General processes. In: Revie, R. W. (eds), Uhlig's Corrosion Handbook, third edition, John Wiley & Sons, Inc, New Jersey, USA and Canada. ISBN: 978-0-470-87285-7;

Guillite O (1995). Bioreceptivity: a new concept for building ecology studies. *The Science of the Total Environment* **167**: 215-220;

Gutarowska B, Celikkol-Aydin S, Bonifay V, Otlewska A, Aydin E, Oldham AL, Brauer JI, Duncan KE, Adamiak J, Sunner JA and Beech IB (2015). Metabolomic and high-throughput sequencing analysis—modern approach for the assessment of biodeterioration of materials from historic buildings. *Frontiers in Microbiology* **6**: 979. DOI: 10.3389/fmicb.2015.00979;

Haldar SK and Tisljar J. Introduction to Mineralogy and Petrology. Chapter 5: Sedimentary Rocks. Elsevier, 2004, pp. 121-212. ISBN: 978-0-12-408133-8;

Hall C and Hoff WD (2007). Rising damp: capillary rise dynamics in walls. *Proceedings of the Royal Society A: Mathematical Physical and Engineering Sciences* **463** (2084). DOI: 10.1098/rspa.2007.1855;

Hallmann C, Fritzlar D, Stannek L and Hoppert M (2011). Ascomycete fungi on dimension stone of the “Burg Gleichen”, Thuringia. *Environmental Earth Sciences* **63** (7): 1713-1722. DOI 10.1007/s12665-011-1076-y.

Hallmann C, Stannek L, Fritzlar D, Hause-Reitner D, Friedl T and Hoppert M (2013). Molecular diversity of phototrophic biofilms on building stone. *FEMS Microbiology Ecology* **84** (2): 355-372. DOI: 10.1111/1574-6941.12065;

Hallman C, Friedenberger H, Hause-Reitner D and Hoppert M (2014). Depth profiles of microbial colonization in sandstones. *Geomicrobiology Journal* **32** (3-4): 365-379. DOI: 10.1080/01490451.2014.929762;

Hedrich S, Schlomann M and Johnson DB (2011). The iron-oxidizing proteobacteria. *Microbiology* **157** (Pt 6): 1551-1564. DOI: 10.1099/mic.0.045344-0;

- Hedrich S and Johnson DB (2013). *Acidithiobacillus ferridurans* sp. nov., an acidophilic iron-, sulfur- and hydrogen-metabolizing chemolithotrophic gammaproteobacterium. *International Journal of Systematic and Evolutionary Microbiology* **63**: 4018-4025. DOI: 10.1099/ijs.0.049759-0;
- Heinrichs G, Hubner I, Schmidt CK, Sybren de Hoog G and Haase G (2013). Analysis of black fungal biofilms occurring at domestic water taps (II): Potential routes of entry. *Mycopathologia* **175** (5-6): 399-412. DOI: 10.1007/s11046-013-9619-2;
- Herlemann DP, Labrenz M, Jurgens K, Bertilsson S, Waniek JJ and Andersson AF (2011). Transitions in bacterial communities along the 2000km salinity gradient of the Baltic Sea. *ISME Journal* **5** (10): 1571-1579. DOI: 10.1038/ismej.2011.41;
- Honegger R, Edwards D and Axe L (2013). The earliest records of internally stratified cyanobacterial and algal lichens from the Lower Devonian of the Welsh Borderland. *New Phytologist* **197**: 264-275. DOI: 10.1111/nph.12009;
- Howe JA (2001). *Geology of building stones*. first edition. Routledge, London, UK. ISBN: 978-131-774-219-7;
- Hueck HJ (1965). The biodeterioration of materials as part of hylobiology. *Mater. Org.* **1**(1): 5-34;
- Isola D, Selbmann L, Meloni P, Maracci E, Onofri S and Zucconi L (2013). Detrimental rock black fungi and biocides: A case study on the monumental cemetery of Cagliari. In: Rogerio-Candelera, Lazzari & Cano (eds), *Science and Technology for the Conservation of Cultural Heritage*, Taylor & Francis Group, London, UK. ISBN: 978-1-138-00009-4;
- Jafari B, Hanifezadeh M and Parvin MSJ (2012). Molecular study of bacteria associated with *Salicornia* symbiotic bacteria as a candidate for Hormozgan salty zone culturing by Persian Gulf water irrigation. *African Journal of Microbiology Research* **6** (22): 4687-4695. DOI: 10.5897/AJMR11.1132;
- Jim CY and Chen WY (2011). Bioreceptivity of buildings for spontaneous arboreal flora in compact city environment. *Urban Forestry & Urban Greening* **10** (1): 19-28. DOI: 10.1016/j.ufug.2010.11.001;
- Jones A (1999). Local colour: Megalithic architecture and colour symbolism in neolithic arran. *Oxford Journal of Archaeology* **18** (4): 339-350. DOI: 10.1111/1468-0092.00088;
- Jroundi F, Fernández-Vivas A, Rodríguez-Navarro C, Bedmar EJ, González-Muñoz MT (2010). Bioconservation of deteriorated monumental calcarenite stone and identification of bacteria with carbonatogenic activity. *Environmental Microbiology* **60** (1):39-54. DOI 10.1007/s00248-010-9665-y;
- Kabacińska Z, Yate L, Wencka M, Krzyminiewski R, Tadyszak K and Coy E (2017). Nanoscale effects of radiation (UV, X-ray, and γ) on calcite surfaces: Implications for its mechanical and physico-chemical properties. *The Journal of Physical Chemistry* **121** (24): 13357-13369. DOI: 10.1021/acs.jpcc.7b03581;

Kabacińska Z, Krzymiński R, Tadyszak K and Coy E (2019). Generation of UV-induced radiation defects in calcite. *Quaternary Geochronology* **51**: 24-42. DOI: 10.1016/j.quageo.2019.01.002;

Kolev H, Tyuliev G, Christov C and Kostov KL (2013). Experimental study of the surface chemical composition of sea salt crystallized during evaporation of seawater under natural conditions. *Bulgarian Chemical Communications* **45** (4): 584-591;

Kalita JM, Wary G (2014) – Thermoluminescence study of X-ray and UV irradiated natural calcite and analysis of its trap and recombination level. *Spectrochimica Acta Part A: Molecular and Biomolecular Spectroscopy*, **125** (5): 99-103. DOI: 10.1016/j.saa.2014.01.090;

Karaca Z, Ozturk A and Çolak E (2015). Biofouling of marbles by oxygenic photosynthetic microorganisms. *Environmental Science and Pollution Research* **22** (15): 11285-11289. DOI: 10.1007/s11356-015-4366-1;

Karagiannis N, Karoglou M, Bakolas A and Moropoulou A (2016). Building Materials Capillary Rise Coefficient: Concepts, Determination and Parameters Involved. In: Delgado, J. (eds), *New Approaches to Building Pathology and Durability. Building Pathology and Rehabilitation*, vol 6, Springer, Singapore. ISBN: 978-981-10-0647-0;

Kemler M, Witfeld F, Begerow D and Yurkov A (2017). Phylloplane yeasts in temperate climates. In: Buzzini P, Lachance MA, Yurkov A (eds), *Yeasts in Natural Ecosystems: Diversity*, Springer, Cham, 2017, pp. 171-197. DOI: 10.1007/978-3-319-62683-3_6;

Keshari N and Adhikary SP (2013). Characterization of cyanobacteria isolated from biofilms on stone monuments at Santiniketan, India. *The Journal of Bioadhesion and Biofilm Research* **29** (5): 525-536. DOI: 10.1080/08927014.2013.794224;

Kirilovsky D and Kerfeld CA (2016). Cyanobacterial photoprotection by the orange carotenoid protein. *Nature Plants* **2**:16180. DOI: 10.1038/nplants.2016.180;

Kirtzel J, Siegel D, Krause K and Kothe E (2017). Chapter three - Stone-eating fungi: Mechanisms in bioweathering and the potential role of laccases in black slate degradation with the Basidiomycete *Schizophyllum commune*. *Advances in Applied Microbiology* **99**: 83-101. DOI: 10.1016/bs.aambs.2017.01.002;

Klindworth A, Pruesse E, Schweer T, Peplies J, Quast C, Horn M and Glockner FO (2013). Evaluation of general 16S ribosomal RNA gene PCR primers for classical and next-generation sequencing-based diversity studies. *Nucleic Acids Research* **41**:e1. DOI: 10.1093/nar/gks808;

Kloppmann W, Bromblet P, Vallet JM, Vergès-Belmin V, Rolland O, Guerrot C and Gosselin C (2011). Building materials as intrinsic sources of sulphate: A hidden face of salt weathering of historical monuments investigated through multi-isotope tracing (B, O, S). *Science of The Total Environment* **409** (9): 1658-1669. DOI: 10.1016/j.scitotenv.2011.01.008;

- Koch A and Siegesmund S (2004). The combined effect of moisture and temperature on the anomalous expansion behaviour of marble. *Environmental Geology* **46** (3-4): 350-363. DOI: 10.1007/s00254-004-1037-9;
- Kompaníková Z, Gomez-Heras M, Michňová J, Durmeková T and Vlčko J (2014). Sandstone alterations triggered by fire-related temperatures. *Environmental Earth Sciences* **72** (7): 2569-2581. DOI: 10.1007/s12665-014-3164-2;
- Korkanç M and Savran A (2015). Impact of the surface roughness of stones used in historical buildings on biodeterioration. *Construction and Building Materials* **80**: 279-294. DOI: 10.1016/j.conbuildmat.2015.01.073;
- Kramar S, Urosevic M, Pristacz H and Mirtic B (2011). Assessment of limestone deterioration due to salt formation by micro-Raman spectroscopy: application to architectural heritage. *Journal of Raman Spectroscopy* **41** (11): 1441-1448. DOI: 10.1002/jrs.2700;
- Krupinska B, Grieken RV and De Wael K (2013). Air quality monitoring in a museum for preventive conservation: Results of a three-year study in the Plantin-Moretus Museum in Antwerp, Belgium. *Microchemical Journal* **110** (2013) 350-360. DOI: 10.1016/j.microc.2013.05.006;
- Kuprina AA, Lesovik VS, Zagorodnyk LH and Elistratkin MY (2014). Anisotropy of materials properties of natural and man-triggered origin. *Research Journal of Applied Sciences* **9** (11): 816-819. ISSN: 1815-932X;
- Kusumi A, Li X, Osuga Y, Kawashima A, Gu JD, Nasu M and Katayama Y (2013). Bacterial Communities in Pigmented Biofilms Formed on the Sandstone Bas-Relief Walls of the Bayon Temple, Angkor Thom, Cambodia. *Microbes and Environments* **28** (4): 422-431. DOI: 10.1264/jsme2.ME13033;
- Laanait N, Callagon EBR, Zhang Z, Sturchio NC, Lee SS and Fenter P (2015). X-ray-driven reaction front dynamics at calcite-water interfaces. *Science* **349** (6254): 1330-1334. DOI: 10.1126/science.aab3272;
- Laiz L, Miller AZ, Akatova E, Sanchez-Moral S, Gonzalez JM, Dionisio A, Macedo M. F and Saiz-Jimenez C. (2009). Isolation of five *Rubrobacter* strains from biodeteriorated monuments. *Naturwissenschaften* **96** (1): 71-79. DOI: 10.1007/s00114-008-0452-2;
- Leite MRM and da Silva AF (2013). Mineral raw materials, concepts, upgrading and potential in Portugal. *Ciência & Tecnologia dos Materiais* **25** (2): 71-74. DOI: 10.1016/j.ctmat.2014.03.001;
- Leverenz RL, Sutter M, Wilson A, Gupta S, Thurotte A, de Carbon CB, Petzold CJ, Ralston C, Perreau F, Kirilovsky D and Kerfeld CA (2015). A 12 Å carotenoid translocation in a photoswitch associated with cyanobacterial photoprotection. *Science* **348** (6242): 1463-1466. DOI: 10.1126/science.aaa7234;

Li L, Dong CF, Xiao K, Yao JZ and Li XG (2014). Effect of pH on pitting corrosion of stainless steel welds in alkaline salt water. *Construction and Building Materials* **68**: 709-715. DOI: 10.1016/j.conbuildmat.2014.06.090;

Li Q, Zhang B, He Z and Yang X (2016). Distribution and diversity of bacteria and fungi colonization in stone monuments analyzed by High-Throughput Sequencing. *Plos One* **11** (9): e0163287. DOI: 10.1371/journal.pone.0163287;

Li T, Hu Y and Zhang B (2018a). Biomineralization induced by *Colletotrichum acutatum*: A potential strategy for cultural relic bioprotection. *Frontiers in Microbiology* **9**: 1884. DOI: 10.3389/fmicb.2018.01884;

Li T, Hu Y, Zhang B and Yang X (2018b). Role of fungi in the formation of patinas on Feilaifeng limestone. *Environmental Microbiology* **76** (2): 352-361. DOI: 10.1007/s00248-017-1132-6;

Lichtenstein D (2017). Life Cycle of *Sordaria Fimicola*. (Website sciencing.com);

Liu Q, Zhang, B, Shen Z and Lu H (2006). A crude protective film on historic stones and its artificial preparation through biomimetic synthesis. *Applied Surface Science* **253** (5): 2625-2632. DOI: 10.1016/j.apsusc.2006.05.032;

Llop E, Álvaro I, Gómez-Bolea A, Mariné MH and Sammut S (2013). Biological crusts contribute to the protection of Neolithic Heritage in the Mediterranean region. In: Rogerio-Candelera M, Lazzari M and Cano E (eds), Science and Technology for the Conservation of Cultural Heritage, Taylor & Francis Group, London, UK. ISBN: 978-1-138-00009-4;

Lo Vetro D and Martini F (2016). Mesolithic in Central -Southern Italy: Overview of lithic productions. *Quaternary International* **423**: 279-302. DOI: 10.1016/j.quaint.2015.12.043;

Lopes L (2003). PhD thesis: Contribuição para o conhecimento tectono – Estratigráfico do Nordeste Alentejano, Transversal Terena-Elvas, Implicações económicas no aproveitamento de rochas ornamentais existentes na região (Mármore e Granitos);

Lopes L and Martins R (2012). Marbles from Portugal. *Naturstein: Platform for Natural Stone*;

Lopes L and Martins R (2014). Global Heritage Stone: Estremoz Marbles, Portugal. In: Global Heritage Stone: Towards International Recognition of Building and Ornamental Stones, *Geological Society*, London, Special Publications **407**: 57-74. DOI: 10.1144/SP407.10;

Lopes L (2016). As pedras portuguesas dos edifícios e monumentos brasileiros. *Geonomos* **24** (2): 45-56. DOI: 10.18285/geonomos.v24i2.840;

Lopes L (2020). Anticlinal de Estremoz: Geologia, Ordenamento do Território e Produção de Rochas Ornamentais após 2000 de exploração. *Boletim de Minas*, DGEG. 28 p. *In press*;

Maciel J and Coutinho H (1990). A utilização dos mármore em Portugal na época Romana, <http://ler.letras.up.pt/uploads/2860.pdf>;

Mamet B, Pr at A and De Ridder C (1997). Bacterial origin of the red pigmentation in the Devonian Slivenec limestone, Czech Republic. *Facies* **36** (1): 173-187. DOI: 10.1007/BF02536883;

Mandeiros JF. Patrim nio religioso de Estremoz. C mara Municipal de Estremoz, Estremoz, Portugal, 2001. ISBN: 972-9700-1-5;

Marks MAW, Hettmann K, Schilling J, Frost BR and Markl G (2011). The Mineralogical Diversity of Alkaline Igneous Rocks: Critical Factors for the Transition from Miaskitic to Agpaitic Phase Assemblages. *Journal of Petrology* **52** (3): 439-455. DOI: 10.1093/petrology/egq086;

Marszalek M (2016). Identification of secondary salts and their sources in deteriorated stone monuments using micro-Raman spectroscopy, SEM-EDS and XRD. *Journal of Raman Spectroscopy* **47** (12): 1473-1485. DOI: 10.1002/jrs.5037;

Martin-Sanchez PM, Bastian F, Alabouvette C, Saiz-Jimenez C (2013). Real-time PCR detection of *Ochroconis lascauxensis* involved in the formation of black stains in the Lascaux Cave, France. *Science of The Total Environment* **443**: 478-484. DOI: 10.1016/j.scitotenv.2012.11.026;

Martinho E, Dion sio A and Mendes M (2017). Simulation of a Portuguese limestone masonry structure submitted to fire: 3D ultrasonic tomography approach. *International Journal of Conservation Science* **8** (4): 565-580. ISSN: 2067-533X.

Martinho E and Dion sio A (2018). Assessment techniques for studying the effects of fire on stone materials: A literature review. *International Journal of Architectural Heritage*. DOI: 10.1080/15583058.2018.1535008;

Martino PD (2016). What about biofilms on the surface of stone monuments? *The Open Conference Proceedings Journal* **7** (1): 14-28. DOI: 10.2174/2210289201607020014;

Martins L, Vasconcelos G, Louren o PB and Palha C (2015). Influence of the Freeze-Thaw Cycles on the Physical and Mechanical Properties of Granites. *Journal of Materials in Civil Engineering* **28** (5). DOI: 10.1061/(ASCE)MT.1943-5533.0001488;

Martins R and Lopes L (2011). M rmoreos de Portugal, *Rochas & Equipamentos* **100**: 32-56;

Marvasi M, Donnarumma F, Frandi A, Mastromei G, Sterflinger K, Tiano P and Perito B (2012). Black microcolonial fungi as deteriogens of two famous marble statues in Florence, Italy. *International Biodeterioration & Biodegradation* **68**: 36-44. DOI: 10.1016/j.ibiod.2011.10.011;

Marzal RME and Scherer GW (2008). Crystallization of sodium sulfate salts in limestone. *Environmental Geology* **56** (3-4): 605-621. DOI: 10.1007/s00254-008-1441-7;

Matero F and Tagle A (1995). Cleaning, iron stain removal, and surface repair of architectural marble and crystalline limestone: The Metropolitan Club. *Journal of the American Institute for Conservation* **34** (1): 49-68. DOI: 10.1179/019713695806113712;

Mazdab FK, Wooden JL and Barth AP (2007). Trace elements variability in titanite from diverse geologic environments. *Geological Society of America Abstr Programs* **39** (6): 406.

McAllister DA (2016). Environmental controls on sandstone decay: the impact of climate and changing dynamics. EThOS Library Online, Queen's University Belfast. ISNI: 0000 0004 5371 4875;

McCabe S, Smith BJ and Warke PA (2010). Exploitation of inherited weakness in fire-damaged building sandstone: the 'fatiguing' of 'shocked' stone. *Engineering Geology* **115** (3-4): 217-225. DOI: 10.1016/j.enggeo.2009.06.003;

McCabe S, McAllister D, Warke PA and Gomez-Heras M (2015). Building sandstone surface modification by biofilm and iron precipitation: emerging block-scale heterogeneity and system response. *Earth Surface Processes and Landforms* **40** (1): 112-122; DOI: 10.1002/esp.3665;

McNamara CJ and Mitchell R (2005). Microbial deterioration of historic stone. *Frontiers in Ecology and the Environment* **3** (8): 445-451;

McNamara CJ, Perry TD, Bearce KA, Hernandez-Duque G and Mitchell R (2006). Epilithic and endolithic bacterial communities in limestone from a Maya archaeological site. *Microbial Ecology* **51** (1): 51-64. DOI: 10.1007/s00248-005-0200-5;

Mendes A, Sanjayan JG, Gates WP and Collins F (2012). The influence of water absorption and porosity on the deterioration of cement paste and concrete exposed to elevated temperatures, as in a fire event. *Cemented and Concrete Composites* **34** (9): 1067-1074. DOI: 10.1016/j.cemconcomp.2012.06.007;

Menningen J, Siegesmund S, Lopes L et al. (2018). The Estremoz marbles: an updated summary on the geological, mineralogical and rock physical characteristics. *Environmental Earth Sciences* **77**: 191. DOI: 10.1007/s12665-018-7328-3.

Mérillou N, Mérillou S, Ghazanfarpour D, Dischler JM and Galin M. Simulating Atmospheric Pollution Weathering on Buildings. 18th International Conference in Central Europe on Computer Graphics, pp. 65-72, Univerzita V Plzni, Czech Republic, 2010;

Mihajlovski A, Seyer D, Benamara H, Bousta F and Di Martino P (2015). An overview of techniques for the characterization and quantification of microbial colonization on stone monuments. *Annals of Microbiology* **65**: 1243-1255. DOI: 10.1007/s13213-014-0956-2;

Mihajlovski A, Gabarre A, Seyer D, Bousta F and Di Martino P (2017). Bacterial diversity on rock surface of the ruined part of a French historic monument: The Chaalis abbey. *International Biodeterioration & Biodegradation* **120**: 161-169. DOI: 10.1016/j.ibiod.2017.02.019;

Miller AZ, Laiz L, Gonzalez JM, Dionísio A, Macedo MF and Saiz-Jimenez C (2008). Reproducing stone monument photosynthetic-based colonization under laboratory conditions. *Science of The Total Environment* **405**: 278-285. DOI: 10.1016/j.scitotenv.2008.06.066;

- Miller AZ, Dionísio A, Laiz L, Macedo MF and Saiz-Jimenez C (2009). The influence of inherent properties of building limestones on their bioreceptivity to phototrophic microorganisms. *Annals of Microbiology* **59** (4): 705-713. DOI: 10.1007/BF03179212;
- Miller AZ, Sanmartín P, Pereira-Pardo L, Dionísio A, Saiz-Jimenez C, Macedo MF and Prieto B (2012). Bioreceptivity of building stones: A review. *Science of The Total Environment* **426**: 1-12. DOI: 10.1016/j.scitotenv.2012.03.026;
- Millero FJ (2009). Carbonate constants for estuarine waters. *Marine and Freshwater Research* **61** (2): 139-142. DOI: 10.1071/MF09254;
- Mitchell R, and Gu JD (2000). Changes in the biofilm microflora of limestone caused by atmospheric pollutants. *International Biodeterioration & Biodegradation* **46** (4): 299-303. DOI: 10.1016/S0964-8305(00)00105-0;
- Mohammadi P and Maghbolí-Balásjin N (2014). Isolation and molecular identification of deteriorating fungi from Cyrus the Great tomb stones. *Iranian Journal of Microbiology* **6** (5): 361-370;
- Mokrzycki W and Tatol M (2011). Color difference Delta E – A survey. *Machine Graphics and Vision* **20** (4): 383-411;
- Monte M (2003). Oxalate film formation on marble specimens caused by fungus. *Journal of Cultural Heritage* **4** (3): 255-258. DOI: 10.1016/S1296-2074(03)00051-7;
- Móricz F, Mádaí F and Walder IF (2012). Pyrite oxidation under circumneutral pH conditions. *GeoScience Engineering* **1**: 111-116. DOI: 10.1016/0016-7037(91)90005-P;
- Morillas H, Maguregui M, Marcaida I, Trebolazabala J, Salcedo I and Madariaga JM (2015). Characterization of the main colonizer and biogenic pigments present in the red biofilm from La Galea Fortress sandstone by means of microscopic observations and Raman imaging. *Microchemical Journal* **121**: 48-55. DOI: 10.1016/j.microc.2015.02.005;
- Mos YM, Vermeulen AC, Buisman CJN and Weijma J (2018). X-ray diffraction of iron containing samples: The importance of a suitable configuration. *Geomicrobiology Journal* **35**: 511-517. DOI: 10.1080/01490451.2017.1401183;
- Mosch S (2009). Optimierung der Exploration, Gewinnung und Materialcharakterisierung von Naturwerksteinen. Diss Univ Göttingen, Göttingen;
- Mosmann T (1983). Rapid colorimetric assay for cellular growth and survival: Application to proliferation and cytotoxicity assays, *Journal of Immunological Methods* **65**:55-63. DOI: 10.1016/0022-1759(83)90303-4;
- Moura AC (2007). Mármore e calcários ornamentais de Portugal. *Gestão de Artes Gráficas, SA*, Amadora, Portugal. ISBN: 978-972-676-204-1;
- Municchia AC, Caneva G, Ricci MA and Sodo A (2014). Identification of endolithic traces on stone monuments and natural outcrops: preliminary evidences. *Journal of Raman Spectroscopy* **45** (11-12): 1180-1185;

Muynck W, Leuridan S, Van Loo D, Verbeken K, Cnudde V, De Belie N and Verstraete W (2011). Influence of Pore Structure on the effectiveness of a biogenic carbonate surface treatment for limestone conservation. *Applied and Environmental Microbiology* **77** (19): 6808-6820. DOI: 10.1128/AEM.00219-11;

Nassau K. The Physics and Chemistry of Color: The Fifteen Causes of Color. second edition, *Wiley-VCH*, New York, USA, 2001. ISBN: 978-0-471-39106-7;

Niyomvong N, Pathom-aree W, Thamchaipenet A and Duangmal K (2012). Actinomycetes from tropical limestone caves. *Chiang Mai Journal of Science* **39** (3): 373-388;

Nordstrom DK (2011). Sulfide Mineral Oxidation. In book: Encyclopedia of Geobiology, pp. 856-858. DOI: 10.1007/978-1-4020-9212-1_198;

Nupur LNU, Vats A, Dhanda SK, Raghava GPS, Pinnaka AK and Kumar A (2016). ProCarDB: a database of bacterial carotenoids. *BMC Microbiology* **16**: 96. DOI: 10.1186/s12866-016-0715-6;

Olson CJ, Ruhe RV and Mausbach MJ (1980). The Terra Rossa limestone contact phenomena in Karst, Southern Indiana. *Soil Science Society of America Journal* **44** (5): 1075-1079. DOI: 10.2136/sssaj1980.03615995004400050040x;

Onofri S, Zucconi L, Isola D and Selbmann L (2014). Rock-inhabiting fungi and their role in deterioration of stone monuments in the Mediterranean area. *Plant Biosystems* **148** (2): 384-391. DOI: 10.1080/11263504.2013.877533;

Orial G, Castanier S, Le Metayer-Levrel G, Loubiere JF (1993). The biomineralization: a new process to protect calcareous stone applied to historic monuments. In: Ktoishi H, Arai T, Yamano K (eds) Proceedings of the 2nd International Conference of Biodeterioration of Cultural Property. International Communications Specialists, Tokyo, Japan, pp 98–116;

Orihuela MF, Abad J, González Martínez JF, Fernández FJ and Colchero J (2014). Nanoscale characterisation of limestone degradation using Scanning Force Microscopy and its correlation to optical appearance. *Engineering Geology* **179**: 158-166. DOI: 10.1016/j.enggeo.2014.06.022;

Ortega-Morales BO, Narváez-Zapata J, Reyes-Estebanez M, Quintana P, Rosa-García SC, Bullen H, Gómez-Cornelio S, Chan-Bacab MJ (2016). Bioweathering Potential of Cultivable Fungi Associated with Semi-Arid Surface Microhabitats of Mayan Buildings. *Frontiers in Microbiology* **7**:201. DOI: 10.3389/fmicb.2016.00201;

Ospitali F, Bersani D, Di Lonardo G and Lottici PP (2008). “Green earths”: vibrational and elemental characterization of glauconites, celadonites and historical pigments. *Journal of Raman Spectroscopy* **39**: 1066-1073. DOI: 10.1002/jrs.1983;

Ozguven A and Ozcelik Y (2013). Investigation of some property changes of natural building stones exposed to fire and high heat. *Construction and Building Materials* **38**: 813-821. DOI: 10.1016/j.conbuildmat.2012.09.072;

- Ozguven A and Ozcelik Y (2014). Effects of high temperature on physico-mechanical properties of Turkish natural building stones. *Engineering Geology* **183**: 127-136. DOI: 10.1016/j.enggeo.2014.10.006;
- Palla F and Barresi G. *Biotechnology and Conservation of Cultural Heritage*. first edition, Springer International Publishing Switzerland, Cham, Switzerland, 2017. ISBN: 978-3319461663;
- Pangallo D, Chovanová A, Simonovicová A and Ferianc P (2009). Investigation of microbial community isolated from indoor artworks and air environment: identification, biodegradative abilities, and DNA typing. *Canadian Journal of Microbiology* **55**: 277-287. DOI: 10.1139/w08-136;
- Páramo-Aguilera P, Ortega-Morales BO, Narváez-Zapata JA (2012). Culturable fungi associated with urban stone surfaces in Mexico City. *Electronic Journal of Biotechnology* **15** (4):1-17. DOI: 10.2225/vol15-issue4-fulltext-6;
- Parisi F and Augenti N (2013). Earthquake damages to cultural heritage constructions and simplified assessment of artworks. *Engineering Failure Analysis* **34**: 735-760. DOI: 10.1016/j.engfailanal.2013.01.005;
- Pereira D and Marker B (2016). The value of original natural stone in the context of architectural heritage. *Geosciences* **6** (1): 13-21. DOI: 10.3390/geosciences6010013;
- Piñar G, Jimenez-Lopez C, Sterflinger K, Eettenauer J, Jroundi F, Fernandez-Vivas A and Gonzalez-Muñoz MT (2010). Bacterial community Dynamics during the application of a *Myxococcus xanthus*-inoculated culture medium used for consolidation of ornamental stone. *Microbial Ecology* **60** (1): 15-28. DOI: 10.1007/s00248-010-9661-2;
- Piñar G, Eettenauer J and Sterflinger K (2014a). “La vie en rose”: A review of the rosy discoloration of subsurface monuments. In: *The conservation of subterranean cultural heritage*, Saiz-Jimenez, C. (ed.), CRC Press/Balkema, Leiden, 113-124. DOI: 10.1201/b17570-16;
- Piñar G, Kraková L, Pangallo D, Piombino-Mascali D, Maixner F, Zink A and Sterflinger K (2014). Halophilic bacteria are colonizing the exhibition areas of the Capuchin Catacombs in Palermo, Italy. *Extremophiles* **18** (4): 677-691. DOI: 10.1007/s00792-014-0649-6;
- Pinheiro AC, Mesquita N, Trovão J, Soares F, Tiago I, Coelho C, Carvalho HP, Gil F, Catarino L, Piñar G and Portugal A (2019). Limestone biodeterioration: A review on the Portuguese cultural heritage scenario. *Journal of Cultural Heritage* **36**: 275-285. DOI: 10.1016/j.culher.2018.07.008;
- Pinna D (2014). Biofilms and lichens on stone monuments: do they damage or protect? *Frontiers in Microbiology* **5**:133. DOI: 10.3389/fmicb.2014.00133;
- Pires V, Silva ZSG, Simão JAR, Galhano C and Amaral PM (2010). “Bianco di Asiago” limestone pavement – Degradation and alteration study. *Construction and Building Materials* **24** (5): 686-694. DOI: 10.1016/j.conbuildmat.2009.10.040;

Pitcher DG, Saunders NA and Owen RJ (1989). Rapid extraction of genomic DNA with guanidinium thiocyanate. *Letters in Applied Microbiology* **8**: 151-156. DOI: 10.1111/j.1472-765X.1989.tb00262.x;

Pokorna D and Zabranska J (2015). Sulfur-oxidizing bacteria in environmental technology. *Biotechnology Advances* **33** (6): 1246-1259. DOI: 10.1016/j.biotechadv.2015.02.007;

Polikreti K and Maniatis Y (2004). Distribution changes of Mn²⁺ and Fe³⁺ on weathered marble surfaces measured by EPR. *Atmospheric Environment* **38** (22): 3617-3624. DOI: 10.1016/j.atmosenv.2004.03.048;

Polo A, Cappitelli F, Brusetti L, Principi P, Villa F, Giacomucci L, Ranalli G and Sorlini C (2010). Feasibility of removing surface deposits on stone using biological and chemical remediation methods. *Microbial Ecology* **60** (1): 1-14. DOI: 10.1007/s00248-009-9633-6;

Pouli P, Oujja M and Castillejo M (2012). Practical issues in laser cleaning of stone and painted artefacts: optimisation procedures and side effects. *Applied Physics A* **106**: 447-464. DOI: 10.1007/s00339-011-6696-2;

Pranjic AM, Mulec J, Muck T, Hladnik A and Mladenovic A (2015). The bioreceptivity of building stone. *Geophysical Research Abstracts*, EGU General Assembly **17**, EGU2015-13017-3;

Rahmani S, Forozandeh M, Mosavi M and Rezaee A (2006). Detection of bacteria amplifying the 16S rRNA gene with universal primers and RFLP. *Medical Journal of the Islamic Republic of Iran* **19** (4): 333-338;

Rampazzi L, Andreotti A, Bonaduce I, Colombini MP, Colombo C and Toniolo L (2004). Analytical investigation of calcium oxalate films on marble monuments. *Talanta* **63** (4): 967-977. DOI: 10.1016/j.talanta.2004.01.005;

Rana A, Kalla P, Verma HK and Mohnot JK (2016). Recycling of dimensional stone waste in concrete: A review. *Journal of Cleaner Production* **135**: 312-331. DOI: 10.1016/j.jclepro.2016.06.126;

Randive KR, Korakoppa MM, Muley SV, Varade AM, Khandare HW, Lanjewar SG, Tiwari RR and Karadhi KK (2015). Paragenesis of Cr-rich muscovite and chlorite in green-mica quartzites of Saigaon-Palasaon area, Western Bastar Craton, India. *Journal of Earth System Science* **124** (1): 213-225. DOI: 10.1007/s12040-014-0514-0;

Rikkinen J (2013). Molecular studies on cyanobacterial diversity in lichen symbioses. *MycoKeys* **6**: 3-32. DOI: 10.3897/mycokeys.6.3869;

Rinta-Kanto J M, Ouellette A J, Boyer G L, Twiss MR, Bridgeman TB and Wilhelm SW (2005). Quantification of toxic *Microcystis* spp. during the 2003 and 2004 blooms in Western Lake Erie using quantitative Real-Time PCR, *Environmental Science & Technology* **39**: 4198-4205, DOI: 10.1021/es048249u;

Ritsema CJ and Groenenberg JE (1993). Pyrite oxidation, carbonate weathering, and gypsum formation in a drained potential acid sulfate soil. *Soil Science Society of America Journal* **57** (4): 968-976. DOI: 10.2136/sssaj1993.03615995005700040015x;

Rivadeneira MA, Párraga J, Delgado R, Ramos-Cormenzana A, and Delgado G (2004). Biomineralization of carbonates by *Halobacillus trueperi* in solid and liquid media with different salinities. *FEMS Microbiology Ecology* **48** (1): 39-46. DOI: 10.1016/j.femsec.2003.12.008;

Robeson DJ and Jalal MAF (1992). Formation of Ent-isophleichrome by *Cladosporium herbarum* isolated from sugar beet. *Bioscience, Biotechnology, and Biochemistry* **56** (6): 949-952;

Rodrigues JD (2006). Stone patina. A controversial concept of relevant importance in conservation. International Seminar Theory and Practice in Conservation. A tribute to Cesare Brandi, Lisbon, Portugal, Volume: 1;

Rodrigues JD (2015). Defining, mapping and assessing deterioration patterns in stone conservation projects. *Journal of Cultural Heritage* **16** (3): 267-275. DOI: 10.1016/j.culher.2014.06.007;

Rodriguez-Navarro C, Hansen E, Sebastian E and Ginell S (1997). The role of clays in the decay of ancient Egyptian limestone sculptures. *Journal of the American Institute for Conservation* **36** (2): 151-163. DOI: 10.2307/3179829;

de la Rosa JP M, Warke PA and Smith BJ (2012). Microscale biopitting by the endolithic lichen *Verrucaria baldensis* and its proposed role in mesoscale solution basin development on limestone. *Earth Surface Processes and Landforms* **37** (4): 374-384. DOI: 10.1002/esp.2244;

de la Rosa JPM, Porcel MC and Warke PA (2013). Mapping stone surface temperature fluctuations: Implications for lichen distribution and biomodification on historic stone surfaces. *Journal of Cultural Heritage* **14** (4): 346-353. DOI: 10.1016/j.culher.2012.09.006;

de la Rosa JPM, Warke PA and Smith BJ (2014). The effects of lichen cover upon the rate of solutional weathering of limestone. *Geomorphology* **220**: 81-92. DOI: 10.1016/j.geomorph.2014.05.030;

Rosa-García SC, Ortega-Morales O, Gaylarde CC, Beltrán-García M, Quintana-Owen P and Reyes-Estebanez M (2011). Influence of fungi in the weathering of limestone of Mayan monuments. *Revista Mexicana de Micología* **33**: 43-51;

Rosado T, Gil M, Mirão J, Candeias A and Caldeira AT (2013a). Oxalate biofilm formation in mural paintings due to microorganisms – A comprehensive study. *International Biodeterioration & Biodegradation* **85**: 1-7. DOI: 10.1016/j.ibiod.2013.06.013;

Rosado T, Martins MR, Pires M, Mirão J, Candeias A and Caldeira AT (2013b). Enzymatic monitorization of mural paintings biodegradation and biodeterioration. *International Journal of Conservation Science* **4**:603-612. ISSN: 2067-533X;

Rosado T, Reis A, Mirão J, Candeias A, Vandenabeele P and Caldeira AT (2014a). Pink! Why not? On the unusual colour of Évora Cathedral, *International Biodeterioration & Biodegradation* **94**: 121-127. 10.1016/j.ibiod.2014.07.010;

Rosado T, Silva M, Galvão A, Mirão J, Candeias A and Caldeira AT (2016). A first insight on the biodegradation of limestone: the case of the World Heritage Convent of Christ. *Applied Physics A* **122**: 1012. DOI: 10.1007/s00339-016-0525-6;

Rosado T, Dias L, Lança M, Nogueira C, Santos R, Martins MR, Candeias A, Mirão J and Caldeira AT (2019). Assessment of microbiota present on outdoor stone materials using high throughput sequencing approaches (article submitted).

Rosso F, Jin W, Pisello AL, Ferrero M and Ghandehari M (2016). Translucent marbles for building envelope applications: Weathering effects on surface lightness and finishing when exposed to simulated acid rain. *Construction and Building Materials* **108**: 146-153. DOI: 10.1016/j.conbuildmat.2016.01.041;

Rothert E, Eggers T, Cassar J, Ruedrich J, Fitzner B and Siegesmund S (2007). Stone properties and weathering induced by salt crystallization of Maltese Globigerina Limestone. In *Building Stone Decay: From Diagnosis to Conservation*, Prikryl R and Smith BJ (eds) Geological Society, London, *Special Publications* **271**: 189-198. ISBN: 978-1-86239-218-2;

Ruedrich J, Kirchner D, Siegesmund S (2011). Physical weathering of building stones induced by freeze–thaw action: a laboratory long-term study. *Environmental Earth Sciences* **63** (7-8): 1573-1586. DOI: 10.1007/s12665-010-0826-6;

Saiz-Jimenez C. Air pollution and cultural heritage. first edition, Taylor & Francis Group, London, UK, 2004. ISBN: 9789058096821;

Saiz-Jimenez C, Miller AZ, Martin-Sanchez PM and Hernandez-Marine M (2012). Uncovering the origin of the black stains in Lascaux Cave in France. *Environmental Microbiology* **14** (12): 3220-3231. DOI: 10.1111/1462-2920.12008;

Saloustros S, Pelà L, Roca P and Portal J (2015). Numerical analysis of structural damage in the church of the Poblet Monastery. *Engineering Failure Analysis* **48**: 41-61. DOI: 10.1016/j.engfailanal.2014.10.015;

Salvadori O and Municchia AC (2016). The Role of Fungi and Lichens in the Biodeterioration of Stone Monuments. *The Open Conference Proceedings Journal* **10**: 39-54. DOI: 10.2174/2210289201607020039;

Sambrook J, Fritsch E and Maniatis T (1989). Molecular cloning: a laboratory manual. second edition. Cold Spring Harbor Laboratory, Cold Spring Harbor, N.Y., ISBN: 978-1-936113-42-2;

- Sánchez-España J, Boehrer B and Yusta I (2014). Extreme Carbon Dioxide Concentrations in Acidic Pit Lakes Provoked by Water/Rock Interaction. *Environmental Science & Technology* **48** (8): 4273-4281. DOI: 10.1021/es5006797;
- Sasso S, Scrano L, Ventrella E, Bonomo MG, Crescenzi A, Salzano G and Bufo SA (2013). Natural biocides to prevent the microbial growth on cultural heritage. Proceeding of Built Heritage 2013 – Monitoring Conservation Management, Milan, Italy, pp. 1035-1042;
- Sassoni E and Franzoni E (2014a). Influence of porosity on artificial deterioration of marble and limestone by heating. *Applied Physics A* **115** (3): 809-816. DOI: 10.1007/s00339-013-7863-4;
- Sassoni E and Franzoni E (2014b). Sugaring marble in the Monumental Cemetery in Bologna (Italy): characterization of naturally and artificially weathered samples and first results of consolidation by hydroxyapatite. *Applied Physics A* **117** (4): 1893-1906. DOI: 10.1007/s00339-014-8629-3;
- Sazanova KV, Shchiparev SM and Vlasov DY (2014). Formation of organic acids by fungi isolated from the surface of stone monuments. *Microbiology* **83** (5): 516-522. DOI: 10.1134/S002626171405021X;
- Scheerer S, Ortega-Morales O and Gaylarde C (2009). Microbial Deterioration of Stone Monuments—An Updated Overview. *Advances in Applied Microbiology* **66**: 97-139. DOI: 10.1016/S0065-2164(08)00805-8;
- Schiavon N (1991). Gypsum crust formation and “stratigraphy” in weathered building limestones: A SEM study of stone decay in the U.K.. *Science, Technology and European Cultural Heritage*, Proceedings of the European Symposium, Bologna, Italy, June 1989: 447-451;
- Schiavon N, De Caro T, Kiros A, Caldeira AT, Parisi IE, Riccucci C and Gigante GE (2013). A multianalytical approach to investigate stone biodeterioration at a UNESCO world heritage site: the volcanic rock-hewn churches of Lalibela, Northern Ethiopia. *Applied Physics A* **113** (4): 843-854. DOI: 10.1007/s00339-013-7757-5;
- Schmidt K (2011). Göbekli Tepe: A Neolithic Site in Southwestern Anatolia. In Steadman, Sharon R.; McMahon, Gregory (eds.). *The Oxford Handbook of Ancient Anatolia*. Oxford: Oxford University Press. p. 917. ISBN: 9780195376142;
- Schmieder R and Edwards R (2011). Quality control and preprocessing of metagenomic datasets. *Bioinformatics* **27** (6): 863-864. DOI: 10.1093/bioinformatics/btr026;
- Schon JH (2015). Physical properties of rocks: Fundamentals and principals of petrophysics. 2nd edition, Elsevier, Amsterdam, Netherlands. ISBN: 978-0-08-100404-3;
- Schubert M, Lindgreen S and Orlando L (2016). AdapterRemoval v2: rapid adapter trimming, identification, and read merging. *BMC Research Notes* **9**: 88-94. DOI: 10.1186/s13104-016-1900-2;
- Schuster SC (2007). Next-generation sequencing transforms today's biology. *Nature Methods* **5**: 16-18. DOI: 10.1038/nmeth1156;

Seaward MRD (2014). Lichens as Agents of Biodeterioration. In: Upreti D, Divakar P, Shukla V and Bajpai R (eds), *Recent Advances in Lichenology*. Springer, New Delhi. DOI: 10.1007/978-81-322-2181-4_9;

Sebastián E, Cultrone G, Benavente D, Linares Fernández L, Elert K and Rodríguez-Navarro C (2008). Swelling damage in clay-rich sandstones used in the church of San Mateo in Tarifa (Spain). *Journal of Cultural Heritage* **9** (1): 66-76. DOI: 10.1016/j.culher.2007.09.002;

Selonen O, Luodes H and Ehlers C (2000). Exploration for dimensional stone—implications and examples from the Precambrian of southern Finland. *Engineering Geology* **56**: 275-291. DOI: 10.1016/S0013-7952(99)00091-5;

Serafeimidis K and Anagnostou G (2014). On the crystallisation pressure of gypsum. *Environmental Earth Sciences* **72** (12): 4985-4994. DOI: 10.1007/s12665-014-3366-7;

Shushakova V, Fuller Jr ER and Siegesmund S (2013). Microcracking in calcite and dolomite marble: microstructural influences and effects on properties. *Environmental Earth Sciences* **69** (4): 1263-1279. DOI: DOI 10.1007/s12665-012-1995-2;

Siedel H and Siegesmund S (2014). Characterization of Stone Deterioration on Buildings. In: Siegesmund, S. and Snethlage, R. (eds), *Stone in Architecture*. Springer, Berlin, Heidelberg. DOI: 10.1007/978-3-642-45155-3_6;

Siegesmund S, Ruedrich J and Weiss T (2004). Marble deterioration In: Prikryl R (ed.) *Dimension Stone 2004*. Taylor & Francis Group, London, 211–217. ISBN: 978-905-809-675-3;

Siegesmund S, Mosch S, Scheffchuk C and Nikolayev DI (2008a). The bowing potential of granitic rocks: rock fabric, thermal properties and residual strain. *Environmental Geology* **55** (7): 1437-1448. DOI: 10.1007/s00254-007-1094-y;

Siegesmund S, Ruedrich J, Koch A (2008b). Marble bowing: Comparative studies of three different public building facades. *Environmental Geology* **56** (3-4):473-494. DOI: 10.1007/s00254-008-1307-z;

Siegesmund S and Snethlage R. *Stone in Architecture, Properties and Durability*, Springer-Verlag, Berlin, fourth edition, 2011. ISBN 978-3-642-14474-5;

Silva, L and Leal, J (2015). Rural tourism and national identity building in contemporary Europe: Evidence from Portugal. *Journal of Rural Studies* **38**: 109-119. DOI: 10.1016/j.jrurstud.2015.02.005;

Silva, M (2017). *Novel Biocides for Cultural Heritage*. PhD thesis.

Simonot L and Elias M (2002). Color change due to surface state modification. *Color Research and Application* **28**: 45-49. DOI: 10.1002/col.10113;

Skipper PJ, Schulze H, Williams DR and Dixon RA (2016). Biodeterioration of limestone built heritage: A multidisciplinary challenge. 13th International Congress on the Deterioration and Conservation of Stone. Glasgow, Scotland, 6-10 September;

Slamova K, Glaser R, Schill C, Wiesmeier S and Kohl M (2012). Mapping atmospheric corrosion in coastal regions: methods and results. *Journal of Photonics for Energy* **2** (1): 1-11. DOI: 10.1117/1.JPE.2.022003;

Smith BJ, Srinivasan S, Gomez-Heras M, Basheer PAM and Viles HA (2011). Near-surface temperature cycling of stone and its implications for scales of surface deterioration. *Geomorphology* **130** (1-2): 76-82. DOI: 10.1016/j.geomorph.2010.10.005;

Sohrabi M, Favero-Longo SE, Pérez-Ortega S, Ascaso C, Haghghat Z, Talebian MH, Fadaei H and de los Ríos A (2017). Lichen colonization and associated deterioration processes in Pasargadae, UNESCO world heritage site, Iran. *International Biodeterioration & Biodegradation* **117**: 171-182. DOI: 10.1016/j.ibiod.2016.12.012;

Sousa LMO (2014). Petrophysical properties and durability of granites employed as building stone: a comprehensive evaluation. *Bulletin of Engineering Geology and the Environment* **73** (2): 569-588. DOI: 10.1007/s10064-013-0553-9;

Spile S, Suzuki T, Bendix J and Simonsen K (2016). Effective cleaning of rust stained marble. *Heritage Science* **4**: 12. DOI: 10.1186/s40494-016-0081-6;

St.Clair L and Seaward M (2004). Biodeterioration of Stone Surfaces: Lichens and Biofilms as Weathering Agents of Rocks and Cultural Heritage. *Springer Netherlands*, first edition. DOI: 10.1007/978-1-4020-2845-8;

Steiger M (2005). Salts in Porous Materials: Thermodynamics of Phase Transitions, Modeling and Preventive Conservation. *Restoration of buildings and monuments* **11** (6): 419-432. DOI: 10.1515/rbm-2005-6002;

Sterflinger K (2000). Fungi as a Geologic Agent. *Geomicrobiology Journal* **17** (2): 97-124. DOI: 10.1080/01490450050023791;

Sterflinger K (2010). Fungi: Their role in deterioration of cultural heritage. *Fungal Biology Reviews* **24** (1-2): 47-55. DOI: 10.1016/j.fbr.2010.03.003;

Sterflinger K, Tesei D and Zakharova K (2012). Fungi in hot and cold deserts with particular reference to microcolonial fungi. *Fungal Ecology* **5** (4): 453-462. DOI: 10.1016/j.funeco.2011.12.007;

Sterflinger K and Piñar G (2013). Microbial deterioration of cultural heritage and works of art - tilting at windmills?. *Applied Microbiology and Biotechnology* **97** (22): 9637-9646. DOI: 10.1007/s00253-013-5283-1;

Sturm EV, Frank-Kamenetskaya O, Vlasov D, Zelenskaya M, Sazanova K, Rusakov A and Kniep R (2015). Crystallization of calcium oxalate hydrates by interaction of calcite marble with fungus *Aspergillus niger*. *American Mineralogist* **100**: (11-12): 2559-2565. DOI: 10.2138/am-2015-5104;

Sudalma S, Purwanto P and Santoso LW (2015). The Effect of SO₂ and NO₂ from Transportation and Stationary Emissions Sources to SO₄²⁻ and NO₃⁻ in Rain Water in Semarang. *Procedia Environmental Sciences* **23**: 247-252. DOI: 10.1016/j.proenv.2015.01.037;

- Tamura K, Peterson D, Peterson N, Stecher G, Nei M and Kumar S (2011). MEGA5: molecular evolutionary genetics analysis using maximum likelihood, evolutionary distance, and maximum parsimony methods. *Molecular Biology Evolution* **28** (10): 2731-2739. DOI: 10.1093/molbev/msr121;
- Tan B, Ng C, Nshimiyimana JP, Loh LL, Gin KY-H and Thompson JR (2015). Next-generation sequencing (NGS) for assessment of microbial water quality: current progress, challenges, and future opportunities. *Frontiers in Microbiology* **6**:1027. DOI: 10.3389/fmicb.2015.01027;
- Tedersoo L, Bahram M et al. (2014). Global diversity and geography of soil fungi. *Science* **346** (6213):1078. DOI: 10.1126/science.1256688;
- Terezopoulos N (2004). The challenge for European ornamental stones. Proceedings of the 1st OSNET Workshop;
- Thompson J. Manual of Curatorship - A guide to museum practice. second edition. Routledge, Third Avenue, New York, 2012. ISBN: 978-0750603515;
- Tiano, P. (2002). Biodegradation of cultural heritage: decay mechanisms and control methods. Proceedings ARIADNE Workshop 9 – historic materials and their diagnostic;
- Tomaselli L, Lamenti G, Bosco M and Tiano P (2000). Biodiversity of photosynthetic micro-organisms dwelling on stone monuments. *International Biodeterioration & Biodegradation* **46** (3): 251-258. DOI: 10.1016/S0964-8305(00)00078-0;
- de la Torre MA, Gomez-Alarcon G and Palacios JM (1993). “In vitro” biofilm formation by *Penicillium frequentans* strains on sandstone, granite, and limestone. *Applied Microbiology and Biotechnology* **40** (2-3): 408-415. DOI: 10.1007/BF00170402;
- Toth T N, Chukhutsina V, Domonkos I, Knoppová J, Komenda J, Kis M, Lénárt Z, Garab G, Kovács L, Gombos Z and van Amerongen H (2015). Carotenoids are essential for the assembly of cyanobacterial photosynthetic complexes. *Biochimica et Biophysica Acta (BBA) – Bioenergetics* **1847** (10): 1153-1165;
- Unkovic N, Eric S, Saric K, Stupar M, Savkovic Z, Stankovic S, Stanojevic O, Dimkic I, Vukojevic J and Grbic ML (2017). Biogenesis of secondary mycogenic minerals related to wall paintings deterioration process. *Micron* **100**: 1-9. DOI: 10.1016/j.micron.2017.04.004;
- Urosevic M, Sebastián E and Cardell C (2013). An experimental study on the influence of surface finishing on the weathering of a building low-porous limestone in coastal environments. *Engineering Geology* **154**: 131-141. DOI: 10.1016/j.enggeo.2012.12.013;
- Uroz S, Calvaruso C, Turpault MP and Frey-Klett P (2009). Mineral weathering by bacteria: ecology, actors and mechanisms. *Trends in Microbiology* **17** (8): 378-387. DOI: 10.1016/j.tim.2009.05.004;
- Urzi C, Brusetti L, Salamone P, Sorlini C, Stackebrandt E and Daffonchio D (2001). Biodiversity of Geodermatophilaceae isolated from altered stones and monuments in the Mediterranean basin. *Environmental Microbiology* **3** (7): 471-479. DOI: 10.1046/j.1462-2920.2001.00217.x;

- Valls del Barrio S, Garcia-Valles M, Pradell T and Vendrell-Saz M (2002). The red-orange patina developed on a monumental dolostone. *Engineering Geology* **63** (1-2): 31-38. DOI: 10.1016/S0013-7952(01)00066-7;
- Vasconcelos G and Lourenço PB (2009). In-Plane experimental behavior of stone masonry walls under cyclic loading, *Journal of Structural Engineering* **135** (10): 1269-1277. DOI: 10.1061/(ASCE)ST.1943-541X.0000053;
- Vázquez P, Luque A, Alonso FJ and Grossi CM (2013). Surface changes on crystalline stones due to salt crystallisation. *Environmental Earth Sciences* **69** (4): 1237-1248. DOI: 10.1007/s12665-012-2003-6;
- Vázquez P, Carrizo L, Thomachot-Schneider C, Gibeaux S and Alonso FJ (2016). Influence of surface finish and composition on the deterioration of building stones exposed to acid atmospheres. *Construction and Building Materials* **106**: 392-403. DOI: 10.1016/j.conbuildmat.2015.12.125;
- Vázquez-Nion D, Silva B and Prieto B (2018). Bioreceptivity index for granitic rocks used as construction material. *Science of The Total Environment* **633**: 112-121. DOI: 10.1016/j.scitotenv.2018.03.171;
- Vignati E, Facchini MC, Rinaldi M, Scannell C, Ceburnis D, Sciare J, Kanakidou M, Myriokefalitakis S, Dentener F and O'Dowd CD (2010). Global scale emission and distribution of sea-spray aerosol: Sea-salt and organic enrichment. *Atmospheric Environment* **44** (5): 670-677. DOI: 10.1016/j.atmosenv.2009.11.013;
- Viles HA (2002). Implications of future climate change for stone deterioration. Geological Society, London, *Special Publications* **205**: 407-418. DOI: 10.1144/GSL.SP.2002.205.01.29;
- Villa F, Stewart PS, Klapper I, Jacob JM and Cappitelli F (2016). Subaerial biofilms on outdoor stone monuments: Changing the Perspective toward an ecological framework. *BioScience* **66** (4): 285-294. DOI: 10.1093/biosci/biw006;
- Vingiani S, Di Iorio E, Colombo C and Terribile F (2018). Integrated study of Red Mediterranean soils from Southern Italy. *Catena*. DOI: 10.1016/j.catena.2018.01.002;
- Vojtková H (2017). Algae and their biodegradation effects on building materials in the Ostrava industrial agglomeration. *IOP Conference Series: Earth and Environmental Science* **92**. DOI: 10.1088/1755-1315/92/1/012073;
- Warscheid T and Braams J (2000). Biodeterioration of stone: a review. *International Biodeterioration & Biodegradation* **46** (4): 343-368. DOI: 10.1016/S0964-8305(00)00109-8;
- Weiss N, Normandin K and Slaton D. Cleaning Techniques in Conservation Practice: A special issue of the Journal of Architectural Conservation. Taylor & Francis, Oxford, UK, 2005. ISBN: 1-873394-74-8;
- White AF and Buss HL (2014). 7.4 - Natural Weathering Rates of Silicate Minerals. *Treatise on Geochemistry* **7**: 115-155. DOI: 10.1016/B978-0-08-095975-7.00504-0;

Wickerham LJ and Kurtzman CP (1975). Synergistic color variants of *Aureobasidium pullulans*. *Mycologia* **67** (2): 342-361. DOI: 10.2307/3758426;

Winkler EM (1994). Stone in architecture: Properties, durability. Third edition. *Springer-Verlag*, Berlin, Germany. ISBN: 978-354-057-626-6;

Winkler EM (1997). Iron in minerals and the formation of rust in stone. In: Stone in Architecture. *Springer*, Berlin, Heidelberg, Germany. DOI: 10.1007/978-3-662-10070-7_9;

Yanxia Z and Qing H (2009). Characteristics of the Acid Rain Variation in China During 1993-2006 and Associated Causes. *Acta Mechanica Sinica* **24** (2): 239-250;

Yavuz H, Demirdag S and Caran S (2010). Thermal effect on the physical properties of carbonate rocks. *International Journal of Rock Mechanics and Mining Sciences* **47** (1): 94-103;

Yuanfeng C, Xiaoxiao H Xiang L and Pan Y (2012). Origin of the red colour in a red limestone from the Vispi Quarry section (central Italy): A high-resolution transmission electron microscopy analysis. *Cretaceous Research* **38**: 97-102. DOI: 10.1016/j.cretres.2011.11.016;

Zammit G, De Leo F, Urzì C and Albertano P (2009). A non-invasive approach to the polyphasic study of biodeteriogenic biofilms at St Agatha Crypt and Catacombs at Rabat, Malta. Science and Cultural Heritage in the Mediterranean Area- Diagnostics, Conservation Experiences and Proposals for a Risk Map, Conference Proceedings pp. 323-327, Palermo, 18-21 October 2007, Italy. ISBN: 978-88-64-086-3;

Zanardini E, May E, Inkpen R, Cappitelli F, Murrell JC, Purdy KJ (2016). Diversity of archaeal and bacterial communities on exfoliated sandstone from Portchester Castle (UK). *International Biodeterioration & Biodegradation* **109**: 78-87. DOI: 10.1016/j.ibiod.2015.12.021;

Zavrel T, Sinetova MA and Cervený J (2015). Measurement of Chlorophyll a and Carotenoids Concentration in Cyanobacteria. *Bio-protocol* **5** (9): e1467. DOI: 10.21769/BioProtoc.1467;

Zeza F, Pascua NG and Macrí F (1995). Rising damp and soluble salts in the weathering processes of biocalcarenes. Case study of cathedrals, churches and buildings of Lecce baroque. In: Preservation and Restoration of Cultural Heritage, Proceedings of the 1995 LCP Congress, Montreux, 161-176;

Zhou C, Gong Z, Hu J, Cao A and Liang H (2015). A cost-benefit analysis of landfill mining and material recycling in China. *Waste Management* **35**: 191-198. DOI: 10.1016/j.wasman.2014.09.029.

Annexes



Annex A. Samples obtained from the blue limestone

Table A-1. Samples of stone collected and their location.

Sample reference	Location of the sampling	
C1	Next to Mosteiro da Batalha	
C2	Next to Mosteiro da Batalha	
C3	Next to Mosteiro da Batalha	
C4	Waterfront in São Martinho do Porto	
C5	Waterfront in São Martinho do Porto	
C6	Waterfront in São Martinho do Porto	

Annex B. Culture media composition**Table B-1.** Composition of the culture media used for microbiological development.



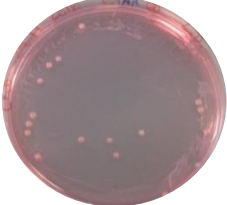
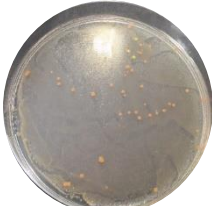




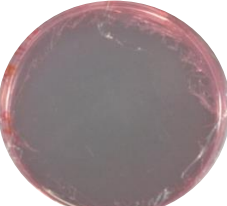



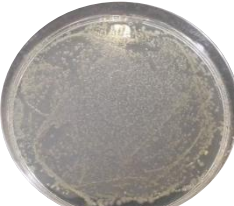

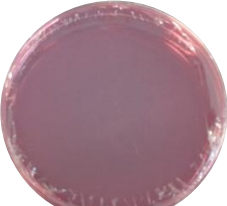
NA	MEA	CRB
5 g/L Peptic digest animals	30 g/L Malt extract	5 g/L Peptone
1.5 g/L Beef extract	5 g/L Peptone mycologic	10 g/L Glucose
1.5 g/L Yeast extract	20 g/L Glucose	1 g/L K ₂ HPO ₄
5 g/L Sodium Chloride	15 g/L Agar	0.5 g/L MgSO ₄
15 g/L Agar		0.05 g/L Rose Bengal
		0.1 g/L Chloramphenicol
		15.5 g/L Agar



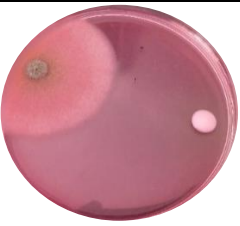

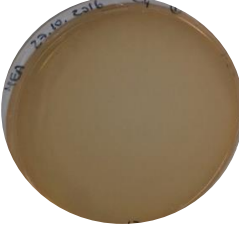
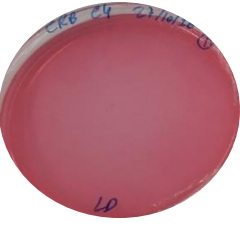


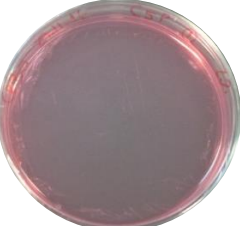




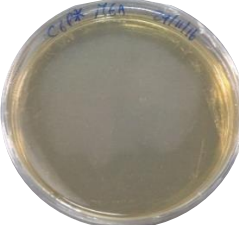
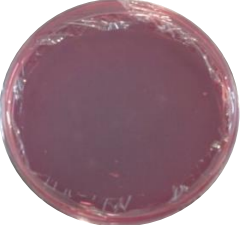

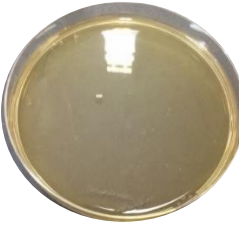
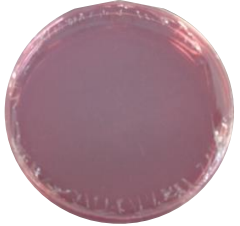
NA – Nutrient Agar; MEA: Malt Extract Agar; CRB – Cook Rose Bengal.

Annex C. Characterisation of the microbial population thriving in the samples obtained from the blue limestone

C.1. Microbial growth resulted from the inoculation of blue limestone samples using CDM

Table C-1. Microbial colonies growth from the inoculated samples of building stone, with and without chromatic alteration.

Sample	Culture medium		
	Nutrient Agar	Malt Extract Agar	Cooke Rose Bengal
C1 non-altered area			
C1 altered area			
C2 non-altered area			
C2 altered area			
C3 non-altered area			

Sample	Culture medium		
	Nutrient Agar	Malt Extract Agar	Cooke Rose Bengal
C3 altered area			
C4 altered area*			
C5 non- altered area			
C5 altered area			
C6 non- altered area			
C6 altered area			

*the samples collected only contained area with chromatic alteration.

C.2. Electrophoresis of the PCR products obtained from the isolated microbial population of the blue limestone

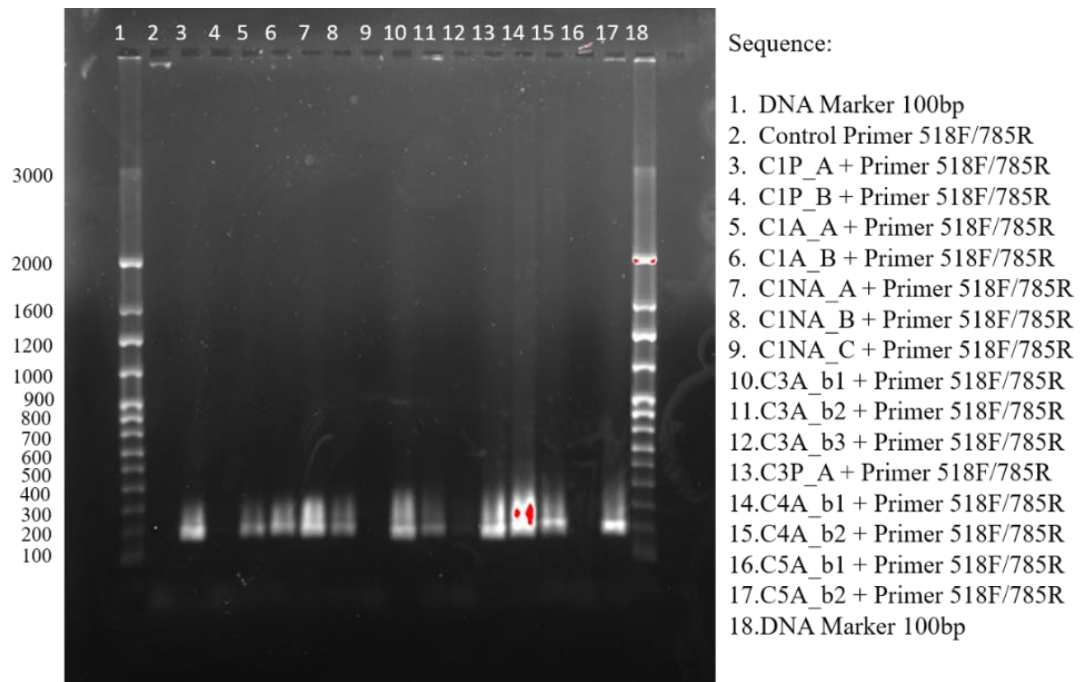


Figure C-1. Electrophoresis of the PCR products performed with DNA extracted from bacteria isolates.

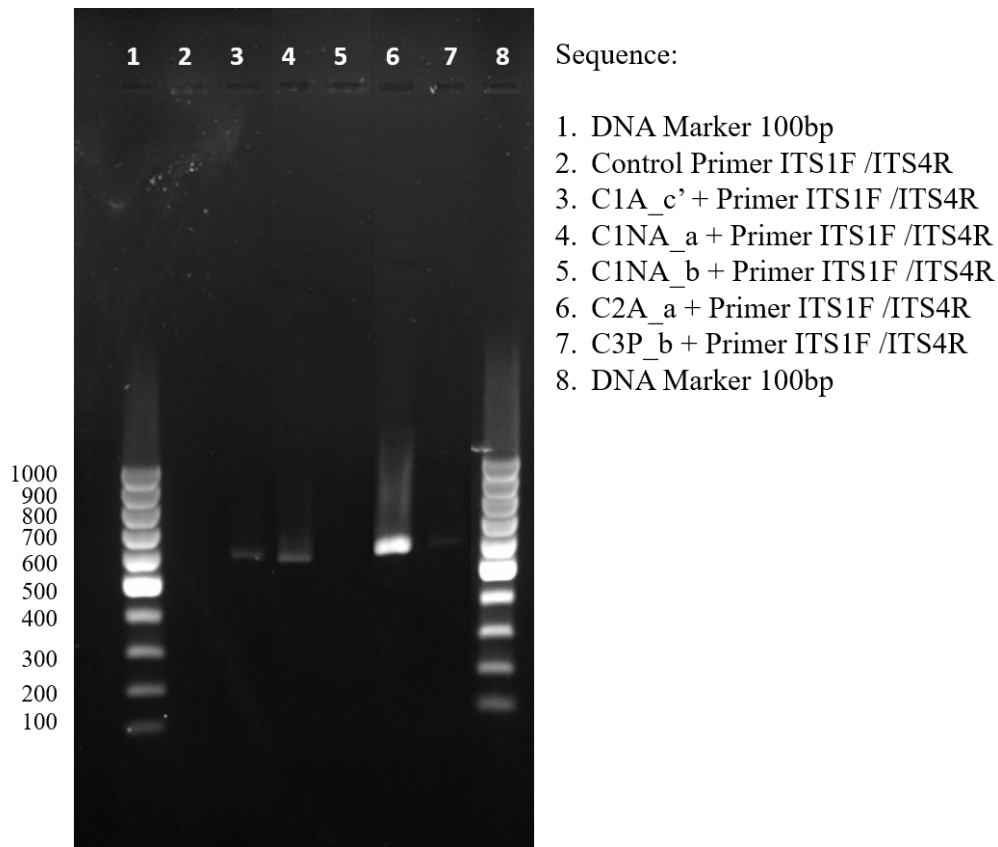


Figure C-2. Electrophoresis of the PCR products performed with DNA extracted from yeast isolates.

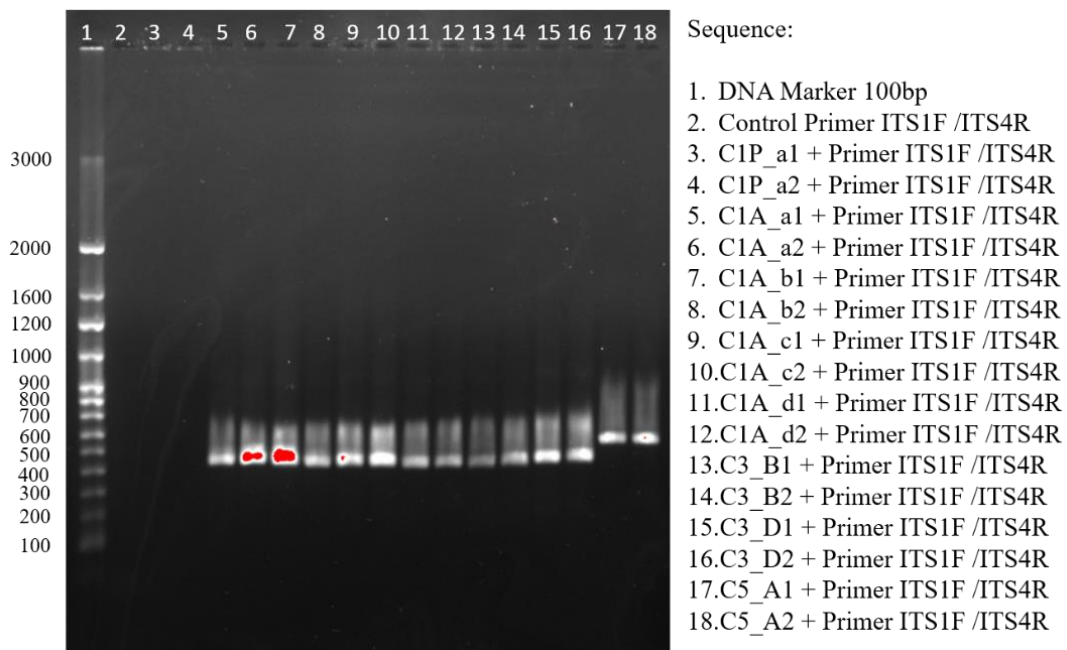


Figure C-3. Electrophoresis of the PCR products performed with DNA extracted from fungi isolates.

C.3. HTS approach for the blue limestone samples

Table C-2. Prokaryotic population present in the altered areas of the stone, identified through HTS approach.

Phylum	Class	Order	Family	Genus
Actinobacteria	Actinobacteria	Actinomycetales	Geodermatophilaceae	<i>Modestobacter</i>
Actinobacteria	Actinobacteria	Actinomycetales	Micrococcaceae	<i>Arthrobacter</i>
Actinobacteria	Actinobacteria	Actinomycetales	Other	Other
Actinobacteria	Actinobacteria	Actinomycetales	Nocardioideaceae	-
Actinobacteria	Actinobacteria	Actinomycetales	Geodermatophilaceae	Other
Actinobacteria	Actinobacteria	Actinomycetales	Micrococcaceae	-
Actinobacteria	Actinobacteria	Actinomycetales	Microbacteriaceae	<i>Agrococcus</i>
Proteobacteria	Alphaproteobacteria	Sphingomonadales	Sphingomonadaceae	-
Actinobacteria	Actinobacteria	Actinomycetales	Kineosporiaceae	-
[Thermi]	Deinococci	Deinococcales	Deinococcaceae	<i>Deinococcus</i>
Actinobacteria	Actinobacteria	Actinomycetales	Geodermatophilaceae	-
Bacteroidetes	Bacteroidia	Bacteroidales	Bacteroidaceae	<i>Bacteroides</i>
Actinobacteria	Actinobacteria	Actinomycetales	Propionibacteriaceae	<i>Propionibacterium</i>
Chloroflexi	Thermomicrobia	JG30-KF-CM45	-	-
Proteobacteria	Alphaproteobacteria	Rhodobacterales	Rhodobacteraceae	<i>Paracoccus</i>
Actinobacteria	Actinobacteria	Actinomycetales	Sporichthyaceae	-
Actinobacteria	Actinobacteria	Actinomycetales	Intrasporangiaceae	-
Cyanobacteria	Chloroplast	Stramenopiles	-	-
Chloroflexi	Ktedonobacteria	Thermogemmatissporales	Thermogemmatissporaceae	-
Actinobacteria	Actinobacteria	Actinomycetales	Geodermatophilaceae	<i>Geodermatophilus</i>
Proteobacteria	Alphaproteobacteria	Rhizobiales	Hyphomicrobiaceae	<i>Rhodoplanes</i>
Proteobacteria	Gammaproteobacteria	Pseudomonadales	Pseudomonadaceae	<i>Pseudomonas</i>
Proteobacteria	Betaproteobacteria	Burkholderiales	Comamonadaceae	<i>Delftia</i>
Proteobacteria	Alphaproteobacteria	Caulobacterales	Caulobacteraceae	-
Proteobacteria	Betaproteobacteria	Burkholderiales	Comamonadaceae	-
Proteobacteria	Gammaproteobacteria	Pseudomonadales	Pseudomonadaceae	-
Actinobacteria	Actinobacteria	Actinomycetales	Microbacteriaceae	-
Bacteroidetes	Cytophagia	Cytophagales	Cytophagaceae	-
Proteobacteria	Alphaproteobacteria	Rhodobacterales	Rhodobacteraceae	<i>Amaricoccus</i>
Proteobacteria	Gammaproteobacteria	Xanthomonadales	Xanthomonadaceae	-
Actinobacteria	Actinobacteria	Actinomycetales	Nocardioideaceae	<i>Nocardioides</i>
Actinobacteria	Actinobacteria	Actinomycetales	Streptomycetaceae	<i>Streptomyces</i>
Proteobacteria	Alphaproteobacteria	Sphingomonadales	Sphingomonadaceae	<i>Sphingomonas</i>
Actinobacteria	Actinobacteria	Actinomycetales	Corynebacteriaceae	<i>Corynebacterium</i>
Bacteroidetes	Cytophagia	Cytophagales	Cytophagaceae	<i>Hymenobacter</i>
Firmicutes	Bacilli	Lactobacillales	Streptococcaceae	<i>Streptococcus</i>
Proteobacteria	Alphaproteobacteria	Rhodospirillales	Acetobacteraceae	<i>Roseomonas</i>
Acidobacteria	Solibacteres	Solibacterales	-	-

Phylum	Class	Order	Family	Genus
Proteobacteria	Gammaproteobacteria	Xanthomonadales	Xanthomonadaceae	<i>Stenotrophomonas</i>
Proteobacteria	Alphaproteobacteria	Sphingomonadales	Sphingomonadaceae	<i>Kaistobacter</i>
Actinobacteria	Actinobacteria	Actinomycetales	-	-
Chloroflexi	TK10	B07_WMSP1	-	-
Proteobacteria	Alphaproteobacteria	Rhizobiales	Methylobacteriaceae	<i>Methylobacterium</i>
Proteobacteria	Deltaproteobacteria	Bdellovibrionales	Bdellovibrionaceae	<i>Bdellovibrio</i>
Actinobacteria	Actinobacteria	Actinomycetales	Streptomycetaceae	-
Bacteroidetes	[Saprospirae]	[Saprospirales]	Chitinophagaceae	-
AD3	ABS-6	-	-	-
Acidobacteria	DA052	Ellin6513	-	-
Chloroflexi	Ktedonobacteria	JG30-KF-AS9	-	-
Proteobacteria	Alphaproteobacteria	Rhodospirillales	Rhodospirillaceae	-
Acidobacteria	Acidobacteriia	Acidobacteriales	Acidobacteriaceae	-
Proteobacteria	Alphaproteobacteria	Rhizobiales	Rhizobiaceae	<i>Agrobacterium</i>
Actinobacteria	Thermoleophilia	Solirubrobacterales	Conexibacteraceae	-
Firmicutes	Bacilli	Bacillales	Staphylococcaceae	<i>Staphylococcus</i>
Firmicutes	Bacilli	Lactobacillales	Leuconostocaceae	<i>Leuconostoc</i>
TM7	SC3	-	-	-
Firmicutes	Bacilli	Bacillales	[Exiguobacteraceae]	<i>Exiguobacterium</i>
Firmicutes	Bacilli	Lactobacillales	Lactobacillaceae	<i>Lactobacillus</i>
Firmicutes	Bacilli	Bacillales	Planococcaceae	<i>Lysinibacillus</i>
Firmicutes	Clostridia	Clostridiales	[Tissierellaceae]	<i>Peptoniphilus</i>
Gemmatimonadetes	Gemm-1	-	-	-
OD1	ABY1	-	-	-
Proteobacteria	Alphaproteobacteria	Rhizobiales	Brucellaceae	<i>Ochrobactrum</i>
Proteobacteria	Alphaproteobacteria	Rhizobiales	Rhizobiaceae	<i>Rhizobium</i>
Proteobacteria	Alphaproteobacteria	Rhodospirillales	Acetobacteraceae	-
Actinobacteria	Thermoleophilia	Solirubrobacterales	Patulibacteraceae	-
Proteobacteria	Gammaproteobacteria	Pasteurellales	Pasteurellaceae	<i>Haemophilus</i>
Gemmatimonadetes	Gemmatimonadetes	Gemmatimonadales	-	-
Proteobacteria	Alphaproteobacteria	Rhodobacterales	Rhodobacteraceae	Other
Proteobacteria	Betaproteobacteria	Burkholderiales	Oxalobacteraceae	-
Proteobacteria	Gammaproteobacteria	Oceanospirillales	Alcanivoracaceae	<i>Alcanivorax</i>
Actinobacteria	Actinobacteria	Actinomycetales	Frankiaceae	Other
Actinobacteria	Actinobacteria	Actinomycetales	Frankiaceae	-
Cyanobacteria	Oscillatoriothycideae	Chroococcales	Xenococcaceae	-
Firmicutes	Bacilli	Lactobacillales	Streptococcaceae	<i>Lactococcus</i>
OD2	ZB2	-	-	-
Proteobacteria	Alphaproteobacteria	Rhizobiales	Bradyrhizobiaceae	-
Verrucomicrobia	Verrucomicrobiae	Verrucomicrobiales	Verrucomicrobiaceae	<i>Prostheco bacter</i>



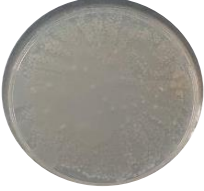






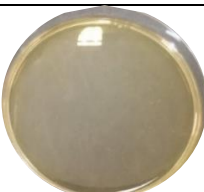




Table C-3. Eukaryotic population present in the altered areas of the stone, identified through HTS approach.

Phylum	Class	Order	Family	Genus
Ascomycota	Eurotiomycetes	Chaetothyriales	Incertae_sedis	<i>Coniosporium</i>
Ascomycota	Dothideomycetes	Capnodiales	Mycosphaerellaceae	<i>Cladosporium</i>
Ascomycota	Saccharomycetes	Saccharomycetales	Incertae_sedis	<i>Candida</i>
Ascomycota	unidentified	unidentified	unidentified	unidentified
Ascomycota	Dothideomycetes	Pleosporales	unidentified	unidentified
Other	Other	Other	Other	Other
Ascomycota	Dothideomycetes	Pleosporales	Pleosporaceae	<i>Alternaria</i>
Basidiomycota	Agaricomycetes	Atheliales	Atheliaceae	<i>Tylospora</i>
Ascomycota	Saccharomycetes	Saccharomycetales	Saccharomycetaceae	<i>Kluyveromyces</i>
Ascomycota	Other	Other	Other	Other
Ascomycota	Saccharomycetes	Saccharomycetales	Saccharomycetaceae	<i>Debaryomyces</i>
Ascomycota	Dothideomycetes	Capnodiales	Mycosphaerellaceae	Other
Basidiomycota	Agaricomycetes	Boletales	Rhizopogonaceae	<i>Rhizopogon</i>
Ascomycota	Sordariomycetes	Hypocreales	Nectriaceae	<i>Fusarium</i>
Basidiomycota	Agaricomycetes	Russulales	Russulaceae	<i>Russula</i>
Basidiomycota	Tremellomycetes	Tremellales	Trichosporonaceae	<i>Trichosporon</i>
Ascomycota	Dothideomycetes	Pleosporales	Other	Other
Basidiomycota	Incertae_sedis	Malasseziales	Other	Other
Ascomycota	Eurotiomycetes	Eurotiales	Trichocomaceae	<i>Penicillium</i>
Ascomycota	Sordariomycetes	Sordariales	Chaetomiaceae	Other
Ascomycota	Dothideomycetes	Pleosporales	Montagnulaceae	<i>Paraphaeosphaeria</i>
Basidiomycota	Tremellomycetes	Filobasidiales	Filobasidiaceae	<i>Cryptococcus</i>
Ascomycota	Saccharomycetes	Saccharomycetales	Debaryomycetaceae	<i>Meyerozyma</i>
Other	Other	Other	Other	Other
Ascomycota	Dothideomycetes	Pleosporales	Incertae_sedis	<i>Phoma</i>
Ascomycota	Eurotiomycetes	Eurotiales	Trichocomaceae	<i>Aspergillus</i>
Ascomycota	Dothideomycetes	Incertae_sedis	Myxotrichaceae	Other
Ascomycota	Dothideomycetes	Pleosporales	Phaeosphaeriaceae	Other
Basidiomycota	Agaricomycetes	Cantharellales	Clavulinaceae	<i>Clavulina</i>
Basidiomycota	Incertae_sedis	Malasseziales	Incertae_sedis	<i>Malassezia</i>
Basidiomycota	Agaricomycetes	Russulales	Russulaceae	unidentified
Zygomycota	Incertae_sedis	Mucorales	Umbelopsidaceae	<i>Umbelopsis</i>
Ascomycota	Leotiomycetes	Helotiales	Incertae_sedis	<i>Cadophora</i>
Basidiomycota	Other	Other	Other	Other
Ascomycota	Saccharomycetes	Saccharomycetales	Pichiaceae	<i>Pichia</i>
Ascomycota	Sordariomycetes	Hypocreales	Nectriaceae	<i>Gibberella</i>
Basidiomycota	Agaricomycetes	Agaricales	Tricholomataceae	Other

Annex D. Characterisation of the microbial population thriving in the limestone sculptures from the Portuguese NMAA

D.1. Microbial growth in the sculpture's samples using CDM

Table D-1. Cultivable microbial colonies present on the limestone sculptures.

Sculpture	Culture Medium	
	NA	MEA
<i>St. John the Baptist</i>		
		
<i>St. Paul</i>		
		
<i>Virgin and the Child</i>		
		
Musician Angel		

D.2. HTS approach for the sculptures' samples

Table D-2. Prokaryotic population present in the *St. John the Baptist* sculpture, identified through HTS approach.

Phylum	Class	Order	Family	Genus	Specie
Firmicutes	Bacilli	Lactobacillales	Streptococcaceae	<i>Lactococcus</i>	<i>Lactococcus</i> sp.
Firmicutes	Bacilli	Lactobacillales	Streptococcaceae	<i>Lactococcus</i>	<i>Lactococcus raffinolactis</i>
Firmicutes	Bacilli	Lactobacillales	Streptococcaceae	<i>Streptococcus</i>	<i>Streptococcus agalactiae</i>
Firmicutes	Bacilli	Lactobacillales	Leuconostocaceae	<i>Leuconostoc</i>	<i>Leuconostoc gasicomitatum</i>
Firmicutes	Bacilli	Lactobacillales	Carnobacteriaceae	<i>Carnobacterium</i>	<i>Carnobacterium maltaromaticum</i>
Firmicutes	Bacilli	Lactobacillales	Streptococcaceae	<i>Streptococcus</i>	<i>Streptococcus</i> sp.
Proteobacteria	Gammaproteobacteria	Pseudomonadales	Pseudomonadaceae	<i>Pseudomonas</i>	<i>Pseudomonas lundensis</i>
Firmicutes	Bacilli	Lactobacillales	Leuconostocaceae	<i>Leuconostoc</i>	<i>Leuconostoc</i> sp.
Firmicutes	Bacilli	Lactobacillales	Streptococcaceae	<i>Lactococcus</i>	<i>Lactococcus fujiensis</i>
Firmicutes	Bacilli	Lactobacillales	Streptococcaceae	<i>Streptococcus</i>	<i>Streptococcus vestibularis</i>
Firmicutes	Bacilli	Lactobacillales	-	-	-
Firmicutes	Bacilli	Lactobacillales	Leuconostocaceae	<i>Leuconostoc</i>	<i>Leuconostoc carnosum</i>
Firmicutes	Bacilli	Lactobacillales	Streptococcaceae	<i>Streptococcus</i>	<i>Streptococcus orisratti</i>
Firmicutes	Bacilli	Lactobacillales	Carnobacteriaceae	<i>Carnobacterium</i>	<i>Carnobacterium inhibens</i>

Table D-3. Prokaryotic population present in *The Virgin and the Child* sculpture, identified through HTS approach.

Phylum	Class	Order	Family	Genus	Specie
Firmicutes	Bacilli	Lactobacillales	Streptococcaceae	<i>Lactococcus</i>	<i>Lactococcus</i> sp.
Firmicutes	Bacilli	Lactobacillales	Streptococcaceae	<i>Lactococcus</i>	<i>Lactococcus raffinolactis</i>
Firmicutes	Bacilli	Lactobacillales	Streptococcaceae	<i>Streptococcus</i>	<i>Streptococcus agalactiae</i>
Firmicutes	Bacilli	Lactobacillales	Leuconostocaceae	<i>Leuconostoc</i>	<i>Leuconostoc gasicomitatum</i>
Firmicutes	Bacilli	Lactobacillales	Streptococcaceae	<i>Streptococcus</i>	<i>Streptococcus</i> sp.
Firmicutes	Bacilli	Lactobacillales	Carnobacteriaceae	<i>Carnobacterium</i>	<i>Carnobacterium maltaromaticum</i>
Proteobacteria	Gammaproteobacteria	Pseudomonadales	Pseudomonadaceae	<i>Pseudomonas</i>	<i>Pseudomonas lundensis</i>
Firmicutes	Bacilli	Lactobacillales	Leuconostocaceae	<i>Leuconostoc</i>	<i>Leuconostoc</i> sp.
Firmicutes	Bacilli	Lactobacillales	Streptococcaceae	<i>Lactococcus</i>	<i>Lactococcus fujiensis</i>
Firmicutes	Bacilli	Lactobacillales	Streptococcaceae	<i>Streptococcus</i>	<i>Streptococcus orisratti</i>

Table D-4. Prokaryotic population present in the *St. Paul* sculpture, identified through HTS approach.

Phylum	Class	Order	Family	Genus	Specie
Firmicutes	Bacilli	Lactobacillales	Streptococcaceae	<i>Lactococcus</i>	<i>Lactococcus</i> sp.
Firmicutes	Bacilli	Lactobacillales	Streptococcaceae	<i>Lactococcus</i>	<i>Lactococcus raffinolactis</i>
Firmicutes	Bacilli	Lactobacillales	Streptococcaceae	<i>Streptococcus</i>	<i>Streptococcus agalactiae</i>
Firmicutes	Bacilli	Lactobacillales	Leuconostocaceae	<i>Leuconostoc</i>	<i>Leuconostoc gasicomitatum</i>
Firmicutes	Bacilli	Lactobacillales	Streptococcaceae	<i>Streptococcus</i>	<i>Streptococcus</i> sp.
Firmicutes	Bacilli	Lactobacillales	Carnobacteriaceae	<i>Carnobacterium</i>	<i>Carnobacterium maltaromaticum</i>
Proteobacteria	Gammaproteobacteria	Pseudomonadales	Pseudomonadaceae	<i>Pseudomonas</i>	<i>Pseudomonas lundensis</i>
Firmicutes	Bacilli	Lactobacillales	Leuconostocaceae	<i>Leuconostoc</i>	<i>Leuconostoc</i> sp.
Firmicutes	Bacilli	Lactobacillales	Streptococcaceae	<i>Lactococcus</i>	<i>Lactococcus fujiensis</i>
Firmicutes	Bacilli	Lactobacillales	-	-	-
Firmicutes	Bacilli	Lactobacillales	Streptococcaceae	<i>Streptococcus</i>	<i>Streptococcus vestibularis</i>

Phylum	Class	Order	Family	Genus	Specie
Firmicutes	Bacilli	Lactobacillales	Streptococcaceae	<i>Streptococcus</i>	<i>Streptococcus orisratti</i>
Firmicutes	Bacilli	Lactobacillales	Leuconostocaceae	<i>Leuconostoc</i>	<i>Leuconostoc carnosum</i>
Proteobacteria	Gammaproteobacteria	Pseudomonadales	Pseudomonadaceae	<i>Pseudomonas</i>	<i>Pseudomonas fragi</i>

Table D-5. Prokaryotic population present in the *Musician Angel* sculpture, identified through HTS approach.

Phylum	Class	Order	Family	Genus	Specie
Firmicutes	Bacilli	Lactobacillales	Streptococcaceae	<i>Lactococcus</i>	<i>Lactococcus</i> sp.
Firmicutes	Bacilli	Bacillales	Bacillaceae	<i>Bacillus</i>	<i>Bacillus aryabhatai</i>
Firmicutes	Bacilli	Lactobacillales	Streptococcaceae	<i>Lactococcus</i>	<i>Lactococcus raffinolactis</i>
Firmicutes	Bacilli	Bacillales	Bacillaceae	<i>Bacillus</i>	<i>Bacillus</i> sp.
Firmicutes	Bacilli	Bacillales	Bacillaceae	<i>Bacillus</i>	<i>Bacillus flexus</i>
Firmicutes	Bacilli	Lactobacillales	Streptococcaceae	<i>Streptococcus</i>	<i>Streptococcus agalactiae</i>
Firmicutes	Bacilli	Bacillales	-	-	-
Firmicutes	Bacilli	Lactobacillales	Leuconostocaceae	<i>Leuconostoc</i>	<i>Leuconostoc gasicomitatum</i>
Firmicutes	Bacilli	Bacillales	Bacillaceae	<i>Bacillus</i>	<i>Bacillus megaterium</i>
Firmicutes	Bacilli	Lactobacillales	Carnobacteriaceae	<i>Carnobacterium</i>	<i>Carnobacterium maltaromaticum</i>
Firmicutes	Bacilli	-	-	-	-
Firmicutes	Bacilli	Lactobacillales	Streptococcaceae	<i>Streptococcus</i>	<i>Streptococcus</i> sp.
Firmicutes	Bacilli	Bacillales	Bacillaceae	<i>Bacillus</i>	<i>Bacillus ginsenggisoli</i>
Proteobacteria	Gammaproteobacteria	Pseudomonadales	Pseudomonadaceae	<i>Pseudomonas</i>	<i>Pseudomonas lundensis</i>
Firmicutes	Bacilli	Bacillales	Planococcaceae	<i>Planococcus</i>	<i>Planococcus maritimus</i>
Firmicutes	Bacilli	Lactobacillales	Streptococcaceae	<i>Lactococcus</i>	<i>Lactococcus fujiensis</i>
Firmicutes	Bacilli	Lactobacillales	Enterococcaceae	-	-
Firmicutes	Bacilli	Lactobacillales	Leuconostocaceae	<i>Leuconostoc</i>	<i>Leuconostoc</i> sp.
Firmicutes	Bacilli	Bacillales	Paenibacillaceae	<i>Paenibacillus</i>	<i>Paenibacillus contaminans</i>

Phylum	Class	Order	Family	Genus	Specie
Firmicutes	Bacilli	Lactobacillales	-	-	-
Firmicutes	Bacilli	Bacillales	Bacillaceae	-	-
Firmicutes	Bacilli	Lactobacillales	Enterococcaceae	<i>Enterococcus</i>	<i>Enterococcus</i> sp.
Proteobacteria	Gammaproteobacteria	Pseudomonadales	Pseudomonadaceae	<i>Pseudomonas</i>	<i>Pseudomonas fragi</i>
Firmicutes	Bacilli	Lactobacillales	Carnobacteriaceae	<i>Carnobacterium</i>	<i>Carnobacterium inihbens</i>
Firmicutes	Bacilli	Lactobacillales	Streptococcaceae	<i>Streptococcus</i>	<i>Streptococcus vestibularis</i>

Annex E. Microbial population thriving on the “São João da Penitência” Convent identified through HTS approach

E.1. Prokaryotic population

Table E-1. Prokaryotic population present in the area CM1 of the Convent, identified through HTS approach.

Phylum	Class	Order	Family	Genus	Specie
Actinobacteria	Rubrobacteria	Rubrobacterales	Rubrobacteraceae	<i>Rubrobacter</i>	<i>Rubrobacter</i> sp.
Proteobacteria	Gammaproteobacteria	Pseudomonadales	Pseudomonadaceae	<i>Pseudomonas</i>	<i>Pseudomonas</i> sp.
Actinobacteria	Actinobacteria	Actinomycetales	Geodermatophilaceae	<i>Geodermatophilus</i>	<i>Geodermatophilus</i> sp.
Proteobacteria	Gammaproteobacteria	Pseudomonadales	Pseudomonadaceae	<i>Pseudomonas</i>	<i>Pseudomonas corrugata</i>
Actinobacteria	Actinobacteria	Actinomycetales	Kineosporiaceae	<i>Kineosporia</i>	<i>Kineosporia</i> sp.
Actinobacteria	Actinobacteria	Actinomycetales	Kineosporiaceae	<i>Kineosporia</i>	<i>Kineosporia rhizophila</i>
Proteobacteria	-	-	-	-	-
Proteobacteria	Betaproteobacteria	Burkholderiales	Oxalobacteraceae	<i>Ralstonia</i>	<i>Ralstonia detusculanense</i>
Proteobacteria	Alphaproteobacteria	Rhizobiales	Aurantimonadaceae	<i>Aurantimonas</i>	<i>Aurantimonas litoralis</i>
Proteobacteria	Alphaproteobacteria	Sphingomonadales	Sphingomonadaceae	<i>Kaistobacter</i>	<i>Kaistobacter</i> sp.
Actinobacteria	Actinobacteria	Actinomycetales	Propionibacteriaceae	<i>Propionibacterium</i>	<i>Propionibacterium humerusii</i>
Bacteroidetes	Sphingobacteriia	Sphingobacteriales	Flexibacteraceae	<i>Hymenobacter</i>	<i>Hymenobacter</i> sp.
Thermi	Deinococci	Deinococcales	Deinococcaceae	<i>Deinococcus</i>	<i>Deinococcus</i> sp.
Proteobacteria	Gammaproteobacteria	-	-	-	-
Actinobacteria	Actinobacteria	Actinomycetales	Pseudonocardiaceae	<i>Pseudonocardia</i>	<i>Pseudonocardia khuvsgulensis</i>
Proteobacteria	Alphaproteobacteria	Rhodobacterales	Rhodobacteraceae	<i>Jannaschia</i>	<i>Jannaschia rubra</i>
Proteobacteria	Gammaproteobacteria	Pseudomonadales	Pseudomonadaceae	<i>Pseudomonas</i>	<i>Pseudomonas borealis</i>
Actinobacteria	Actinobacteria	Actinomycetales	-	-	-
Proteobacteria	Gammaproteobacteria	Enterobacteriales	Enterobacteriaceae	<i>Erwinia</i>	<i>Erwinia papayae</i>
Proteobacteria	Gammaproteobacteria	Enterobacteriales	Enterobacteriaceae	-	-
Actinobacteria	Actinobacteria	Actinomycetales	Geodermatophilaceae	<i>Modestobacter</i>	<i>Modestobacter</i> sp.

Phylum	Class	Order	Family	Genus	Specie
Proteobacteria	Gammaproteobacteria	Enterobacteriales	Enterobacteriaceae	<i>Candidatus Blochmannia</i>	<i>Candidatus Blochmannia</i> sp.
Cyanobacteria	Oscillatoriothycideae	Chroococcales	Phormidiaceae	<i>Microcoleus</i>	<i>Microcoleus antarcticus</i>
Actinobacteria	Actinobacteria	Actinomycetales	Geodermatophilaceae	<i>Modestobacter</i>	<i>Modestobacter marinus</i>
Proteobacteria	Gammaproteobacteria	Pseudomonadales	Pseudomonadaceae	<i>Pseudomonas</i>	<i>Pseudomonas lutea</i>
Firmicutes	Bacilli	Lactobacillales	Streptococcaceae	<i>Lactococcus</i>	<i>Lactococcus</i> sp.
Proteobacteria	Alphaproteobacteria	Sphingomonadales	Erythrobacteraceae	<i>Erythromicrobium</i>	<i>Erythromicrobium ramosum</i>
Actinobacteria	Actinobacteria	Actinomycetales	Geodermatophilaceae	-	-
Proteobacteria	Gammaproteobacteria	Pseudomonadales	Pseudomonadaceae	<i>Pseudomonas</i>	<i>Pseudomonas abietaniphila</i>

Table E-2. Prokaryotic population present in the area CM2 of the Convent, identified through HTS approach.

Phylum	Class	Order	Family	Genus	Specie
Proteobacteria	Gammaproteobacteria	Pseudomonadales	Pseudomonadaceae	<i>Pseudomonas</i>	<i>Pseudomonas viridiflava</i>
Proteobacteria	Gammaproteobacteria	Pseudomonadales	Pseudomonadaceae	<i>Pseudomonas</i>	<i>Pseudomonas lutea</i>
Proteobacteria	Gammaproteobacteria	Pseudomonadales	Pseudomonadaceae	<i>Pseudomonas</i>	<i>Pseudomonas</i> sp.
Proteobacteria	Gammaproteobacteria	Pseudomonadales	Pseudomonadaceae	<i>Pseudomonas</i>	<i>Pseudomonas tremae</i>
Proteobacteria	-	-	-	-	-
Proteobacteria	Gammaproteobacteria	Pseudomonadales	Pseudomonadaceae	<i>Pseudomonas</i>	<i>Pseudomonas migulae</i>
Proteobacteria	Alphaproteobacteria	Rickettsiales	Anaplasmataceae	<i>Ehrlichia</i>	<i>Ehrlichia ovina</i>
Firmicutes	Bacilli	Lactobacillales	Streptococcaceae	<i>Streptococcus</i>	<i>Streptococcus marimammalium</i>
Proteobacteria	Gammaproteobacteria	Pseudomonadales	Pseudomonadaceae	<i>Pseudomonas</i>	<i>Pseudomonas abietaniphila</i>
Proteobacteria	Gammaproteobacteria	Pseudomonadales	Pseudomonadaceae	<i>Pseudomonas</i>	<i>Pseudomonas lundensis</i>

Table E-3. Prokaryotic population present in the area CM3 of the Convent, identified through HTS approach.

Phylum	Class	Order	Family	Genus	Specie
Proteobacteria	Gammaproteobacteria	Pseudomonadales	Pseudomonadaceae	<i>Pseudomonas</i>	<i>Pseudomonas viridiflava</i>
Proteobacteria	Gammaproteobacteria	Pseudomonadales	Pseudomonadaceae	<i>Pseudomonas</i>	<i>Pseudomonas</i> sp.
Proteobacteria	Gammaproteobacteria	Pseudomonadales	Pseudomonadaceae	<i>Pseudomonas</i>	<i>Pseudomonas lutea</i>
Proteobacteria	Alphaproteobacteria	Sphingomonadales	Sphingomonadaceae	<i>Sphingomonas</i>	<i>Sphingomonas leidyia</i>
Firmicutes	Bacilli	Lactobacillales	Streptococcaceae	<i>Lactococcus</i>	<i>Lactococcus</i> sp.
Proteobacteria	Gammaproteobacteria	Pseudomonadales	Pseudomonadaceae	<i>Pseudomonas</i>	<i>Pseudomonas abietaniphila</i>
Actinobacteria	Actinobacteria	Actinomycetales	Propionibacteriaceae	<i>Propionibacterium</i>	<i>Propionibacterium acnes</i>
Proteobacteria	Alphaproteobacteria	Caulobacterales	Caulobacteraceae	<i>Phenylobacterium</i>	<i>Phenylobacterium</i> sp.
Proteobacteria	Gammaproteobacteria	Xanthomonadales	Xanthomonadaceae	<i>Stenotrophomonas</i>	<i>Stenotrophomonas</i> sp.
Proteobacteria	Alphaproteobacteria	Sphingomonadales	Sphingomonadaceae	<i>Sphingomonas</i>	<i>Sphingomonas</i> sp.
Proteobacteria	Gammaproteobacteria	Enterobacteriales	Enterobacteriaceae	<i>Enterobacter</i>	<i>Enterobacter hormaechei</i>

Proteobacteria	-	-	-	-	-
Proteobacteria	Gammaproteobacteria	Pseudomonadales	Pseudomonadaceae	<i>Pseudomonas</i>	<i>Pseudomonas tremae</i>
Proteobacteria	Betaproteobacteria	Burkholderiales	Oxalobacteraceae	<i>Ralstonia</i>	<i>Ralstonia pickettii</i>
Actinobacteria	Actinobacteria	Actinomycetales	Corynebacteriaceae	<i>Corynebacterium</i>	<i>Corynebacterium</i> sp.
Proteobacteria	Alphaproteobacteria	Rhodobacterales	Rhodobacteraceae	<i>Paracoccus</i>	<i>Paracoccus</i> sp.
Firmicutes	Bacilli	Bacillales	Staphylococcaceae	<i>Staphylococcus</i>	<i>Staphylococcus</i> sp.
Firmicutes	Bacilli	Lactobacillales	Streptococcaceae	<i>Lactococcus</i>	<i>Lactococcus raffinolactis</i>
Proteobacteria	Alphaproteobacteria	Rhizobiales	Phyllobacteriaceae	<i>Mesorhizobium</i>	<i>Mesorhizobium</i> sp.
Proteobacteria	Gammaproteobacteria	-	-	-	-
Proteobacteria	Gammaproteobacteria	Pseudomonadales	Pseudomonadaceae	<i>Pseudomonas</i>	<i>Pseudomonas graminis</i>
Proteobacteria	Gammaproteobacteria	Enterobacteriales	Enterobacteriaceae	<i>Plesiomonas</i>	<i>Plesiomonas</i> sp.

Table E-4. Prokaryotic population present in the area CM4 of the Convent, identified through HTS approach.

Phylum	Class	Order	Family	Genus	Specie
Proteobacteria	Gammaproteobacteria	Pseudomonadales	Pseudomonadaceae	<i>Pseudomonas</i>	<i>Pseudomonas</i> sp.
Firmicutes	Bacilli	Lactobacillales	Streptococcaceae	<i>Lactococcus</i>	<i>Lactococcus</i> sp.
Proteobacteria	-	-	-	-	-
Proteobacteria	Gammaproteobacteria	Pseudomonadales	Pseudomonadaceae	<i>Pseudomonas</i>	<i>Pseudomonas abietaniphila</i>
Proteobacteria	Gammaproteobacteria	-	-	-	-
Proteobacteria	Alphaproteobacteria	Sphingomonadales	Sphingomonadaceae	<i>Sphingomonas</i>	<i>Sphingomonas leidyia</i>
Firmicutes	Bacilli	Lactobacillales	Streptococcaceae	<i>Streptococcus</i>	<i>Streptococcus</i> sp.
Proteobacteria	Alphaproteobacteria	Caulobacterales	Caulobacteraceae	<i>Phenylobacterium</i>	<i>Phenylobacterium</i> sp.
Actinobacteria	Actinobacteria	Actinomycetales	Propionibacteriaceae	<i>Propionibacterium</i>	<i>Propionibacterium acnes</i>
Proteobacteria	Gammaproteobacteria	Pseudomonadales	Pseudomonadaceae	<i>Pseudomonas</i>	<i>Pseudomonas viridiflava</i>
Proteobacteria	Gammaproteobacteria	Pseudomonadales	Pseudomonadaceae	<i>Pseudomonas</i>	<i>Pseudomonas moraviensis</i>
Proteobacteria	Gammaproteobacteria	Pseudomonadales	Pseudomonadaceae	<i>Pseudomonas</i>	<i>Pseudomonas lutea</i>

Phylum	Class	Order	Family	Genus	Specie
Proteobacteria	Alphaproteobacteria	Sphingomonadales	Sphingomonadaceae	<i>Sphingomonas</i>	<i>Sphingomonas oligophenolica</i>
Proteobacteria	Alphaproteobacteria	Sphingomonadales	Sphingomonadaceae	<i>Sphingomonas</i>	<i>Sphingomonas</i> sp.
Proteobacteria	Betaproteobacteria	Burkholderiales	Oxalobacteraceae	<i>Ralstonia</i>	<i>Ralstonia detusculanense</i>
Actinobacteria	Actinobacteria	Actinomycetales	Microbacteriaceae	<i>Microbacterium</i>	<i>Microbacterium</i> sp.
Firmicutes	Bacilli	Lactobacillales	Streptococcaceae	-	-
Proteobacteria	Gammaproteobacteria	Pseudomonadales	Moraxellaceae	<i>Moraxella</i>	<i>Moraxella caviae</i>
Firmicutes	Bacilli	Lactobacillales	Streptococcaceae	<i>Lactococcus</i>	<i>Lactococcus fujiensis</i>
Actinobacteria	Actinobacteria	Actinomycetales	Corynebacteriaceae	<i>Corynebacterium</i>	<i>Corynebacterium kroppenstedtii</i>
Actinobacteria	Actinobacteria	Actinomycetales	Propionibacteriaceae	<i>Propionibacterium</i>	<i>Propionibacterium</i> sp.
Proteobacteria	Gammaproteobacteria	Pseudomonadales	Pseudomonadaceae	<i>Pseudomonas</i>	<i>Pseudomonas mucidolens</i>
Proteobacteria	Gammaproteobacteria	Pseudomonadales	Moraxellaceae	<i>Enhydrobacter</i>	<i>Enhydrobacter aerosaccus</i>
Actinobacteria	Actinobacteria	Actinomycetales	Geodermatophilaceae	<i>Geodermatophilus</i>	<i>Geodermatophilus</i> sp.
Proteobacteria	Gammaproteobacteria	Pseudomonadales	Pseudomonadaceae	<i>Pseudomonas</i>	<i>Pseudomonas lundensis</i>
Proteobacteria	Betaproteobacteria	-	-	-	-
Proteobacteria	Alphaproteobacteria	Rhodospirillales	Acetobacteraceae	<i>Roseomonas</i>	<i>Roseomonas</i> sp.
Proteobacteria	Alphaproteobacteria	Caulobacterales	Caulobacteraceae	<i>Arthrospira</i>	<i>Arthrospira</i> sp.
Proteobacteria	Gammaproteobacteria	Pseudomonadales	Moraxellaceae	<i>Acinetobacter</i>	<i>Acinetobacter tjernbergiae</i>
Proteobacteria	Betaproteobacteria	Burkholderiales	Oxalobacteraceae	<i>Ralstonia</i>	<i>Ralstonia pickettii</i>
Proteobacteria	Alphaproteobacteria	Sphingomonadales	Sphingomonadaceae	-	-
Actinobacteria	Actinobacteria	Actinomycetales	-	-	-
Proteobacteria	Alphaproteobacteria	Rhizobiales	Bradyrhizobiaceae	<i>Bradyrhizobium</i>	<i>Bradyrhizobium</i> sp.
Proteobacteria	Alphaproteobacteria	Rhodobacterales	Rhodobacteraceae	<i>Paracoccus</i>	<i>Paracoccus</i> sp.
Proteobacteria	Gammaproteobacteria	Pseudomonadales	Pseudomonadaceae	<i>Pseudomonas</i>	<i>Pseudomonas chloritidismutans</i>
Proteobacteria	Alphaproteobacteria	Rhodobacterales	Rhodobacteraceae	<i>Paracoccus</i>	<i>Paracoccus aestuarii</i>
Tenericutes	Mollicutes	Acholeplasmatales	Acholeplasmataceae	<i>Candidatus Phytoplasma</i>	<i>Candidatus Phytoplasma</i> sp.
Proteobacteria	Alphaproteobacteria	Sphingomonadales	Sphingomonadaceae	<i>Sphingomonas</i>	<i>Sphingomonas melonis</i>

Phylum	Class	Order	Family	Genus	Specie
Proteobacteria	Alphaproteobacteria	Caulobacterales	Caulobacteraceae	-	-
Firmicutes	Clostridia	Clostridiales	Peptostreptococcaceae	<i>Peptostreptococcus</i>	<i>Peptostreptococcus stomatis</i>
Proteobacteria	Gammaproteobacteria	Pseudomonadales	Pseudomonadaceae	<i>Pseudomonas</i>	<i>Pseudomonas azotoformans</i>
Firmicutes	Bacilli	Lactobacillales	Streptococcaceae	<i>Lactococcus</i>	<i>Lactococcus raffinolactis</i>
Proteobacteria	Betaproteobacteria	Burkholderiales	Alcaligenaceae	<i>Oligella</i>	<i>Oligella ureolytica</i>
Actinobacteria	Actinobacteria	Actinomycetales	Micrococcaceae	<i>Micrococcus</i>	<i>Micrococcus yunnanensis</i>
Firmicutes	Bacilli	Lactobacillales	-	-	-
Proteobacteria	Gammaproteobacteria	Pseudomonadales	Pseudomonadaceae	<i>Pseudomonas</i>	<i>Pseudomonas putida</i>
Proteobacteria	Alphaproteobacteria	Caulobacterales	Caulobacteraceae	<i>Brevundimonas</i>	<i>Brevundimonas olei</i>
Proteobacteria	Gammaproteobacteria	Pseudomonadales	Moraxellaceae	<i>Acinetobacter</i>	<i>Acinetobacter seohaensis</i>
Proteobacteria	Gammaproteobacteria	Enterobacteriales	Enterobacteriaceae	<i>Enterobacter</i>	<i>Enterobacter</i> sp.
Cyanobacteria	Nostocophycideae	Stigonematales	Rivulariaceae	<i>Calothrix</i>	<i>Calothrix parietina</i>
Proteobacteria	Gammaproteobacteria	Enterobacteriales	Enterobacteriaceae	<i>Serratia</i>	<i>Serratia marcescens</i>
Proteobacteria	Gammaproteobacteria	Pseudomonadales	Pseudomonadaceae	<i>Pseudomonas</i>	<i>Pseudomonas xanthomarina</i>
Spirochaetes	Leptospirae	Leptospirales	Leptospiraceae	<i>Leptospira</i>	<i>Leptospira licerasiae</i>
Actinobacteria	Actinobacteria	Actinomycetales	Micrococcaceae	<i>Arthrobacter</i>	<i>Arthrobacter uratoxydans</i>
Proteobacteria	Gammaproteobacteria	Pseudomonadales	Pseudomonadaceae	<i>Pseudomonas</i>	<i>Pseudomonas borealis</i>
Firmicutes	Bacilli	Lactobacillales	Lactobacillaceae	<i>Lactobacillus</i>	<i>Lactobacillus</i> sp.
Firmicutes	Bacilli	Lactobacillales	Leuconostocaceae	<i>Leuconostoc</i>	<i>Leuconostoc</i> sp.
Firmicutes	Bacilli	Bacillales	Bacillaceae	<i>Virgibacillus</i>	<i>Virgibacillus salexigens</i>
Actinobacteria	Actinobacteria	Actinomycetales	Propionibacteriaceae	<i>Propionibacterium</i>	<i>Propionibacterium avidum</i>
Firmicutes	Bacilli	Lactobacillales	Streptococcaceae	<i>Streptococcus</i>	<i>Streptococcus bovis</i>

Table E-5. Prokaryotic population present in the area CM5 of the Convent, identified through HTS approach.

Phylum	Class	Order	Family	Genus	Specie
Proteobacteria	Gammaproteobacteria	Pseudomonadales	Pseudomonadaceae	<i>Pseudomonas</i>	<i>Pseudomonas corrugata</i>
Proteobacteria	Gammaproteobacteria	Enterobacteriales	Enterobacteriaceae	<i>Erwinia</i>	<i>Erwinia mallotivora</i>
Proteobacteria	Gammaproteobacteria	Pseudomonadales	Pseudomonadaceae	<i>Pseudomonas</i>	<i>Pseudomonas</i> sp.
Proteobacteria	Gammaproteobacteria	Enterobacteriales	Enterobacteriaceae	<i>Erwinia</i>	<i>Erwinia papayae</i>
Proteobacteria	Gammaproteobacteria	Enterobacteriales	Enterobacteriaceae	<i>Erwinia</i>	<i>Erwinia</i> sp.
Proteobacteria	Gammaproteobacteria	Pseudomonadales	Pseudomonadaceae	<i>Pseudomonas</i>	<i>Pseudomonas moraviensis</i>
Proteobacteria	Gammaproteobacteria	Pseudomonadales	Pseudomonadaceae	<i>Pseudomonas</i>	<i>Pseudomonas viridiflava</i>
Proteobacteria	Gammaproteobacteria	Pseudomonadales	Pseudomonadaceae	<i>Pseudomonas</i>	<i>Pseudomonas borealis</i>
Proteobacteria	Gammaproteobacteria	Pseudomonadales	Pseudomonadaceae	<i>Pseudomonas</i>	<i>Pseudomonas lurida</i>
Proteobacteria	Gammaproteobacteria	Pseudomonadales	Pseudomonadaceae	<i>Pseudomonas</i>	<i>Pseudomonas azotoformans</i>
Proteobacteria	Gammaproteobacteria	Enterobacteriales	Enterobacteriaceae	-	-
Proteobacteria	Gammaproteobacteria	Enterobacteriales	Enterobacteriaceae	<i>Enterobacter</i>	<i>Enterobacter hormaechei</i>
Proteobacteria	Gammaproteobacteria	Enterobacteriales	Enterobacteriaceae	<i>Erwinia</i>	<i>Erwinia psidii</i>

Table E-6. Prokaryotic population present in the area CM6 of the Convent, identified through HTS approach.

Phylum	Class	Order	Family	Genus	Specie
Proteobacteria	Gammaproteobacteria	Pseudomonadales	Pseudomonadaceae	<i>Pseudomonas</i>	<i>Pseudomonas fragi</i>
Proteobacteria	Gammaproteobacteria	Pseudomonadales	Pseudomonadaceae	<i>Pseudomonas</i>	<i>Pseudomonas lundensis</i>
Proteobacteria	Gammaproteobacteria	Pseudomonadales	Pseudomonadaceae	<i>Pseudomonas</i>	<i>Pseudomonas</i> sp.
Proteobacteria	Gammaproteobacteria	Pseudomonadales	Pseudomonadaceae	<i>Pseudomonas</i>	<i>Pseudomonas abietaniphila</i>
Cyanobacteria	Nostocophycideae	Nostocales	Nostocaceae	<i>Anabaena</i>	<i>Anabaena augstumalis</i>
Proteobacteria	Gammaproteobacteria	-	-	-	-

Phylum	Class	Order	Family	Genus	Specie
Proteobacteria	Gammaproteobacteria	Pseudomonadales	Pseudomonadaceae	<i>Pseudomonas</i>	<i>Pseudomonas moraviensis</i>
Proteobacteria	Gammaproteobacteria	Pseudomonadales	Pseudomonadaceae	<i>Pseudomonas</i>	<i>Pseudomonas borealis</i>

E.2. Eukaryotic population

Table E-7. Eukaryotic population present in the area CM1 of the Convent, identified through HTS approach.

Phylum	Class	Order	Family	Genus	Specie
Ascomycota	Dothideomycetes	Capnodiales	Cladosporiaceae	<i>Cladosporium</i>	<i>Cladosporium</i> sp.
Ascomycota	Dothideomycetes	Capnodiales	Neodevriesiaceae	unidentified	unidentified
Ascomycota	Dothideomycetes	Capnodiales	-	-	-
Ascomycota	Dothideomycetes	Pleosporales	Pleosporaceae	<i>Alternaria</i>	<i>Alternaria</i> sp.
Ascomycota	Dothideomycetes	Capnodiales	Neodevriesiaceae	-	-
Ascomycota	Dothideomycetes	Pleosporales	Pleosporaceae	<i>Alternaria</i>	<i>Alternaria didymospora</i>
Ascomycota	Dothideomycetes	Pleosporales	Pleosporaceae	<i>Alternaria</i>	<i>Alternaria hordeicola</i>
Chlorophyta	Trebouxiophyceae	Trebouxiales	Trebouxiaceae	<i>Trebouxia</i>	<i>Trebouxia arboricola</i>
Ascomycota	Dothideomycetes	Pleosporales	Pleosporaceae	<i>Alternaria</i>	<i>Alternaria alternata</i>
Ascomycota	Dothideomycetes	Capnodiales	Cladosporiaceae	<i>Cladosporium</i>	<i>Cladosporium sphaerospermum</i>
Ascomycota	Dothideomycetes	Pleosporales	Phaeosphaeriaceae	<i>Phaeosphaeriopsis</i>	<i>Phaeosphaeriopsis glaucopunctata</i>
Ascomycota	-	-	-	-	-
Ascomycota	Lecanoromycetes	Lecanorales	Ramalinaceae	<i>Toninia</i>	<i>Toninia physaroides</i>
Ascomycota	Dothideomycetes	Pleosporales	Didymellaceae	<i>Didymella</i>	<i>Didymella</i> sp.
Ascomycota	Dothideomycetes	Capnodiales	Cladosporiaceae	<i>Cladosporium</i>	<i>Cladosporium fusiforme</i>
Ascomycota	Dothideomycetes	Pleosporales	Didymosphaeriaceae	<i>Neokalmusia</i>	<i>Neokalmusia brevispora</i>
Ascomycota	Dothideomycetes	Pleosporales	Didymellaceae	-	-
Ascomycota	Dothideomycetes	Pleosporales	Pleosporaceae	<i>Stemphylium</i>	<i>Stemphylium</i> sp.
Ascomycota	Dothideomycetes	Pleosporales	Pleosporaceae	<i>Alternaria</i>	<i>Alternaria metachromatica</i>
Ascomycota	Dothideomycetes	Capnodiales	Mycosphaerellaceae	<i>Mycosphaerella</i>	<i>Mycosphaerella tassiana</i>
Ascomycota	Dothideomycetes	Capnodiales	Cladosporiaceae	<i>Cladosporium</i>	<i>Cladosporium grevilleae</i>

Phylum	Class	Order	Family	Genus	Specie
Ascomycota	Dothideomycetes	Capnodiales	Neodevriesiaceae	<i>Neodevriesia</i>	<i>Neodevriesia</i> sp.
Chlorophyta	Trebouxiophyceae	Trebouxiales	Trebouxiaceae	<i>Trebouxia</i>	<i>Trebouxia decolorans</i>
Ascomycota	Dothideomycetes	Pleosporales	-	-	-
Ascomycota	Dothideomycetes	Pleosporales	Pleosporales_fam _Incertae_sedis	<i>Ochrocladosporium</i>	<i>Ochrocladosporium frigidarii</i>
Ascomycota	Dothideomycetes	Capnodiales	Cladosporiaceae	<i>Cladosporium</i>	<i>Cladosporium velox</i>
Ascomycota	Dothideomycetes	Pleosporales	Pleosporaceae	-	-
Chytridiomycota	-	-	-	-	-
Ascomycota	Dothideomycetes	Capnodiales	Mycosphaerellaceae	<i>Ramularia</i>	<i>Ramularia</i> sp.
Ascomycota	Dothideomycetes	Dothideales	Aureobasidiaceae	<i>Aureobasidium</i>	<i>Aureobasidium pullulans</i>
Ascomycota	Dothideomycetes	Capnodiales	Mycosphaerellaceae	<i>Zasmidium</i>	<i>Zasmidium</i> sp.
Chlorophyta	Trebouxiophyceae	Trebouxiales	Trebouxiaceae	<i>Trebouxia</i>	<i>Trebouxia</i> sp.
Ascomycota	Sordariomycetes	Sordariales	Sordariaceae	<i>Sordaria</i>	<i>Sordaria fimicola</i>
Ascomycota	Leotiomycetes	Helotiales	-	-	-
Ascomycota	Sordariomycetes	Diaporthales	Diaporthaceae	<i>Diaporthe</i>	<i>Diaporthe mayteni</i>
Ascomycota	Dothideomycetes	-	-	-	-
Basidiomycota	Agaricomycetes	Polyporales	Meruliaceae	<i>Phlebia</i>	<i>Phlebia</i> sp.
Ascomycota	Dothideomycetes	Capnodiales	Teratosphaeriaceae	-	-
Ascomycota	Lecanoromycetes	-	-	-	-
Ascomycota	Dothideomycetes	Capnodiales	Teratosphaeriaceae	<i>Meristemomyces</i>	<i>Meristemomyces frigidus</i>
Ascomycota	Dothideomycetes	Capnodiales	Cladosporiaceae	<i>Cladosporium</i>	<i>Cladosporium dominicanum</i>
Basidiomycota	Agaricomycetes	-	-	-	-
Ascomycota	Dothideomycetes	Capnodiales	Teratosphaeriaceae	<i>Teratosphaeria</i>	<i>Teratosphaeria xenocryptica</i>
Ascomycota	Leotiomycetes	Thelebolales	Thelebolaceae	<i>Thelebolus</i>	<i>Thelebolus globosus</i>
Ascomycota	Dothideomycetes	Capnodiales	Neodevriesiaceae	<i>Neodevriesia</i>	<i>Neodevriesia coryneliae</i>
Ascomycota	Dothideomycetes	Capnodiales	Cladosporiaceae	<i>Cladosporium</i>	<i>Cladosporium halotolerans</i>

Phylum	Class	Order	Family	Genus	Specie
Ascomycota	Saccharomycetes	Saccharomycetales	Saccharomycetales _fam_Incertae_sedis	<i>Candida</i>	<i>Candida galli</i>
Ascomycota	Lecanoromycetes	Umbilicariales	Umbilicariaceae	<i>Umbilicaria</i>	<i>Umbilicaria torrefacta</i>
Ascomycota	Saccharomycetes	Saccharomycetales	Saccharomycetaceae	<i>Kazachstania</i>	<i>Kazachstania naganishii</i>
Ascomycota	Dothideomycetes	Pleosporales	Pleosporaceae	<i>Bipolaris</i>	<i>Bipolaris</i> sp.
Ascomycota	Dothideomycetes	Capnodiales	Mycosphaerellaceae	-	-
Ascomycota	Sordariomycetes	Sordariales	Sordariaceae	<i>Neurospora</i>	<i>Neurospora</i> sp.
Ascomycota	Eurotiomycetes	Eurotiales	Aspergillaceae	<i>Penicillium</i>	<i>Penicillium</i> sp.
Ascomycota	Dothideomycetes	Capnodiales	Mycosphaerellaceae	<i>Ramularia</i>	<i>Ramularia beticola</i>
Ascomycota	Sordariomycetes	Coniochaetales	Coniochaetaceae	<i>Coniochaeta</i>	<i>Coniochaeta decumbens</i>
Glomeromycota	Glomeromycetes	Diversisporales	Diversisporaceae	<i>Diversispora</i>	<i>Diversispora</i> sp.
Basidiomycota	-	-	-	-	-
Ascomycota	Dothideomycetes	Capnodiales	Cladosporiaceae	<i>Cladosporium</i>	<i>Cladosporium aphidis</i>
Ascomycota	Dothideomycetes	Capnodiales	Mycosphaerellaceae	<i>Cercosporidium</i>	<i>Cercosporidium bougainvilleae</i>
Basidiomycota	Agaricomycetes	Polyporales	Meruliaceae	<i>Phlebia</i>	<i>Phlebia tuberculata</i>
Ascomycota	Geoglossomycetes	Geoglossales	Geoglossaceae	<i>Geoglossum</i>	<i>Geoglossum simile</i>
Ascomycota	Dothideomycetes	Capnodiales	Capnodiales_fam _Incertae_sedis	<i>Phaeotheca</i>	<i>Phaeotheca triangularis</i>
Ascomycota	Dothideomycetes	Capnodiales	Mycosphaerellaceae	<i>Ramularia</i>	<i>Ramularia acris</i>
Ascomycota	Sordariomycetes	Microascales	Microascaceae	<i>Scopulariopsis</i>	<i>Scopulariopsis fusca</i>
Ascomycota	Dothideomycetes	Capnodiales	Mycosphaerellaceae	<i>Pseudocercospora</i>	<i>Pseudocercospora</i> sp.
Ascomycota	Dothideomycetes	Capnodiales	Teratosphaeriaceae	<i>Teratosphaeria</i>	<i>Teratosphaeria mexicana</i>
Ascomycota	Dothideomycetes	Pleosporales	Sporormiaceae	<i>Preussia</i>	<i>Preussia</i> sp.
Ascomycota	Dothideomycetes	Capnodiales	Teratosphaeriaceae	<i>Capnobotryella</i>	<i>Capnobotryella</i> sp.
Ascomycota	Dothideomycetes	Capnodiales	Mycosphaerellaceae	<i>Ramulispora</i>	<i>Ramulispora sorghi</i>
Ascomycota	Sordariomycetes	Trichosphaeriales	Trichosphaeriaceae	<i>Nigrospora</i>	<i>Nigrospora oryzae</i>
Ascomycota	Eurotiomycetes	Coryneliales	Coryneliaceae	<i>Corynelia</i>	<i>Corynelia</i> sp.

Phylum	Class	Order	Family	Genus	Specie
Ascomycota	Dothideomycetes	Capnodiales	Teratosphaeriaceae	<i>Melanodothis</i>	<i>Melanodothis caricis</i>
Ascomycota	Leotiomycetes	Helotiales	Sclerotiniaceae	<i>Botrytis</i>	<i>Botrytis caroliniana</i>
Ascomycota	Dothideomycetes	Pleosporales	Didymosphaeriaceae	<i>Pseudopithomyces</i>	<i>Pseudopithomyces</i> sp.
Basidiomycota	Agaricomycetes	Agaricales	-	-	-
Ascomycota	Dothideomycetes	Pleosporales	Didymosphaeriaceae	-	-
Ascomycota	Sordariomycetes	-	-	-	-

Table E-8. Eukaryotic population present in the area CM2 of the Convent, identified through HTS approach.

Phylum	Class	Order	Family	Genus	Specie
Ascomycota	Dothideomycetes	Pleosporales	Didymellaceae	<i>Stagonosporopsis</i>	<i>Stagonosporopsis dorenboschii</i>
Ascomycota	Dothideomycetes	Pleosporales	Didymellaceae	-	-
Ascomycota	Dothideomycetes	Capnodiales	Cladosporiaceae	<i>Cladosporium</i>	<i>Cladosporium</i> sp.
Ascomycota	Leotiomycetes	Helotiales	Helotiaceae	<i>Articulospora</i>	<i>Articulospora</i> sp.
Ascomycota	Dothideomycetes	Capnodiales	Mycosphaerellaceae	<i>Mycosphaerella</i>	<i>Mycosphaerella tassiana</i>
Ascomycota	Dothideomycetes	Pleosporales	Pleosporaceae	<i>Alternaria</i>	<i>Alternaria alternata</i>
Ascomycota	Dothideomycetes	Pleosporales	Didymellaceae	<i>Didymella</i>	<i>Didymella</i> sp.
Basidiomycota	Tremellomycetes	Tremellales	Bulleribasidiaceae	<i>Vishniacozyma</i>	<i>Vishniacozyma carnescens</i>
Ascomycota	Leotiomycetes	Helotiales	Helotiaceae	<i>Articulospora</i>	<i>Articulospora proliferata</i>
Ascomycota	Dothideomycetes	Pleosporales	Pleosporaceae	<i>Alternaria</i>	<i>Alternaria</i> sp.
Ascomycota	Dothideomycetes	Pleosporales	Didymellaceae	unidentified	unidentified
Ascomycota	Leotiomycetes	Helotiales	Helotiaceae	<i>Articulospora</i>	<i>Articulospora</i> sp.
Ascomycota	Dothideomycetes	Pleosporales	Didymellaceae	<i>Ascochyta</i>	<i>Ascochyta rabiei</i>
Ascomycota	Dothideomycetes	Dothideales	Aureobasidiaceae	<i>Aureobasidium</i>	<i>Aureobasidium namibiae</i>
Ascomycota	Dothideomycetes	Pleosporales	-	-	-
Ascomycota	Dothideomycetes	Pleosporales	Didymellaceae	<i>Neoscochyta</i>	<i>Neoscochyta desmazieri</i>

Phylum	Class	Order	Family	Genus	Specie
Ascomycota	Dothideomycetes	Capnodiales	-	-	-
Ascomycota	Leotiomycetes	Helotiales	-	-	-
Ascomycota	-	-	-	-	-
Basidiomycota	Tremellomycetes	Filobasidiales	Filobasidiaceae	<i>Naganishia</i>	<i>Naganishia adeliensis</i>
Ascomycota	Dothideomycetes	Dothideales	Aureobasidiaceae	<i>Aureobasidium</i>	<i>Aureobasidium pullulans</i>
Ascomycota	Dothideomycetes	Pleosporales	Didymellaceae	<i>Didymella</i>	<i>Didymella chenopodii</i>
Ascomycota	Dothideomycetes	Pleosporales	Didymellaceae	<i>Stagonosporopsis</i>	<i>Stagonosporopsis</i> sp.
Basidiomycota	Cystobasidiomycetes	Cystobasidiomycetes _ord_Incertae_sedis	Symmetrosporaceae	<i>Symmetrospora</i>	<i>Symmetrospora foliicola</i>
Ascomycota	Lecanoromycetes	Lecanorales	Ramalinaceae	<i>Toninia</i>	<i>Toninia physaroides</i>
Ascomycota	Dothideomycetes	Pleosporales	Didymellaceae	<i>Allophoma</i>	<i>Allophoma minor</i>
Ascomycota	Dothideomycetes	Capnodiales	Cladosporiaceae	<i>Cladosporium</i>	<i>Cladosporium halotolerans</i>
Ascomycota	Dothideomycetes	Pleosporales	Didymellaceae	<i>unidentified</i>	<i>Didymellaceae</i> sp.
Ascomycota	Dothideomycetes	Dothideales	Aureobasidiaceae	<i>Aureobasidium</i>	<i>Aureobasidium subglaciale</i>
Ascomycota	Dothideomycetes	Pleosporales	Didymellaceae	<i>Epicoccum</i>	<i>Epicoccum</i> sp.
Ascomycota	Dothideomycetes	Pleosporales	Pleosporaceae	-	-
Ascomycota	Dothideomycetes	Capnodiales	Capnodiales_fam _Incertae_sedis	<i>Phaeotheca</i>	<i>Phaeotheca triangularis</i>
Basidiomycota	Tremellomycetes	Tremellales	Bulleribasidiaceae	<i>Vishniacozyma</i>	<i>Vishniacozyma dimennae</i>
Ascomycota	Dothideomycetes	Pleosporales	Didymellaceae	<i>Boeremia</i>	<i>Boeremia exigua</i>
Ascomycota	Dothideomycetes	Pleosporales	Didymellaceae	<i>Phoma</i>	<i>Phoma multirostrata</i>
Ascomycota	Dothideomycetes	Pleosporales	Pleosporaceae	<i>Alternaria</i>	<i>Alternaria hordeicola</i>
Ascomycota	Dothideomycetes	Pleosporales	Didymellaceae	<i>Xenodidymella</i>	<i>Xenodidymella humicola</i>
Basidiomycota	-	-	-	-	-
Ascomycota	Dothideomycetes	Pleosporales	Morosphaeriaceae	<i>Acrocalymma</i>	<i>Acrocalymma cycadis</i>
Ascomycota	Dothideomycetes	Pleosporales	Didymellaceae	<i>Didymella</i>	<i>Didymella gardeniae</i>
Ascomycota	Eurotiomycetes	Eurotiales	Aspergillaceae	<i>Penicillium</i>	<i>Penicillium</i> sp.

Phylum	Class	Order	Family	Genus	Specie
Ascomycota	Saccharomycetes	Saccharomycetales	Saccharomycetaceae	<i>Saccharomyces</i>	<i>Saccharomyces</i> sp.
Ascomycota	Leotiomycetes	Helotiales	Vibrisseaceae	<i>Phialocephala</i>	<i>Phialocephala virens</i>
Ascomycota	Dothideomycetes	Venturiales	Venturiaceae	<i>Venturia</i>	<i>Venturia hystrioides</i>
Ascomycota	Dothideomycetes	Pleosporales	Didymellaceae	<i>Neosascochyta</i>	<i>Neosascochyta</i> sp.
Basidiomycota	Microbotryomycetes	Sporidiobolales	Sporidiobolaceae	<i>Sporobolomyces</i>	<i>Sporobolomyces oryzicola</i>
Ascomycota	Dothideomycetes	Pleosporales	Sporormiaceae	unidentified	unidentified
Ascomycota	Dothideomycetes	Pleosporales	Didymellaceae	<i>Stagonosporopsis</i>	<i>Stagonosporopsis helianthi</i>
Ascomycota	Dothideomycetes	Pleosporales	Leptosphaeriaceae	<i>Neophaeosphaeria</i>	<i>Neophaeosphaeria</i> sp.
Ascomycota	Dothideomycetes	Pleosporales	Pleosporaceae	<i>Stemphylium</i>	<i>Stemphylium</i> sp.
Ascomycota	Dothideomycetes	Capnodiales	Cladosporiaceae	<i>Cladosporium</i>	<i>Cladosporium grevilleae</i>
Ascomycota	Dothideomycetes	Capnodiales	Neodevriesiaceae	-	-
Ascomycota	Lecanoromycetes	-	-	-	-
Ascomycota	Dothideomycetes	Pleosporales	Didymellaceae	<i>Boeremia</i>	<i>Boeremia noackiana</i>
Ascomycota	Dothideomycetes	Pleosporales	Phaeosphaeriaceae	-	-
Ascomycota	Dothideomycetes	Pleosporales	Didymellaceae	<i>Stagonosporopsis</i>	<i>Stagonosporopsis loticola</i>
Ascomycota	Dothideomycetes	Pleosporales	Didymellaceae	<i>Nothophoma</i>	<i>Nothophoma infossa</i>
Ascomycota	Saccharomycetes	Saccharomycetales	Saccharomycetaceae	<i>Kazachstania</i>	<i>Kazachstania</i> sp.
Basidiomycota	Tremellomycetes	Tremellales	Bulleribasidiaceae	<i>Vishniacozyma</i>	<i>Vishniacozyma</i> sp.
Basidiomycota	Microbotryomycetes	Leucosporidiales	Leucosporidiaceae	<i>Leucosporidium</i>	<i>Leucosporidium muscorum</i>
Basidiomycota	Tremellomycetes	Tremellales	unidentified	unidentified	unidentified
Ascomycota	Eurotiomycetes	Eurotiales	Aspergillaceae	<i>Penicillium</i>	<i>Penicillium corylophilum</i>
Ascomycota	Dothideomycetes	Pleosporales	Pleosporaceae	<i>Alternaria</i>	<i>Alternaria metachromatica</i>
Ascomycota	Dothideomycetes	Pleosporales	Pleosporaceae	<i>Pleospora</i>	<i>Pleospora</i> sp.
Ascomycota	Saccharomycetes	Saccharomycetales	Saccharomycetaceae	<i>Saccharomyces</i>	<i>Saccharomyces cerevisiae</i>
Ascomycota	Dothideomycetes	Capnodiales	Cladosporiaceae	<i>Cladosporium</i>	<i>Cladosporium fusiforme</i>
Ascomycota	Sordariomycetes	Hypocreales	Stachybotryaceae	<i>Sirastachys</i>	<i>Sirastachys cylindrospora</i>

Phylum	Class	Order	Family	Genus	Specie
Basidiomycota	Tremellomycetes	Tremellales	Bulleribasidiaceae	<i>Vishniacozyma</i>	<i>Vishniacozyma psychrotolerans</i>
Ascomycota	Dothideomycetes	Pleosporales	Didymellaceae	<i>Ascochyta</i>	<i>Ascochyta</i> sp.
Ascomycota	Dothideomycetes	Pleosporales	Didymellaceae	<i>Calophoma</i>	<i>Calophoma aquilegiicola</i>
Basidiomycota	Agaricomycetes	-	-	-	-
Ascomycota	Dothideomycetes	Dothideales	Dothioraceae	<i>Sydowia</i>	<i>Sydowia polyspora</i>
Ascomycota	Dothideomycetes	-	-	-	-
Ascomycota	Dothideomycetes	Pleosporales	Pleosporaceae	<i>Dendryphiella</i>	<i>Dendryphiella paravinosa</i>
Ascomycota	Dothideomycetes	Dothideales	Aureobasidiaceae	-	-
Basidiomycota	Tremellomycetes	Tremellales	Tremellaceae	<i>Cryptococcus</i>	<i>Cryptococcus frias</i>
Ascomycota	Sordariomycetes	-	-	-	-
Ascomycota	Saccharomycetes	Saccharomycetales	-	-	-
Basidiomycota	Tremellomycetes	Tremellales	Bulleribasidiaceae	<i>Vishniacozyma</i>	<i>Vishniacozyma victoriae</i>
Ascomycota	Dothideomycetes	Pleosporales	Leptosphaeriaceae	<i>Sphaerellopsis</i>	<i>Sphaerellopsis paraphysata</i>
Ascomycota	Dothideomycetes	Pleosporales	Didymellaceae	<i>Didymella</i>	<i>Didymella urticicola</i>
Ascomycota	Sordariomycetes	Glomerellales	Plectosphaerellaceae	<i>Plectosphaerella</i>	<i>Plectosphaerella cucumerina</i>
Ascomycota	Dothideomycetes	Dothideales	Aureobasidiaceae	<i>Aureobasidium</i>	<i>Aureobasidium</i> sp.
Ascomycota	Dothideomycetes	Pleosporales	Leptosphaeriaceae	<i>Leptosphaeria</i>	<i>Leptosphaeria polylepidis</i>
Ascomycota	Dothideomycetes	Pleosporales	Didymellaceae	<i>Ascochyta</i>	<i>Ascochyta phacae</i>
Ascomycota	Dothideomycetes	Dothideales	-	-	-

Table E-9. Eukaryotic population present in the area CM3 of the Convent, identified through HTS approach.

Phylum	Class	Order	Family	Genus	Specie
Ascomycota	Dothideomycetes	Capnodiales	Cladosporiaceae	<i>Cladosporium</i>	<i>Cladosporium</i> sp.
Ascomycota	Dothideomycetes	Capnodiales	Mycosphaerellaceae	<i>Mycosphaerella</i>	<i>Mycosphaerella tassiana</i>
Ascomycota	Dothideomycetes	Pleosporales	Pleosporaceae	<i>Stemphylium</i>	<i>Stemphylium</i> sp.

Phylum	Class	Order	Family	Genus	Specie
Ascomycota	Dothideomycetes	Pleosporales	Pleosporaceae	<i>Alternaria</i>	<i>Alternaria metachromatica</i>
Ascomycota	Dothideomycetes	Dothideales	Aureobasidiaceae	<i>Aureobasidium</i>	<i>Aureobasidium namibiae</i>
Ascomycota	Dothideomycetes	Pleosporales	Pleosporaceae	<i>Alternaria</i>	<i>Alternaria hordeicola</i>
Ascomycota	Dothideomycetes	Pleosporales	Didymellaceae	<i>Phoma</i>	<i>Phoma polemonii</i>
Ascomycota	Dothideomycetes	Pleosporales	Pleosporaceae	<i>Alternaria</i>	<i>Alternaria eureka</i>
Ascomycota	Dothideomycetes	Pleosporales	Pleosporaceae	<i>Alternaria</i>	<i>Alternaria sp.</i>
Ascomycota	Dothideomycetes	Pleosporales	Pleosporaceae	<i>Stemphylium</i>	<i>Stemphylium vesicarium</i>
Ascomycota	Dothideomycetes	Pleosporales	Pleosporaceae	-	-
Ascomycota	Dothideomycetes	Capnodiales	-	-	-
Ascomycota	Dothideomycetes	Pleosporales	Pleosporaceae	<i>Stemphylium</i>	<i>Stemphylium sp.</i>
Ascomycota	Dothideomycetes	Dothideales	Dothioraceae	<i>Hormonema</i>	<i>Hormonema sp.</i>
Ascomycota	Dothideomycetes	Pleosporales	-	-	-
Ascomycota	Dothideomycetes	Pleosporales	Didymellaceae	-	-
Basidiomycota	Agaricostilbomycetes	Agaricostilbales	Kondoaceae	<i>Kondoa</i>	<i>Kondoa aeria</i>
Ascomycota	-	-	-	-	-
Ascomycota	Dothideomycetes	Pleosporales	Pleosporaceae	<i>Alternaria</i>	<i>Alternaria alternata</i>
Basidiomycota	Exobasidiomycetes	Microstromatales	Microstromataceae	<i>Microstroma</i>	<i>Microstroma album</i>
Ascomycota	Dothideomycetes	Pleosporales	Pleosporaceae	<i>Bipolaris</i>	<i>Bipolaris sp.</i>
Ascomycota	Dothideomycetes	Pleosporales	Pleosporaceae	<i>Alternaria</i>	<i>Alternaria breviramosa</i>
Ascomycota	Dothideomycetes	Pleosporales	Pleosporaceae	<i>Alternaria</i>	<i>Alternaria infectoria</i>
Ascomycota	Lecanoromycetes	Lecanorales	Ramalinaceae	<i>Toninia</i>	<i>Toninia physaroides</i>
Basidiomycota	Agaricomycetes	Agaricales	Physalacriaceae	<i>Cylindrobasidium</i>	<i>Cylindrobasidium sp.</i>
Ascomycota	Dothideomycetes	Capnodiales	Capnodiales_fam _Incertae_sedis	<i>Phaeotheca</i>	<i>Phaeotheca triangularis</i>
Ascomycota	Leotiomycetes	Thelebolales	Pseudeurotiaceae	unidentified	unidentified
Ascomycota	Dothideomycetes	Dothideales	Aureobasidiaceae	<i>Aureobasidium</i>	<i>Aureobasidium sp.</i>

Phylum	Class	Order	Family	Genus	Specie
Ascomycota	Sordariomycetes	Hypocreales	Nectriaceae	<i>Fusarium</i>	<i>Fusarium</i> sp.
Ascomycota	Dothideomycetes	Dothideales	Aureobasidiaceae	-	-
Ascomycota	Dothideomycetes	Pleosporales	Pleosporaceae	<i>Paradendryphiella</i>	<i>Paradendryphiella arenariae</i>
Ascomycota	Dothideomycetes	Capnodiales	Cladosporiaceae	<i>Cladosporium</i>	<i>Cladosporium fusiforme</i>
Ascomycota	Dothideomycetes	Pleosporales	Pleosporaceae	<i>Stemphylium</i>	<i>Stemphylium loti</i>
Ascomycota	Saccharomycetes	Saccharomycetales	Saccharomycetaceae	<i>Saccharomyces</i>	<i>Saccharomyces</i> sp.
Basidiomycota	Cystobasidiomycetes	Cystobasidiomycetes _ord_Incertae_sedis	Symmetrosporaceae	<i>Symmetrospora</i>	<i>Symmetrospora foliicola</i>
Ascomycota	Eurotiomycetes	Eurotiales	Aspergillaceae	<i>Penicillium</i>	Penicillium sp.
Ascomycota	Dothideomycetes	Capnodiales	Cladosporiaceae	<i>Cladosporium</i>	<i>Cladosporium halotolerans</i>
Ascomycota	Dothideomycetes	Pleosporales	Didymellaceae	<i>Didymella</i>	<i>Didymella negriana</i>
Ascomycota	Leotiomycetes	Helotiales	-	-	-
Ascomycota	Dothideomycetes	Pleosporales	unidentified	unidentified	unidentified
Ascomycota	Dothideomycetes	Pleosporales	Leptosphaeriaceae	<i>Sphaerellopsis</i>	<i>Sphaerellopsis paraphysata</i>
Ascomycota	Lecanoromycetes	Acarosporales	Acarosporaceae	<i>Sarcogyne</i>	<i>Sarcogyne hypophaeoides</i>
Ascomycota	Dothideomycetes	Capnodiales	Cladosporiaceae	<i>Cladosporium</i>	<i>Cladosporium grevilleae</i>
Ascomycota	Dothideomycetes	Dothideales	-	-	-
Ascomycota	Dothideomycetes	-	-	-	-
Ascomycota	Leotiomycetes	Thelebolales	Thelebolaceae	<i>Thelebolus</i>	<i>Thelebolus globosus</i>
Basidiomycota	Agaricostilbomycetes	Agaricostilbales	Kondoaceae	<i>Bensingtonia</i>	<i>Bensingtonia</i> sp.
Ascomycota	Lecanoromycetes	-	-	-	-
Ascomycota	Dothideomycetes	Pleosporales	Morosphaeriaceae	<i>Acrocalymma</i>	<i>Acrocalymma</i> sp.
Ascomycota	Dothideomycetes	Pleosporales	Pleosporaceae	<i>Curvularia</i>	<i>Curvularia clavata</i>
Ascomycota	Dothideomycetes	Dothideales	Aureobasidiaceae	<i>Aureobasidium</i>	<i>Aureobasidium pullulans</i>
Ascomycota	Sordariomycetes	Hypocreales	Cordycipitaceae	<i>Lecanicillium</i>	<i>Lecanicillium dimorphum</i>
Ascomycota	Dothideomycetes	Dothideales	Dothideaceae	<i>Celosporium</i>	<i>Celosporium</i> sp.

Phylum	Class	Order	Family	Genus	Specie
Basidiomycota	Cystobasidiomycetes	Cystobasidiomycetes _ord_Incertae_sedis	Buckleyzymaceae	<i>Buckleyzyma</i>	<i>Buckleyzyma aurantiaca</i>
Basidiomycota	Microbotryomycetes	Sporidiobolales	Sporidiobolaceae	<i>Rhodotorula</i>	<i>Rhodotorula mucilaginosa</i>
Ascomycota	Saccharomycetes	Saccharomycetales	-	-	-
Ascomycota	Dothideomycetes	Pleosporales	Didymellaceae	<i>Phoma</i>	<i>Phoma aloes</i>
Basidiomycota	Microbotryomycetes	Sporidiobolales	Sporidiobolaceae	<i>Sporobolomyces</i>	<i>Sporobolomyces roseus</i>
Ascomycota	Sordariomycetes	Diaporthales	Diaporthaceae	<i>Diaporthe</i>	<i>Diaporthe mayteni</i>
Basidiomycota	Agaricomycetes	Agaricales	Agaricaceae	<i>Lepiota</i>	<i>Lepiota subincarnata</i>
Ascomycota	Leotiomycetes	-	-	-	-
Ascomycota	Saccharomycetes	Saccharomycetales	Saccharomycetaceae	-	-
Ascomycota	Saccharomycetes	Saccharomycetales	Saccharomycetaceae	<i>Kazachstania</i>	<i>Kazachstania</i> sp.
Basidiomycota	Tremellomycetes	Filobasidiales	Filobasidiaceae	<i>Naganishia</i>	<i>Naganishia albida</i>
Ascomycota	Sordariomycetes	Hypocreales	Nectriaceae	-	-
Ascomycota	Dothideomycetes	Capnodiales	Neodevriesiaceae	unidentified	unidentified
Ascomycota	Dothideomycetes	Pleosporales	Pleosporaceae	<i>Curvularia</i>	<i>Curvularia uncinata</i>
Ascomycota	Dothideomycetes	Dothideales	Dothioraceae	<i>Sydowia</i>	<i>Sydowia polyspora</i>
Basidiomycota	Agaricomycetes	-	-	-	-
Ascomycota	Dothideomycetes	Capnodiales	Mycosphaerellaceae	<i>Ramulispora</i>	<i>Ramulispora sorghi</i>
Ascomycota	Dothideomycetes	Capnodiales	Mycosphaerellaceae	<i>Pseudocercospora</i>	<i>Pseudocercospora</i> sp.
Ascomycota	Saccharomycetes	Saccharomycetales	Saccharomycetaceae	<i>Saccharomyces</i>	<i>Saccharomyces cerevisiae</i>
Basidiomycota	Malasseziomycetes	Malasseziales	Malasseziaceae	<i>Malassezia</i>	<i>Malassezia restricta</i>
Ascomycota	Dothideomycetes	Pleosporales	Pleosporaceae	<i>Curvularia</i>	<i>Curvularia bothriochloae</i>
Ascomycota	Dothideomycetes	Pleosporales	Pleosporaceae	<i>Curvularia</i>	<i>Curvularia</i> sp.
Ascomycota	Dothideomycetes	Pleosporales	Pleosporaceae	<i>Exserohilum</i>	<i>Exserohilum rostratum</i>
Ascomycota	Dothideomycetes	Pleosporales	Phaeosphaeriaceae	-	-
Ascomycota	Dothideomycetes	Capnodiales	Cladosporiaceae	<i>Rachicladosporium</i>	<i>Rachicladosporium</i> sp.

Phylum	Class	Order	Family	Genus	Specie
Ascomycota	Eurotiomycetes	Chaetothyriales	Trichomeriaceae	<i>Knufia</i>	<i>Knufia peltigerae</i>
Ascomycota	Dothideomycetes	Pleosporales	Pleosporaceae	<i>Cochliobolus</i>	<i>Cochliobolus</i> sp.
Mucoromycota	Mucoromycetes	Mucorales	Mucoraceae	<i>Mucor</i>	<i>Mucor plumbeus</i>
Ascomycota	Dothideomycetes	Pleosporales	Phaeosphaeriaceae	<i>Tintelnotia</i>	<i>Tintelnotia destructans</i>
Basidiomycota	-	-	-	-	-
Basidiomycota	Tremellomycetes	Tremellales	-	-	-

Table E-10. Eukaryotic population present in the area CM4 of the Convent, identified through HTS approach.

Phylum	Class	Order	Family	Genus	Specie
Ascomycota	Dothideomycetes	Dothideales	Aureobasidiaceae	<i>Aureobasidium</i>	<i>Aureobasidium pullulans</i>
Ascomycota	Dothideomycetes	Capnodiales	Cladosporiaceae	<i>Cladosporium</i>	<i>Cladosporium</i> sp.
Basidiomycota	Tremellomycetes	Tremellales	Bulleribasidiaceae	<i>Vishniacozyma</i>	<i>Vishniacozyma carnescens</i>
Basidiomycota	Tremellomycetes	Tremellales	Bulleribasidiaceae	<i>Vishniacozyma</i>	<i>Vishniacozyma victoriae</i>
Ascomycota	Dothideomycetes	Pleosporales	Didymellaceae	<i>Stagonosporopsis</i>	<i>Stagonosporopsis</i> sp.
Basidiomycota	Microbotryomycetes	Sporidiobolales	Sporidiobolaceae	<i>Sporobolomyces</i>	<i>Sporobolomyces roseus</i>
Ascomycota	Dothideomycetes	Pleosporales	Pleosporaceae	<i>Alternaria</i>	<i>Alternaria metachromatica</i>
Ascomycota	Dothideomycetes	Pleosporales	Didymellaceae	-	-
Ascomycota	Dothideomycetes	Dothideales	Aureobasidiaceae	-	-
Ascomycota	Dothideomycetes	Pleosporales	Pleosporaceae	<i>Alternaria</i>	<i>Alternaria hordeicola</i>
Ascomycota	Dothideomycetes	Dothideales	Aureobasidiaceae	<i>Aureobasidium</i>	<i>Aureobasidium subglaciale</i>
Ascomycota	Dothideomycetes	Dothideales	Aureobasidiaceae	<i>Kabatiella</i>	<i>Kabatiella lini</i>
Basidiomycota	Tremellomycetes	Filobasidiales	Filobasidiaceae	<i>Filobasidium</i>	<i>Filobasidium oeirense</i>
Ascomycota	-	-	-	-	-
Ascomycota	Dothideomycetes	Capnodiales	-	-	-
Ascomycota	Dothideomycetes	Capnodiales	Mycosphaerellaceae	<i>Mycosphaerella</i>	<i>Mycosphaerella tassiana</i>

Phylum	Class	Order	Family	Genus	Specie
Ascomycota	Dothideomycetes	Dothideales	Aureobasidiaceae	<i>Aureobasidium</i>	<i>Aureobasidium</i> sp.
Basidiomycota	Tremellomycetes	Tremellales	Bulleribasidiaceae	<i>Vishniacozyma</i>	<i>Vishniacozyma</i> sp.
Ascomycota	Dothideomycetes	Dothideales	Aureobasidiaceae	<i>Aureobasidium</i>	<i>Aureobasidium namibiae</i>
Ascomycota	Dothideomycetes	Dothideales	-	-	-
Ascomycota	Dothideomycetes	Pleosporales	Pleosporaceae	<i>Alternaria</i>	<i>Alternaria</i> sp.
Ascomycota	Dothideomycetes	Dothideales	Aureobasidiaceae	<i>Aureobasidium</i>	<i>Aureobasidium microstictum</i>
Ascomycota	Lecanoromycetes	Lecanorales	Ramalinaceae	<i>Toninia</i>	<i>Toninia physaroides</i>
Ascomycota	Dothideomycetes	Capnodiales	Cladosporiaceae	<i>Verrucocladosporium</i>	<i>Verrucocladosporium dirinae</i>
Ascomycota	Dothideomycetes	Capnodiales	Neodevriesiaceae	<i>Neodevriesia</i>	<i>Neodevriesia bulbilosa</i>
Ascomycota	Dothideomycetes	Pleosporales	Didymellaceae	<i>Stagonosporopsis</i>	<i>Stagonosporopsis lupini</i>
Ascomycota	Sordariomycetes	Hypocreales	Hypocreaceae	<i>Trichoderma</i>	<i>Trichoderma</i> sp.
Ascomycota	Lecanoromycetes	Pertusariales	Megasporaceae	<i>Megaspora</i>	<i>Megaspora</i> sp.
Ascomycota	Dothideomycetes	Capnodiales	Neodevriesiaceae	unidentified	unidentified
Ascomycota	Dothideomycetes	Pleosporales	-	-	-
Ascomycota	Lecanoromycetes	-	-	-	-
Basidiomycota	-	-	-	-	-
Ascomycota	Eurotiomycetes	Eurotiales	Aspergillaceae	<i>Penicillium</i>	<i>Penicillium</i> sp.
Ascomycota	Dothideomycetes	Capnodiales	Capnodiales_fam _Incertae_sedis	<i>Phaeotheca</i>	<i>Phaeotheca triangularis</i>
Ascomycota	Dothideomycetes	Capnodiales	Teratosphaeriaceae	-	-
Basidiomycota	Agaricomycetes	-	-	-	-
Ascomycota	Saccharomycetes	Saccharomycetales	Saccharomycetaceae	<i>Saccharomyces</i>	<i>Saccharomyces</i> sp.
Ascomycota	Dothideomycetes	Capnodiales	Mycosphaerellaceae	<i>Ramulispora</i>	<i>Ramulispora sorghi</i>
Basidiomycota	Agaricomycetes	Agaricales	-	-	-
Ascomycota	Leotiomycetes	Helotiales	-	-	-
Ascomycota	Dothideomycetes	Capnodiales	Cladosporiaceae	<i>Cladosporium</i>	<i>Cladosporium aphidis</i>

Phylum	Class	Order	Family	Genus	Specie
Ascomycota	Dothideomycetes	Pleosporales	Pleosporaceae	<i>Alternaria</i>	<i>Alternaria infectoria</i>
Basidiomycota	Agaricomycetes	Hymenochaetales	Hymenochaetaceae	<i>Phellinus</i>	<i>Phellinus andinus</i>
Ascomycota	Dothideomycetes	-	-	-	-
Ascomycota	Dothideomycetes	Pleosporales	Pleosporaceae	-	-
Ascomycota	Sordariomycetes	Hypocreales	Nectriaceae	unidentified	unidentified
Ascomycota	Saccharomycetes	Saccharomycetales	-	-	-
Ascomycota	Dothideomycetes	Pleosporales	Didymellaceae	<i>Didymella</i>	<i>Didymella boeremae</i>
Ascomycota	Dothideomycetes	Pleosporales	Phaeosphaeriaceae	<i>Phaeosphaeria</i>	<i>Phaeosphaeria triglochicola</i>
Ascomycota	Dothideomycetes	Pleosporales	unidentified	unidentified	unidentified
Ascomycota	Dothideomycetes	Dothideales	Aureobasidiaceae	<i>Kabatiella</i>	<i>Kabatiella zeae</i>
Ascomycota	Dothideomycetes	Capnodiales	Cladosporiaceae	<i>Cladosporium</i>	<i>Cladosporium grevilleae</i>
Ascomycota	Lecanoromycetes	Acarosporales	Acarosporaceae	-	-
Ascomycota	Dothideomycetes	Pleosporales	Pleosporaceae	<i>Bipolaris</i>	<i>Bipolaris</i> sp.
Ascomycota	Saccharomycetes	Saccharomycetales	Saccharomycetaceae	<i>Lachancea</i>	<i>Lachancea</i> sp.
Basidiomycota	Agaricomycetes	Russulales	Peniophoraceae	<i>Subulicystidium</i>	<i>Subulicystidium</i> sp.
Ascomycota	Dothideomycetes	Botryosphaeriales	Botryosphaeriaceae	-	-
Ascomycota	Sordariomycetes	Hypocreales	Nectriaceae	<i>Fusarium</i>	<i>Fusarium</i> sp.
Ascomycota	Lecanoromycetes	Umbilicariales	Ophioparmaceae	<i>Hypocenomyce</i>	<i>Hypocenomyce scalaris</i>
Basidiomycota	Tremellomycetes	Tremellales	-	-	-
Basidiomycota	Tremellomycetes	Tremellales	Bulleribasidiaceae	<i>Hannaella</i>	<i>Hannaella luteola</i>
Basidiomycota	Cystobasidiomycetes	Cystobasidiales	Cystobasidiaceae	<i>Cystobasidium</i>	<i>Cystobasidium slooffiae</i>
Basidiomycota	Malasseziomycetes	Malasseziales	Malasseziaceae	<i>Malassezia</i>	<i>Malassezia restricta</i>
Ascomycota	Dothideomycetes	Capnodiales	Cladosporiaceae	<i>Cladosporium</i>	<i>Cladosporium halotolerans</i>
Ascomycota	Dothideomycetes	Pleosporales	Pleosporaceae	<i>Alternaria</i>	<i>Alternaria breviramosa</i>
Ascomycota	Sordariomycetes	Hypocreales	Nectriaceae	<i>Volutella</i>	<i>Volutella lini</i>
Basidiomycota	Microbotryomycetes	Sporidiobolales	Sporidiobolaceae	<i>Sporobolomyces</i>	<i>Sporobolomyces</i> sp.

Phylum	Class	Order	Family	Genus	Specie
Ascomycota	Saccharomycetes	Saccharomycetales	Saccharomycetaceae	<i>Kazachstania</i>	<i>Kazachstania</i> sp.
Ascomycota	Dothideomycetes	Capnodiales	Cladosporiaceae	<i>Cladosporium</i>	<i>Cladosporium fusiforme</i>
Ascomycota	Sordariomycetes	Hypocreales	Nectriaceae	<i>Fusarium</i>	<i>Fusarium domesticum</i>
Ascomycota	Dothideomycetes	Pleosporales	Morosphaeriaceae	<i>Acrocalymma</i>	<i>Acrocalymma cycadis</i>
Ascomycota	Saccharomycetes	Saccharomycetales	Saccharomycetaceae	-	-
Ascomycota	Saccharomycetes	Saccharomycetales	Saccharomycetaceae	<i>Saccharomyces</i>	<i>Saccharomyces cerevisiae</i>
Ascomycota	Dothideomycetes	Pleosporales	Didymellaceae	<i>Stagonosporopsis</i>	<i>Stagonosporopsis helianthi</i>
Ascomycota	Dothideomycetes	Capnodiales	Mycosphaerellaceae	<i>Pseudocercospora</i>	<i>Pseudocercospora</i> sp.
Ascomycota	Dothideomycetes	Tubeufiales	Tubeufiaceae	<i>Acanthostigma</i>	<i>Acanthostigma multiseptatum</i>
Ascomycota	Leotiomycetes	Thelebolales	Thelebolaceae	<i>Thelebolus</i>	<i>Thelebolus globosus</i>
Basidiomycota	Agaricomycetes	Agaricales	Tricholomataceae	-	-
Ascomycota	Eurotiomycetes	Eurotiales	Aspergillaceae	-	-

Table E-11. Eukaryotic population present in the area CM5 of the Convent, identified through HTS approach.

Phylum	Class	Order	Family	Genus	Specie
Ascomycota	Sordariomycetes	Sordariales	Sordariaceae	<i>Sordaria</i>	<i>Sordaria fimicola</i>
Ascomycota	Dothideomycetes	Capnodiales	Cladosporiaceae	<i>Cladosporium</i>	<i>Cladosporium</i> sp.
Ascomycota	Dothideomycetes	Dothideales	Aureobasidiaceae	<i>Aureobasidium</i>	<i>Aureobasidium pullulans</i>
Basidiomycota	Tremellomycetes	Cystofilobasidiales	Cystofilobasidiaceae	<i>Guehomyces</i>	<i>Guehomyces pullulans</i>
Ascomycota	Dothideomycetes	Capnodiales	Mycosphaerellaceae	<i>Mycosphaerella</i>	<i>Mycosphaerella tassiana</i>
Basidiomycota	Tremellomycetes	Tremellales	Bulleribasidiaceae	<i>Vishniacozyma</i>	<i>Vishniacozyma victoriae</i>
Ascomycota	Dothideomycetes	Dothideales	Aureobasidiaceae	<i>Aureobasidium</i>	<i>Aureobasidium namibiae</i>
Ascomycota	Dothideomycetes	Pleosporales	Didymellaceae	-	-
Ascomycota	Dothideomycetes	Pleosporales	Pleosporaceae	<i>Alternaria</i>	<i>Alternaria hordeicola</i>

Phylum	Class	Order	Family	Genus	Specie
Ascomycota	Dothideomycetes	Pleosporales	Pleosporaceae	<i>Alternaria</i>	<i>Alternaria metachromatica</i>
Ascomycota	Sordariomycetes	Sordariales	Sordariaceae	<i>Neurospora</i>	<i>Neurospora</i> sp.
Ascomycota	Sordariomycetes	Hypocreales	Nectriaceae	<i>Gibberella</i>	<i>Gibberella tricineta</i>
Ascomycota	Dothideomycetes	Capnodiales	-	-	-
Ascomycota	Dothideomycetes	Capnodiales	Neodevriesiaceae	<i>Neodevriesia</i>	<i>Neodevriesia pakbiae</i>
Ascomycota	-	-	-	-	-
Ascomycota	Dothideomycetes	Pleosporales	Pleosporaceae	<i>Alternaria</i>	<i>Alternaria</i> sp.
Ascomycota	Dothideomycetes	Pleosporales	Pleosporaceae	<i>Alternaria</i>	<i>Alternaria alternata</i>
Ascomycota	Dothideomycetes	Capnodiales	Mycosphaerellaceae	<i>Readeriella</i>	<i>Readeriella</i> sp.
Ascomycota	Lecanoromycetes	Lecanorales	Ramalinaceae	<i>Toninia</i>	<i>Toninia physaroides</i>
Ascomycota	Dothideomycetes	Pleosporales	Anteagloniaceae	<i>Flammeascoma</i>	<i>Flammeascoma bambusae</i>
Ascomycota	Dothideomycetes	Pleosporales	Didymellaceae	<i>Stagonosporopsis</i>	<i>Stagonosporopsis dorenboschii</i>
Ascomycota	Sordariomycetes	Sordariales	Sordariaceae	<i>Neurospora</i>	<i>Neurospora crassa</i>
Ascomycota	Sordariomycetes	Sordariales	Sordariaceae	-	-
Basidiomycota	Tremellomycetes	Tremellales	Rhynchogastremataceae	<i>Papiliotrema</i>	<i>Papiliotrema fuscus</i>
Ascomycota	Dothideomycetes	Pleosporales	Didymellaceae	<i>Didymella</i>	<i>Didymella</i> sp.
Ascomycota	Leotiomycetes	Helotiales	Sclerotiniaceae	<i>Botrytis</i>	<i>Botrytis porri</i>
Ascomycota	Dothideomycetes	Dothideales	Aureobasidiaceae	-	-
Ascomycota	Dothideomycetes	Pleosporales	-	-	-
Basidiomycota	Tremellomycetes	Tremellales	Rhynchogastremataceae	<i>Papiliotrema</i>	<i>Papiliotrema</i> sp.
Ascomycota	Dothideomycetes	unidentified	unidentified	unidentified	unidentified
Ascomycota	Dothideomycetes	Pleosporales	Didymellaceae	<i>Didymella</i>	<i>Didymella chenopodii</i>
Ascomycota	Dothideomycetes	Dothideales	Aureobasidiaceae	<i>Kabatiella</i>	<i>Kabatiella lini</i>
Ascomycota	Dothideomycetes	Pleosporales	Didymellaceae	<i>Didymella</i>	<i>Didymella boeremae</i>
Ascomycota	Sordariomycetes	-	-	-	-

Phylum	Class	Order	Family	Genus	Specie
Ascomycota	Dothideomycetes	Dothideales	Aureobasidiaceae	<i>Aureobasidium</i>	<i>Aureobasidium</i> sp.
Ascomycota	Dothideomycetes	Dothideales	Aureobasidiaceae	<i>Aureobasidium</i>	<i>Aureobasidium subglaciale</i>
Ascomycota	Dothideomycetes	Capnodiales	Cladosporiaceae	<i>Cladosporium</i>	<i>Cladosporium aphidis</i>
Ascomycota	Dothideomycetes	Capnodiales	Neodevriesiaceae	<i>Neodevriesia</i>	<i>Neodevriesia modesta</i>
Basidiomycota	Agaricomycetes	-	-	-	-
Ascomycota	Dothideomycetes	Dothideales	-	-	-
Ascomycota	Dothideomycetes	Pleosporales	Didymellaceae	<i>Ascochyta</i>	<i>Ascochyta rabiei</i>
Ascomycota	Lecanoromycetes	-	-	-	-
Ascomycota	Saccharomycetes	Saccharomycetales	Saccharomycetaceae	<i>Saccharomyces</i>	<i>Saccharomyces</i> sp.
Ascomycota	Sordariomycetes	Sordariales	Sordariaceae	<i>Neurospora</i>	<i>Neurospora terricola</i>
Ascomycota	Dothideomycetes	Dothideales	Aureobasidiaceae	<i>Aureobasidium</i>	<i>Aureobasidium microstictum</i>
Ascomycota	Leotiomycetes	Helotiales	-	-	-
Ascomycota	Dothideomycetes	Pleosporales	Didymellaceae	<i>Phoma</i>	<i>Phoma polemonii</i>
Ascomycota	Dothideomycetes	Botryosphaeriales	Botryosphaeriaceae	<i>Dothiorella</i>	<i>Dothiorella santali</i>
Basidiomycota	Agaricomycetes	Agaricales	-	-	-
Ascomycota	Dothideomycetes	Pleosporales	Phaeosphaeriaceae	<i>Chaetosphaeronema</i>	<i>Chaetosphaeronema</i> sp.
Ascomycota	Dothideomycetes	-	-	-	-
Ascomycota	Sordariomycetes	Hypocreales	Stachybotryaceae	<i>Myrothecium</i>	<i>Myrothecium verrucaria</i>
Basidiomycota	Tremellomycetes	Tremellales	Bulleribasidiaceae	<i>Vishniacozyma</i>	<i>Vishniacozyma carnescens</i>
Ascomycota	Dothideomycetes	Pleosporales	unidentified	unidentified	unidentified
Basidiomycota	Tremellomycetes	Tremellales	Bulleribasidiaceae	<i>Vishniacozyma</i>	<i>Vishniacozyma</i> sp.
Basidiomycota	-	-	-	-	-
Ascomycota	Dothideomycetes	Pleosporales	Pleosporaceae	-	-
Ascomycota	Sordariomycetes	Hypocreales	Nectriaceae	<i>Gibberella</i>	<i>Gibberella baccata</i>
Ascomycota	Dothideomycetes	Pleosporales	Pleosporaceae	<i>Alternaria</i>	<i>Alternaria breviramosa</i>
Ascomycota	Sordariomycetes	Hypocreales	Nectriaceae	<i>Nalanthamala</i>	<i>Nalanthamala diospyri</i>

Phylum	Class	Order	Family	Genus	Specie
Ascomycota	Sordariomycetes	Hypocreales	Nectriaceae	<i>Fusarium</i>	<i>Fusarium</i> sp.
Ascomycota	Dothideomycetes	Capnodiales	Cladosporiaceae	<i>Cladosporium</i>	<i>Cladosporium grevilleae</i>
Ascomycota	Dothideomycetes	Pleosporales	Didymosphaeriaceae	<i>Paraconiothyrium</i>	<i>Paraconiothyrium</i> sp.
Ascomycota	Dothideomycetes	Pleosporales	Phaeosphaeriaceae	<i>Nodulosphaeria</i>	<i>Nodulosphaeria aconiti</i>
Basidiomycota	Tremellomycetes	Tremellales	Phaeotremellaceae	<i>Gelidatrema</i>	<i>Gelidatrema spencermartinsiae</i>
Ascomycota	Dothideomycetes	Pleosporales	Pleosporaceae	<i>Stemphylium</i>	<i>Stemphylium</i> sp.
Ascomycota	Sordariomycetes	Hypocreales	Stachybotryaceae	<i>Myrothecium</i>	<i>Myrothecium roridum</i>
Basidiomycota	Tremellomycetes	Tremellales	Tremellaceae	<i>Tremella</i>	<i>Tremella globispora</i>
Basidiomycota	Tremellomycetes	Tremellales	Rhynchogastremataceae	<i>Papiliotrema</i>	<i>Papiliotrema bandonii</i>
Ascomycota	Dothideomycetes	Pleosporales	Pleosporaceae	<i>Alternaria</i>	<i>Alternaria eureka</i>
Ascomycota	Dothideomycetes	Pleosporales	Morosphaeriaceae	<i>Acrocalymma</i>	<i>Acrocalymma cycadis</i>
Ascomycota	Dothideomycetes	Pleosporales	Periconiaceae	<i>Periconia</i>	<i>Periconia digitata</i>
Ascomycota	Dothideomycetes	Capnodiales	Cladosporiaceae	<i>Rachicladosporium</i>	<i>Rachicladosporium</i> sp.
Ascomycota	Dothideomycetes	Capnodiales	Extremaceae	-	-
Ascomycota	Dothideomycetes	Pleosporales	Arthopyreniaceae	<i>Arthopyrenia</i>	<i>Arthopyrenia salicis</i>
Ascomycota	Saccharomycetes	Saccharomycetales	Saccharomycetaceae	-	-
Ascomycota	Dothideomycetes	Pleosporales	Pleosporaceae	<i>Alternaria</i>	<i>Alternaria infectoria</i>
Ascomycota	Dothideomycetes	Capnodiales	Extremaceae	<i>Vermiconia</i>	<i>Vermiconia calcicola</i>
Ascomycota	Sordariomycetes	Sordariales	Sordariaceae	<i>Sordaria</i>	<i>Sordaria</i> sp.
Basidiomycota	Agaricomycetes	Agaricales	Psathyrellaceae	<i>Coprinellus</i>	<i>Coprinellus xanthothrix</i>
Ascomycota	Dothideomycetes	Capnodiales	Neodevriesiaceae	unidentified	unidentified
Ascomycota	Dothideomycetes	Pleosporales	Pleosporaceae	<i>Bipolaris</i>	<i>Bipolaris</i> sp.
Ascomycota	Lecanoromycetes	Acarosporales	Acarosporaceae	-	-
Ascomycota	Saccharomycetes	Saccharomycetales	Saccharomycetaceae	<i>Lachancea</i>	<i>Lachancea</i> sp.
Ascomycota	Dothideomycetes	Pleosporales	Cucurbitariaceae	<i>Pyrenochaeta</i>	<i>Pyrenochaeta</i> sp.

Phylum	Class	Order	Family	Genus	Specie
Ascomycota	Sordariomycetes	Hypocreales	Nectriaceae	unidentified	unidentified
Ascomycota	Lecanoromycetes	Lecanorales	-	-	-
Ascomycota	Saccharomycetes	Saccharomycetales	Saccharomycetaceae	<i>Kazachstania</i>	<i>Kazachstania</i> sp.
Ascomycota	Saccharomycetes	Saccharomycetales	-	-	-
Ascomycota	Sordariomycetes	Diaporthales	Diaporthaceae	<i>Diaporthe</i>	<i>Diaporthe mayteni</i>
Chytridiomycota	Spizellomycetes	Spizellomycetales	Spizellomycetaceae	<i>Spizellomyces</i>	<i>Spizellomyces</i> sp.
Ascomycota	Eurotiomycetes	Eurotiales	Aspergillaceae	<i>Penicillium</i>	<i>Penicillium</i> sp.
Ascomycota	Dothideomycetes	Capnodiales	Mycosphaerellaceae	<i>Ramulispora</i>	<i>Ramulispora sorghi</i>
Ascomycota	Sordariomycetes	Hypocreales	Nectriaceae	-	-
Ascomycota	Dothideomycetes	Capnodiales	Cladosporiaceae	<i>Cladosporium</i>	<i>Cladosporium fusiforme</i>
Ascomycota	Sordariomycetes	Glomerellales	Glomerellaceae	<i>Colletotrichum</i>	<i>Colletotrichum</i> sp.
Ascomycota	Dothideomycetes	Capnodiales	Teratosphaeriaceae	<i>Devriesia</i>	<i>Devriesia fraseriae</i>
Ascomycota	Dothideomycetes	Capnodiales	Mycosphaerellaceae	<i>Ramularia</i>	<i>Ramularia beticola</i>
Ascomycota	Dothideomycetes	Pleosporales	Didymellaceae	<i>Epicoccum</i>	<i>Epicoccum</i> sp.
Ascomycota	Dothideomycetes	Capnodiales	Teratosphaeriaceae	-	-
Ascomycota	Eurotiomycetes	Eurotiales	Aspergillaceae	-	-
Ascomycota	Dothideomycetes	Pleosporales	Didymosphaeriaceae	<i>Montagnula</i>	<i>Montagnula aloes</i>
Ascomycota	Dothideomycetes	Capnodiales	Teratosphaeriaceae	<i>Capnobotryella</i>	<i>Capnobotryella</i> sp.
Ascomycota	Dothideomycetes	Dothideales	Dothioraceae	<i>Hormonema</i>	<i>Hormonema viticola</i>
Ascomycota	Dothideomycetes	Tubeufiales	Tubeufiaceae	<i>Acanthostigma</i>	<i>Acanthostigma multiseptatum</i>
Ascomycota	Dothideomycetes	Capnodiales	Mycosphaerellaceae	<i>Zasmidium</i>	<i>Zasmidium</i> sp.
Ascomycota	Dothideomycetes	Capnodiales	Extremaceae	<i>Incertomyces</i>	<i>Incertomyces vagans</i>
Ascomycota	Dothideomycetes	Dothideales	Dothioraceae	<i>Sydowia</i>	<i>Sydowia polyspora</i>
Basidiomycota	Tremellomycetes	Cystofilobasidiales	-	-	-
Ascomycota	Sordariomycetes	Calosphaeriales	Calosphaeriaceae	<i>Jattaea</i>	<i>Jattaea</i> sp.
Ascomycota	Dothideomycetes	Pleosporales	Phaeosphaeriaceae	-	-

Phylum	Class	Order	Family	Genus	Specie
Ascomycota	Dothideomycetes	Capnodiales	Mycosphaerellaceae	<i>Pseudocercospora</i>	<i>Pseudocercospora</i> sp.
Ascomycota	Saccharomycetes	Saccharomycetales	Saccharomycetaceae	<i>Kazachstania</i>	<i>Kazachstania naganishii</i>
Arthropoda	Insecta	Lepidoptera	Crambidae	<i>Petrophila</i>	<i>Petrophila incerta</i>
Ascomycota	Dothideomycetes	Botryosphaeriales	Botryosphaeriaceae	-	-
Ascomycota	Eurotiomycetes	Chaetothyriales	Cyphellophoraceae	<i>Cyphellophora</i>	<i>Cyphellophora europaea</i>
Ascomycota	Sordariomycetes	Sordariales	-	-	-
Ascomycota	Leotiomycetes	Helotiales	Helotiaceae	<i>Glarea</i>	<i>Glarea lozoyensis</i>
Ascomycota	Leotiomycetes	Helotiales	Sclerotiniaceae	-	-
Ascomycota	Dothideomycetes	Capnodiales	Mycosphaerellaceae	<i>Protostegia</i>	<i>Protostegia eucleae</i>
Ascomycota	Eurotiomycetes	Eurotiales	Aspergillaceae	<i>Aspergillus</i>	<i>Aspergillus</i> sp.

Table E-12. Eukaryotic population present in the area CM6 of the Convent, identified through HTS approach.

Phylum	Class	Order	Family	Genus	Specie
Ascomycota	Dothideomycetes	Capnodiales	Cladosporiaceae	<i>Cladosporium</i>	<i>Cladosporium</i> sp.
Ascomycota	Leotiomycetes	Thelebolales	Thelebolaceae	<i>Thelebolus</i>	<i>Thelebolus globosus</i>
Ascomycota	Dothideomycetes	Dothideales	Aureobasidiaceae	<i>Aureobasidium</i>	<i>Aureobasidium namibiae</i>
Ascomycota	Dothideomycetes	Pleosporales	Didymellaceae	-	-
Ascomycota	Dothideomycetes	Capnodiales	Neodevriesiaceae	<i>Neodevriesia</i>	<i>Neodevriesia pakbiae</i>
Ascomycota	Dothideomycetes	Pleosporales	Pleosporaceae	<i>Alternaria</i>	<i>Alternaria hordeicola</i>
Basidiomycota	Tremellomycetes	Tremellales	Bulleribasidiaceae	<i>Vishniacozyma</i>	<i>Vishniacozyma victoriae</i>
Ascomycota	Dothideomycetes	Pleosporales	Sporormiaceae	unidentified	unidentified
Ascomycota	Sordariomycetes	Hypocreales	Nectriaceae	<i>Gibberella</i>	<i>Gibberella tricincta</i>
Ascomycota	Dothideomycetes	Dothideales	Aureobasidiaceae	<i>Aureobasidium</i>	<i>Aureobasidium pullulans</i>
Basidiomycota	Tremellomycetes	Tremellales	Bulleribasidiaceae	<i>Vishniacozyma</i>	<i>Vishniacozyma carnescens</i>

Phylum	Class	Order	Family	Genus	Specie
Ascomycota	Dothideomycetes	Pleosporales	Pleosporaceae	<i>Alternaria</i>	<i>Alternaria</i> sp.
Ascomycota	Dothideomycetes	Pleosporales	Pleosporaceae	<i>Alternaria</i>	<i>Alternaria metachromatica</i>
Ascomycota	Sordariomycetes	Xylariales	Amphisphaeriaceae	unidentified	unidentified
Ascomycota	Dothideomycetes	Pleosporales	Pleosporaceae	<i>Stemphylium</i>	<i>Stemphylium</i> sp.
Ascomycota	Dothideomycetes	Capnodiales	Mycosphaerellaceae	<i>Readeriella</i>	<i>Readeriella</i> sp.
Ascomycota	Dothideomycetes	Pleosporales	Didymellaceae	<i>Didymella</i>	<i>Didymella chenopodii</i>
Ascomycota	Dothideomycetes	Pleosporales	Didymellaceae	<i>Stagonosporopsis</i>	<i>Stagonosporopsis</i> sp.
Ascomycota	Dothideomycetes	Pleosporales	Pleosporaceae	<i>Alternaria</i>	<i>Alternaria eureka</i>
Ascomycota	-	-	-	-	-
Basidiomycota	Tremellomycetes	Holtermanniales	Holtermanniales_fam _Incertae_sedis	<i>Holtermanniella</i>	<i>Holtermanniella takashimae</i>
Ascomycota	Dothideomycetes	Capnodiales	Mycosphaerellaceae	<i>Mycosphaerella</i>	<i>Mycosphaerella tassiana</i>
Ascomycota	Dothideomycetes	Capnodiales	-	-	-
Ascomycota	Sordariomycetes	Hypocreales	Stachybotryaceae	<i>Myrothecium</i>	<i>Myrothecium roridum</i>
Ascomycota	Dothideomycetes	Pleosporales	Didymellaceae	<i>Stagonosporopsis</i>	<i>Stagonosporopsis dorenboschii</i>
Ascomycota	Dothideomycetes	Pleosporales	-	-	-
Ascomycota	Lecanoromycetes	Lecanorales	Ramalinaceae	<i>Toninia</i>	<i>Toninia physaroides</i>
Ascomycota	Dothideomycetes	Pleosporales	Sporormiaceae	-	-
Ascomycota	Dothideomycetes	Pleosporales	Didymosphaeriaceae	<i>Neokalmusia</i>	<i>Neokalmusia brevispora</i>
Ascomycota	Dothideomycetes	Pleosporales	Anteagloniaceae	<i>Flammeascoma</i>	<i>Flammeascoma bambusae</i>
Ascomycota	Dothideomycetes	Pleosporales	Sporormiaceae	<i>Sporormiella</i>	<i>Sporormiella leporina</i>
Ascomycota	Dothideomycetes	Pleosporales	Phaeosphaeriaceae	unidentified	unidentified
Ascomycota	Dothideomycetes	unidentified	unidentified	unidentified	unidentified
Basidiomycota	Tremellomycetes	Filobasidiales	Filobasidiaceae	<i>Filobasidium</i>	<i>Filobasidium wieringae</i>
Ascomycota	Dothideomycetes	Dothideales	Dothioraceae	<i>Sydowia</i>	<i>Sydowia polyspora</i>
Ascomycota	Sordariomycetes	Hypocreales	Nectriaceae	<i>Fusarium</i>	<i>Fusarium oxysporum</i>

Phylum	Class	Order	Family	Genus	Specie
Ascomycota	Lecanoromycetes	-	-	-	-
Ascomycota	Dothideomycetes	Dothideales	Aureobasidiaceae	-	-
Ascomycota	Dothideomycetes	Pleosporales	Sporormiaceae	<i>Sporormiella</i>	<i>Sporormiella</i> sp.
Ascomycota	Dothideomycetes	Dothideales	Aureobasidiaceae	<i>Aureobasidium</i>	<i>Aureobasidium</i> sp.
Ascomycota	Dothideomycetes	Pleosporales	Pleosporaceae	<i>Alternaria</i>	<i>Alternaria infectoria</i>
Ascomycota	Dothideomycetes	Pleosporales	Pleosporaceae	<i>Alternaria</i>	<i>Alternaria alternata</i>
Ascomycota	Sordariomycetes	Hypocreales	Nectriaceae	<i>Gibberella</i>	<i>Gibberella baccata</i>
Ascomycota	Eurotiomycetes	Verrucariales	Verrucariaceae	<i>Verrucaria</i>	<i>Verrucaria nigrescens</i>
Ascomycota	Dothideomycetes	Pleosporales	Pleosporaceae	-	-
Ascomycota	Dothideomycetes	Pleosporales	Didymellaceae	<i>Didymella</i>	<i>Didymella</i> sp.
Ascomycota	Dothideomycetes	Pleosporales	Didymosphaeriaceae	<i>Montagnula</i>	<i>Montagnula aloes</i>
Ascomycota	Sordariomycetes	Togniniales	Togniniaceae	<i>Phaeoacremonium</i>	<i>Phaeoacremonium</i> sp.
Ascomycota	Eurotiomycetes	Chaetothyriales	Herpotrichiellaceae	<i>Phialophora</i>	<i>Phialophora cyclaminis</i>
Basidiomycota	Tremellomycetes	Tremellales	Bulleribasidiaceae	<i>Vishniacozyma</i>	<i>Vishniacozyma dimennae</i>
Ascomycota	Dothideomycetes	Pleosporales	Cucurbitariaceae	<i>Pyrenochaeta</i>	<i>Pyrenochaeta</i> sp.
Ascomycota	Dothideomycetes	Pleosporales	Phaeosphaeriaceae	<i>Chaetosphaeronema</i>	<i>Chaetosphaeronema</i> sp.
Ascomycota	Sordariomycetes	Hypocreales	Stachybotryaceae	<i>Alfaria</i>	<i>Alfaria</i> sp.
Ascomycota	Sordariomycetes	Hypocreales	Nectriaceae	<i>Ilyonectria</i>	<i>Ilyonectria macroconidialis</i>
Ascomycota	Dothideomycetes	Pleosporales	Didymellaceae	<i>Boeremia</i>	<i>Boeremia sambuci-nigrae</i>
Ascomycota	Dothideomycetes	Pleosporales	Didymellaceae	<i>Didymella</i>	<i>Didymella negriana</i>
Ascomycota	Dothideomycetes	Pleosporales	Didymellaceae	<i>Epicoccum</i>	<i>Epicoccum</i> sp.
Ascomycota	Lecanoromycetes	Acarosporales	Acarosporaceae	-	-
Ascomycota	Dothideomycetes	Pleosporales	Pleosporaceae	<i>Stemphylium</i>	<i>Stemphylium</i> sp.
Ascomycota	Sordariomycetes	Hypocreales	Stachybotryaceae	-	-
Ascomycota	Eurotiomycetes	Eurotiales	Aspergillaceae	<i>Penicillium</i>	<i>Penicillium</i> sp.
Ascomycota	Dothideomycetes	Pleosporales	Sporormiaceae	<i>Preussia</i>	<i>Preussia pilosella</i>

Phylum	Class	Order	Family	Genus	Specie
Ascomycota	Sordariomycetes	Hypocreales	Stachybotryaceae	unidentified	unidentified
Ascomycota	Sordariomycetes	Hypocreales	Nectriaceae	<i>Fusarium</i>	<i>Fusarium domesticum</i>
Ascomycota	Dothideomycetes	-	-	-	-
Ascomycota	Dothideomycetes	Pleosporales	Phaeosphaeriaceae	<i>Wojnowicia</i>	<i>Wojnowicia viburni</i>
Ascomycota	Dothideomycetes	Pleosporales	unidentified	unidentified	unidentified
Ascomycota	Dothideomycetes	Dothideales	-	-	-
Ascomycota	Sordariomycetes	Hypocreales	Nectriaceae	-	-
Ascomycota	Dothideomycetes	Capnodiales	Cladosporiaceae	<i>Cladosporium</i>	<i>Cladosporium grevilleae</i>
Ascomycota	Dothideomycetes	Capnodiales	Extremaceae	<i>Vermiconia</i>	<i>Vermiconia calcicola</i>
Ascomycota	Sordariomycetes	-	-	-	-
Ascomycota	Leotiomycetes	-	-	-	-
Basidiomycota	Tremellomycetes	Tremellales	Bulleribasidiaceae	<i>Vishniacozyma</i>	<i>Vishniacozyma</i> sp.
Ascomycota	Eurotiomycetes	Verrucariales	Verrucariaceae	<i>Psoroglaena</i>	<i>Psoroglaena</i> sp.
Ascomycota	Dothideomycetes	Pleosporales	Phaeosphaeriaceae	-	-
Ascomycota	Dothideomycetes	Pleosporales	Didymellaceae	<i>Phomatodes</i>	<i>Phomatodes aubrietiae</i>
Ascomycota	Leotiomycetes	Helotiales	Hyaloscyphaceae	<i>Lachnum</i>	<i>Lachnum fuscescens</i>
Ascomycota	Lecanoromycetes	Lecanorales	-	-	-
Ascomycota	Sordariomycetes	Hypocreales	Nectriaceae	<i>Gibberella</i>	<i>Gibberella</i> sp.
Ascomycota	Dothideomycetes	Pleosporales	Leptosphaeriaceae	<i>Subplenodomus</i>	<i>Subplenodomus</i> sp.
Ascomycota	Dothideomycetes	Pleosporales	Pleosporaceae	<i>Alternaria</i>	<i>Alternaria breviramosa</i>
Ascomycota	Dothideomycetes	Pleosporales	Didymellaceae	<i>Didymella</i>	<i>Didymella boeremae</i>
Ascomycota	Dothideomycetes	Pleosporales	Didymellaceae	<i>Ascochyta</i>	<i>Ascochyta rabiei</i>
Ascomycota	Dothideomycetes	Capnodiales	Teratosphaeriaceae	<i>Devriesia</i>	<i>Devriesia fraserae</i>
Ascomycota	Leotiomycetes	Helotiales	-	-	-
Basidiomycota	Tremellomycetes	Tremellales	Rhynchogastremataceae	<i>Papiliotrema</i>	<i>Papiliotrema flavescens</i>
Ascomycota	Dothideomycetes	Pleosporales	Pleosporaceae	<i>Bipolaris</i>	<i>Bipolaris</i> sp.

Phylum	Class	Order	Family	Genus	Specie
Ascomycota	Sordariomycetes	Hypocreales	Hypocreales_fam _Incertae_sedis	<i>Acremonium</i>	<i>Acremonium persicinum</i>
Ascomycota	Dothideomycetes	Dothideales	Aureobasidiaceae	<i>Aureobasidium</i>	<i>Aureobasidium subglaciale</i>
Ascomycota	Lecanoromycetes	Lecanorales	Parmeliaceae	<i>Karoowia</i>	<i>Karoowia scitula</i>
Ascomycota	Dothideomycetes	Pleosporales	Didymellaceae	<i>Boeremia</i>	<i>Boeremia exigua</i>
Ascomycota	Leotiomycetes	Helotiales	Helotiaceae	<i>Tetracladium</i>	<i>Tetracladium marchalianum</i>
Ascomycota	Leotiomycetes	Helotiales	Helotiaceae	<i>Crocicreas</i>	<i>Crocicreas epicalamia</i>
Ascomycota	Dothideomycetes	Dothideales	Aureobasidiaceae	<i>Kabatiella</i>	<i>Kabatiella lini</i>
Ascomycota	Dothideomycetes	Pleosporales	Pleosporaceae	<i>Stemphylium</i>	<i>Stemphylium loti</i>
Ascomycota	Dothideomycetes	Pleosporales	Phaeosphaeriaceae	<i>Phaeosphaeria</i>	<i>Phaeosphaeria triglochinicola</i>
Ascomycota	Dothideomycetes	Capnodiales	Mycosphaerellaceae	<i>Zasmidium</i>	<i>Zasmidium sp.</i>
Ascomycota	Leotiomycetes	Helotiales	Sclerotiniaceae	<i>Botrytis</i>	<i>Botrytis caroliniana</i>
Ascomycota	Sordariomycetes	Xylariales	-	-	-
Ascomycota	Dothideomycetes	Pleosporales	Didymellaceae	<i>Phoma</i>	<i>Phoma multirostrata</i>
Ascomycota	Sordariomycetes	Sordariales	Sordariaceae	<i>Neurospora</i>	<i>Neurospora crassa</i>
Ascomycota	Dothideomycetes	Pleosporales	Cucurbitariaceae	<i>Pyrenochaeta</i>	<i>Pyrenochaeta inflorescentiae</i>
Ascomycota	Eurotiomycetes	-	-	-	-
Ascomycota	Dothideomycetes	Pleosporales	Didymellaceae	<i>Stagonosporopsis</i>	<i>Stagonosporopsis lupini</i>
Ascomycota	Dothideomycetes	Capnodiales	Extremaceae	<i>Incertomyces</i>	<i>Incertomyces vagans</i>
Ascomycota	Dothideomycetes	Pleosporales	Pleosporaceae	<i>Dendryphiella</i>	<i>Dendryphiella paravivosa</i>
Ascomycota	Sordariomycetes	Xylariales	Bartaliniaceae	<i>Truncatella</i>	<i>Truncatella spadicea</i>
Basidiomycota	Agaricomycetes	-	-	-	-
Ascomycota	Dothideomycetes	Capnodiales	Extremaceae	-	-
Basidiomycota	-	-	-	-	-
Basidiomycota	Tremellomycetes	Cystofilobasidiales	Cystofilobasidiaceae	<i>Cystofilobasidium</i>	<i>Cystofilobasidium capitatum</i>
Ascomycota	Saccharomycetes	Saccharomycetales	Saccharomycetaceae	-	-

Phylum	Class	Order	Family	Genus	Specie
Ascomycota	Dothideomycetes	Capnodiales	Neodevriesiaceae	<i>Neodevriesia</i>	<i>Neodevriesia modesta</i>
Ascomycota	Dothideomycetes	Pleosporales	Didymosphaeriaceae	-	-
Ascomycota	Lecanoromycetes	Lecanorales	Ramalinaceae	<i>Lecania</i>	<i>Lecania proteiformis</i>
Ascomycota	Dothideomycetes	Dothideales	Aureobasidiaceae	<i>Aureobasidium</i>	<i>Aureobasidium microstictum</i>
Ascomycota	Dothideomycetes	Pleosporales	Didymosphaeriaceae	<i>Pseudopithomyces</i>	<i>Pseudopithomyces</i> sp.
Ascomycota	Dothideomycetes	Pleosporales	Didymellaceae	<i>Ascochyta</i>	<i>Ascochyta phacae</i>
Ascomycota	Dothideomycetes	Pleosporales	Arthopyreniaceae	<i>Arthopyrenia</i>	<i>Arthopyrenia salicis</i>
Ascomycota	Lecanoromycetes	Trapeliales	Phlyctidaceae	<i>Phlyctis</i>	<i>Phlyctis argena</i>
Ascomycota	Sordariomycetes	Xylariales	Apiosporaceae	<i>Arthrimum</i>	<i>Arthrimum sacchari</i>
Ascomycota	Sordariomycetes	Hypocreales	-	-	-
Ascomycota	Dothideomycetes	Botryosphaeriales	Botryosphaeriaceae	<i>Lasiodiplodia</i>	<i>Lasiodiplodia crassispora</i>
Ascomycota	Dothideomycetes	Pleosporales	Didymellaceae	<i>Phoma</i>	<i>Phoma saxea</i>
Ascomycota	Saccharomycetes	Saccharomycetales	-	-	-
Ascomycota	Sordariomycetes	Sordariales	Sordariaceae	<i>Neurospora</i>	<i>Neurospora</i> sp.
Ascomycota	Leotiomycetes	Rhytismatales	Cudoniaceae	-	-
Ascomycota	Dothideomycetes	Capnodiales	Cladosporiaceae	<i>Cladosporium</i>	<i>Cladosporium fusiforme</i>
Ascomycota	Leotiomycetes	Helotiales	Sclerotiniaceae	<i>Botrytis</i>	<i>Botrytis porri</i>
Ascomycota	Sordariomycetes	Sordariales	Sordariaceae	<i>Neurospora</i>	<i>Neurospora terricola</i>
Ascomycota	Sordariomycetes	Xylariales	Bartaliniaceae	<i>Hyalotiella</i>	<i>Hyalotiella spartii</i>
Ascomycota	Dothideomycetes	Pleosporales	Morosphaeriaceae	<i>Acrocalymma</i>	<i>Acrocalymma cycadis</i>
Ascomycota	Sordariomycetes	Hypocreales	Stachybotryaceae	<i>Sirastachys</i>	<i>Sirastachys cylindrospora</i>
Ascomycota	Dothideomycetes	Capnodiales	Teratosphaeriaceae	<i>Devriesia</i>	<i>Devriesia compacta</i>
Ascomycota	Dothideomycetes	Pleosporales	Pleosporales_fam _Incertae_sedis	<i>Monodictys</i>	<i>Monodictys</i> sp.
Basidiomycota	Tremellomycetes	Holtermanniales	Holtermanniales_fam _Incertae_sedis	<i>Holtermannia</i>	<i>Holtermannia corniformis</i>
Ascomycota	Dothideomycetes	Pleosporales	Pleosporaceae	<i>Alternaria</i>	<i>Alternaria didymospora</i>

Phylum	Class	Order	Family	Genus	Specie
Ascomycota	Dothideomycetes	Pleosporales	Phaeosphaeriaceae	<i>Nodulosphaeria</i>	<i>Nodulosphaeria aconiti</i>
Ascomycota	Dothideomycetes	Capnodiales	Capnodiales_fam _Incertae_sedis	<i>Arthrocatena</i>	<i>Arthrocatena tenebrio</i>
Ascomycota	Dothideomycetes	Capnodiales	Cladosporiaceae	<i>Cladosporium</i>	<i>Cladosporium aphidis</i>
Ascomycota	Lecanoromycetes	Acarosporales	Acarosporaceae	<i>Sarcogyne</i>	<i>Sarcogyne hypophaeoides</i>
Ascomycota	Eurotiomycetes	Chaetothyriales	Herpotrichiellaceae	<i>Coniosporium</i>	<i>Coniosporium apollinis</i>
Ascomycota	Sordariomycetes	Xylariales	Amphisphaeriaceae	<i>Seimatosporium</i>	<i>Seimatosporium</i> sp.
Ascomycota	Lecanoromycetes	Lecanorales	Ramalinaceae	<i>Lecania</i>	<i>Lecania erysibe</i>
Basidiomycota	Tremellomycetes	Cystofilobasidiales	Cystofilobasidiaceae	<i>Guehomyces</i>	<i>Guehomyces pullulans</i>
Ascomycota	Dothideomycetes	Pleosporales	Lentitheciaceae	<i>Keissleriella</i>	<i>Keissleriella taminensis</i>
Basidiomycota	Agaricomycetes	Agaricales	-	-	-
Basidiomycota	Agaricomycetes	Agaricales	Strophariaceae	<i>Psilocybe</i>	<i>Psilocybe inquilina</i>
Ascomycota	Saccharomycetes	Saccharomycetales	Dipodascaceae	<i>Dipodascus</i>	<i>Dipodascus australiensis</i>
Ascomycota	Dothideomycetes	Capnodiales	Mycosphaerellaceae	<i>Pseudocercospora</i>	<i>Pseudocercospora</i> sp.
Ascomycota	Eurotiomycetes	Eurotiales	Aspergillaceae	<i>Aspergillus</i>	<i>Aspergillus</i> sp.
Ascomycota	Lecanoromycetes	Acarosporales	Acarosporaceae	<i>Polysporina</i>	<i>Polysporina</i> sp.
Ascomycota	Dothideomycetes	Pleosporales	Didymellaceae	<i>Xenodidymella</i>	<i>Xenodidymella humicola</i>